Treatment effect of Low Intensity Pulsed Ultrasound either alone, with functional appliance and with gene therapy on the mandibular condylar growth

by

Harmanpreet Kaur

A thesis submitted in partial fulfillment of the requirements for the degree of

Doctor of Philosophy

Medical Sciences - Dentistry
University of Alberta

Abstract:

The aim of this thesis was to investigate the effect of Low intensity pulsed ultrasound (LIPUS) with or without the use of forward bite jumping appliance, also known as functional appliance (FA) on the mandibular condylar growth in the rat model and also to investigate the biological effect on MC 3T3E1 pre-osteoblast and C28/I2 chondrocyte cell lines. In addition, we need to explore the effect of LIPUS and local injection of gene therapy on the mandibular condylar growth. In the animal study, fifty four Sprague-Dawley (SD) rats were divided into six groups (n=9) namely: control, LIPUS 20 minutes, LIPUS 40 minutes, Functional Appliance (FA), FA + LIPUS 20 minutes and FA + LIPUS 40 minutes. Right mandibular condyle was used as the experimental side and the left mandibular condyle was the internal control. After 4 weeks, the mandibles were evaluated for morphometric analysis while the condylar heads were evaluated using Micro-CT, histomorphometric and immunohistochemistry analyses. 20 minutes LIPUS application either alone or in combination with FA showed a significant increase in mandibular condylar length, increased cell number and layer width of proliferative and hypertrophic layers along with increased protein expression of SOX9, Collagen II, Collagen X and Aggrecan in the mandible condyle. Also, Micro-CT analysis demonstrated a significant increase in bone micro-architecture and bone mineral density.

We hypothesized that LIPUS application leads to reactive oxygen species (ROS) generation which is involved in mitogen-activated protein kinases (MAPKs) activation. C28/I2 chondrocyte and MC 3T3E1 pre-osteoblast cell lines were stimulated with one time LIPUS application for either 10 minutes or 20 minutes; control groups were treated with sham transducers. For ROS inhibition, diphenylene iodonium was added to the culture medium before LIPUS application. In C28/I2 chondrocytes, LIPUS showed a significant increase in ROS generation, ERK1/2 activation as well as increased gene expressions of *SOX9*, *COL2A1*, and *ACAN* while the effect was reversed in ROS inhibition. On the contrary, in MC 3T3E1 pre-osteoblasts, LIPUS increased ERK1/2 activation and increased gene expressions of *RUNX2*, *OCN*, and *OPN* in ROS inhibition. In both the cell lines, the amount of ROS generated was non-toxic.

Gene therapy is rapidly growing treatment modality in the field of tissue engineering and bone regeneration. We conducted a pilot study to investigate the effect of LIPUS with non-viral gene delivery of basic fibroblast growth factor (bFGF). Fifteen SD rats were divided into 5 groups (n=3): control, gWiz, bFGF plasmid- polyethyleneimine- linoleic acid (bFGF-PEI-LA), LIPUS 20 minutes and bFGF-PEI-LA + LIPUS 20 minutes. The plasmid-polymer complex was injected on the left side of the mandible condyle on the first day of the experiment and LIPUS was applied for 20 minutes for next 4 weeks. After 4 weeks, the mandibles were analyzed for morphometric, histomorphometric and Micro-CT

analyses. There was a significant increase in mandibular condyle length in either bFGF-PEI-LA or LIPUS alone groups while the combination group showed an increase in bone volume fraction. Collectively, these results are indicative of distinct anabolic effect of LIPUS application that enhances the mandibular condylar growth.

Preface:

This thesis is an original work by Harmanpreet Kaur. The research project, of which this thesis is a part, received research ethics approval from University of Alberta Animal Care and Use Committee, Project titled "Dose dependent effect of Low Intensity Pulsed Ultrasound on the condylar growth during functional appliance application", No 694/04/13/C (AUP #381) approved on April 20, 2012.

Chapter 2 of this thesis has been published as H. Kaur, H. Uludag, D. Dederich and T. El-Bialy "Effect of increasing Low Intensity Pulsed Ultrasound and Functional Appliance on Mandibular condyle in the growing rats" Journal of Ultrasound in Medicine. doi: 10.7863/ultra.15.06063. I was responsible for the study design, data collection and analysis as well as the manuscript composition. H. Uludag and D. Dederich contributed to manuscript edits. T. El-Bialy was the supervisory author and was involved with manuscript composition.

Chapter 5 of this thesis has been published as H. Kaur, H. Uludag and T. El-Bialy "Effect of nonviral plasmid delivered basic fibroblast growth factor and Low intensity pulsed ultrasound on the mandibular condylar growth – a preliminary study" BioMed Research International Volume 2014, Article ID 426710, 9 pages http://dx.doi.org/10.1155/2014/426710. I was responsible for the data collection and analysis as well as the manuscript composition. H. Uludag and D. Dederich contributed to manuscript edits. T. El-Bialy was the supervisory author and was involved with manuscript composition.

Dedication:

To my family

Acknowledgement:

First and foremost, I would like to thanks my supervisors- Dr. Tarek El-Bialy and Dr. Hasan Uludag for their guidance and support. I also wish my sincere gratitude to my supervisory committee members Dr. Arno Siraki, Dr. Douglas Dederich and Dr. Patrick Flood for their suggestions and directions.

My sincere thanks to the past and present El-Bialy lab members, specially Cezary Kucharski for cell culture, Monika Sharma for teaching me Western blot; Manoj Parmar for his support with qPCR; and Zeba Malik for her help with immunohistochemistry.

I would also like to acknowledge my funding sources- Medical Science Graduate Program Scholarships, MITACS Accelerate and my heartfelt gratitude to Dr. Hasan Uludag for supporting me, and giving me the opportunity to work in his lab.

Table of Contents

List of Tables

List of Figures

Chapter 1

Chapter 2

Chapter 3:

Chapter 4

Chapter 5:

List of Abbreviations:

AP-1: Activator protein-1

ACAN: Aggrecan

ABC: Avidin biotin complex

AAV: Adeno associated virus

ALP: Alkaline phosphatase

ANOVA: Analysis of variance

bFGF: Basic fibroblast growth factor

BSSO: Bilateral sagittal split osteotomy

BMD: Bone mineral density

BMP: Bone morphogenetic protein

BSP: Bone sialoprotein

B.Vol: Bone volume

BV/TV: Bone volume fraction (Bone volume/Tissue volume)

BSA: Bovine serum albumin

CCD: Charge couple device

COL2A1: Collagen type 2 alpha 1

Ct: Cycle of threshold

DNA: Deoxyribonucleic acid

DAB: Diaminobenzidine

DHE: Dihydroethidine

DMSO: Dimethyl sulfoxide

DPI: Diphenylene iodonium

DO: Distraction osteogenesis

DUOX: Dual oxidase

DMEM: Dulbecco's modified eagle medium

DPBS: Dulbecco's phosphate buffered saline

EO: Endochondral ossification

ECL: Enhanced chemiluminiscence

ECM: Extracellular matrix

ELISA: Enzyme-linked immunosorbent assay

ERK: Extracellular signal-regulated kinase

FBS: Fetal bovine serum

FGF: Fibroblast growth factor

FGFR: Fibroblast growth factor receptor

FAD: Flavin adenine dinucleotide

FAK: Focal adhesion kinase

FDA: Food and drug administration

FA: Functional appliance

GAPDH: Glyceraldehydes 3 phosphate dehydrogenase

GFP: Green fluorescent protein

GPCR: G-protein coupled receptor

GAGs: Glycosaminoglycans

GoT: Gonial tangent point

GP: Gonion point

HBSS: Hank's balanced salt solution

HEPES: 4-(2 hydroxyethyl)-1-piperazineethanesulfonic acid

HIF1: Hypoxia inducible factor 1

IRES: Internal ribosome entry site

ICC: Intraclass correlation coefficient

Ihh: Indian hedgehog

IGF-1: Insulin growth factor -1

IL: Interleukin

JNK: c-Jun N-terminal kinase

JIA: Juvenile idiopathic osteoarthritis

LA: Linoleic acid

LIPUS: Low intensity pulsed ultrasound

MCC: Mandibular condylar cartilage

MMP: Matrix metaloproteinase

MAPK: Mitogen- associated protein kinase

Micro-CT: Micro computed tomography

MTT: (3-(4, 5 Dimethylthiazol- 2-yl)-2,5 diphenyltetrazolium bromide

NIH: National Institute of Health

NAC: N-acetyl cysteine

NADPH Nicotinamide adenine dinucleotide phosphate

NOX: NADPH (Nicotinamide adenine dinucleotide phosphate) oxidase

OA: Osteoarthritis

OCN: Osteocalcin

OPN: Osteopontin

PTHrP: Parathyroid hormone related protein

PBS: Phosphate buffered saline

PI3K: Phosphotidylinositol 3 kinase

pDNA: Plasmid deoxyribonucleic acid

PAGE: Polyacrylamide gel electrophoresis

PEI: Polyethyleneimine

PAS: Periodic acid Schiff

PAGE: Polyacrylamide gel electrophoresis

PTK: Protein tyrosine kinase

PTP: Protein tyrosine phosphatase

ROS: Reactive oxygen species

ROI: Region of interest

RNA: Ribonucleic acid

RUNX2: Runt related transcription factor 2

STAT1: Signal transducers and activators of transcription 1

si RNA: Small interfering RNA

SDS: Sodium dodecyl sulfate

SATA: Spatial average and temporal average

SOX9: SRY (Sex determining region Y) –related HMG (high mobility group) box 9

SD: Standard deviation

SPSS: Statistical package for social sciences

SAC: Stretch activated ion channel

SZP: Superficial zone protein

TMD: Temporomandibular disorder

TMJ: Temporomandibular joint

Tb.N: Trabecular number

Tb.Sep: Trabecular separation

Tb.Th: Trabecular thickness

TGF β1: Transforming growth factor beta 1

TCOF1: Treacle ribosome biogenesis factor 1

TNF α: Tumor necrosis factor alpha

VEGF: Vascular endothelial growth factor

VHL: Von Hippel Lindau

Chapter 1: General introduction

1. Background and literature review:

1.1 Temporomandibular joint and mandibular condylar cartilage:

Temporomandibular joint (TMJ) is a ginglymus diarthrodial joint present anterior to external auditory meatus in the mandibular fossa of the temporal bone. It is formed by temporal bone and mandible, and separating these bones is a specialized fibrous tissue called articular disc. It is the only site of articulation between the skull and the lower jaw. Movement of the joint is directed by surrounding muscles and ligaments which along with other orofacial structures perform various functions like mastication, speech, breathing, deglutition and facial expression. The articulating surface of the mandible has a special cartilage called mandibular condylar cartilage (MCC) (1). The growth of this cartilage is closely related to the growth and development of the mandible as well as its growth is critical for the craniofacial complex development. Endochondral ossification (EO) at the deeper surface of the cartilage is an important contributor to mandible growth. EO is an organized program of chondrocyte proliferation, differentiation, and maturation. As EO progresses, the condyle elongates and ramus increases in height.

1.1.1 MCC as a major growth center:

MCC appears during the 12^{th} week of embryonic life adjacent to the developing mandible from alkaline phosphatase positive cells that are periosteal in origin (2). The first sign of endochondral ossification appears by the 14^{th} week and by the middle of

intrauterine life, the cartilage is completely replaced by bone. However, the superior most part of the mandible condyle has been reported to have the cartilage that acts both as a growth center and as an articular cartilage (3) (4). The growth of the mandibular condyle ceases by the age of 12- 14 years but in the actual sense, the growth and remodeling occur throughout life as evidenced by morphological changes in the mandible shape from childhood to adulthood and later in the old age. This is to compensate for the changes in muscular dynamics and continuous wear and tear of the condylar cartilage (5). However, in post-pubertal stage, the mandibular growth occurs at the condylar cartilage and posterior border of the ramus (6).

MCC is designated as a secondary cartilage as the morphogenesis of TMJ occurs late in the prenatal development (around 12^{th} week) in contrast to the primary cartilages that present at the articular ends of the long bones which are developed by the 7^{th} week. Apart from developmental time, there are other features that differentiate MCC from the primary cartilage which are explained further. Primary cartilage is predominantly composed of collagen II and grows by interstitial proliferation while a superficial layer of secondary cartilage constitutes undifferentiated cells called prechondroblasts. This layer is rich in collagen I (7) (8). Prechondroblastic cells of the superficial layer are continuous with the osteogenic layer of the periosteum (9). Also, secondary cartilage is present in relation to the membranous bone that is subjected to mechanical loading by the muscular activity (10). Mechanical stress is an important factor that differentiates the progenitor cells in the superficial layer of MCC to either chondroblasts or

osteoblasts as these cells have shown to express both SOX9 (a transcription factor for chondrocyte differentiation) and RUNX2 (transcription factor for osteoblast differentiation) (11). Increased mechanical loading on MCC has shown to increase cell proliferation and increased collagen II synthesis (12) (13) (14). However, when the cartilage was subjected to a non-functional environment like in the study by Meikle in which TMJ from 7 day old rats were placed in left cerebral hemisphere (15), the proliferative cells in the cartilage differentiated into osteoblasts. Lastly, the most evident difference between primary and secondary cartilage is the presence of more cellular component and lack of intercellular matrix in the secondary cartilage (10).

In brief, MCC is different from epiphyseal cartilage as MCC has the capability to grow in multi-direction while epiphyseal cartilage grows longitudinally. There is an absence of fibrocartilage cap and presence of thin perichondrium layer (16). These factors give MCC a unique characteristic to adapt to the external stimuli throughout life (17). Like epiphyseal cartilage, MCC also grows by the process of endochondral ossification but there is an absence of epiphysis, a secondary ossification center, in MCC. During mandibular development, when hyaline condylar growth cartilage is replaced by bone, the articular cartilage becomes the center for growth (18).

1.1.2. Endochondral ossification at MCC:

MCC growth occurs through endochondral ossification (EO) which is identical to the long bones with a distinct difference in gene expression which leads to a difference

in histological and biochemical composition between these two tissues. EO is an organized process of chondrocyte proliferation, differentiation, and maturation. Here the cartilage matrix formed by chondrocytes is substituted by bone due to ossification by osteoblast in contrast to intramembranous ossification where osteoblast directly lay down the bone matrix with the absence of intermediate cartilage formation (19). In EO, there is a sequential expression of various factors like SRY-box containing gene 9 (SOX9), parathyroid hormone related peptide (PTHrP), Indian hedgehog (Ihh) and Runt-related transcription factor 2 (RUNX2) that causes differentiation of prechondroblasts to chondroblasts to mature chondrocytes and hypertrophic chondrocytes. Hypertrophic chondrocytes undergo apoptosis and are replaced by osteoblast.

Histologically, the condylar cartilage is divided into four layers based on the distribution of collagen I, II and X. Superficial layer adjacent to the joint cavity is the articular or fibrous layer. Superficial zone protein (SZP) is expressed in this layer which acts as a lubricant for the joint activity. There is no cellular differentiation in this zone as this layer mainly function as a protective covering for the underlying layers (20) (21). Next layer is the proliferative or polymorphic zone and is composed of irregular polygonal cells in the upper layer while lower layer has flattened cells with their long axis parallel to the articular layer. Cells in this layer are actively proliferating and express PTHrP and SOX9. These cells have multilineage potential to differentiate either into chondroblasts, osteoblasts or fat progenitor cells depending on the presence of

mechanical load (22). PTHrP is highly expressed in the proliferative layer while its receptors are expressed in the pre-hypertrophic layer. PTHrP enhances and sustains prechondrogenic cell proliferation and prevents the differentiation of these cells to hypertrophic chondrocytes (23). Increased expression of PTHrP inhibits cartilage maturation and delays bone formation (24). SOX9 is an important transcription factor for chondrocyte differentiation and expression of collagen II, collagen IX and XI and aggrecan. Like PTHrP, it regulates chondrocyte proliferation and inhibits their hypertrophy. Studies with SOX9 gene deletion showed a complete absence of cartilage formation due to the inability of mesenchymal cells to differentiate into chondrocytes (25). The lower sublayer of the proliferative zone shows higher expression of SOX9 and collagen II.

The third layer is the chondrocyte cell layer in which there is a change in cellular morphology from flattened to spherical cells. This layer shows increased deposition of collagen, proteoglycans and glycosaminoglycans (GAGs) (2) (26) (27). Ihh is expressed in a pre-hypertrophic layer that regulates PTHrP level by a negative feedback loop. It causes the delay in cartilage mineralization and inhibition of hypertrophic chondrocyte differentiation by increasing PTHrP expression in the proliferative layer. Ihh is considered as a central coordinator of EO. In the fourth layer, which is the hypertrophic cell layer, the chondrocytes increase in volume and become hypertrophic. There is a transition from collagen II to collagen X. With this, the degradation of cartilage begins, a preliminary stage of EO (28). Chondrocyte hypertrophic differentiation is believed to

be regulated by RUNX2. It is also an important transcription factor for osteoblast differentiation (29). Furthermore, RUNX2 positively control Ihh expression by activating its promoter gene and hence regulating PTHrP expression. It is also involved in blood vessel invasion in the degenerating cartilage since RUNX2 deficient mice showed complete absence o vasculature in the cartilage (30).

Other factors involved in EO of MCC are fibroblast growth factor (FGF) and its receptor, bone morphogenetic protein (BMP), hypoxia-inducible factor 1 (HIF1), and vascular endothelial growth factor (VEGF). FGF and its receptor (FGFR3) are believed to accelerate chondrocyte hypertrophy and osteoblast differentiation while negatively regulating chondrocyte proliferation by signal transducer and activator of transcription 1 (STAT1) and mitogen-activate protein kinases (MAPKs) signaling pathway (31) (32). BMP is another factor that leads to cartilage and bone formation by binding to their serine-threonine receptors leading to Smad and MAPKs signaling pathway. Its expression is positively induced by Ihh activation. Along with PTHrP and Ihh, BMP regulates proliferation of chondrocytes while inhibits its maturation. HIF-1 is composed of two subunits HIF-1α and HIF-1β, and it is expressed in relation to hypoxic response. Under normal oxygen tension, HIF-1α level is detected and degraded by von Hippel-Lindau (VHL) protein. In hypoxic condition, HIF-1α binds with HIF-1β and translocate to the nucleus where it activates VEGF expression (33). VEGF is a potent angiogenic factor that helps in blood vessels formation during cartilage degradation. All these factors interact together during EO in MCC. Disturbance in the form of mutation or

deletion of any factor besides mechanical loading severely affects MCC growth and development. There are several anomalies associated with the deficient mandible that might be related to deficiency of the aforementioned growth factors.

1.2 Anomalies associated with deficient lower jaw:

Underdeveloped or complete absence of the mandibular condyle is associated with various craniofacial deformities which could be congenital or acquired. Congenital malformed condyle mainly occurs due to problems associated with first and/ or second branchial arches while acquired condition is caused by trauma, infection of mandibular bone or middle ear or due to rheumatoid arthritis. Underdeveloped mandible results in the lack of symmetrical growth of the lower face.

1.2.1 Hemifacial microsomia (HFM):

This is caused by the underdevelopment of the craniofacial structures that develop from 1st and 2nd branchial arches. It occurs in 1:3000 to 1:5000 live birth and is the second most common congenital anomaly after cleft palate/lip (34). The cause of this condition is unknown. It is believed that damage to stapedial artery causes a hematoma which interferes with branchial arch development. The characteristic features are deficient mandible, distortion of the face, epibulbar dermoid (benign tumor located at the junction between cornea and conjunctiva), and failure of the segmentation of cervical spine. HFM can be present as a mild form affecting only an ear tag with or without malformed ear or as the most severe case affecting the ear, temporal bone with

missing glenoid fossa, malformed TMJ including condylar and coronoid processes (35). Based on mandibular and TMJ malformation and midface and lower face involvement, HFM is classified into Type I, II A, II B and III (34). Mandibular and TMJ malformation range from hypoplastic mandible and attached muscle in Type I to a cone-shaped or missing condyle with hypoplastic muscles in Type II A and B to congenital absence of ramus and muscles (34). Goldenhar syndrome is a variant of HFM. It is also known as an oculoauriculovertebral syndrome characterized by hypoplastic mandible and renal, genitourinary and skeletal abnormalities. Deletion of 5q and trisomy 18 and duplication of 7q are the multiple chromosomal abnormalities involved in the complex (36).

1.2.2 Treacher Collin syndrome:

Also known as Mandibulofacial Dysostosis. This condition is characterized by bilateral abnormality of 1st and 2nd branchial arches. Occurrence rate is 1:25000 to 1:50000 in live births. It is an autosomal dominant inherited disorder with the mutation in gene called treacle ribosome biogenesis factor 1 (TCOF1). This gene encodes for nucleolar phosphoprotein treacle that forms mature ribosomes in neuroepithelium and neural crest cells (37). It is expressed during embryogenesis in the 1st and 2nd branchial arches. Mutation of TCOF1 gene leads to the disturbed proliferation of neural crest cells and hence deficient migration of the cells to the branchial arches (38). Involved patients are reported to have characteristic features include a convex face, hypoplasia of zygoma, maxilla and mandible, TMJ and the muscles of mastication, hearing loss due to

hypoplasia of external auditory meatus, eyes are dropping laterally of palpebral fissure (37) (38).

1.2.3 Pierre Robin Syndrome (PRS):

This condition is characterized by cleft palate, mandibular micrognathia and airway obstruction due to posterior displacement of the tongue. It may occur as an isolated case or in association with a variety of syndromes. The prevalence rate is 1/2000 to 1/8500 in live births. SOX9 deficiency has been associated with PRS due to translocation of chromosome 2 and 17 (39).

1.2.4 Nager Syndrome:

Also called Nager acrofacial dysostosis. It is a rare condition with only 35 cases presented in the literature. This condition is caused by either sporadic occurrence or due to autosomal dominant trait as well as an autosomal recessive inheritance (40) (41). Characteristic features include spine and mandibular malformation ranging from missing joint structure to limited jaw movement; ear abnormalities with hearing loss and absence of soft palate (42).

1.2.5 Other related syndromes:

Other related syndromes associated with deficient lower jaw are Turner syndrome, Parry-Romberg syndrome. In Turner syndrome, there is a short mandibular body with posterior rotation of mandible condyle. Parry-Romberg or hemifacial atrophy causes

facial asymmetry affecting mandibular condyle. Patients with oculomandibuodyscephaly or Hallermann-Streiff syndrome present with birdlike appearance due to craniofacial disproportion, bilateral congenital cataract and bilateral microphthalmia (36) (43). Secondary condylar hypoplasia or acquired hypoplasia is caused by local factors like trauma, infection of the middle ear, mandible condyle or by systemic factors like rheumatoid arthritis (44) during active growth phase which affects either one or both sides of TMJ. Juvenile idiopathic arthritis (JIA) is a chronic inflammation condition present in 1-2/1000 children (45). The condition is characterized by an articular surface covered by tumor-like granulation tissue called pannus and increased blood vessel proliferation. This results in the destruction of the joint and the cartilage (46). Destruction of MCC in JIA causes posterior mandibular rotation, reduced ramal height and mandibular length (47) (48). Another acquired condition frequently associated with hypoplasia is mandibular trauma to the condylar region during childhood which leads to the retrognathic mandible, temporomandibular disorders, anterior open bite, and in severe cases trauma leads to ankylosis.

1.2.6 Class II Malocclusion:

Malocclusion is defined as the occlusion in which there is mal-relationship between the upper and lower arches in any of the three planes of spaces or in which there are anomalies in tooth position beyond normal limit. Class I malocclusion normally is established when the upper and lower arches are in normal relation but there might be some problems like spacing and crowding etc. Class II malocclusion is when

the lower jaw is more backward position compared to the upper jaw. This could be either due to underdeveloped mandible or oversized maxilla. In Class III malocclusion, the upper jaw is posteriorly positioned in relation to the lower jaw. 80% of the cases with Class II malocclusion have underdeveloped mandible (49). It is present in about one-third of the world's adult population and is considered to be the most common in patients attending the orthodontic clinics (50). In a study conducted on Canadian children of 6 and 9 yr, 11.2% of 6 yr old and 17.5% of 9 year old had an increased overjet (horizontal overlap/distance between the top and bottom front teeth when all teeth are biting together) of more than 5mm (normal overjet is 2-3 mm) (51). Micrognathia of the mandible can be present as an isolated condition or in association with over 450 syndromic conditions. Class II malocclusion is more prevalent in Caucasian compared to the black population. There are many factors related to the development of malocclusion. Habits like thumb or finger sucking or tongue thrusting are some of the examples that lead to the development of Class II malocclusion. In another study, 55% of children in mixed dentition had Class II malocclusion due to sucking habits (52).

Lower jaw deficiency not only affects the functional occlusion and aesthetic appearance of the affected patients but may also can lead to upper airway obstruction and sleep apnea (53)(54). Deficient mandible leads to posterior displacement of the tongue causing chronic hypoxia and fatigue leading to behavioral issues, neurological and cognitive delay and cardiopulmonary complications like bradycardia in the

developing child (55). Patient with deficient lower jaw may suffer from dental problems (like decayed or missing teeth), poor oral health, bruxism, teeth crowding, higher incidences of dental trauma due to the relatively protruded upper anterior teeth, mastication difficulties and digestion disturbance (56). Bruxism leads to muscle pain and fatigue, tooth attrition which in turn leads to hypersensitive dentition (57). Imbalance of muscle activity also causes pain in the head, neck and ear region with the formation of trigger points (58). There is a large impact of lower jaw deficiency on both the individual and the society in terms of discomfort, quality of life as well as social and functional limitations like speech, mastication and swallowing (59).

1.3 Treatments available for correction of the deficient lower jaw:

The treatment of the affected cases depends on the age of the patient, severity of the problem, expected success rate and impact on the facial profile (60). Preadolescents growing patients with moderate jaw discrepancy due to mandibular deficiency are frequently treated with appliances designed to induce mandibular forward positioning. For adolescent and young adults, the treatment is more likely to be either repositioning the teeth by orthodontic treatment and/or surgical correction (61).

1.3.1 Surgical treatment:

Surgical treatments of mandibular deficient mandibles in adults include advancement using bilateral sagittal split osteotomy (BSSO) and/or distraction osteogenesis (DO). Other than being costly, these surgical methods have other several

limitations and complications (62) (63). DO has proven to be a major advance for the treatment of numerous congenital and acquired craniofacial deformities. DO is a steady procedure of increasing the length of bone after surgical cut of the short bone then separating the cut bones after initial healing of the cut bones with the help of a distraction device. It was first performed by Codvilla in 1905 and later re-introduced by Ilizarov in 1940 for long bone lengthening. Recovery time has three phases- latency, distraction, and consolidation. There are a number of factors that affect the outcome of surgical treatment. Masticatory muscles have great influence on the surgical outcome as they affect the shape, size, and orientation of mandible. Also, suprahyoid muscles can cause relapse after surgery if they are stretched more than 15% of their original length. Failure to position the condyle in the glenoid fossa after surgery, severely cause relapse after removal of inter-maxillary fixation (64). Both BSSO and DO showed similar relapse rate for the mandibular advancement between 6 - 10mm. There are higher incidences of neurosensory disturbances and condylar resorption in the case of BSSO. Complications include problems with distraction device, occlusal disturbance due to the device, patient's compliance problem and chronic infection, damage to the inferior alveolar nerve, TMJ dysfunction and condylar resorption (63).

1.3.2 Functional appliances (FAs):

Also known as forward bite jumping appliances or orthopedic appliances, are devices that are believed to alter the patient's functional environment by producing biomechanical forces in an attempt to influence and, ideally, permanently change the

contiguous hard tissue inter-relationship (65). The principal goal of the early treatment using FAs is to correct the existing muscular, skeletal and dental imbalances.

The theoretical basis of functional appliance treatment is the principle has been described as ‘a new pattern of function’ dictated by the appliance leads to the development of a corresponding ‘new morphological pattern’ (65) (66). Bone is one of the hardest tissues in the human body but it is one of the most responsive to the external stimuli (66). The theory of bone plasticity was given by Wolff who believed that the form and function of bone are related intimately. When the bone is subjected to the functional stress, there is a change in the internal bone architecture and external shape. When the functional appliance is placed in the mouth, it leads to increased contractile activity of the lateral pterygoid muscle. This leads to increase in the production of growth factors. Moreover, the forward position of the lower jaw produces a change in the trabecular orientation of the condyle, growth of the condylar cartilage and ossification of the posterior border of the mandible. All these changes are believed to lead to lengthening of the mandible (65). Mechanical loading initiates specific biomechanical responses in the chondrocytes (12,13). This distinctive characteristic is the fundamental rationale for therapies with different types of functional appliance.

Treatment with functional appliance can produce satisfactory improvement of the facial esthetics and minimizes the need for surgical intervention. Treatment with functional appliance is more economical compared to surgery and fixed orthodontic appliances. It reduces the treatment time with fixed orthodontic braces and decreases

adverse fixed appliance problems like gingival hyperplasia, extraction, caries and periodontal problems (69). The appliances help to reduce or eliminate dysfunctional habits and treatment of temporomandibular disorders associated with retruded mandible (70). However, the effectiveness of these appliances in modifying mandibular growth is still debatable especially with regards to treatment duration and long term effectiveness on the lower jaw growth. Several studies have reported positive response (71) (72) (73) while some researchers consider that this response is due to the actual growth (74) (75). Clinical trials have demonstrated that either no growth enhancement or the increased growth occurs only at the preliminary stage and the mandible returning to its original position afterward (14,15).

Hence there is a need to new treatment modalities to correct the deficient mandible. Treatment with gene delivery and Low intensity pulsed ultrasound are new emerging methods that may be used to treat cases with deficient mandibles.

1.4 Novel approaches for the treatment of deficient lower jaw:

1.4.1 Gene therapy

It is a fast developing technology in which small DNA or RNA is delivered into the targeted cells. This therapy offers sustained and regulated the local production of one or more morphogens in situ (78) and represent a significant advantage over protein delivery based system. It has become a primary focus for bone and joint disorder in the field of regenerative medicine and tissue engineering. More than 85% of the world population need replacement of craniofacial structure in the form tooth decay treatment

and/or bone regeneration after periodontal surgeries (79). Direct delivery of protein can suffer from protein instability and inadequate post-translational modifications of recombinant proteins which may limit their bioactivity (80). A possible successful treatment outcome depends on several factors including scaffold (carrier), growth factor and the vector. A plasmid containing genetic information is delivered to the cell enters the nucleus and start the protein expression. However, the gene delivery and its retention in the cell are two limiting factors for the success (81). A vector is used to transfer genes into the host cells which could either be a virus or a non-virus vector. Viral vectors prove efficient gene delivery carriers and are widely used to deliver genes to the targeted tissue and for gene expression over a long period of time because of their natural ability to translocate their own genetic material efficiently. However, there are safety concerns associated with viral vectors like immunogenicity and oncogenicity (82). For these reasons, non-viral vectors are preferred gene delivery approaches. Non-viral gene delivery involves a transfer of genetic material either by direct injection of the plasmid or by physical or chemical methods. Direct delivery is the most simple and convenient method. Electroporation (using electric current) and sonoporation (using ultrasound) are two examples of physical methods that have been used in gene delivery.

Bone morphogenetic proteins (BMPs) are the most commonly used and clinically approved growth factors that possess osteoinductive properties which make them attractive growth factor for the use of gene therapy. Several studies in the literature both in-vitro and in-vivo showed a positive effect of BMP for inducing osteogenic differentiation of mesenchymal stem cells and ectopic de novo bone formation and

healing of critical-sized bone defects (83). In the craniofacial region, most studies conducted have used recombinant Adeno associated virus (rAAV) as a vector for the delivery of the gene of interest. Studies in rodent models using BMP7 have successfully enhanced healing of bone defect (81). Other growth factors- insulin growth factor-1 (IGF-1), FGF, and VEGF and Wnt are under investigation for bone regeneration and cartilage repair. Gugale et al study (84) showed new bone formation after 14 days of implantation of collagen seeded with the AVV-BMP2 gene. Application of gene therapy for spine fusion, bone rehabilitation after avascular necrosis, repair of alveolar, mandibular and periodontal defect has already shown positive results (85).

Injury to articular cartilage, avascular tissue, leads to osteoarthritis. Several studies in the literature have shown positive results with BMP-2, Ihh, transforming growth factor-β1 (TGF- β1) and IGF-1 (86) (87) (88). Till date, only one study has been conducted using rAAV and VEGF for TMJ repair (89). Basic Fibroblast Growth Factor (bFGF) is another important growth factor that is involved in the development and skeletal morphogenesis. It has been shown its profound effect on the craniofacial bone formation. Blocking of bFGF by antibody showed prevention of cranial suture osteogenesis.

1.4.2 Low Intensity Pulsed Ultrasound (LIPUS):

In the field of medicine, ultrasound is classified according to its waveform to continuous and pulsed (Fig 1.1); or on the basis of its application to diagnostic, operative and therapeutic (94).

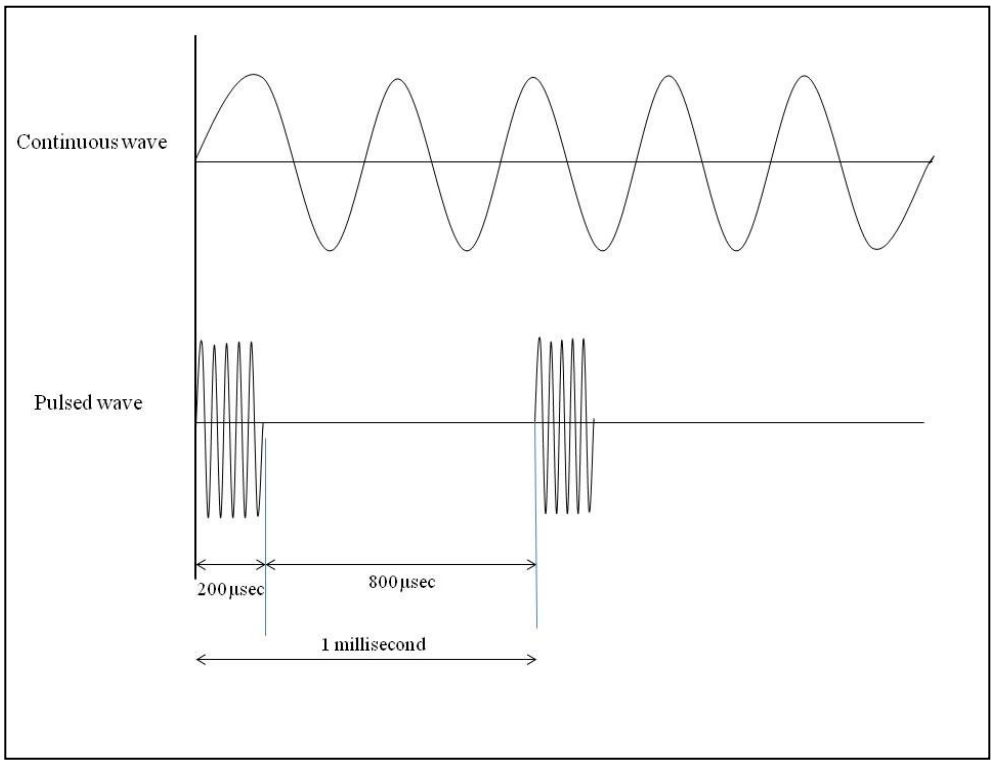

Fig 1.1: Ultrasound waveform: Continuous and Pulsed.

In recent years, some noninvasive approaches to augment the lower jaw growth have been proposed by various research groups (89) (90) (91) (92) (93). One of these methods is the application of Low Intensity Pulsed Ultrasound (LIPUS) on the condylar region, especially when it is accompanied by the use of a functional appliance. It is a safe, easy to use and cost effective method. Its application for non-healing fractured bone have been approved by Food and Drug Administration (FDA) (94) (95). It has been used to enhance bone growth, healing, and reduces treatment time after distraction osteogenesis (96). LIPUS also stimulates new blood vessel formation and hence enhances endochondral bone formation (97) (98). In-vitro studies have shown to

increase cell count in fibroblast, and osteoblast cell culture (99) (100) with increased transforming growth factor β1 (TGF-β1) expression and decreased IL-6 and tumor necrosis factor-α (TNF-α) (101); increased RUNX2, ALP, VEGF, OCN and BMP-2 expression (102) (103) (104) (105). Similar results were seen in bone marrow derived stem cells and animal studies. Increased aggrecan and collagen II expression have been supported in several studies (106) (107) (108) (109) (110).

The exact mechanism of LIPUS is still not completely understood. LIPUS produces a non-thermal effect which causes cavitation, micro streaming and affects the cell membrane. Cavitation is the growth and oscillation of gaseous cavities which grows rapidly and collapse leading to change in the cell membrane. These changes increase the cell membrane permeability and hence increase the cellular uptake of the extracellular ions, growth factors and drugs (111). But when the bubble grows in size so that when it collapses, it results in permanent membrane damage and cell death, this is known as unstable cavitation (112). Acoustic streaming is the circular movement of the fluid around the vibrating structures like the cell membranes or the oscillating gas bubbles. These movements produce stress on the structures leading to the formation of pores for a short period of time. The increase in the membrane permeability and movement of fluid around it causes the delivery of the therapeutic agents into the cell (113). However, the intensity of LIPUS is too low to induce cavitation or the cell membrane destruction (114). The mechanical energy of LIPUS when applied to biological tissues or cells induces strain on the cell membrane affecting the mechanosensitive elements (115). In

'bilayer sonophore model' proposed by Krasovitski et al (116), it explains the changes in cell membranes bilayer with ultrasound application. In positive pressure, the cell membrane layers are pushed together while in negative pressure, the membranes are pulled apart. These movements also cause the activation of mechanosensitive elements. The process by which cell sense the mechanical load and transducer it to the cascade of cellular and molecular events is called mechanotransduction. Mechanosensitive elements, including cytoskeleton, stretch-activated ion channels, integrins, G-protein receptors, have been extensively explained in the literature.

1.4.2.1 Mechanotransduction and LIPUS:

Microfilaments, microtubules and intermediate filaments like actin, talin, vinculin and filamin A are the structural units of the cytoskeleton that maintain the cellular shape during the application of mechanical load. The cytoskeleton components provide a direct link between the adhesion receptors and the nucleus. Integrins and cadherins are coupled with cytoskeleton filament on one end and nuclear scaffold, nucleoli, chromatin or DNA in the nucleus on the other end (117). When the mechanical load is applied, cytoskeleton filaments bear the impact and reorganize themselves and activate the biochemical events that influences cell survival, protein synthesis in addition to spreading and migration (118). Many studies have shown activation of signal transduction and gene expression with alteration in cytoskeleton structure (119) (120) (121). Previous studies have shown increased polymerization of actin filament and activation of integrin with ultrasound application (122) (123) (124).

Stretch-activated ion channels (SAC) play an important role not only in maintaining the resting membrane potential but also in cell volume. Upon activation, these channels allow movement of ions like Na^+, Ca^{2+}, K^+ in or out of the cells. Na^+ ion first enters the cells causing depolarization of the membrane which is followed by Ca^{2+} entry (125). Ca^{2+} ion concentration in the cell also increases due to the release of ions from intracellular reservoirs: endoplasmic reticulum, sarcoplasmic reticulum, and mitochondria. Increased Ca^{2+} ions after mechanical stimulation are seen in different cell types including smooth muscle cells, fibroblasts, osteoblasts and chondrocytes. SAC after mechanical loading causes phosphorylation of focal adhesion kinase (FAK) and paxillin (126), aggrecan gene expression and cell proliferation (127) (128). LIPUS has also shown increased Ca^{2+} ion concentration causing proteoglycan synthesis in chondrocytes and this effect was abolished by inhibiting Ca^{2+} ions (107).

Integrins are transmembrane glycoprotein receptors composed of two subunits- α and β. Their primary function is the attachment of the cell to its extracellular matrix (ECM). The combination of α and β subunits are specific for the cell type and determine the ligand specificity. α5β1 is a fibronectin specific integrin present in chondrocytes. Integrin signaling across the cell membrane can be 'inside out' where the binding of integrin to its ECM components is regulated by the inside of the cell, or it can be 'outside in' i.e. integrin binding to ECM component leads to biochemical events in the cell (129). The structure of integrin has three domains – extracellular domain, membrane-spanning region, and a cytoplasmic tail. At resting stage, the extracellular

domain has ‘bent’ conformation. When the mechanical load is applied, this changes to ‘upright’ structure exposing the binding sites to ECM (130). The cytoplasmic tail end activates FAK and further recruit talin and paxillin which are cytoplasmic proteins. These proteins are triggered to form large multi protein complex called focal adhesion molecule during integrin activation. This further leads to activation and organization of either cytoskeleton component of the cell (131) (132). Studies have shown that mechanical stresses produced by LIPUS have lead to increase in gene expression and protein synthesis in chondrocytes and osteoblasts via integrin activation (133) (134) (135). Many studies in the literature have shown that ultrasound exposure augments membrane expression of integrins (133) (136) and hence results in reorganization of cytoskeleton and maturation of osteoblasts (137) and chondrogenic differentiation of human mesenchymal stem cell (138). Mechanical loading by LIPUS has shown to increase phosphorylation of focal adhesion molecule like FAK and Src which are downstream regulators of MAPK signaling pathway (139) (140) (141).

Mitogen Activated Protein Kinases (MAPKs) are serine-threonine protein kinases that are extensively studied in many cell types, especially in osteoblast and chondrocyte. These protein kinases respond to the external stimuli and regulate the cellular events by affecting the gene and protein expression in various cellular processes like cell growth, differentiation, survival and cell death. These include extracellular signal-regulated kinase1/2 (ERK1/2), c-Jun N-terminal kinase (JNK) and p38 kinase. ERK1/2 is preferentially activated in response to growth factors while JNK and p38 kinase are

more responsive to stress stimuli. In osteoblast, MAPKs regulate bone mass by acting as a mediator in osteoblast differentiation. There is an increase in activator protein-1 (AP-1), a transcription factor for osteoblast differentiation, with MAPK activation (142). In chondrocytes, JNK plays a minor role while ERK1/2 and p38 are important for chondrogenesis (143). Activated MAPK further phosphorylates various intracellular factors involved in cellular metabolism including membrane transporters, cytoskeletal elements and transcription factors (144).

Studies on LIPUS have shown increased phosphorylation of ERK1/2 and p38 in osteoblasts and chondrocytes (145) (146) (147) (148) (149) (141). Activation of MAPK employs core 3 kinases cascade consisting of MAP3K which phosphorylates and activates MAP2K which then phosphorylates and increases the activity of MAPK. De-phosphorylation of MAPK by phosphatase is an important negative control. MAPK are believed to be redox regulated i.e. phosphorylation and dephosphorylation of MAPKs is under the control of reactive oxygen species (ROS).

1.5 Reactive oxygen species (ROS) and signal transduction:

ROS including superoxide ($O_2\bullet^-$), hydroxyl radical (•OH) and hydrogen peroxide (H_2O_2) are small molecules generated due to incomplete one-electron reduction of oxygen. Production of $O_2\bullet^-$ generally starts the cascade of ROS generation. Two-electron reduction of $O_2\bullet^-$ forms H_2O_2 in the presence of superoxide dismutase. In the presence of catalase and glutathione peroxidase, H_2O_2 is reduced to water. However, in the presence of iron, O_2^- and H_2O_2 interact to •OH which is highly reactive free radical

(150) (151). ROS are mainly generated as by-products of the reactions taking place in mitochondria, peroxisome and cytochrome P450 (152). However, due to a high level of mitochondrial enzymes like superoxide dismutase, superoxide generated is readily reduced to H_2O_2. Nicotinamide adenine dinucleotide phosphate (NADPH) oxidases (NOX) are considered the main source where ROS are generated as the main product.

NOX family enzymes are transmembrane protein complex that reduces O_2 to $O_2\bullet^-$. There are seven types of NOX enzymes present in the animal cell – NOX1-5 and two larger dual oxidases (DUOX) 1 and 2. The complex has one NADPH binding site at COOH terminus, flavin adenine dinucleotide (FAD) binding site, six transmembrane domains and four heme binding histidines and an additional NH2 domain in DUOX enzymes (153). NOX2 or $gp91^{phox}$ is the prototype NOX which requires the assembly of other components for its activation. $p22^{phox}$ is another membrane bound subunit that stabilizes NOX and two cytosolic subunits – $p47^{phox}$ and $p67^{phox}$. Small GTPase protein Rac1 and $p40^{phox}$ act as modulator proteins that help in assembly of $p47^{phox}$ and $p67^{phox}$.

During the past decade, reduction- oxidation (redox) reactions that generate ROS have been identified as an important chemical mediator in the regulation of signal transduction processes involved in cell growth and differentiation. These radicals play the dual role in a living organism as both deleterious and beneficial effects that are depending upon the amount produced and the availability of the cellular antioxidants. In low amount, they are involved in normal physiological functions like signal

transduction, platelet aggregation, immune system control and regulation of cellular growth and synthesis of biological compounds (154)(155). ROS ideally fulfill the prerequisites for intracellular signaling molecule since they are rapidly generated, highly diffusible, easily degraded and ubiquitously present in all cell types (152). A study by Morita et al (156) showed that free radicals are involved in hypertrophy of chondrocytes in endochondral ossification and when the cells were treated with N-acetylcysteine (free radical scavenger) hypertrophy was inhibited.

1.5.1 ROS as a second messenger:

The signal transduction pathways are regulated by ROS not through activation of protein tyrosine kinase (PTK) but by deactivation of protein tyrosine phosphatase (PTP). These enzymes contain Cysteine residue in their active sites (157) which are highly susceptible to oxidation by ROS and undergo diverse oxidation modification (158). ROS causes oxidative modification by forming disulfide bonds (-S-S-), sulfenyl (-SOH), sulfinyl ($-SO_2H$) and sulfonyl moiety ($-SO_3H$). By oxidative modification, ROS decreases the phosphatase activity which in turn enhances PTK activity. This leads to increased phosphorylation of MAPK signaling pathway. Studies have shown increased activation of p38 MAPK with H_2O_2 in rat alveolar macrophages, NIH3T3, HEK 293 cells, human fibroblasts cells while ERK1/2 was activated in bovine coronary artery and rat mesangial cells (159) (160).

1.6 Rationale:

LIPUS is a non-invasive treatment modality that has been approved by FDA for the treatment of non-healing bone fractures. In the previous studies, LIPUS has shown the stimulatory effect on the mandibular condylar growth. In rabbits, daily 20 min LIPUS application showed increased mandibular growth after four weeks (161); in baboon monkeys, it took four months (162) and one year in human patients (163). With 40 min LIPUS application Schumann et al (138) and Chan et al (164) showed increased enhanced chondrogenesis and rapid bone healing in distraction osteogenesis. Further, the mechanism of LIPUS in chondrocyte and osteoblast are not completely understood. ROS generation has only been studied in leukemia cell line with ultrasound application with higher intensity (> 0.1 W/cm2 – 0.5 W/cm2). Finally, there were no studies on the effect of LIPUS and non-viral gene delivery on the mandibular condylar growth.

1.6.1 Research Hypotheses and Objectives:

***Hypothesis # 1*:** Stimulatory effect of LIPUS on the mandibular condylar growth in young growing rats either alone or when combined with functional appliance treatment is dose-dependent.

Objective #1: To determine the possible effect of increasing LIPUS daily dose (from 20 min to 40 min) and functional appliance on the mandible condyle in young growing rats.

***Hypothesis #2*:** LIPUS application leads to free radical generation that causes phosphorylation of MAPKs and leads to increased gene and protein expression in chondrocyte and osteoblasts.

Objective #2: To understand possible effect of LIPUS on chondrocytes and osteoblasts:

a. By determining free radical production after LIPUS application.
b. Evaluate the effect of LIPUS on chondrocytes and osteoblasts *in-vitro* on the gene and protein expression of ERK 1 /2, p38 and JNK by qPCR, Western Blot.

Hypothesis #3: Basic FGF plasmid (gene), when combined with LIPUS will enhance the mandibular condylar growth more than each modality alone.

Objective #3: To study the effect of basic Fibroblast Growth Factor (bFGF) pDNA delivery on mandibular condyle and to explore the possible effect of local injection of bFGF plasmid and daily low intensity pulsed ultrasound (LIPUS) application on mandibular condylar growth.

1.7 Scope of the thesis:

This study was framed to test all the hypotheses and address all objectives in four chapters with two additional chapters for the introduction and literature review and a final chapter for general discussion and conclusion. In Chapter 2, LIPUS application on the mandibular condylar growth was studied. Two time-points i.e. 20 min or 40 min LIPUS application per day were compared either alone or in combination with the use of functional appliance. This chapter presented morphometric, histology, immunohistochemistry and Micro-CT analyses outcome of the animal study. These results were crucial since it will provide data about the optimized LIPUS duration with or without FAs to be used for the future studies. This chapter tested our first hypothesis.

Chapter 3 and 4 addressed the in-vitro part of this study where we presented the effect of LIPUS application on chondrocytes and pre-osteoblast cell lines respectively. The cells were exposed to either 10 min or 20 min single LIPUS application. Single LIPUS application effect was studied for ROS generation, cell viability, gene expressions for transcription factor and ECM synthesis; and protein expression for MAPK signaling in the presence or absence of ROS inhibitor. These chapters tested the second hypothesis of this thesis.

Chapter 5 is focused on exploring the possible effect of non-viral gene delivery and LIPUS application on the mandibular condylar growth. There is only one study in the literature that investigated condylar growth by viral gene delivery. In this pilot study, we attempted to deliver polyethyleneimine (PEI) - bFGF plasmid in the animal

model and studied its effect either alone or in combination with LIPUS on the mandibular condylar growth using histology and Micro-CT analyses. This chapter tested our third hypothesis. Finally, we discussed the outcomes of all the performed studies, their inter-relationships, limitations with future directions for the studies to improve the clinical outcomes of LIPUS for cartilage and bone regeneration.

1.8 References:

1. Shaffer SM, Brismée J-M, Sizer PS, Courtney CA. Temporomandibular disorders. Part 1: anatomy and examination/diagnosis. J Man Manip Ther. 2014 Feb;22(1):2–12.

2. Shibata S, Suda N, Suzuki S, Fukuoka H, Yamashita Y. An in situ hybridization study of Runx2, Osterix, and Sox9 at the onset of condylar cartilage formation in fetal mouse mandible. J Anat. 2006 Feb;208(2):169–77.

3. Symons NBB. Studies on the growth and form of the mandible. Dent Rec (London). 1951 Mar;71(3):41–53.

4. Copray JC, Jansen HW, Duterloo HS. Growth and growth pressure of mandibular condylar and some primary cartilages of the rat in vitro. Am J Orthod Dentofacial Orthop. 1986 Jul;90(1):19–28.

5. Ogston A. The Growth and Maintenance of the Articular Ends of Adult Bones. J Anat Physiol. 1878 Jul;12(Pt 4):503–17.

6. Sperber GH, Sperber SM, Guttmann GD. Craniofacial Embryogenetics and Development. PMPH-USA; 2010. 264 p.

7. Mizoguchi I, Nakamura M, Takahashi I, Kagayama M, Mitani H. An immunohistochemical study of localization of type I and type II collagens in mandibular condylar cartilage compared with tibial growth plate. Histochemistry. 1990 Apr 1;93(6):593–9.

8. Livne E, Oliver C, Silbermann M. Further characterization of the chondroprogenitor zone in mandibular condyles of suckling mice. An ultrastructural and cytochemical study. Acta Anat (Basel). 1987;129(3):231–7.

9. Hinton RJ. Genes that regulate morphogenesis and growth of the temporomandibular joint: a review. Dev Dyn. 2014 Jul;243(7):864–74.

10. Symons NBB. A histochemical study of the secondary cartilage of the mandibular condyle in the rat. Archives of Oral Biology. 1965 Jul;10(4):579–IN3.

11. Glineburg RW, Laskin DM, Blaustein DI. The effects of immobilization on the primate temporomandibular joint: a histologic and histochemical study. J Oral Maxillofac Surg. 1982 Jan;40(1):3–8.

12. Nakao Y, Konno-Nagasaka M, Toriya N, Arakawa T, Kashio H, Takuma T, et al. Proteoglycan Expression Is Influenced by Mechanical Load in TMJ Discs. J DENT RES. 2014 Oct 27;22034514553816.

13. Yamashiro T, Takano-Yamamoto T. Differential responses of mandibular condyle and femur to oestrogen deficiency in young rats. Arch Oral Biol. 1998 Mar;43(3):191–5.

14. Ghafari J, Degroote C. Condylar cartilage response to continuous mandibular displacement in the rat. Angle Orthod. 1986 Jan;56(1):49–57.

15. Meikle MC. In vivo transplantation of the mandibular joint of the rat; an autoradiographic investigation into cellular changes at the condyle. Arch Oral Biol. 1973 Aug;18(8):1011–20.

16. Voudouris JC, Kuftinec MM. Improved clinical use of Twin-block and Herbst as a result of radiating viscoelastic tissue forces on the condyle and fossa in treatment and long-term retention: growth relativity. Am J Orthod Dentofacial Orthop. 2000 Mar;117(3):247–66.

17. Rabie ABM, Hägg U. Factors regulating mandibular condylar growth. Am J Orthod Dentofacial Orthop. 2002 Oct;122(4):401–9.

18. Moffett B. The morphogenesis of the temporomandibular joint. American Journal of Orthodontics. 1966 Jun 1;52(6):401–15.

19. Li QF, Rabie ABM. A new approach to control condylar growth by regulating angiogenesis. Arch Oral Biol. 2007 Nov;52(11):1009–17.

20. Luder HU, Leblond CP, von der Mark K. Cellular stages in cartilage formation as revealed by morphometry, radioautography and type II collagen immunostaining of the mandibular condyle from weanling rats. Am J Anat. 1988 Jul;182(3):197–214.

21. Ohno S, Schmid T, Tanne Y, Kamiya T, Honda K, Ohno-Nakahara M, et al. Expression of superficial zone protein in mandibular condyle cartilage. Osteoarthr Cartil. 2006 Aug;14(8):807–13.

22. Mizoguchi I, Toriya N, Nakao Y. Growth of the mandible and biological characteristics of the mandibular condylar cartilage. Japanese Dental Science Review. 2013 Nov;49(4):139–50.

23. Shibukawa Y, Young B, Wu C, Yamada S, Long F, Pacifici M, et al. Temporomandibular joint formation and condyle growth require Indian hedgehog signaling. Dev Dyn. 2007 Feb;236(2):426–34.

24. Provot S, Schipani E. Molecular mechanisms of endochondral bone development. Biochemical and Biophysical Research Communications. 2005 Mar 18;328(3):658–65.

25. Lefebvre V, Smits P. Transcriptional control of chondrocyte fate and differentiation. Birth Defects Res C Embryo Today. 2005 Sep;75(3):200–12.

26. Shibata S, Suda N, Yoda S, Fukuoka H, Ohyama K, Yamashita Y, et al. Runx2-deficient mice lack mandibular condylar cartilage and have deformed Meckel's cartilage. Anat Embryol. 2004 Jul;208(4):273–80.

27. Fukada K, Shibata S, Suzuki S, Ohya K, Kuroda T. In situ hybridisation study of type I, II, X collagens and aggrecan mRNas in the developing condylar cartilage of fetal mouse mandible. J Anat. 1999 Oct;195 (Pt 3):321–9.

28. Shen G, Rabie AB, Zhao Z-H, Kaluarachchi K. Forward deviation of the mandibular condyle enhances endochondral ossification of condylar cartilage indicated by increased expression of type X collagen. Arch Oral Biol. 2006 Apr;51(4):315–24.

29. Park JH, Park BH, Kim HK, Park TS, Baek HS. Hypoxia decreases Runx2/Cbfa1 expression in human osteoblast-like cells. Molecular and Cellular Endocrinology. 2002 Jun 28;192(1–2):197–203.

30. Hartmann C, Tabin CJ. Dual roles of Wnt signaling during chondrogenesis in the chicken limb. Development. 2000 Jul;127(14):3141–59.

31. Sahni M, Ambrosetti DC, Mansukhani A, Gertner R, Levy D, Basilico C. FGF signaling inhibits chondrocyte proliferation and regulates bone development through the STAT-1 pathway. Genes Dev. 1999 Jun 1;13(11):1361–6.

32. Ornitz DM. FGF signaling in the developing endochondral skeleton. Cytokine Growth Factor Rev. 2005 Apr;16(2):205–13.

33. Yang Z, Jiao H, Chao W, Yan Z, Changhong H, Li G, et al. Application of HIF-1α by gene therapy enhances angiogenesis and osteogenesis in alveolar bone defect regeneration. J Gene Med. 2016 Feb 29;

34. Wink JD, Goldstein JA, Paliga JT, Taylor JA, Bartlett SP. The mandibular deformity in hemifacial microsomia: a reassessment of the Pruzansky and Kaban classification. Plast Reconstr Surg. 2014 Feb;133(2):174e–81e.

35. Vargervik K. Mandibular malformations: growth characteristics and management in hemifacial microsomia and Nager syndrome. Acta Odontol Scand. 1998 Dec;56(6):331–8.

36. Kaneyama K, Segami N, Hatta T. Congenital deformities and developmental abnormalities of the mandibular condyle in the temporomandibular joint. Congenit Anom (Kyoto). 2008 Sep;48(3):118–25.

37. Gonzales B, Henning D, So RB, Dixon J, Dixon MJ, Valdez BC. The Treacher Collins syndrome (TCOF1) gene product is involved in pre-rRNA methylation. Hum Mol Genet. 2005 Jul 15;14(14):2035–43.

38. Dixon J, Jones NC, Sandell LL, Jayasinghe SM, Crane J, Rey J-P, et al. Tcof1/Treacle is required for neural crest cell formation and proliferation deficiencies that cause craniofacial abnormalities. Proc Natl Acad Sci USA. 2006 Sep 5;103(36):13403–8.

39. Jakobsen LP, Ullmann R, Christensen SB, Jensen KE, Mølsted K, Henriksen KF, et al. Pierre Robin sequence may be caused by dysregulation of SOX9 and KCNJ2. J Med Genet. 2007 Jun;44(6):381–6.

40. Battaglia A, Magit A. Nager acrofacial dysostosis with autosomal dominant inheritance: implications for the otolaryngologist. Otolaryngol Head Neck Surg. 2000 Sep;123(3):276–7.

41. Verrotti C, Benassi G, Piantelli G, Magnani C, Giordano G, Gramellini D. Acrofacial dysostosis syndromes: a relevant prenatal dilemma. A case report and brief literature review. J Matern Fetal Neonatal Med. 2007 Jun;20(6):487–90.

42. Friedman RA, Wood E, Pransky SM, Seid AB, Kearns DB. Nager acrofacial dysostosis: management of a difficult airway. Int J Pediatr Otorhinolaryngol. 1996 Mar;35(1):69–72.

43. Pirttiniemi P, Peltomäki T, Müller L, Luder HU. Abnormal mandibular growth and the condylar cartilage. Eur J Orthod. 2009 Feb;31(1):1–11.

44. Tank W, Wright D, Iizuka T. Unilateral dysplasia of the mandibular condyle: report of a case. J Oral Maxillofac Surg. 1998 Jun;56(6):765–9.

45. Saurenmann RK, Rose JB, Tyrrell P, Feldman BM, Laxer RM, Schneider R, et al. Epidemiology of juvenile idiopathic arthritis in a multiethnic cohort: ethnicity as a risk factor. Arthritis Rheum. 2007 Jun;56(6):1974–84.

46. Yang L, Thornton S, Grom AA. Interleukin-15 inhibits sodium nitroprusside-induced apoptosis of synovial fibroblasts and vascular endothelial cells. Arthritis Rheum. 2002 Nov;46(11):3010–4.

47. Hanna VE, Rider SF, Moore TL, Wilson VK, Osborn TG, Rotskoff KS, et al. Effects of systemic onset juvenile rheumatoid arthritis on facial morphology and temporomandibular joint form and function. J Rheumatol. 1996 Jan;23(1):155–8.

48. Kjellberg H. Craniofacial growth in juvenile chronic arthritis. Acta Odontol Scand. 1998 Dec;56(6):360–5.

49. McNamara JA Jr. Components of class II malocclusion in children 8-10 years of age. Angle Orthod. 1981 Jul;51(3):177–202.

50. Proffit WR, Fields HW Jr, Moray LJ. Prevalence of malocclusion and orthodontic treatment need in the United States: estimates from the NHANES III survey. Int J Adult Orthodon Orthognath Surg. 1998;13(2):97–106.

51. Karaiskos N, Wiltshire WA, Odlum O, Brothwell D, Hassard TH. Preventive and interceptive orthodontic treatment needs of an inner-city group of 6- and 9-year-old Canadian children. J Can Dent Assoc. 2005 Oct;71(9):649.

52. Warren JJ, Slayton RL, Yonezu T, Bishara SE, Levy SM, Kanellis MJ. Effects of Nonnutritive Sucking Habits on Occlusal Characteristics in the Mixed Dentition. Pediatric Dentistry. 2005 Nov 1;27(6):445–50.

53. Randerath WJ, Verbraecken J, Andreas S, Bettega G, Boudewyns A, Hamans E, et al. Non-CPAP therapies in obstructive sleep apnoea. Eur Respir J. 2011 May;37(5):1000–28.

54. Kinzinger G, Czapka K, Ludwig B, Glasl B, Gross U, Lisson J. Effects of fixed appliances in correcting Angle Class II on the depth of the posterior airway space: FMA vs. Herbst appliance--a retrospective cephalometric study. J Orofac Orthop. 2011 Aug;72(4):301–20.

55. Sedaghat AR, Anderson ICW, McGinley BM, Rossberg MI, Redett RJ, Ishman SL. Characterization of obstructive sleep apnea before and after tongue-lip adhesion in children with micrognathia. Cleft Palate Craniofac J. 2012 Jan;49(1):21–6.

56. Joshi N, Hamdan AM, Fakhouri WD. Skeletal malocclusion: a developmental disorder with a life-long morbidity. J Clin Med Res. 2014 Dec;6(6):399–408.

57. Ghafournia M, Hajenourozali Tehrani M. Relationship between Bruxism and Malocclusion among Preschool Children in Isfahan. J Dent Res Dent Clin Dent Prospects. 2012;6(4):138–42.

58. Rondeau BH. Class II malocclusion in mixed dentition. J Clin Pediatr Dent. 1994;19(1):1–11.

59. Ritto AK. Class II malocclusion: why, when and how to treat this anomaly in mixed dentition with fixed functional appliances. J Gen Orthod. 2001;12(4):9–21.

60. Bock NC, Ruf S. Dentoskeletal changes in adult Class II division 1 Herbst treatment--how much is left after the retention period? Eur J Orthod. 2012 Dec;34(6):747–53.

61. Camilla Tulloch JF, Lenz BE, Phillips C. Surgical Versus Orthodontic Correction for Class II Patients: Age and Severity in Treatment Planning and Treatment Outcome. Semin Orthod. 1999 Dec;5(4):231–40.

62. Kersey ML, Nebbe B, Major PW. Temporomandibular joint morphology changes with mandibular advancement surgery and rigid internal fixation: a systematic literature review. Angle Orthod. 2003 Feb;73(1):79–85.

63. Ow A, Cheung LK. Skeletal stability and complications of bilateral sagittal split osteotomies and mandibular distraction osteogenesis: an evidence-based review. J Oral Maxillofac Surg. 2009 Nov;67(11):2344–53.

64. Epker BN, Wolford LM, Fish LC. Mandibular deficiency syndrome. II. Surgical considerations for mandibular advancement. Oral Surg Oral Med Oral Pathol. 1978 Mar;45(3):349–63.

65. Graber TM, Rakosi T, Petrovic AG. Dentofacial orthopedics with functional appliances. St. Louis: Mosby; 1997.

66. Graber TM, Vanarsdall RL, Vig KWL. Orthodontics: current principles & techniques. St. Louis: Elsevier Mosby; 2005.

67. Tingey TF, Shapiro PA. Selective inhibition of condylar growth in the rabbit mandible using intra-articular papain. Am J Orthod. 1982 Jun;81(6):455–64.

68. Peltomäki T, Kylämarkula S, Vinkka-Puhakka H, Rintala M, Kantomaa T, Rönning O. Tissue-separating capacity of growth cartilages. Eur J Orthod. 1997 Oct;19(5):473–81.

69. Dannan A. An update on periodontic-orthodontic interrelationships. J Indian Soc Periodontol. 2010 Jan;14(1):66–71.

70. Pancherz H, Ruf S, Thomalske-Faubert C. Mandibular articular disk position changes during Herbst treatment: a prospective longitudinal MRI study. Am J Orthod Dentofacial Orthop. 1999 Aug;116(2):207–14.

71. Kochel J, Meyer-Marcotty P, Witt E, Stellzig-Eisenhauer A. Effectiveness of bionator therapy for Class II malocclusions. J Orofac Orthop. 2012 Apr;73(2):91–103.

72. Angelieri F, Franchi L, Cevidanes LHS, Scanavini MA, McNamara JA. Long-term treatment effects of the FR-2 appliance: a prospective evalution 7 years post-treatment. Eur J Orthod [Internet]. 2013 Jun 4 [cited 2013 Jul 20]; Available from: http://ejo.oxfordjournals.org/content/early/2013/06/03/ejo.cjt026

73. Franchi L, Pavoni C, Faltin K, McNamara JA, Cozza P. Long-term skeletal and dental effects and treatment timing for functional appliances in Class II malocclusion. Angle Orthod. 2013 Mar;83(2):334–40.

74. O'Brien K, Wright J, Conboy F, Chadwick S, Connolly I, Cook P, et al. Effectiveness of early orthodontic treatment with the Twin-block appliance: a multicenter, randomized, controlled trial. Part 2: Psychosocial effects. Am J Orthod Dentofacial Orthop. 2003 Nov;124(5):488-494-495.

75. Siara-Olds NJ, Pangrazio-Kulbersh V, Berger J, Bayirli B. Long-term dentoskeletal changes with the Bionator, Herbst, Twin Block, and MARA functional appliances. Angle Orthod. 2010 Jan;80(1):18–29.

76. Du X, Hägg U, Rabie ABM. Effects of headgear Herbst and mandibular step-by-step advancement versus conventional Herbst appliance and maximal jumping of the mandible. Eur J Orthod. 2002 Apr;24(2):167–74.

77. Bendeus M, Hägg U, Rabie B. Growth and treatment changes in patients treated with a headgear-activator appliance. Am J Orthod Dentofacial Orthop. 2002 Apr;121(4):376–84.

78. Evans CH, Huard J. Gene therapy approaches to regenerating the musculoskeletal system. Nat Rev Rheumatol. 2015 Apr;11(4):234–42.

79. Scheller EL, Krebsbach PH, Kohn DH. Tissue engineering: state of the art in oral rehabilitation. J Oral Rehabil. 2009 May;36(5):368–89.

80. Huang Y-C, Simmons C, Kaigler D, Rice KG, Mooney DJ. Bone regeneration in a rat cranial defect with delivery of PEI-condensed plasmid DNA encoding for bone morphogenetic protein-4 (BMP-4). Gene Ther. 2005 Mar;12(5):418–26.

81. Scheller EL, Villa-Diaz LG, Krebsbach PH. Gene therapy: implications for craniofacial regeneration. J Craniofac Surg. 2012 Jan;23(1):333–7.

82. Hacein-Bey-Abina S, Von Kalle C, Schmidt M, McCormack MP, Wulffraat N, Leboulch P, et al. LMO2-associated clonal T cell proliferation in two patients after gene therapy for SCID-X1. Science. 2003 Oct 17;302(5644):415–9.

83. Jin H, Zhang K, Qiao C, Yuan A, Li D, Zhao L, et al. Efficiently engineered cell sheet using a complex of polyethylenimine-alginate nanocomposites plus bone morphogenetic protein 2 gene to promote new bone formation. Int J Nanomedicine. 2014;9:2179–90.

84. Gugala Z, Davis AR, Fouletier-Dilling CM, Gannon FH, Lindsey RW, Olmsted-Davis EA. Adenovirus BMP2-induced osteogenesis in combination with collagen carriers. Biomaterials. 2007 Oct;28(30):4469–79.

85. Evans CH. Advances in regenerative orthopedics. Mayo Clin Proc. 2013 Nov;88(11):1323–39.

86. Sieker JT, Kunz M, Weißenberger M, Gilbert F, Frey S, Rudert M, et al. Direct bone morphogenetic protein 2 and Indian hedgehog gene transfer for articular cartilage repair using bone marrow coagulates. Osteoarthr Cartil. 2015 Mar;23(3):433–42.

87. Ivkovic A, Pascher A, Hudetz D, Maticic D, Jelic M, Dickinson S, et al. Articular cartilage repair by genetically modified bone marrow aspirate in sheep. Gene Ther. 2010 Jun;17(6):779–89.

88. Goodrich LR, Hidaka C, Robbins PD, Evans CH, Nixon AJ. Genetic modification of chondrocytes with insulin-like growth factor-1 enhances cartilage healing in an equine model. J Bone Joint Surg Br. 2007 May;89(5):672–85.

89. Rabie ABM, Dai J, Xu R. Recombinant AAV-mediated VEGF gene therapy induces mandibular condylar growth. Gene Ther. 2007 Jun;14(12):972–80.

90. Suzuki S, Itoh K, Ohyama K. Local administration of IGF-I stimulates the growth of mandibular condyle in mature rats. J Orthod. 2004 Jun;31(2):138–43.

91. Seifi M, Maghzi A, Gutknecht N, Mir M, Asna-Ashari M. The effect of 904 nm low level laser on condylar growth in rats. Lasers Med Sci. 2010 Jan;25(1):61–5.

92. Wan Q, Li Z-B. Intra-articular injection of parathyroid hormone in the temporomandibular joint as a novel therapy for mandibular asymmetry. Med Hypotheses. 2010 Apr;74(4):685–7.

93. Liu Q, Wan Q, Yang R, Zhou H, Li Z. Effects of intermittent versus continuous parathyroid hormone administration on condylar chondrocyte proliferation and differentiation. Biochem Biophys Res Commun. 2012 Jul 20;424(1):182–8.

94. Kasturi G, Adler RA. Mechanical means to improve bone strength: ultrasound and vibration. Curr Rheumatol Rep. 2011 Jun;13(3):251–6.

95. Bashardoust Tajali S, Houghton P, MacDermid JC, Grewal R. Effects of low-intensity pulsed ultrasound therapy on fracture healing: a systematic review and meta-analysis. Am J Phys Med Rehabil. 2012 Apr;91(4):349–67.

96. El-Bialy TH, Elgazzar RF, Megahed EE, Royston TJ. Effects of ultrasound modes on mandibular osteodistraction. J Dent Res. 2008 Oct;87(10):953–7.

97. Shimazaki A, Inui K, Azuma Y, Nishimura N, Yamano Y. Low-intensity pulsed ultrasound accelerates bone maturation in distraction osteogenesis in rabbits. J Bone Joint Surg Br. 2000 Sep;82(7):1077–82.

98. Katano M, Naruse K, Uchida K, Mikuni-Takagaki Y, Takaso M, Itoman M, et al. Low intensity pulsed ultrasound accelerates delayed healing process by reducing the time required for the completion of endochondral ossification in the aged mouse femur fracture model. Exp Anim. 2011;60(4):385–95.

99. Doan N, Reher P, Meghji S, Harris M. In vitro effects of therapeutic ultrasound on cell proliferation, protein synthesis, and cytokine production by human fibroblasts, osteoblasts, and monocytes. J Oral Maxillofac Surg. 1999 Apr;57(4):409–419; discussion 420.

100. Sun JS, Hong RC, Chang WH, Chen LT, Lin FH, Liu HC. In vitro effects of low-intensity ultrasound stimulation on the bone cells. J Biomed Mater Res. 2001 Dec 5;57(3):449–56.

101. Li JK, Chang WH, Lin JC, Ruaan RC, Liu HC, Sun JS. Cytokine release from osteoblasts in response to ultrasound stimulation. Biomaterials. 2003 Jun;24(13):2379–85.

102. Naruse K, Sekiya H, Harada Y, Iwabuchi S, Kozai Y, Kawamata R, et al. Prolonged endochondral bone healing in senescence is shortened by low-intensity pulsed ultrasound in a manner dependent on COX-2. Ultrasound Med Biol. 2010 Jul;36(7):1098–108.

103. Naruse K, Miyauchi A, Itoman M, Mikuni-Takagaki Y. Distinct Anabolic Response of Osteoblast to Low-Intensity Pulsed Ultrasound. Journal of Bone and Mineral Research. 2003;18(2):360–369.

104. Ikeda K, Takayama T, Suzuki N, Shimada K, Otsuka K, Ito K. Effects of low-intensity pulsed ultrasound on the differentiation of C2C12 cells. Life Sci. 2006 Oct 12;79(20):1936–43.

105. Takayama T, Suzuki N, Ikeda K, Shimada T, Suzuki A, Maeno M, et al. Low-intensity pulsed ultrasound stimulates osteogenic differentiation in ROS 17/2.8 cells. Life Sci. 2007 Feb 13;80(10):965–71.

106. Parvizi J, Wu CC, Lewallen DG, Greenleaf JF, Bolander ME. Low-intensity ultrasound stimulates proteoglycan synthesis in rat chondrocytes by increasing aggrecan gene expression. J Orthop Res. 1999 Jul;17(4):488–94.

107. Parvizi J, Parpura V, Greenleaf JF, Bolander ME. Calcium signaling is required for ultrasound-stimulated aggrecan synthesis by rat chondrocytes. J Orthop Res. 2002 Jan;20(1):51–7.

108. Mukai S, Ito H, Nakagawa Y, Akiyama H, Miyamoto M, Nakamura T. Transforming growth factor-beta1 mediates the effects of low-intensity pulsed ultrasound in chondrocytes. Ultrasound Med Biol. 2005 Dec;31(12):1713–21.

109. Zhang Z-J, Huckle J, Francomano CA, Spencer RGS. The effects of pulsed low-intensity ultrasound on chondrocyte viability, proliferation, gene expression and matrix production. Ultrasound Med Biol. 2003 Nov;29(11):1645–51.

110. Zhang Z i-Jun, Huckle J, Francomano CA, Spencer RGS. The influence of pulsed low-intensity ultrasound on matrix production of chondrocytes at different stages of differentiation: an explant study. Ultrasound Med Biol. 2002 Dec;28(11–12):1547–53.

111. Mitragotri S. Healing sound: the use of ultrasound in drug delivery and other therapeutic applications. Nat Rev Drug Discov. 2005 Mar;4(3):255–60.

112. Dyson M. Non-thermal cellular effects of ultrasound. Br J Cancer Suppl. 1982 Mar;5:165–71.

113. Frenkel V. Ultrasound mediated delivery of drugs and genes to solid tumors. Adv Drug Deliv Rev. 2008 Jun 30;60(10):1193–208.

114. Padilla F, Puts R, Vico L, Raum K. Stimulation of bone repair with ultrasound: a review of the possible mechanic effects. Ultrasonics. 2014 Jul;54(5):1125–45.

115. Sarvazyan A. Diversity of biomedical applications of acoustic radiation force. Ultrasonics. 2010 Feb;50(2):230–4.

116. Krasovitski B, Frenkel V, Shoham S, Kimmel E. Intramembrane cavitation as a unifying mechanism for ultrasound-induced bioeffects. Proc Natl Acad Sci USA. 2011 Feb 22;108(8):3258–63.

117. Wang N, Tytell JD, Ingber DE. Mechanotransduction at a distance: mechanically coupling the extracellular matrix with the nucleus. Nat Rev Mol Cell Biol. 2009 Jan;10(1):75–82.

118. Wang JH-C, Thampatty BP. An introductory review of cell mechanobiology. Biomech Model Mechanobiol. 2006 Mar;5(1):1–16.

119. Schmidt CE, Horwitz AF, Lauffenburger DA, Sheetz MP. Integrin-cytoskeletal interactions in migrating fibroblasts are dynamic, asymmetric, and regulated. J Cell Biol. 1993 Nov;123(4):977–91.

120. Wang N, Butler JP, Ingber DE. Mechanotransduction across the cell surface and through the cytoskeleton. Science. 1993 May 21;260(5111):1124–7.

121. Urbich C, Dernbach E, Reissner A, Vasa M, Zeiher AM, Dimmeler S. Shear stress-induced endothelial cell migration involves integrin signaling via the fibronectin receptor subunits alpha(5) and beta(1). Arterioscler Thromb Vasc Biol. 2002 Jan;22(1):69–75.

122. Juffermans LJM, van Dijk A, Jongenelen CAM, Drukarch B, Reijerkerk A, de Vries HE, et al. Ultrasound and microbubble-induced intra- and intercellular bioeffects in primary endothelial cells. Ultrasound Med Biol. 2009 Nov;35(11):1917–27.

123. Uddin SMZ, Hadjiargyrou M, Cheng J, Zhang S, Hu M, Qin Y-X. Reversal of the detrimental effects of simulated microgravity on human osteoblasts by modified low intensity pulsed ultrasound. Ultrasound Med Biol. 2013 May;39(5):804–12.

124. Yang R-S, Lin W-L, Chen Y-Z, Tang C-H, Huang T-H, Lu B-Y, et al. Regulation by ultrasound treatment on the integrin expression and differentiation of osteoblasts. Bone. 2005 Feb 1;36(2):276–83.

125. Guilak F. The deformation behavior and viscoelastic properties of chondrocytes in articular cartilage. Biorheology. 2000;37(1–2):27–44.

126. Lee HS, Millward-Sadler SJ, Wright MO, Nuki G, Salter DM. Integrin and mechanosensitive ion channel-dependent tyrosine phosphorylation of focal adhesion proteins and beta-catenin in human articular chondrocytes after mechanical stimulation. J Bone Miner Res. 2000 Aug;15(8):1501–9.

127. Salter DM, Millward-Sadler SJ, Nuki G, Wright MO. Differential responses of chondrocytes from normal and osteoarthritic human articular cartilage to mechanical stimulation. Biorheology. 2002;39(1–2):97–108.

128. Wu QQ, Chen Q. Mechanoregulation of chondrocyte proliferation, maturation, and hypertrophy: ion-channel dependent transduction of matrix deformation signals. Exp Cell Res. 2000 May 1;256(2):383–91.

129. Giancotti FG, Ruoslahti E. Integrin signaling. Science. 1999 Aug 13;285(5430):1028–32.

130. Campbell ID, Humphries MJ. Integrin structure, activation, and interactions. Cold Spring Harb Perspect Biol. 2011 Mar;3(3).

131. Kuo J-C, Han X, Hsiao C-T, Yates JR, Waterman CM. Analysis of the myosin-II-responsive focal adhesion proteome reveals a role for β-Pix in negative regulation of focal adhesion maturation. Nat Cell Biol. 2011 Apr;13(4):383–93.

132. Schiller HB, Friedel CC, Boulegue C, Fässler R. Quantitative proteomics of the integrin adhesome show a myosin II-dependent recruitment of LIM domain proteins. EMBO Rep. 2011 Mar;12(3):259–66.

133. Whitney NP, Lamb AC, Louw TM, Subramanian A. Integrin-mediated mechanotransduction pathway of low-intensity continuous ultrasound in human chondrocytes. Ultrasound Med Biol. 2012 Oct;38(10):1734–43.

134. Watabe H, Furuhama T, Tani-Ishii N, Mikuni-Takagaki Y. Mechanotransduction activates $\alpha_5\beta_1$ integrin and PI3K/Akt signaling pathways in mandibular osteoblasts. Exp Cell Res. 2011 Nov 1;317(18):2642–9.

135. Iwabuchi Y, Tanimoto K, Tanne Y, Inubushi T, Kamiya T, Kunimatsu R, et al. Effects of low-intensity pulsed ultrasound on the expression of cyclooxygenase-2 in mandibular condylar chondrocytes. J Oral Facial Pain Headache. 2014;28(3):261–8.

136. Lee D-Y, Yeh C-R, Chang S-F, Lee P-L, Chien S, Cheng C-K, et al. Integrin-mediated expression of bone formation-related genes in osteoblast-like cells in response to fluid shear stress: roles of extracellular matrix, Shc, and mitogen-activated protein kinase. J Bone Miner Res. 2008 Jul;23(7):1140–9.

137. Yang R-S, Lin W-L, Chen Y-Z, Tang C-H, Huang T-H, Lu B-Y, et al. Regulation by ultrasound treatment on the integrin expression and differentiation of osteoblasts. Bone. 2005 Feb;36(2):276–83.

138. Schumann D, Kujat R, Zellner J, Angele MK, Nerlich M, Mayr E, et al. Treatment of human mesenchymal stem cells with pulsed low intensity ultrasound enhances the chondrogenic phenotype in vitro. Biorheology. 2006;43(3–4):431–43.

139. Cheng K, Xia P, Lin Q, Shen S, Gao M, Ren S, et al. Effects of Low-Intensity Pulsed Ultrasound on Integrin-FAK-PI3K/Akt Mechanochemical Transduction in Rabbit Osteoarthritis Chondrocytes. Ultrasound in Medicine & Biology. 2014 Jul;40(7):1609–18.

140. Barberis L, Wary KK, Fiucci G, Liu F, Hirsch E, Brancaccio M, et al. Distinct roles of the adaptor protein Shc and focal adhesion kinase in integrin signaling to ERK. J Biol Chem. 2000 Nov 24;275(47):36532–40.

141. Choi BH, Choi MH, Kwak M-G, Min B-H, Woo ZH, Park SR. Mechanotransduction pathways of low-intensity ultrasound in C-28/I2 human chondrocyte cell line. Proc Inst Mech Eng H. 2007 Jul;221(5):527–35.

142. Greenblatt MB, Shim J-H, Glimcher LH. Mitogen-Activated Protein Kinase Pathways in Osteoblasts. Annual Review of Cell and Developmental Biology. 2013;29(1):63–79.

143. Stanton L-A, Underhill TM, Beier F. MAP kinases in chondrocyte differentiation. Dev Biol. 2003 Nov 15;263(2):165–75.

144. Kyriakis JM, Avruch J. Mammalian MAPK signal transduction pathways activated by stress and inflammation: a 10-year update. Physiol Rev. 2012 Apr;92(2):689–737.

145. Li X, Li J, Cheng K, Lin Q, Wang D, Zhang H, et al. Effect of low-intensity pulsed ultrasound on MMP-13 and MAPKs signaling pathway in rabbit knee osteoarthritis. Cell Biochem Biophys. 2011 Nov;61(2):427–34.

146. Ren L, Yang Z, Song J, Wang Z, Deng F, Li W. Involvement of p38 MAPK pathway in low intensity pulsed ultrasound induced osteogenic differentiation of human periodontal ligament cells. Ultrasonics. 2012 Nov 5;

147. Sato M, Nagata K, Kuroda S, Horiuchi S, Nakamura T, Karima M, et al. Low-Intensity Pulsed Ultrasound Activates Integrin-Mediated Mechanotransduction Pathway in Synovial Cells. Ann Biomed Eng. 2014 Aug 6;

148. Xia P, Ren S, Lin Q, Cheng K, Shen S, Gao M, et al. Low-Intensity Pulsed Ultrasound Affects Chondrocyte Extracellular Matrix Production via an Integrin-Mediated p38 MAPK Signaling Pathway. Ultrasound Med Biol. 2015 Jun;41(6):1690–700.

149. Chen M-H, Sun J-S, Liao S-Y, Tai P-A, Li T-C, Chen M-H. Low-intensity pulsed ultrasound stimulates matrix metabolism of human annulus fibrosus cells mediated by transforming growth factor β1 and extracellular signal-regulated kinase pathway. Connect Tissue Res. 2015 Jun;56(3):219–27.

150. Son Y, Kim S, Chung H-T, Pae H-O. Reactive oxygen species in the activation of MAP kinases. Meth Enzymol. 2013;528:27–48.

151. Klebanoff SJ. Oxygen metabolism and the toxic properties of phagocytes. Ann Intern Med. 1980 Sep;93(3):480–9.

152. Sauer H, Wartenberg M, Hescheler J. Reactive oxygen species as intracellular messengers during cell growth and differentiation. Cell Physiol Biochem. 2001;11(4):173–86.

153. Bedard K, Krause K-H. The NOX family of ROS-generating NADPH oxidases: physiology and pathophysiology. Physiol Rev. 2007 Jan;87(1):245–313.

154. Suzuki YJ, Forman HJ, Sevanian A. Oxidants as stimulators of signal transduction. Free Radic Biol Med. 1997;22(1–2):269–85.

155. Slutsky V, Kozyrev D. Handbook of Free Radicals : Formation, Types and Effects. New York: Nova Science Publishers; 2010. (Cell Biology Research Progress Series).

156. Morita K, Miyamoto T, Fujita N, Kubota Y, Ito K, Takubo K, et al. Reactive oxygen species induce chondrocyte hypertrophy in endochondral ossification. J Exp Med. 2007 Jul 9;204(7):1613–23.

157. Bartosz G. Reactive oxygen species: Destroyers or messengers? Biochemical Pharmacology. 2009 Apr 15;77(8):1303–15.

158. Hobbs GA, Mitchell LE, Arrington ME, Gunawardena HP, DeCristo MJ, Loeser RF, et al. Redox regulation of Rac1 by thiol oxidation. Free Radical Biology and Medicine. 2015 Feb;79:237–50.

159. Poli G, Leonarduzzi G, Biasi F, Chiarpotto E. Oxidative stress and cell signalling. Current Medicinal Chemistry. 2004;11(9):1163–82.

160. Goldstein BJ, Mahadev K, Kalyankar M, Wu X. Redox paradox: insulin action is facilitated by insulin-stimulated reactive oxygen species with multiple potential signaling targets. Diabetes. 2005 Feb;54(2):311–21.

161. El-Bialy T, El-Shamy I, Graber TM. Growth modification of the rabbit mandible using therapeutic ultrasound: is it possible to enhance functional appliance results? Angle Orthod. 2003 Dec;73(6):631–9.

162. El-Bialy T, Hassan A, Albaghdadi T, Fouad HA, Maimani AR. Growth modification of the mandible with ultrasound in baboons: a preliminary report. Am J Orthod Dentofacial Orthop. 2006 Oct;130(4):435.e7-14.

163. El-Bialy T. Nonsurgical treatment of hemifacial microsomia by therapeutic ultrasound and hybrid functional appliance. J Clin Trials. 2010 Mar;29.

164. Chan CW, Qin L, Lee KM, Cheung WH, Cheng JCY, Leung KS. Dose-dependent effect of low-intensity pulsed ultrasound on callus formation during rapid distraction osteogenesis. J Orthop Res. 2006 Nov;24(11):2072–9.

Chapter 2: Effect of increasing daily Low Intensity Pulsed Ultrasound application and Functional Appliance on mandibular condyle in growing rats.

A version of this chapter was published in: Kaur H, Uludag H, Dederich D and El-Bialy T. J of Ultrasound in Medicine. doi: 10.7863/ultra.15.0606

2.1 Introduction:

The temporomandibular joint (TMJ) is the only movable joint in the craniofacial region and is important because of its role in critical activities like mastication, speaking and clenching. This joint is covered by fibrocartilage which not only serves as a cushion for dispersion of mechanical load but also as a main growth center for craniofacial region (1). Class II malocclusion, where the lower teeth bite in backward position to the upper teeth, is one of the prevalent non-syndromic deformity usually characterized by mandibular retrusion [retrusion or backward position] (2). It not only affects jaw function and aesthetic appearance, but it may also cause airway obstruction and functional limitations such as speech, mastication and swallowing (3). Class II malocclusion affects 15% of the world population and is present in most of the patients attending orthodontic clinics (4).

Treatment of mandibular deficiency depends on the patient's age, severity of the problem, expected success rate and impact on facial profile (5). For a growing patient with retruded mandible, functional appliances (FAs) which are also known as forward bite jumping appliances can be one of treatments of choice. FAs are devices that are believed to enhance condylar growth by displacing the mandible forward and downward and eliminating abnormal muscular forces that interfere with normal dental and skeletal development of the mandible (6). Several animals and human studies have shown improvement of mandibular forward projection with FAs use (7) (8). However, the effectiveness of these appliances is still debatable, especially with regards to the

patient's age, treatment duration and long term effectiveness on mandibular growth modification. Some authors reported that effect of FAs is not skeletal but only dentoalveolar [teeth and their surrounding bone] (9) while others reported that their best skeletal effect is observed when treatment is started just before the growth spurt (8).

The mandibular condylar head undergoes endochondral ossification during growth while bone formation in glenoid fossa occurs by intra-membranous ossification. Cellular activity in glenoid fossa is slower than condylar head. This could be the reason for failure or insignificant clinical results after FAs treatment to modify mandibular growth (10). In recent years, low intensity pulsed ultrasound (LIPUS) has shown positive results in bone growth and regeneration in several studies (11) (12).

LIPUS was shown to be effective in increasing the intracellular calcium level in bone and cartilage cell culture and increasing secretion of angiogenesis related cytokines, which is important in endochondral bone formation involved in mandibular condyle (13). Human studies have also shown enhanced bone fracture healing (14) reduced treatment duration and increased bone strength in distraction osteogenesis using daily LIPUS application (15). Previous studies have shown significant increase in mandibular growth with daily 20 minute LIPUS application in combination with the use of FA (16) (7) (17). However, in a human study, it took a year of daily use of 20 minutes LIPUS in addition to FAs to show clinical improvement in mandibular growth. Therefore, there is a need for an optimized technique that may reduce daily LIPUS treatment time to a few months in humans. Previous studies have shown that daily 40

minute LIPUS application enhanced chondrogenic differentiation *in vitro* (18) and bone regeneration during distraction osteogenesis (19) compared to daily application of 20 min.

The aim of this study was to investigate the effect of increasing daily LIPUS treatment duration from 20 to 40 minutes per day with or without FA on the mandibular condylar growth in growing rats. We hypothesized that increasing daily treatment with LIPUS from 20 to 40 minutes per day will have additive effect on mandibular condylar growth, particularly if combined with FA therapy.

2.2 Materials and Methods:

2.2.1 Animal care and experimental design:

This study was approved by University of Alberta Animal Care and Use Committee (Protocol# 694/04/13/C/AUP381). Fifty four, 21-day old male Sprague Dawley rats were divided into six groups (n=9) namely: 1) Control (no FA or LIPUS application); 2) 20 min/day LIPUS (LIPUS 20 min); 3) 40 min/day LIPUS (LIPUS 40 min); 4) FA alone; 5) FA and LIPUS 20 min/day (FA+ LIPUS 20 min) and 6) FA and LIPUS 40 min/day (FA+ LIPUS 40 min). The rats were acclimatized for a period of one week. FA was attached to upper and lower incisors in the FA allocated groups when the rats were 28 days old (first day of the experiment) and received LIPUS application for 20 min or 40 min for 28 days according to treatment group. All animals were weighed on the first day of acclimatization and after each week until the end of procedures (just

before the euthanasia). Twenty four hours after the final application of LIPUS, the animals were euthanized by using Euthansol IP injection.

2.2.2 Functional Appliance:

FA was made from self-cure polymethyl methacrylate Orthodontic Resin (DENTSPLY, Milford, DE, USA) for each rat and was cemented to the upper and lower incisors, when they were 28 days old, using resin cement Panavia F2.0 (Kuraray Medical Inc, Okayama, Japan). The appliance induced 3 mm of vertical displacement of the jaw (20) and had identical inclined plane to cause anterior displacement of the mandible on mouth closing (Fig 2.1.A). All animals with FA were fed with powdered rat chow while others were fed with normal rat chow (Lab Diet, St. Louis, MO, USA).

2.2.3 Ultrasound device:

LIPUS device was custom-made and was provided by SmileSonica Inc Edmonton, AB, Canada. The device generated 200 μs bursts of 1.5 MHz sine wave with repetition rate of 1 kHz and temporal averaged intensity of 30 mW/cm^2. These parameters have been used in our lab and has been approved by Food and Drug Administration (USA) for the clinical use in promoting healing of fractured bone (7, 14, 17-20, 24, 25). It was calibrated at the beginning and end of the experiment to evaluate consistency of LIPUS parameters. In each animal in the LIPUS groups, the right mandibular condyle was used as the experimental side which was shaved and coupling

gel was applied to ensure LIPUS wave propagation and left side was used as an internal control (Fig 2.1.B).

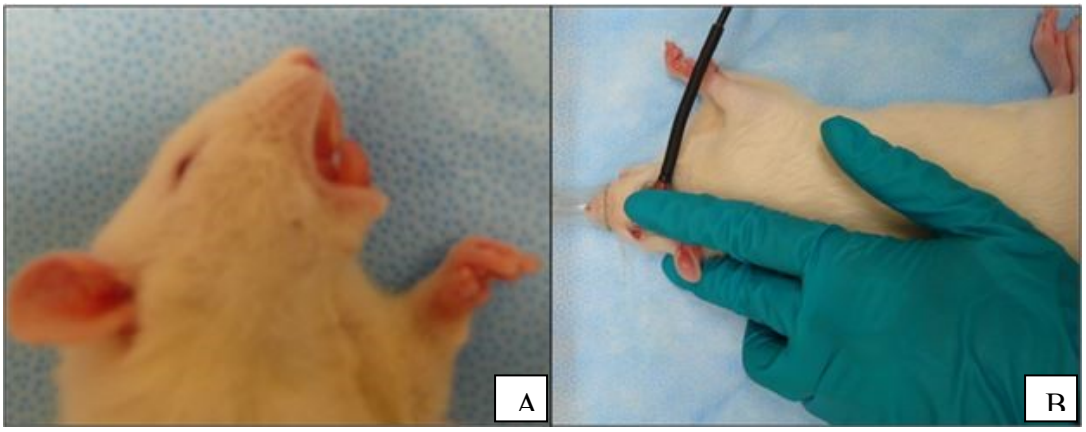

Fig 2.1: A: Picture shows functional appliance attached to the upper and lower incisors of the rat. B: Tranducer of the ultrasound device applied to the right side of the mandible while the rat was under anesthesia.

2.2.4 Morphometric measurements:

Mandibles were dissected and fixed in 10% formalin solution (Sigma-Aldrich, St Louis, MO, USA) for 24 hours at room temperature. Landmark measurements were performed using digital caliper. Fig 2.2 shows the landmarks and linear measurements analyzed and description of variables is presented in Table 2.1.

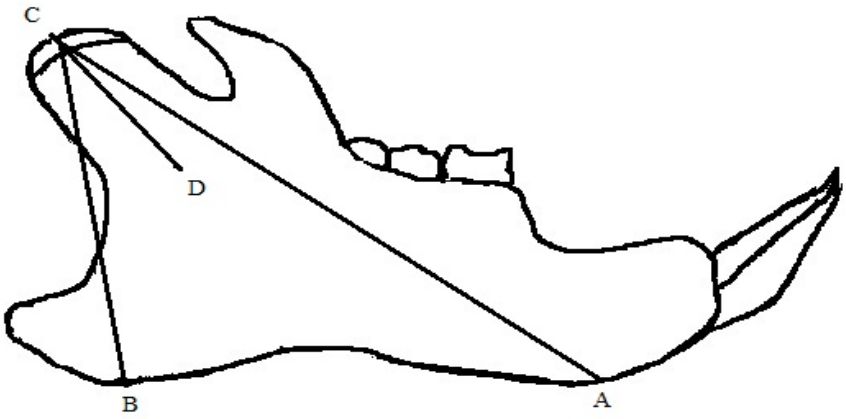

Fig 2.2: The landmarks and linear measurements of the mandible. Mandible lenght (A-C)- distance from the posteriosuperior most point on the condylar head to menton which is anterio inferior point on the lower border of the mandible.– ; Ramus height (C-B) distance from the condylar point to Gonial tangent point (posterio inferior point on the lower border of the mandible); Condyle process length (C-D) distance from the lower border of the mandibular foramen to the condylar point.

Table 2.1: Morphometric landmarks and linear measurements of the mandible.

Points	**Description**
Menton (A)	The most inferior point on the mandibular symphysis.
Gonion tangent point (B)	Assuming that the mandible is placed on a plane. The point of the mandibular gonion at its junction with that plane.
Condylar point (C)	The most posterior and superior point on the mandible condyle.
Mandibular Foramen (D)	The entry of mandibular nerve and blood vessels in the mandibular canal.
Linear measurement	
Menton–Condylar point(A-C)	Total mandibular length. The distance measured between the menton and the condylar point.
Condylar - GoT(C-B)	Ramus height. The distance measured between the condylar point and the gonial tangent point.
Condylar process length (C-D)	The distance measured from the mandibular foramen to the condylar point.

2.2.5 Histology and Histomorphometric measurement:

Condylar processes were separated from the mandibles by dissection and were decalcified using Cal-Ex II (Fisher Scientific, Ottawa, CA) for 2 weeks. Decalcified condyles were embedded in paraffin and sectioned at 6 μm thickness. Slides were stained with Periodic Acid Schiff's reagent (PAS) and Alcian blue stain to identify the cartilage and new bone formation (21)(22). Alcian blue stains the cartilage with blue color while it is stained magenta with PAS which shows calcification of the cartilage matrix. Proliferative layer is composed of undifferentiated mesenchymal cells that stain positive for Alcian blue. Extracellular matrix is stained blue in hypertrophic layer with Alcian blue while the chondrocytes in erosive layer where calcification begins are stained magenta with PAS. Photographs were taken using Leica Fluorescent Digital Microscope with CCD digital camera (Leica, Wetzlar, Germany) and using RS Image software 1.73 (Photometric, Roper Scientific Inc, Tucson, AZ, USA) and analyzed using Metamorph Software. The used magnification was 20X. Cell number and width of proliferative and hypertrophic layers were measured. Readings from 3 slides of each sample were then averaged to get the final reading for every sample. For the thickness measurement, 6 lines were drawn in the proliferative and hypertrophic layers separately and then averaged to get final value from 1 slide. To measure the cell count for proliferative and hypertrophic layers, fixed measurement frame of 500 X 500 μm was drawn in the posterior region (Fig 2.3.A and 2.3.B).

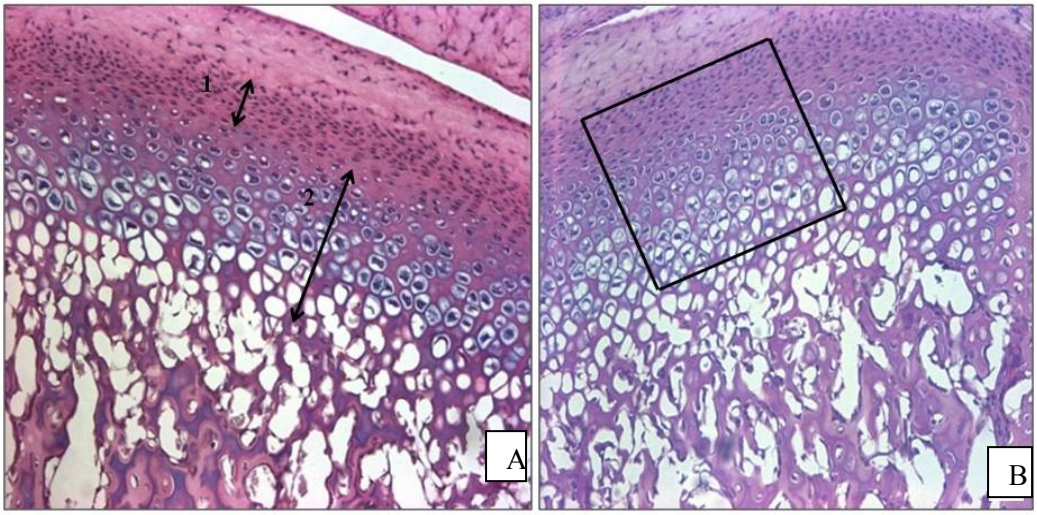

Fig 2.3.A: Line 1 shows the width of the proliferative layer and Line 2 shows the width of hypertrophic layer. B: Square of 500 X500 µm drawn in the posterior region of the condyle and the cell count of proliferative and hypertrophic layers were counted within the square.

2.2.6 Immunohistochemistry:

After the sections were dewaxed and rehydrated, the antigenic sites were exposed by heat treatment using 10 mM Trisodium Citrate buffer. After washing with PBS, the slides were submerged in 6% Hydrogen Peroxide solution for 20 min. The slides were then washed with phosphate buffered solution (PBS) and incubated with 1% bovine serum albumin (BSA) for 30 min. The sections were then incubated overnight at 4ºC with the primary antibody. The primary antibodies used in this study were SOX9 (1:100), Collagen II (1:100), Collagen X (1:50) and Aggrecan (1:100). The incubation with secondary antibody i.e. IgG (1:500) was performed for 1 hr followed by PBS washing. The reaction product was visualized using Avidin-biotin complex (ABC) peroxidase kit (Vectastain) and diaminobenzidine (DAB) substrate (Vectastain). The slides were counterstained with Mayer hematoxylin. To ascertain the specificity of immunostaining is from the primary antibody, negative controls were included on which primary antibody was replaced by 1% BSA.

2.2.7 Micro-Computed Tomography (Micro CT) imaging:

Dissected mandibles were scanned by Skyscan 1176 Micro CT imager (Kontich, Belgium) using vendor supplied imaging control software. Resolution selected was 18 microns. All scans were conducted at 85 kV, 293 µA using 10 mm aluminum filter through 180°rotation at 0.5° step increment. Analysis was performed using CTAn software (version 1.12.0.0 Skyscan, Belgium). Trabecular bone of the condylar head areas were manually selected using the first appearance of trabecular bone as the

reference point up to the 100th slice. Bone structural parameters studied were bone volume to tissue volume ratio or bone volume fraction (BV/TV), trabecular thickness (Tb.Th), trabecular number (Tb.N), trabecular separation (Tb.Sep) and bone mineral density (BMD). From each sample 5 readings were taken and values were averaged to get the final value.

2.2.8 Statistical analysis:

Data were first analyzed for normal distribution using Kolmogrov Smirnoff test. For normally distributed data, one-way ANOVA followed by Bonferroni post hoc test using SPSS version 21.0 (Chicago, IL, USA) was used. The significance level was set at $p < 0.05$. For the left and right side readings, paired t-test was applied. Intra rater reliability for 6 randomly selected animals for each measured variables were tested using Intra Class Correlation Coefficient (ICC) test and measurements were performed twice with an interval of 2 weeks for morphometric analysis and 4 weeks for histology and Micro CT analyses.

2.3 Results:

All measured variables showed normally distributed data except for Trabecular Number, hence Kruskal Wallis test was applied. ICC test also showed absolute agreement ($r > 0.78$-0.99).

2.3.1 Body weight:

There was no difference in body weight among treatment groups on the first day of the experiment ($p=0.18$) but there were significant differences among the groups ($p<0.001$) at the end of the experiment (Fig 2.4). However there was no difference between FA and FA + LIPUS 20 min; and between LIPUS 20 min and LIPUS 40 min groups.

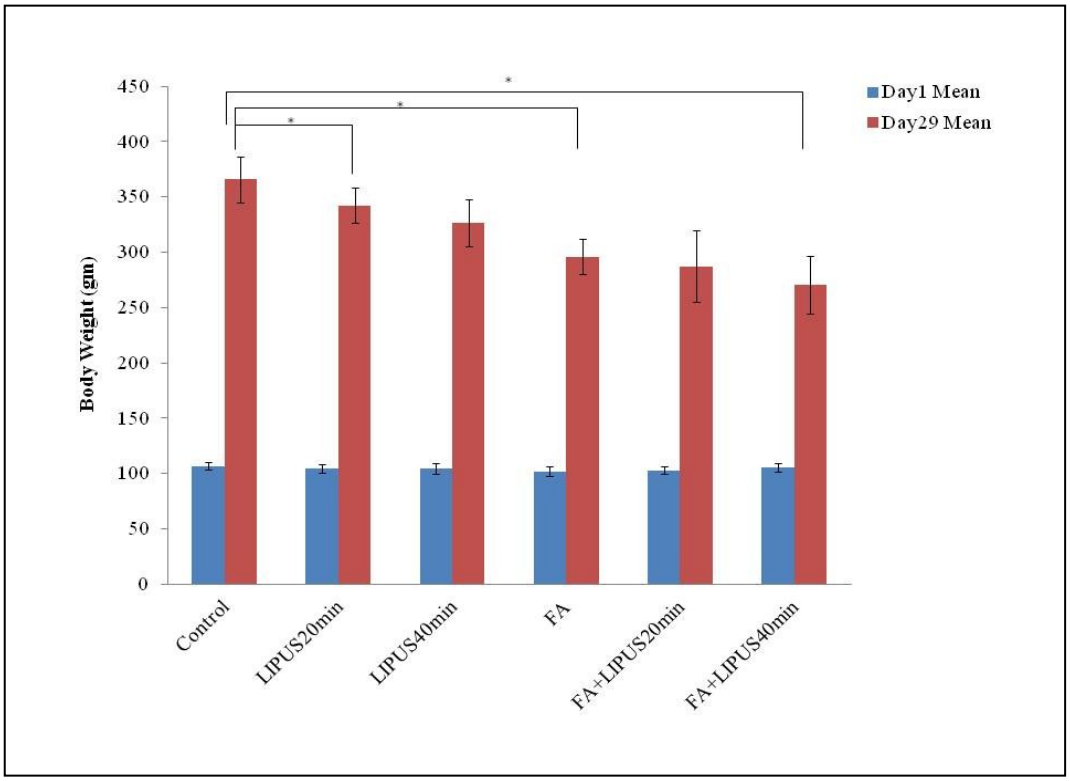

Fig 2.4: Bar chart showing the weights measured on Day 1 and Day 29. No significant difference in the body weight of the animals were seen in on day 1 while there is significant difference among the groups on day 29 specially in Functional Appliance groups (* $p < 0.05$)

2.3.2 Morphometric analysis:

There was a statistical significant increase in all 3 measurements in LIPUS 20 min group ($p<0.05$) except for condylar process length between LIPUS 20 and LIPUS 40 min groups where $p= 0.182$. Mandibular length showed the highest value in LIPUS 20 min group followed by LIPUS 40 min group as compared to control group. However, the mean difference between control and LIPUS 40 min group was small (0.2mm) and was not statistically significant ($p > 0.05$). There was no significant difference between control and FA groups, control and LIPUS 40 min groups and between FA and FA+ LIPUS 40 min groups (Fig 2.5.A). Ramus height (C-B) showed increase in LIPUS 20 min group as compared to control and the difference was statistically significant ($p < 0.05$) (Fig 2.5.B). Condylar length (C-D) also showed increase in LIPUS 20 min group followed by LIPUS 40 min. There was also significant difference between LIPUS 20 min and FA groups; FA + LIPUS 20 min and FA + LIPUS 40 min groups (Fig 2.5.C). On comparing the left and right readings, LIPUS 20 min and FA+ LIPUS 20 min showed significant difference for all the measured variables. Overall, by comparing means of all treatment groups, LIPUS 20 min group showed statistical increase in all 3 linear measurements while FA + LIPUS 40 min group showed decrease in all the measurements.

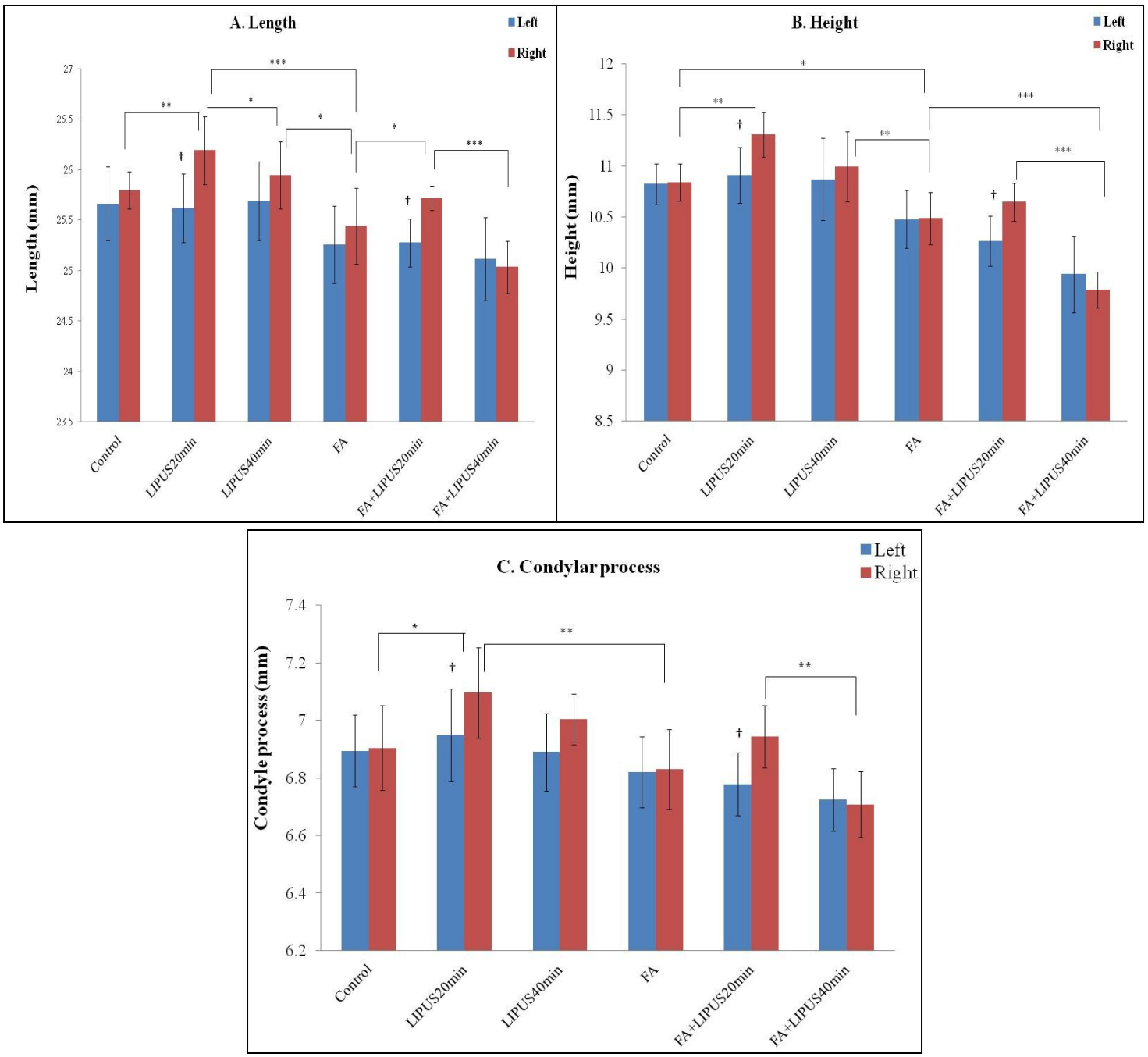

Fig 2.5: Bar charts depict anthropometric measurements of the left and right mandible (A Mandible length. B Ramus height and C Condylar process length.) LIPUS 20 min showed significant increase in mandibular length (A-C), ramus height (B-C) and condylar process (C-D) as compared to other treatment groups while FA + LIPUS 40

min showed least values in all the measured variables. (*p< 0.05, ** p < 0.001 and *** p < 0.0001) († p < 0.05 between the left and right condyle).

2.3.3 Histomorphometric analysis:

Qualitatively, the width of proliferative and hypertrophic cell layers is evident from the slides (Fig 2.6). One-way ANOVA showed significant difference in all the measured histomorphometric variables; i.e., proliferative cell number and width, and hypertrophic cell number and width. LIPUS 20 min group showed significant difference from all other treatment groups in proliferative cell number ($p<0.05$) while there was no significant difference between control and FA groups and control and FA+ LIPUS 40 groups (Fig 2.7.A). In proliferative layer width, again LIPUS 20 min group showed significant increase followed by LIPUS 40 min and FA+ LIPUS 20 min groups. There was no significant difference between control and FA; control and FA+ LIPUS 40 min groups ($p>0.4$ in both cases) (Fig 2.7.B). In the case of hypertrophic cell numbers, there was no significant difference between control and FA groups, and FA and FA+ LIPUS 40 min groups, (Fig 2.7.C). In the case of hypertrophic width, there was no difference between control and FA groups, LIPUS 20 min and LIPUS 40 min groups and LIPUS 40 min and FA+ 20 min LIPUS groups (Fig 2.7.D). On comparing the left and right side readings from histomorphometric analysis, there was significant difference in the groups treated with 20 min of LIPUS application either alone or with FA in proliferative cell count and width and hypertrophic cell count and width. Also LIPUS 40 min showed statistically significant difference between left and right side of the condyle.

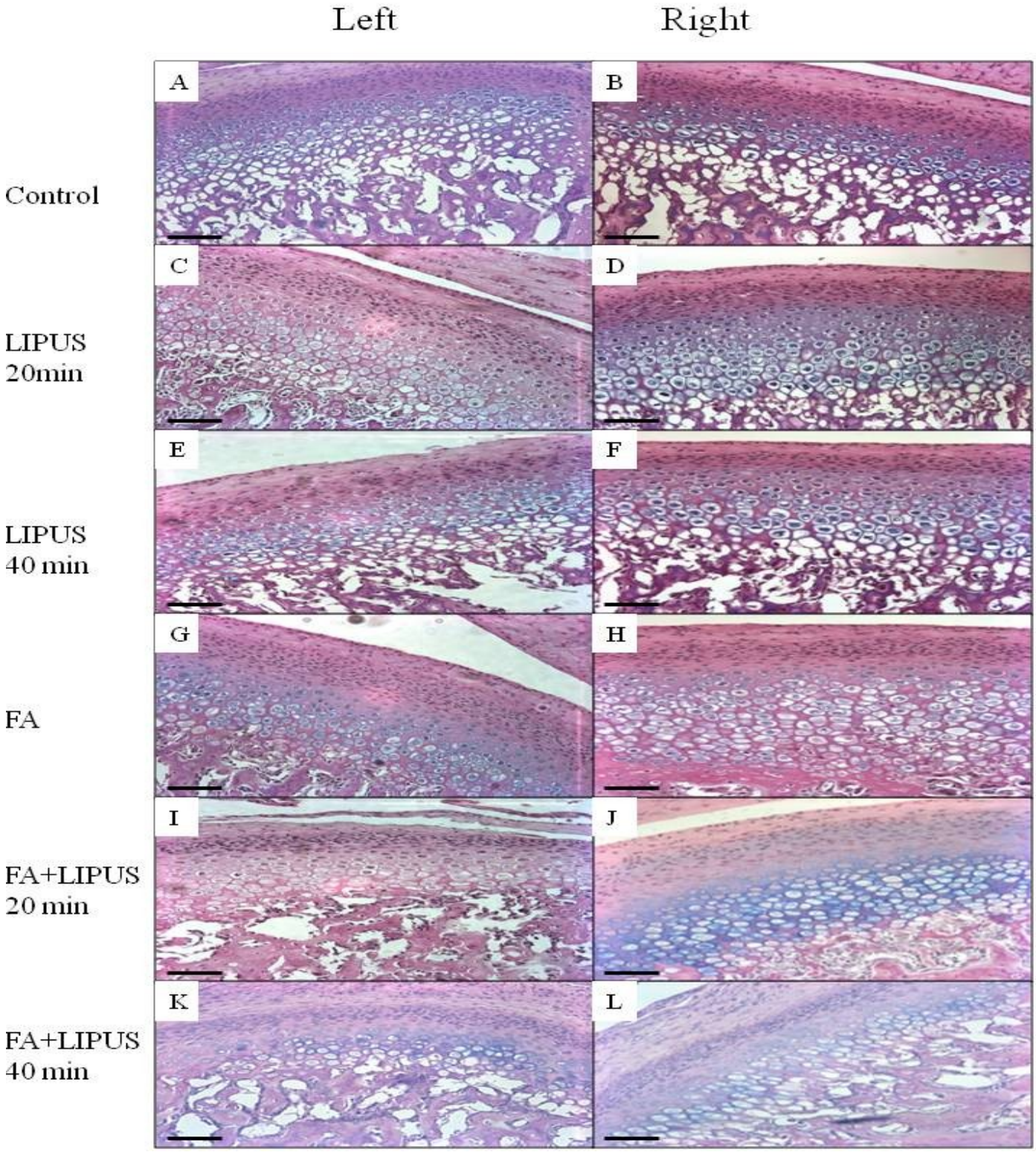

Fig 2.6: Alcian blue and periodic acid Schiff (PAS) stained slides showing the left and right sides of the mandible condyle. Qualitatively, LIPUS 20 min showed increased cell count and width both in proliferative and hypertrophic layers followed by FA+ LIPUS 20 min. There was decrease in both the cell count and width in FA + LIPUS 40 min group as compared to control.

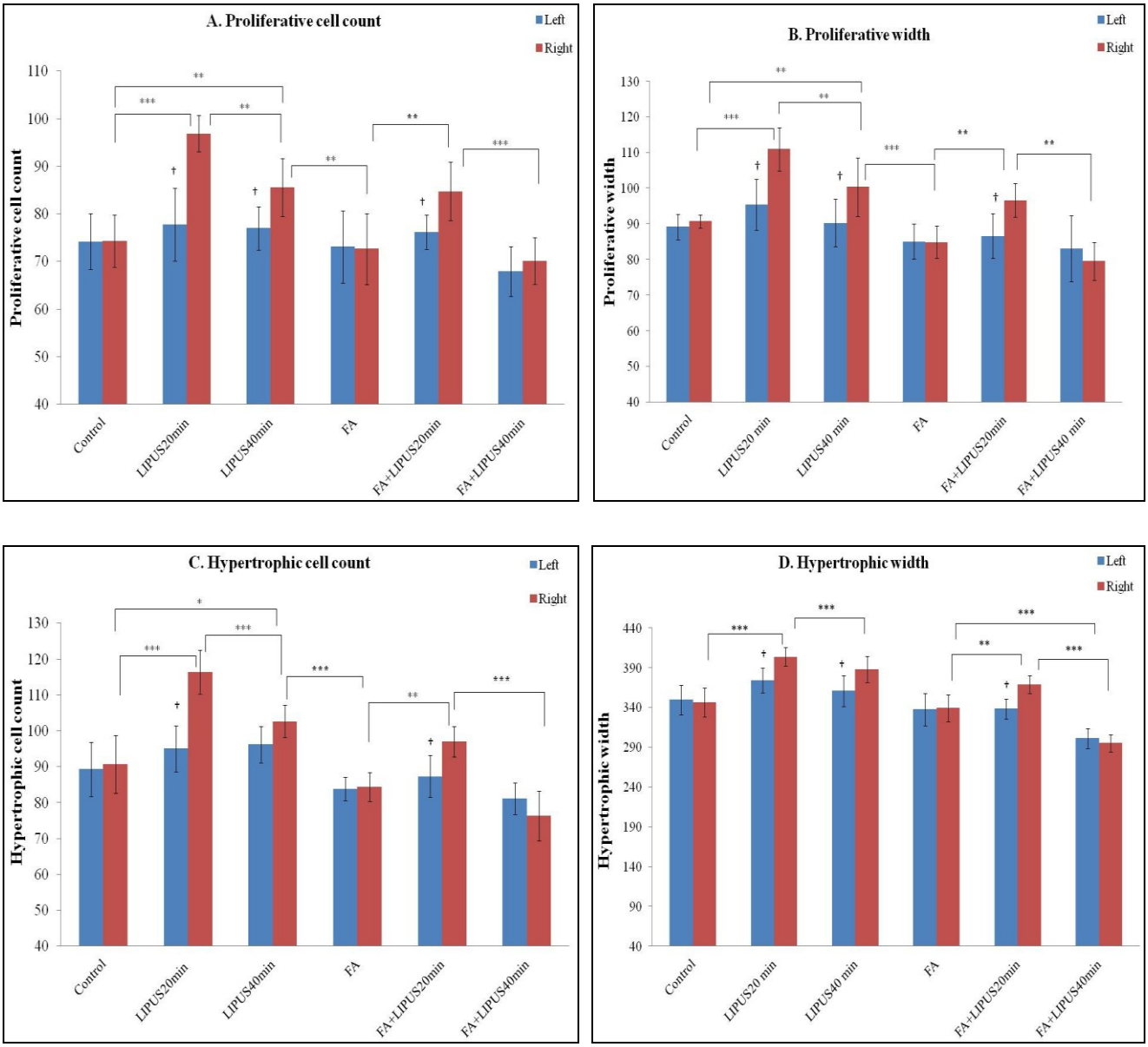

Fig 2.7: Bar charts depict histomorphometric analysis of the left and right mandible condyles. A. Proliferative cell count B. Proliferative width C. Hypertrophic cell count D. Hypertrophic width. After 28 days of the experimental procedure, LIPUS 20 min showed increase in Proliferative and Hypertrophic cell count and layer width. Similar results are seen in Functional Appliance groups where 20 min LIPUS application in combination with FA showed significant increase in all the measured variables. (* $p<0.05$, **$p< 0.001$ and *** $p <0.0001$) († $p <0.05$ between the left and right side of the mandible condyle.)

2.3.4 Immunohistochemistry:

Qualitatively, the groups treated with 20 min LIPUS either alone or with FA showed increased expression of SOX9, Aggrecan, Collagen II and Collagen X. The right side i.e. the treatment sides showed higher expression of these proteins as compared to the left side (Fig 2.8.A, 2.8.C, 2.8.E and 2.8.G).

SOX9: SOX9 transcription factor was detected in the proliferative and upper part of hypertrophic layer. In control and FA groups, SOX9 positive cells were mainly expressed in the proliferative layer while in LIPUS treated groups, some SOX9 positive cells were also expressed in the upper part of hypertrophic layer (Fig 2.8.A). LIPUS 20 min showed increased expression of SOX9 as compared to other treatment groups and the difference was statistically significant ($p<0.05$). In FA treated groups, again FA + LIPUS 20 min showed increased SOX9 expression as compared to FA alone and FA + LIPUS 40 min ($p<0.05$). Right side of the groups showed increased SOX9 expression as compared to left side and the difference was statistically significant in LIPUS 20 min, FA + LIPUS 20 min and FA + LIPUS 40 min ($p<0.05$) (Fig 2.8.B).

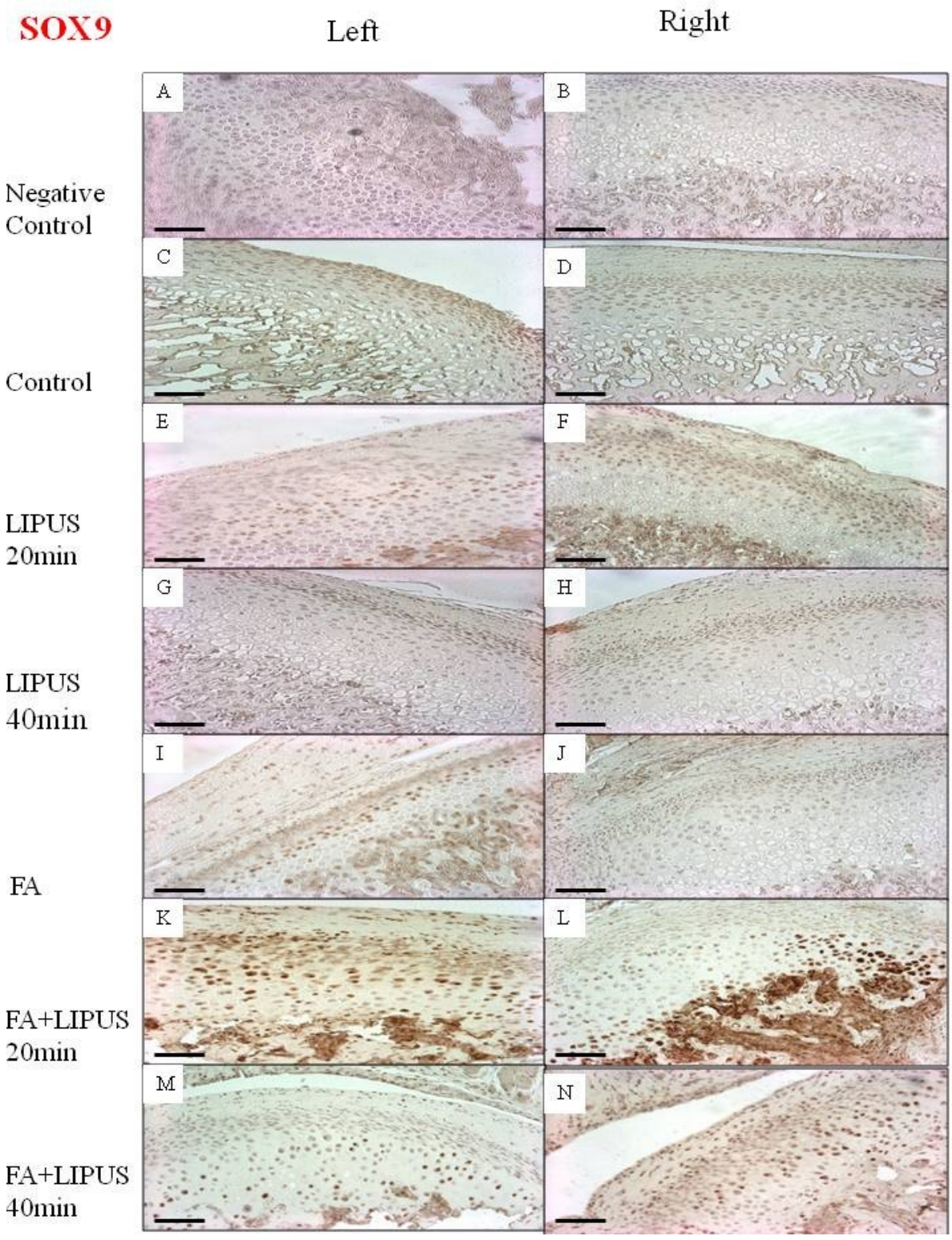

Fig 2.8.A: Expression of Sox 9 in the left and right mandible condyles.

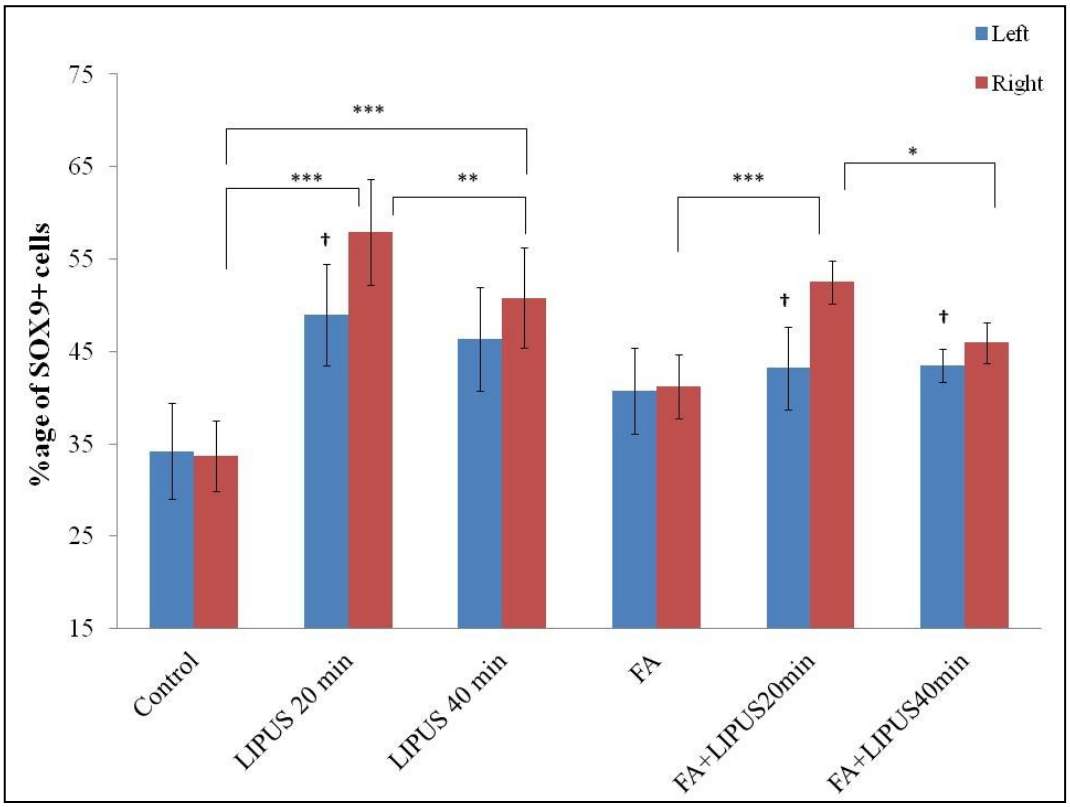

Fig 2.8.B: Bar graph depict the percentage of SOX9 immunopositive cells in the posterior part of the mandible condyle (*** p <0.0005, **p<0.005 and *p<0.05) (†p <0.05 between left and right side of the mandible condyle).

Aggrecan: Mechanical strain produced by LIPUS and FA showed increased expression of Aggrecan in both LIPUS 20 min and FA + LIPUS 20 min groups with treatment showing higher expression as compared to non treatment side (Fig 2.8.C). This increase in expression is statistically significant ($p<0.05$). Aggrecan is mainly expressed in the upper part of hypertrophic layer. On comparing treated and non treated sides within the groups, LIPUS 20 min, LIPUS 40 min, FA + LIPUS 20 min and FA + LIPUS 40 min showed statistically significant increase in Aggrecan expression in the treatment side of the mandible (Fig 2.8.D).

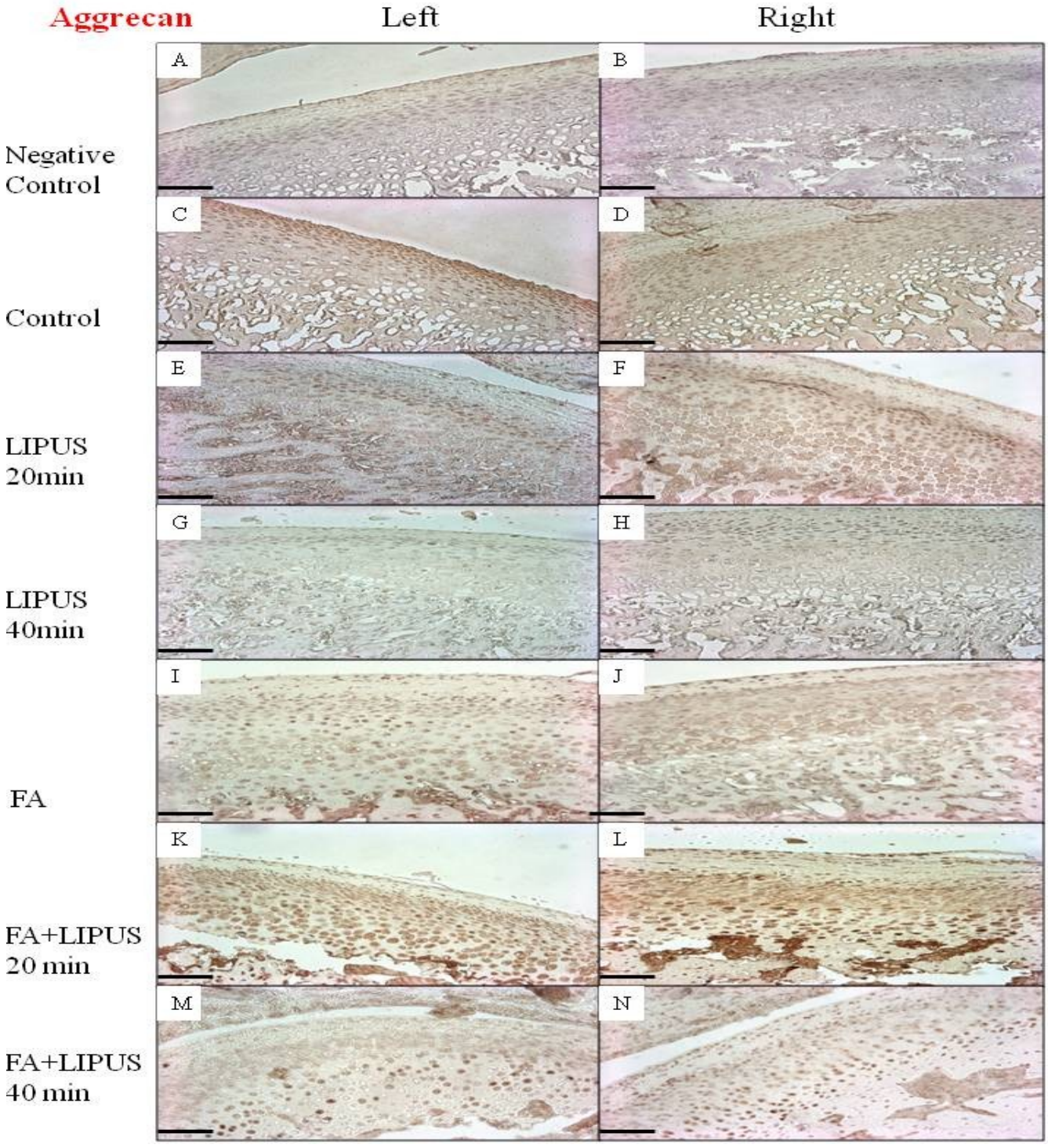

Fig 2.8.C: Expression of Aggrecan in the left and right mandible condyles

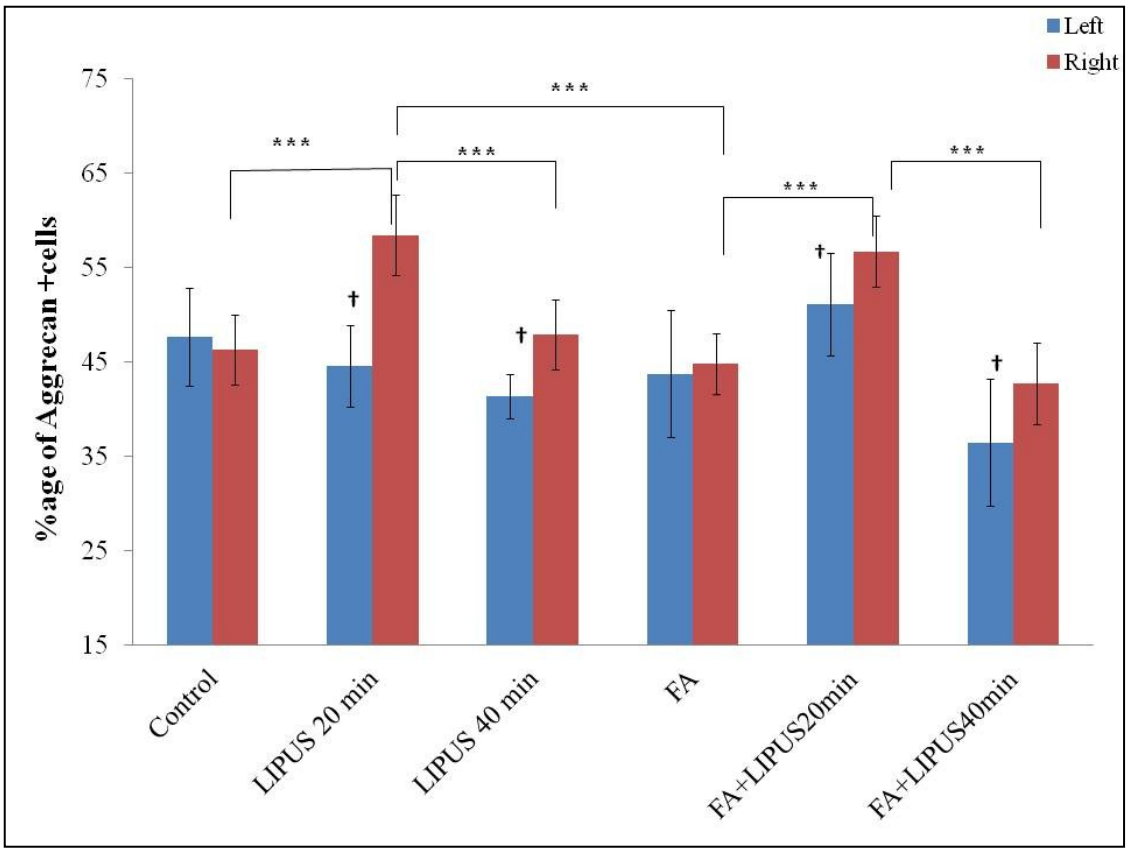

Fig 2.8.D: Bar graph depict the percentage of Aggrecan immunopositive cells in the posterior part of the mandible condyle (*** p <0.0005, **p<0.005 and *p<0.05) (†p <0.05 between left and right side of the mandible condyle).

Collagen II: Collagen II expression is mainly detected in the hypertrophic layer of the mandibular condyle (Fig 2.8.E). Collagen II expression was significantly higher in 20 min LIPUS application both in LIPUS alone and with FA groups. There was no significant difference between FA and FA + LIPUS 20 min while LIPUS 40 min and FA showed similar values in the right side of mandible. On comparing treatment and non treatment sides, the right side of the mandibular condyle showed increased expression in LIPUS 20 min and FA + LIPUS 20 min while FA + LIPUS 40 min showed increased expression of Collagen II on the left side of mandible condyle ($p < 0.05$) (Fig 2.8.F).

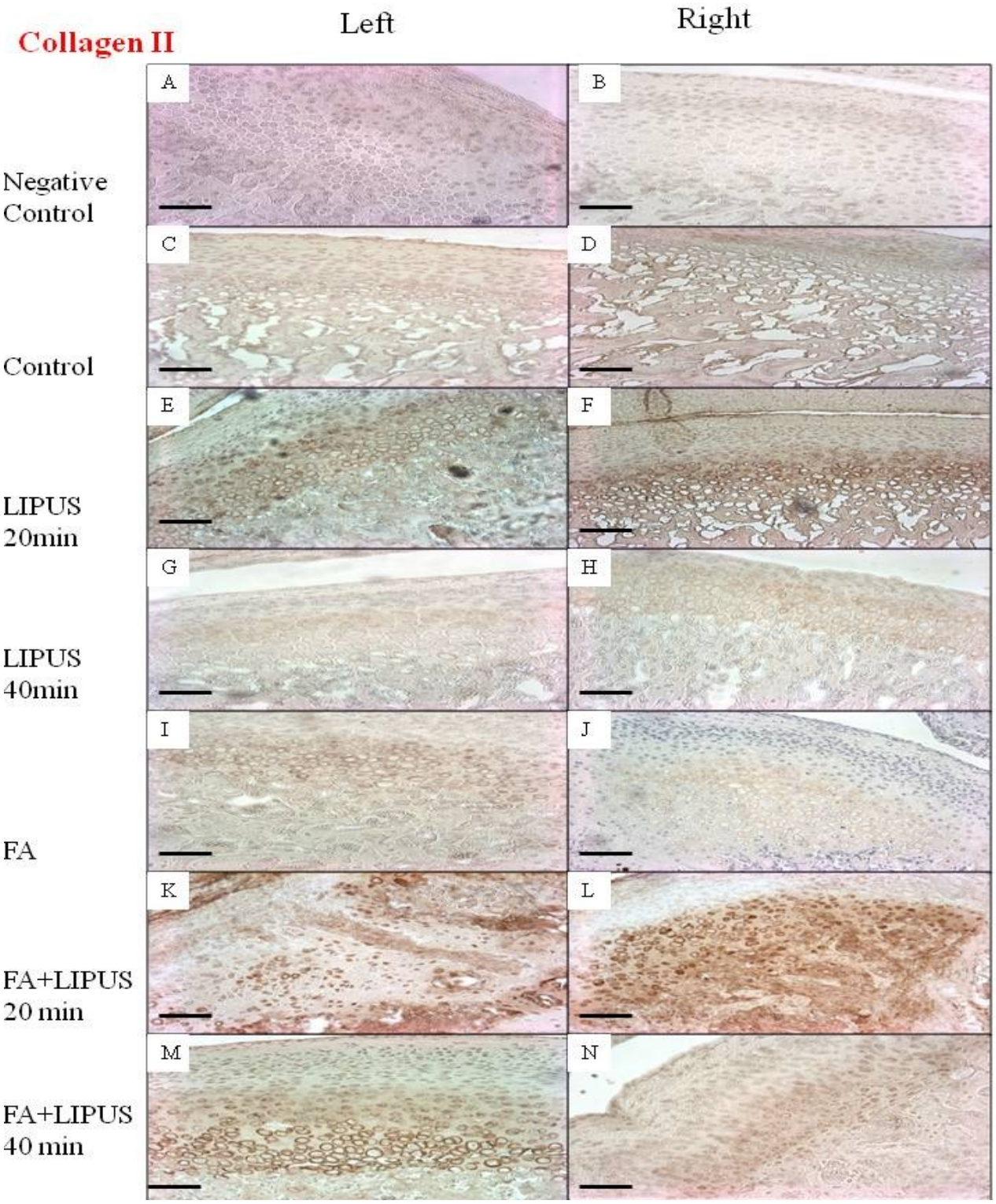

Fig 2.8.E: Expression of Collagen II in the left and right mandible condyles.

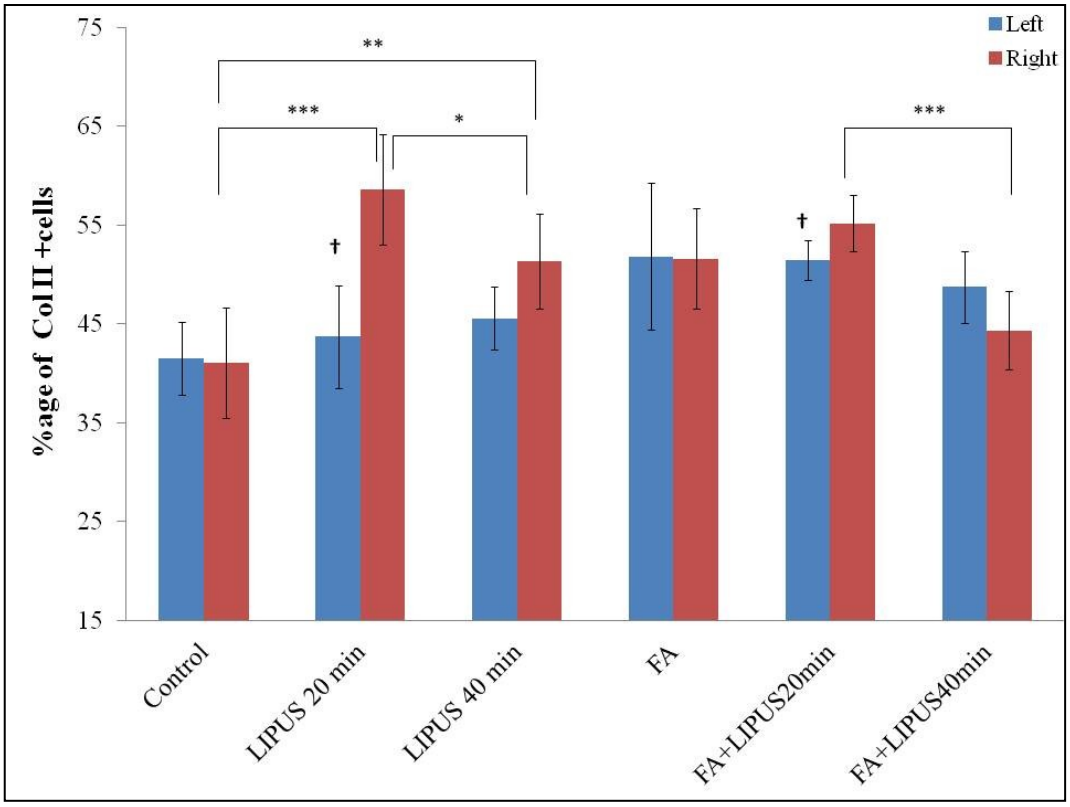

Fig 2.8.F: Bar graph depict the percentage of Collagen II immunopositive cells in the posterior part of the mandible condyle (*** p <0.0005, **p<0.005 and *p<0.05) (†p <0.05 between left and right side of the mandible condyle).

Collagen X: Collagen X is mainly expressed in the hypertrophic layer (Fig 2.8.G). LIPUS 20 min showed increased expression of Collagen X as compared to other treatment groups followed by LIPUS 40 min and FA + LIPUS 20 min and the difference is statistically significant ($p<0.05$). Between left and right side, same groups showed significant difference in Collagen X expression in the right side (Fig 2.8.H).

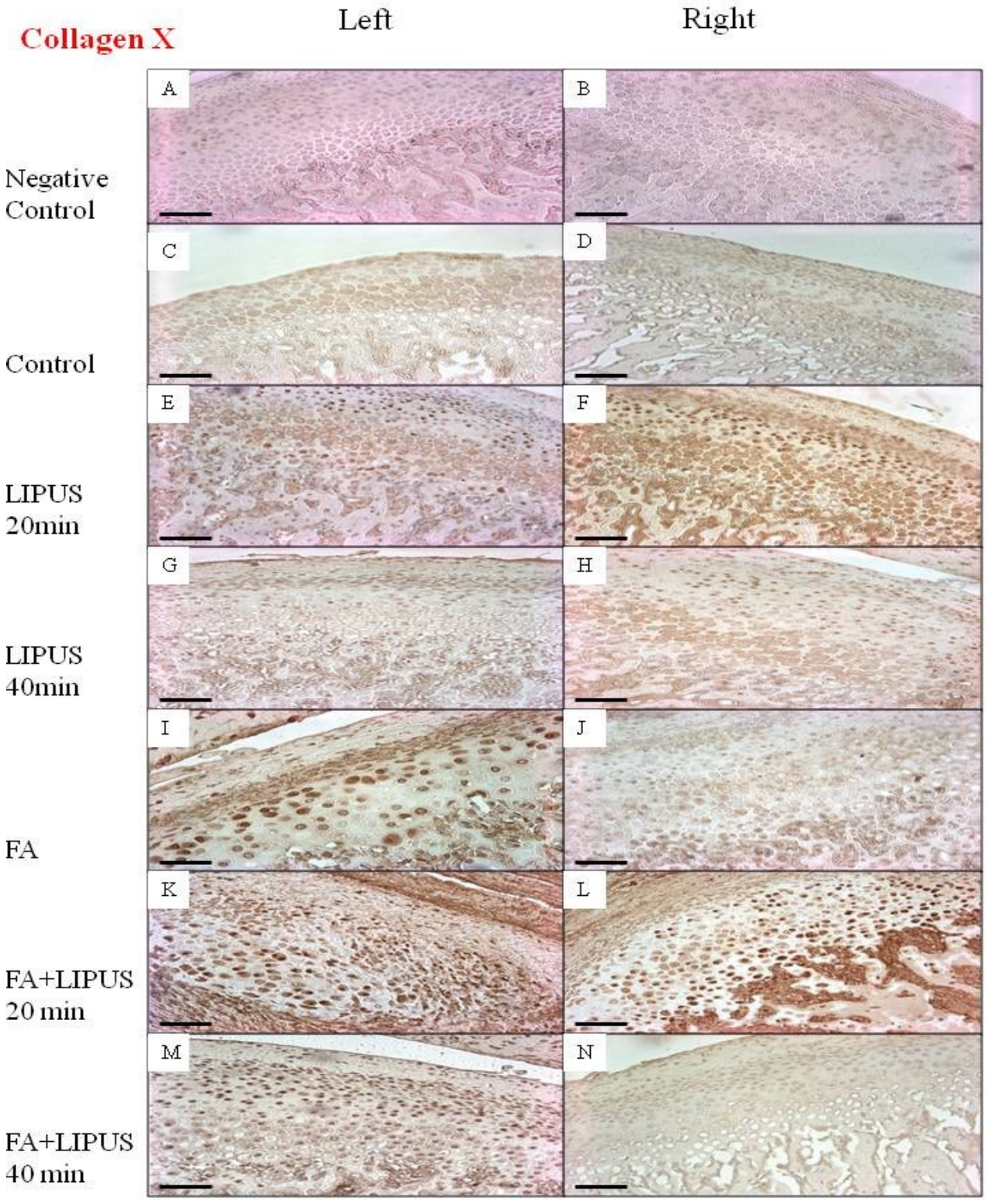

Fig 2.8.G: Expression of Collagen X in the left and right mandible condyles.

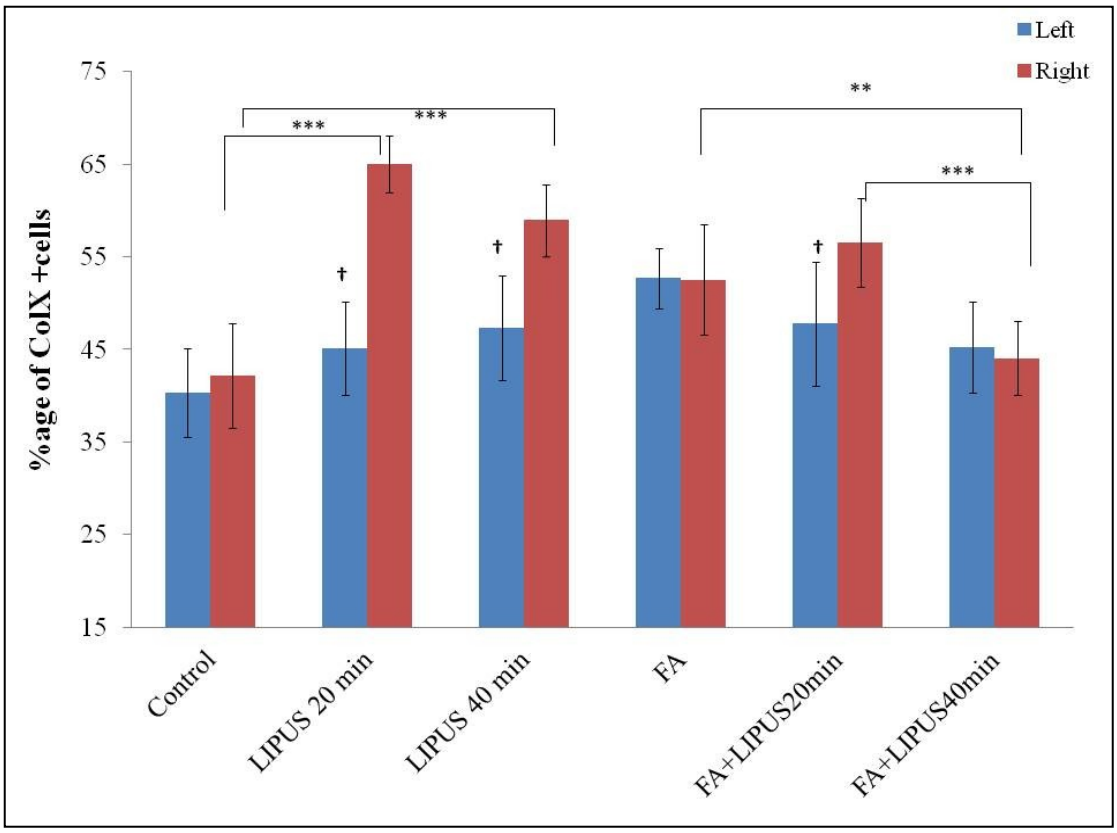

Fig 2.8.H: Bar graph depict the percentage of Collagen X immunopositive cells in the posterior part of the mandible condyle (*** p <0.0005, **p<0.005 and *p<0.05) (†p <0.05 between left and right side of the mandible condyle).

2.3.5 Micro-Computed Tomography (Micro CT) analysis:

There was a significant increase in BV/TV in the treatment groups with 20 min LIPUS application as compared to control. Both LIPUS 20 min and LIPUS 40 min groups showed the highest increase while FA + LIPUS 40 min group showed the lowest value for BV/TV (Fig 2.9.A). There was a significant difference between LIPUS 20 min group and the other treatment groups for Tb.Th (Fig 2.9.B). Tb.Sep showed the highest value in FA + LIPUS 40 min group and the difference was statistically significant (Fig 2.9.C). LIPUS 20 min group showed a significantly ($p<0.05$) higher Tb.N when compared with other groups, except for LIPUS 40 min group ($p>0.05$) (Fig 2.9.D). BMD showed significant increase in LIPUS 20 min group and the difference was statistically significant. FA + LIPUS 40 min group showed the lowest BMD value. Among the groups that received FA, there was no significant difference between the FA and FA + LIPUS 20 min groups ($p>0.05$), while there was a significant difference between FA + LIPUS 20 min and FA + LIPUS 40 min groups ($p<0.05$) (Fig 2.9.E). Right side of LIPUS 20 min, LIPUS 40 min and FA + LIPUS 20 min groups showed statistic significant increase in BV/TV, while LIPUS 20 min and FA + LIPUS 20 min showed significant increase in BMD and Tb.N values. Non treated side of FA + LIPUS 40 min showed significant increase in BV/TV, Tb.N and BMD values as compared to LIPUS treated right side. Tb. Sep showed no significant difference between the left and right side in all the six groups.

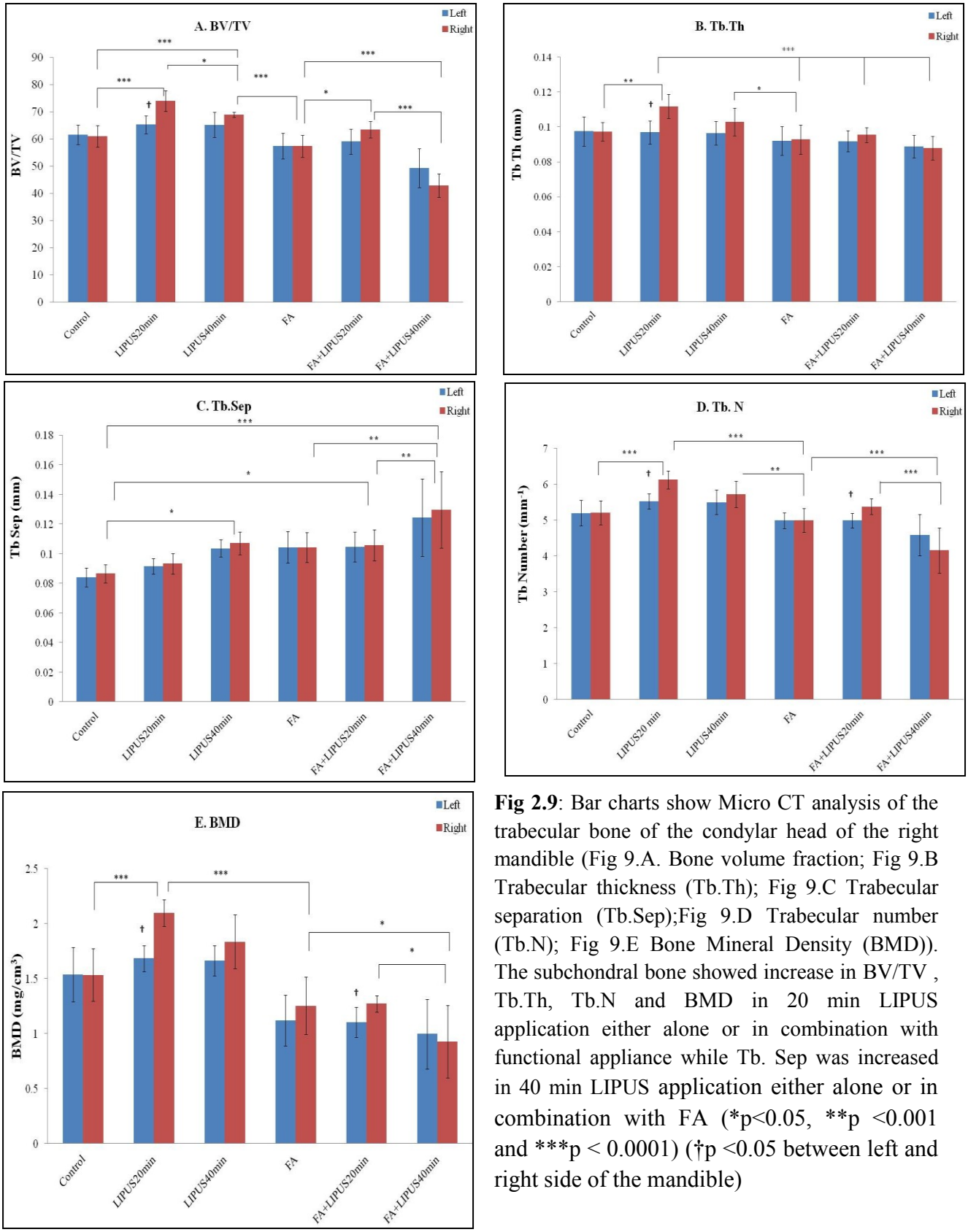

Fig 2.9: Bar charts show Micro CT analysis of the trabecular bone of the condylar head of the right mandible (Fig 9.A. Bone volume fraction; Fig 9.B Trabecular thickness (Tb.Th); Fig 9.C Trabecular separation (Tb.Sep);Fig 9.D Trabecular number (Tb.N); Fig 9.E Bone Mineral Density (BMD)). The subchondral bone showed increase in BV/TV , Tb.Th, Tb.N and BMD in 20 min LIPUS application either alone or in combination with functional appliance while Tb. Sep was increased in 40 min LIPUS application either alone or in combination with FA (*p<0.05, **p <0.001 and ***p < 0.0001) (†p <0.05 between left and right side of the mandible)

2.4 Discussion:

Morphometric results demonstrated that 20 min/day LIPUS application increased condylar and mandibular length and height in the young growing rats while 40 min/day LIPUS application either alone or in combination with FA showed insignificant results as compared to either control or 20 min/day LIPUS application. This is in contrast to other dose response studies reported (18)(19). The mandibular condyle is the primary growth center where the growth mainly takes place by endochondral ossification. Histologically, the condyle is divided into four zones; 1) the fibrous or articular layer which is the most superficial layer which is composed of dense collagen matrix; 2) the proliferative layer which contain undifferentiated mesenchymal cells; 3) the hypertrophic layer of mature chondrocytes and 4) the erosive layer where chondrogenesis ends and osteogenesis begins. In the present study, groups treated with LIPUS 20 min/day showed significant increase in the proliferative and hypertrophic cell numbers and the layer width and the results are supported by earlier published papers with both *in vitro* and *in vivo* where LIPUS application had stimulatory effect on chondrocytes proliferation and collagen synthesis (23)(24).

Bone is an essential part of the musculoskeletal system and is well connected to its surrounding muscles, which influence bone shape and strength via application of muscular forces. Trabecular bone comprises only 20% of bone, but its turnover rate is higher (approx 8 times) than that of cortical bone (25). Hence it is the primary site for detection of changes following any therapeutic treatment. Basic parameters studied for

trabecular micro-architecture are BV/TV, Tb.Th, Tb. N and Tb.Sep in 3D analysis. BV/TV is the ratios of volume of bone present (BV) to total volume of interest (TV) and is a surrogate measure of bone density (26). Bone mineral density (BMD) is volumetric density of calcium hydroxyapatite in the bone in terms of mg/cm^3 and is the best predictor of fracture risk.

Micro CT analysis demonstrated that 20 min/day LIPUS application either alone or with the FA had higher BV/TV, Tb.Th, Tb.N and BMD and lower Tb.Sp than the LIPUS 40 min and control groups. BV/TV values indicate that trabecular network is well connected and thus protecting overlying cortical bone. The well connected network is expected to better diffuse the load because of its structure and hence increases bone strength (26). Tb.Sp represents average distance between trabecular strands in the region of interest and was lower in 20 min/day treatment group and higher in LIPUS 40 min/day group. While 20 min/day LIPUS application has been already shown to create better bone formation in animals and clinical studies, some *in vitro* studies and distraction osteogenesis cases found that 40 min/day LIPUS application showed better results by increasing chondrogenic gene maker, extracellular matrix deposition (18) and enhancing bone regeneration in the distracted callus (19). In contrast to these studies, this study showed better micro-architecture of trabecular bone (and presumably more strength) with 20 min/day LIPUS application. This adverse effect could be due to a thermal effect of LIPUS when it was applied for 40 minutes (39, 40). Also, the longer period of anesthesia for 40 min/day LIPUS group could have had a negative effect on

general body growth, including the mandibular growth compared to LIPUS 20 min group, since a study by Kim et al (27) showed increased DNA damage caused by oxidative stress in rats exposed to Isoflurane anesthesia for 30 and 60 min.

The exact mechanism of action of LIPUS is still not fully understood, however, several possible mechanisms have been proposed. First, ultrasound waves cause movement of the fluid around the cells which could have an effect on cell permeability and activation of secondary messenger (28). Second, ultrasound waves cause mechanical pressure on the cell surface that could activate the stretch receptors of cation channels on cell membrane and affect intracellular gene expression (29). Third, since the bone has the ability to remodel depending on functional demands, the mechanical stresses produced by LIPUS application could help in remodeling of the bone micro architecture (30)(31).

Mechanical stresses induced by LIPUS can causes potential difference in osteoblasts and alter bone remodeling (32). Chondrocytes are mechanosensitive cells and mechanical forces are required for growth and maintenance of the cartilage. These stresses are sensed by transmembrane receptors-integrins, whose stimulation leads to intracellular signaling and hence affects chondrocytes activity. Previous studies have shown that mechanical stress produced by LIPUS increased gene expression and protein synthesis in chondrocytes and osteoblasts via integrin activation (33)(34). FA studies have also indicated the roles of integrin, mechanical forces and cellular proliferation in the condylar cartilage (35)(36). In these studies, an increase in integrin

expression and cellular proliferation was shown in cartilage with the use of FA. Hence, it could be hypothesized that LIPUS along with FA stimulated integrin receptors present on chondrocytes membrane and lead to increase in cellular proliferation and micro-architecture properties of trabecular bone as increase in hypertrophic chondrocytes has been closely related to subchondral bone.

40 min/day LIPUS application showed lower condylar growth as compared to the 20 min/day application. The detrimental effect could be due to thermal effect of LIPUS on the bone. Biological effect of LIPUS is due to a combination of thermal and non-thermal effects which depends on the energy density and is a product of ultrasound intensity applied and exposure time (37). In an *in-vitro* (38) and an *in vivo* study (37), 30 mW/cm^2 of LIPUS application showed 3°C increase in temperature after 20 min. It is possible that temperature increase could double after 40 min of LIPUS application. In our experiment, it was difficult to measure temperature because of the inaccessibility of intra-oral site. This could cause trauma in oral cavity in anesthetized rats as the mandibular condyle is located superiorly and posterior in the glenoid fossa of the skull and is covered with thick layer of oral tissue that requires deep dissection to reach the condyle. The thermal effect of 40 min/day LIPUS application might have resulted in cell destruction, decreased gene expression for bone protein and hence lower micro-architecture of trabecular bone. However, this postulation needs more experiments in vivo to test it. Alternatively, the longer anesthesia used in the LIPUS 40 min group might have affected general body growth including the condyles. Future studies in

higher animals that can use LIPUS with sedation (rather than anesthesia) or equal length of anesthesia for all groups (including control) might better reveal the role anesthesia plays on LIPUS effects.

One confounding factor in this study was the food consistency. Masticatory forces are important as they can stimulate bone remodeling. These forces are transmitted not only to the body and alveolar process but also to condylar head which affect its growth and remodeling (39). The rats that were fed with powdered diet in FA groups had reduced stimulatory effect as force required to cut and chew food was minimal when compared to the groups fed with normal pellet diet. There might not be enough mechanical load to stimulate bone structure in these groups. However decrease in the body weight of rats cannot be due to change in the food consistency since both food type had similar protein and fat content. In the study by Bozzini et al (40), in which the rats were given soft and hard pellet diet, no change in the total body weights were observed. Hence food consistency effect on body weight could be excluded. In this study, ultrasound was applied to one side of the mandible only, where as the FA treatment is usually bilateral. Hence, bilateral LIPUS application is recommended in future studies to get clinically relevant results. Moreover, psychological stress caused by FA and prolonged anesthesia i.e. 40 min as compared to 20 min might also have an effect on rat metabolism. Stress lead to increase in metabolism and hence body weight loss (40).

2.5 Conclusion:

Within the limitations of this study, 20 min/day LIPUS showed more growth in the condyle as compared to 40 min/day LIPUS application. The clinical application of LIPUS along with FA treatment will reduce orthodontic treatment duration. Before that, further long-term studies are advocated using similar diet in all groups to evaluate the combination effect of FA and LIPUS on the mandible condyle and to study the long term effects of combination therapy. Lastly, it will be important to follow the observed changes in temporal patterns for a longer duration of time, since bone is in a continuous process of remodeling.

2.6 References:

1. Delatte M, Von den Hoff JW, van Rheden REM, Kuijpers-Jagtman AM. Primary and secondary cartilages of the neonatal rat: the femoral head and the mandibular condyle. Eur J Oral Sci. 2004 Apr;112(2):156–62.

2. McNamara JA Jr. Components of class II malocclusion in children 8-10 years of age. Angle Orthod. 1981 Jul;51(3):177–202.

3. Ritto AK. Class II malocclusion: why, when and how to treat this anomaly in mixed dentition with fixed functional appliances. J Gen Orthod. 2001;12(4):9–21.

4. Proffit WR, Fields HW Jr, Moray LJ. Prevalence of malocclusion and orthodontic treatment need in the United States: estimates from the NHANES III survey. Int J Adult Orthodon Orthognath Surg. 1998;13(2):97–106.

5. Bock NC, Ruf S. Dentoskeletal changes in adult Class II division 1 Herbst treatment--how much is left after the retention period? Eur J Orthod. 2012 Dec;34(6):747–53.

6. Graber TM, Rakosi T, Petrovic AG. Dentofacial orthopedics with functional appliances. St. Louis: Mosby; 1997.

7. El-Bialy T, El-Shamy I, Graber TM. Growth modification of the rabbit mandible using therapeutic ultrasound: is it possible to enhance functional appliance results? Angle Orthod. 2003 Dec;73(6):631–9.

8. Cozza P, Baccetti T, Franchi L, De Toffol L, McNamara JA Jr. Mandibular changes produced by functional appliances in Class II malocclusion: a systematic review. Am J Orthod Dentofac Orthop Off Publ Am Assoc Orthod Its Const Soc Am Board Orthod. 2006 May;129(5):599.e1-12; discussion e1-6.

9. Pangrazio MNK, Pangrazio-Kulbersh V, Berger JL, Bayirli B, Movahhedian A. Treatment effects of the mandibular anterior repositioning appliance in patients with Class II skeletal malocclusions. Angle Orthod. 2012 Nov;82(6):971–7.

10. Owtad P, Park JH, Shen G, Potres Z, Darendeliler MA. The biology of TMJ growth modification: a review. J Dent Res. 2013 Apr;92(4):315–21.

11. Ustun Y, Erdogan O, Kurkcu M, Akova T, Damlar I. Effects of low-intensity pulsed ultrasound on dental implant osseointegration: a preliminary report. Eur J Dent. 2008 Oct;2(4):254–62.

12. Baker KG, Robertson VJ, Duck FA. A Review of Therapeutic Ultrasound: Biophysical Effects. Phys Ther. 2001 Jul 1;81(7):1351–8.

13. Doan N, Reher P, Meghji S, Harris M. In vitro effects of therapeutic ultrasound on cell proliferation, protein synthesis, and cytokine production by human fibroblasts, osteoblasts, and monocytes. J Oral Maxillofac Surg Off J Am Assoc Oral Maxillofac Surg. 1999 Apr;57(4):409–419; discussion 420.

14. Snyder BM, Conley J, Koval KJ. Does low-intensity pulsed ultrasound reduce time to fracture healing? A meta-analysis. Am J Orthop Belle Mead NJ. 2012 Feb;41(2):E12-19.

15. Dudda M, Hauser J, Muhr G, Esenwein SA. Low-intensity pulsed ultrasound as a useful adjuvant during distraction osteogenesis: a prospective, randomized controlled trial. J Trauma. 2011 Nov;71(5):1376–80.

16. El-Bialy T, Hassan A, Albaghdadi T, Fouad HA, Maimani AR. Growth modification of the mandible with ultrasound in baboons: a preliminary report. Am J Orthod Dentofac Orthop Off Publ Am Assoc Orthod Its Const Soc Am Board Orthod. 2006 Oct;130(4):435.e7-14.

17. El-Bialy T. Nonsurgical treatment of hemifacial microsomia by therapeutic ultrasound and hybrid functional appliance. Open Access J Clin Trials. 2010 Mar;29.

18. Schumann D, Kujat R, Zellner J, Angele MK, Nerlich M, Mayr E, et al. Treatment of human mesenchymal stem cells with pulsed low intensity ultrasound enhances the chondrogenic phenotype in vitro. Biorheology. 2006;43(3–4):431–43.

19. Chan CW, Qin L, Lee KM, Cheung WH, Cheng JCY, Leung KS. Dose-dependent effect of low-intensity pulsed ultrasound on callus formation during rapid distraction osteogenesis. J Orthop Res Off Publ Orthop Res Soc. 2006 Nov;24(11):2072–9.

20. Rabie ABM, She TT, Hägg U. Functional appliance therapy accelerates and enhances condylar growth. Am J Orthod Dentofacial Orthop. 2003 Jan;123(1):40–8.

21. Rabie AB, Zhao Z, Shen G, Hägg EU, Dr O, Robinson W. Osteogenesis in the glenoid fossa in response to mandibular advancement. Am J Orthod Dentofac Orthop Off Publ Am Assoc Orthod Its Const Soc Am Board Orthod. 2001 Apr;119(4):390–400.

22. Rabie ABM, Xiong H, Hägg U. Forward mandibular positioning enhances condylar adaptation in adult rats. Eur J Orthod. 2004 Aug;26(4):353–8.

23. Oyonarte R, Zárate M, Rodriguez F. Low-intensity pulsed ultrasound stimulation of condylar growth in rats. Angle Orthod. 2009 Sep;79(5):964–70.

24. Rawool NM, Goldberg BB, Forsberg F, Winder AA, Hume E. Power Doppler assessment of vascular changes during fracture treatment with low-intensity ultrasound. J Ultrasound Med Off J Am Inst Ultrasound Med. 2003 Feb;22(2):145–53.

25. Fajardo RJ, Müller R. Three-dimensional analysis of nonhuman primate trabecular architecture using micro-computed tomography. Am J Phys Anthropol. 2001 Aug;115(4):327–36.

26. Kazama JJ, Koda R, Yamamoto S, Narita I, Gejyo F, Tokumoto A. Cancellous bone volume is an indicator for trabecular bone connectivity in dialysis patients. Clin J Am Soc Nephrol CJASN. 2010 Feb;5(2):292–8.

27. Kim H, Oh E, Im H, Mun J, Yang M, Khim J-Y, et al. Oxidative damages in the DNA, lipids, and proteins of rats exposed to isofluranes and alcohols. Toxicology. 2006 Mar 15;220(2–3):169–78.

28. Sachs F. Mechanical transduction by membrane ion channels: a mini review. Mol Cell Biochem. 1991 Jun 29;104(1–2):57–60.

29. Bassett CA. Electrical effects in bone. Sci Am. 1965 Oct;213(4):18–25.

30. Behari J, Singh S. Ultrasound propagation in “in vivo” bone. Ultrasonics. 1981 Mar;19(2):87–90.

31. Schortinghuis J, Stegenga B, Raghoebar GM, de Bont LGM. Ultrasound stimulation of maxillofacial bone healing. Crit Rev Oral Biol Med Off Publ Am Assoc Oral Biol. 2003;14(1):63–74.

32. Schuster A, Schwab T, Bischof M, Klotz M, Lemor R, Degel C, et al. Cell specific ultrasound effects are dose and frequency dependent. Ann Anat Anat Anz Off Organ Anat Ges. 2013 Jan;195(1):57–67.

33. Whitney NP, Lamb AC, Louw TM, Subramanian A. Integrin-mediated mechanotransduction pathway of low-intensity continuous ultrasound in human chondrocytes. Ultrasound Med Biol. 2012 Oct;38(10):1734–43.

34. Cheng K, Xia P, Lin Q, Shen S, Gao M, Ren S, et al. Effects of Low-Intensity Pulsed Ultrasound on Integrin-FAK-PI3K/Akt Mechanochemical Transduction in Rabbit Osteoarthritis Chondrocytes. Ultrasound Med Biol. 2014 Jul;40(7):1609–18.

35. Marques MR, Hajjar D, Oliveira Crema V, Kimura ET, Santos MF. A mandibular propulsive appliance modulates collagen-binding integrins distribution in the young rat condylar cartilage. Biorheology. 2006;43(3–4):293–302.

36. Marques MR, Hajjar D, Franchini KG, Moriscot AS, Santos MF. Mandibular appliance modulates condylar growth through integrins. J Dent Res. 2008 Feb;87(2):153–8.

37. Xue H, Zheng J, Cui Z, Bai X, Li G, Zhang C, et al. Low-intensity pulsed ultrasound accelerates tooth movement via activation of the BMP-2 signaling pathway. PloS One. 2013;8(7):e68926.

38. Leskinen JJ, Hynynen K. Study of factors affecting the magnitude and nature of ultrasound exposure with in vitro set-ups. Ultrasound Med Biol. 2012 May;38(5):777–94.

39. Kuroda S, Tanimoto K, Izawa T, Fujihara S, Koolstra JH, Tanaka E. Biomechanical and biochemical characteristics of the mandibular condylar cartilage. Osteoarthr Cartil OARS Osteoarthr Res Soc. 2009 Nov;17(11):1408–15.

40. Bozzini C, Picasso E, Champin G, Bozzini CE, Alippi RM. Effect of physical consistency of food on the biomechanical behaviour of the mandible in the growing rat. Eur J Oral Sci. 2015 Sep 4;

41. Li Q, Zhang M, Chen Y-J, Zhou Q, Wang Y-J, Liu J. Psychological stress alters microstructure of the mandibular condyle in rats. Physiol Behav. 2013;110–111:129–39.

Chapter 3: Superoxide mediates Low Intensity Pulsed Ultrasound induced Mitogen Activated Protein Kinases activation in C28/I2 human chondrocytes.

3.1. Introduction:

Chondrocytes are mechanosensitive cells and are the only cells present in the cartilage. Their primary function is to synthesise and maintain the extracellular matrix of the cartilage. These cells are surrounded by an abundant extracellular matrix containing collagen and proteoglycan. Chondrocytes also participate in bone formation via the endochondral ossification process. In endochondral ossification, the chondrocytes undergo a chronological process of differentiation leading to cartilage formation which acts as a scaffold that is further replaced by bone. Mechanical loading of chondrocytes is important for growth and maintenance of cartilage and lead to an increase in the expression of the extracellular matrix genes (1). Chondrocytes in the articular cartilage environment experience a variety of mechanical stimuli during physiology movements like walking, exercising, mastication and speaking. Loading chondrocytes within physiological limits has an anabolic effect on the cells while either excessive or absence of mechanical load leads to cartilage destruction. Studies have showed reduced mechanical loading, such as animals fed on soft diet (2) or artificially immobilized (3), led to reduced compressive load which impacted not only the cartilage but also the underlying subchondral bone (4).

Low intensity pulsed ultrasound (LIPUS) is a form of an acoustic wave that produces micromechanical strain in the tissue through which it passes, leading to specific biochemical events (5) (6). In recent years, LIPUS stimulation has been employed to exert an anabolic effect on osteoblasts, on bone formation (7) (8), and to

augment new blood vessel formation in wound healing and bone fracture sites (9). LIPUS enhanced the expression of genes involved in matrix production, such as *SOX9*, *COL2A1*, and *ACAN*, and stimulating chondrogenesis and matrix production (10) (11). Because of its stimulatory effect on bone healing, LIPUS has been approved by USA Food and Drug Administration for treatment of delayed and non-union bone fracture. Previous studies have also reported on the stimulatory effect of LIPUS on the growth of the mandible condyle either alone or together with the orthopedic bite jumping appliance (12) (13) (14). LIPUS has shown to enhance lower jaw growth by stimulating chondrogenesis and increase ECM production. Because of its chondrogenic property, LIPUS has also been proposed for the treatment of early stage of OA (15) (16).

The exact mechanism for the beneficial effects of LIPUS is still not fully understood. Mechanical stimulation by LIPUS has shown to augment integrin expression (17), increase phosphoinositide 3 kinase (PI3K) activation (18), enhance actin polymerization (19) and increase mitogen-activated protein kinases (MAPKs) signaling (20). MAPKs are evolutionarily conserved signaling pathways that play an important role in various cellular processes like cell growth, differentiation, survival, and apoptosis. This multifunctional signaling pathway consists of three classes of serine/threonine kinases: extracellular signal regulated kinase 1/2 (ERK1/2), p38 and c-Jun N-terminal kinase (JNK). ERK1/2 is mainly activated by growth factors and mediates cell proliferation and differentiation while p38 and JNK are mainly activated by external stresses in the form of physical and chemical stimulation, X-Rays, heat,

shock and inflammatory cytokines like lipopolysacchrides (LPS), tumor necrotic factor α (TNF-α) and interleukin 1β (IL-1β) (21)(22). MAPK activation is a three-step process consisting of phosphorylation of MAP3K, which then activates and phosphorylates MAP2K and increases the activity of one or more MAPKs, i.e., ERK1/2, p38 and JNK. MAPK phosphatase (MKP) enzyme dephosphorylates and deactivates MAPK pathway.

Studies in the last decade have shown that MAPKs are regulated by the oxidation-reduction reactions that produce ROS like superoxide ($O_2\bullet^-$), hydrogen peroxide (H_2O_2), and hydroxyl radical (•OH). ROS are reactive molecules derived from the partial reduction of oxygen. In addition, they are intracellular second messengers in cell signaling as they are promptly generated, extremely diffusible, effortlessly metabolized and present in all cell types (23). The chief source of ROS in the cell is from the electron transport chain in mitochondria. However, owing to the presence of mitochondrial superoxide dismutase, superoxide levels are kept at a low level. Another source of ROS is NADPH oxidases (NOX), which are a group of seven plasma membrane-bound enzymes NOX 1-5, DUOX 1 and 2. These enzymes contain six transmembrane domains, two histidines, one heme and FAD and NADPH binding domains. NOX2 is the prototype of NOX enzyme and all other types are closely related to NOX2 while NOX4 showed only 39% similarity to NOX2. The main target of ROS in MAPK regulation is protein tyrosine phosphatase (PTP), which contains a cysteine residue in its active site. ROS induces oxidative modification of the active site cysteine by the formation of a disulfide bond (-S-S) causing inactivation of PTP thereby

increasing phosphorylation by tyrosine kinase (24). Previous studies have shown nitric oxide (NO) generation by LIPUS in osteoblasts (25), (26); and in endothelial cells (27), but there have not been reports of ROS generated from LIPUS.

In the present study, we hypothesized that LIPUS application affects ROS levels in chondrocytes and activates MAPKs pathway. To investigate this hypothesis, we employed C28/I2 human chondrocyte cell model, and investigated intracellular signalling involving MAPK as well as expression of genes affecting extracellular matrix turnover (*SOX9, ACAN and COL2A1*).

3.2. Materials and Methods:

3.2.1. Materials:

C28/I2 human chondrocytes cell line was a kind gift from Dr. Mary Goldring (Hospital for Special Surgery, Weill Medical College of Cornell University, NY, USA); Dulbecco's modified eagle's medium F12 (DMEM F12) with L-glutamine and 4-(2-hydroxyethyl)-1-piperazineethanesulfonic acid (HEPES), fetal bovine serum (FBS), and Dulbecco's phosphate buffered saline (DPBS) were purchased from Life technologies, NY, USA; penicillin and streptomycin (Hyclone GE, Uttah, USA). dihydroethidine (DHE), diphenylene iodonium (DPI), MTT [(3-(4, 5- dimethylthiazol–2-yl)-2, 5-diphenyltetrazolium bromide], chloroform, isopropanol, bovine serum albumin (BSA) all were purchased from Sigma Aldrich, MO, USA. Sodium dodecyl sulfate (SDS), polyacrylamide and nitrocellulose membrane were purchased from BioRad, Japan. High

capacity reverse transcription kit for cDNA preparation was purchased from Applied Biosystems, USA. For protein estimation, Pierce BCA protein assay kit was purchased from Thermo Fisher, USA. Enhanced chemiluminiscence (ECL) western blot reagent kit was purchased from GE Health Care.

3.2.2. Cell culture:

1.5 X 10^5 /ml C28/I2 human chondrocytes were cultures in 6 well plates in the medium containing DMEM/F12, 10% FBS and 50 units/ml of penicillin and 50 µg/ ml of streptomycin. Cells were incubated at 37º C in humid chamber with 5% CO_2 and cultured for 24 hours till the first LIPUS application. The cells were washed twice with DPBS and harvested after 1, 3, 6, 12 and 24 hours after LIPUS application. For ROS inhibition, cells were cultured with similar cell density and condition. Before the addition of DPI, cells were starved by removing the medium containing FBS and were replaced with DMEM/F12 only. DPI was added to DMEM/F12 at least 1 hour before LIPUS application.

3.2.3. Low intensity pulsed ultrasound application:

The cells were treated for 10 min and 20 min LIPUS while the control group received sham LIPUS transducer. The LIPUS device was custom made and was provided by SmileSonica Inc. (Edmonton, AB, Canada). The device generates 200 micro seconds burst of 1.5 MHz sine wave with repetition rate of 1 kHz and spatial averaged intensity of 30 mW/cm^2. The six well plates were placed on the surface of

transducer and coupling gel (SmileSonica Inc., Edmonton, AB, Canada) was applied between the LIPUS transducer and base of the six well plates for the transmission of ultrasound waves. The groups were: control DPI (-), LIPUS 10 min DPI (-) and LIPUS 20 min DPI (-). In DPI treatment, the groups were: control DPI (+), LIPUS 10 min DPI (+) and LIPUS 20 min DPI (+).

3.2.4. Dihydroethidine Fluorescence Assay:

The cells were washed with pre warmed (37ºC) DPBS solution and were suspended in DMEM/F12 (without phenol red) in the concentration of 1 X 10^5 cells/ ml in the presence or absence of DPI (10 µM). The suspended cells were incubated with DHE (25 µM) for 20 min in the incubator before LIPUS application. Cells were sonicated with LIPUS according to the treatment groups and 100 µl of cell suspension was collected from each sample in triplicates at 0, 15, 30, 45, 60, 90 and 120 min and were dispended in 96 black view plate. The fluorescence intensity was quantified using Tecan M2000 micro plate reader with excitation and emission wavelengths of 480 and 570 nm respectively.

3.2.5. Cell viability assay:

The cells were seeded on 6-well plate in the presence and absence of DPI and the readings were taken after 24 hrs of LIPUS application. MTT [(3-(4, 5- dimethylthiazol–2-yl)-2, 5- diphenyltetrazolium bromide] assay was used as a measure of cell viability. 800 µl of MTT solution (dissolved in Hank's Balanced Salt Solution HBSS using

concentration of 5 mg/ml) was added to each well containing 2 ml of the medium and incubated for 2 hrs at 37 C. The medium was replaced with 2 ml of dimethyl sulfoxide (DMSO) to dissolve MTT formazan crystals. The optical density was measured at 570 nm using Tecan M2000 micro plate reader.

3.2.6. Real-time quantitative polymerase chain reaction:

Total RNA was prepared using TRIzol reagent according to the manufacturer's instructions. RNA concentration was measured using NanoDrop 2000C spectrophotometer. First strand of cDNA was synthesized from 1µg total RNA by using High Capacity cDNA Reverse Transcriptase kit following the kit instruction in the reaction volume of 20 µl. After reverse transcription reaction, 1 out of 10 dilutions were made from the template to be used in real time PCR. 10 µl real time reaction mixture consisting of 3 µl of cDNA, 1 µl each of forward and reverse primers and 5 µl of the master mix containing SYBR green dye. The mixtures were heated at 95º C for 2 min before going through 40 cycles of denaturation step (15 sec. at 95º C) and an annealing step (1 min at 60º C) using 7500 Real-Time PCR system during which the data were collected. Glyceraldehyde-3-phosphate dehydrogenase (GAPDH) was used as an internal control in each run. Normalized fluorescence was plotted against cycle number (amplification plot), and the threshold suggested by the software was used to calculate Ct (cycle at threshold). ΔΔ Ct analysis was used to determine the differences in gene expression as compared to the control. Primer sequences listed in Table 3.1.

Table 3.1: Primers sequence used in RT qPCR analysis.

	Primer	Direction	Primer Sequence (5' to 3')
1	*SOX9*	Forward	GCTCTGGAGACTTCTGAACGA
		Reverse	GCGGCTGGTACTTGTAATCC
2	*ACAN*	Forward	GTGGTGATGATCTGGCACGA
		Reverse	CGTTTGTAGGTGGTGGCTGT
3	*COL2A1*	Forward	AACCAGGACCAAAGGGACAG
		Reverse	TCTGGGTCCTTGTTCCCCTG
4	*NOX2*	Forward	CAACACATTCAACCTCTGCCA
		Reverse	CCCCAGCCAAACCAGAATGAC
5	*NOX4*	Forward	ACACCTCTGCCTGTTCATCT
		Reverse	GTGATACTCTGGCCCTTGGT
6	*GAPDH*	Forward	GAAGTCAGGTGGAGCGAGG
		Reverse	GCCCAATACGACCAAATCAGAG

3.2.7 Immunoblotting:

For the western blotting analysis, the cells were cultured for 1, 3, 6, 12 and 24 hrs after single ultrasound exposure. The cells were then washed with cold PBS twice and then lysed using NP-40 lysis buffer (50mM Tris-pH8.0, 150mM NaCl, 1% NP-40 and freshly added 10^{-6} M Protease inhibitor). The lysates were used as samples after centrifugation. Total protein concentration was determined using Pierce BCA kit (Thermo Fisher) and SDS polyacrylamide gel electrophoresis (PAGE) was performed for 25 µg of each protein. After SDS-PAGE, proteins were transferred onto a nitrocellulose membrane. The membrane was blocked for 1 h at room temperature with 5% Bovine serum albumin in 1% tri-buffered saline-tween (TBS-T) (Sigma-Aldrich, St. Louis, MO, USA) and incubated overnight at 4 ºC with primary antibody (Total ERK1/2, phospho ERK1/2, Total p38, phospho p38, Total JNK and phospho JNK Cell Signaling Technology, Boston, MA, USA), diluted 1 to 1000 with 5% BSA in 1% TBS-Tween. After incubation with HRP-conjugated anti-rabbit IgG (1:3000, Cell Signaling Technology) for 1hour at room temperature, the blots were detected with Amersham ECL Western Blotting detection reagent and quantified using Image J software.

3.2.8. Statistical analysis:

The data was summarized as mean ± standard deviation where the error bars represent standard deviation. All data were tested for normal distribution (Kolmogorov Smirnoff test) and equal variance (Levene's test) using SPSS software version SPSS 21.0 (Chicago, IL, USA). Two statistical tests were applied: a) Two-way repeated

measure analysis of variance (ANOVA) was used followed by Bonferroni test as post hoc to study significance for treatment and time. b) To study the effect of DPI at each time point, One-way ANOVA followed by Bonferroni post hoc test was used. The level of significance was set at $p< 0.05$.

3.3. Results:

3.3.1. Effect of LIPUS on ROS generation:

To determine whether LIPUS stimulation induced ROS generation in C28/I2 chondrocyte, we first suspended the cells, in the concentration of 1 X 10^5 cells/ml, in DMEM/F12 (without phenol red) in the presence or absence of DPI (10 μM) and added DHE (25 μM). The cell suspension was incubated for 30 min and treated with LIPUS according to the assigned treatment groups. The solution was collected at 0', 15 min, 30 min, 45 min, 60 min, 90 min and 120 min after LIPUS application. In DPI non-treated groups, LIPUS showed increase in the ROS generation as compared to control DPI (-), indicating the ability of LIPUS to increase ROS levels. From 30 min time point onward, LIPUS 10 min DPI (-) showed statistically increased ROS levels as compared to the other groups. In DPI treated groups, the levels of ROS in LIPUS treated groups (both 10 and 20 min) was reduced as compared to DPI (-) groups, indicating active quenching of the ROS by the DPI. Effect of LIPUS and DHE on cellular ROS levels as a function of time is shown in Fig 3.1

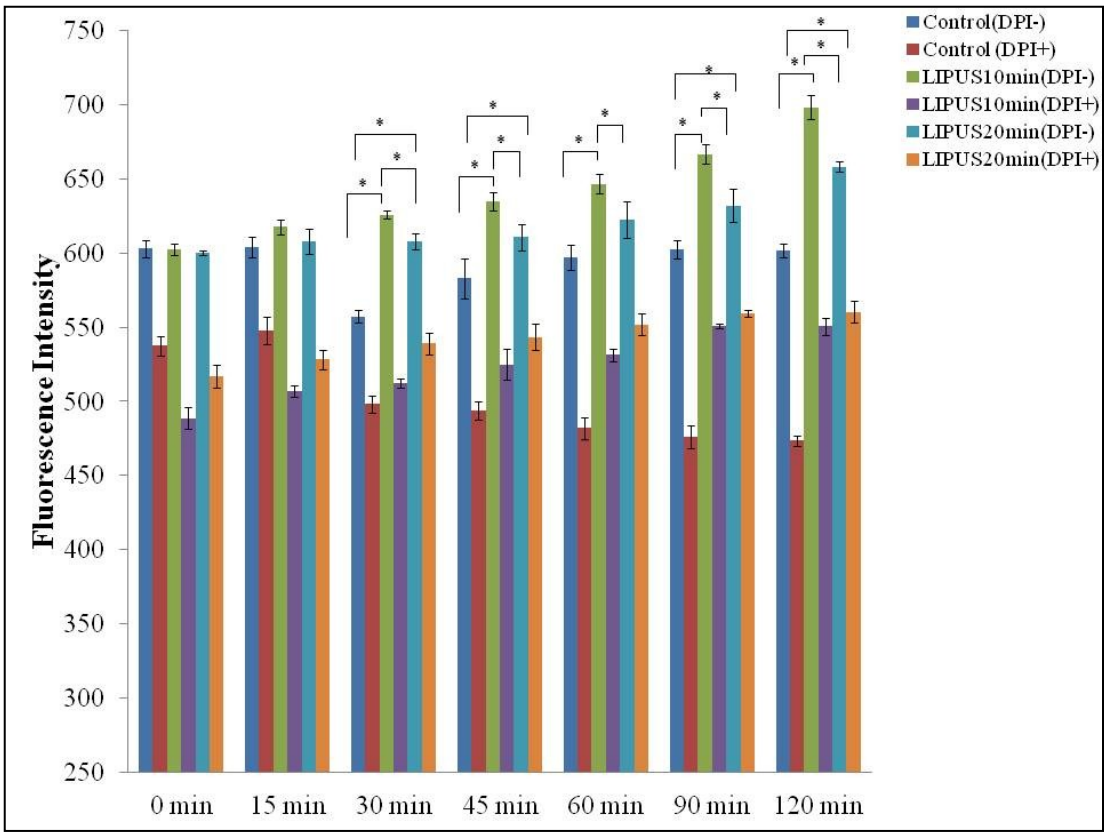

Fig 3.1: Effect of LIPUS stimulation on ROS generation. C28/I2 chondrocytes were suspended in DMEM/F12 (without phenol red) in the concentration of $1X10^5$cells/ml and incubated with DHE (25 µM). For ROS inhibitor, DPI (10 µM) was added to the cell suspension prior to DHE. The cells were treated with LIPUS and the samples were collected at time points- 0', 15', 30', 45', 60', 90' and 120' after LIPUS application. The values (mean ±SD) represent fluorescence unit. LIPUS application showed significant increase in ROS generation from 30' onwards while DPI treated groups showed significant reduction in ROS generation. (* $p<0.05$)

3.3.2. LIPUS effect on C28/I2 cell viability:

We speculated that the amount of ROS generated by LIPUS stimulation is non-toxic to the cells. Thus, we tested the effect of LIPUS on the cell viability in the presence and absence of DPI. After one day of LIPUS application, there was significant increase in cell viability in the group treated with LIPUS 10 min DPI (-) as compared to other groups. In DPI treated groups, there was significant decrease in the cell viability as compared to DPI non treated groups (Fig 3.2).

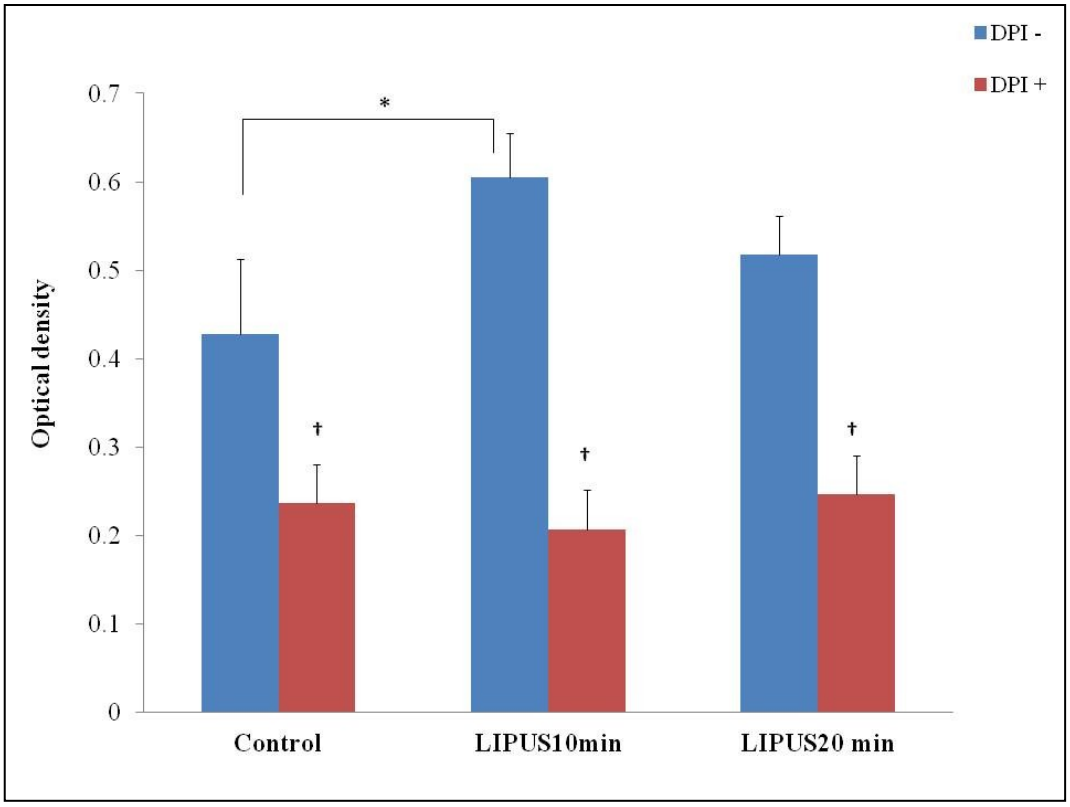

Fig 3.2: Detection of C28/I2 chondrocytes cell viability after LIPUS application using MTT absorbance assay. After 24 hrs of LIPUS application in the presence and absence of DPI (10 μM), the chondrocytes were incubated in MTT solution (5mg/ml) for 2 hrs. Formazan crystals formed were dissolved in DMSO and absorbance was measured. Values in the bar graph are presented as mean± SD. LIPUS stimulation showed significant increase in cell viability as compared to control while DPI treated groups showed significant decrease in cell viability. (* $p<0.05$; † $p<0.05$ between the corresponding DPI treated and non-treated groups.)

3.3.3. Effect of LIPUS on NOX2 and NOX4 gene expression:

To study whether LIPUS stimulation increased *NOX2* and *NOX4* generation, C28/I2 cells were stimulated with LIPUS in the presence or absence of DPI and the samples were collected at 1, 3, 6, 12 and 24 hrs after LIPUS application. In DPI non-treated groups, LIPUS showed significant increase in *NOX2* mRNA expression at 1, 12 and 24 hrs while in DPI treated groups LIPUS showed increased *NOX2* gene expression at 1 and 12 hrs time points. There was no significant effect of LIPUS on *NOX4* gene expression except at 3 hour time point. (Fig 3.3 and 3.4)

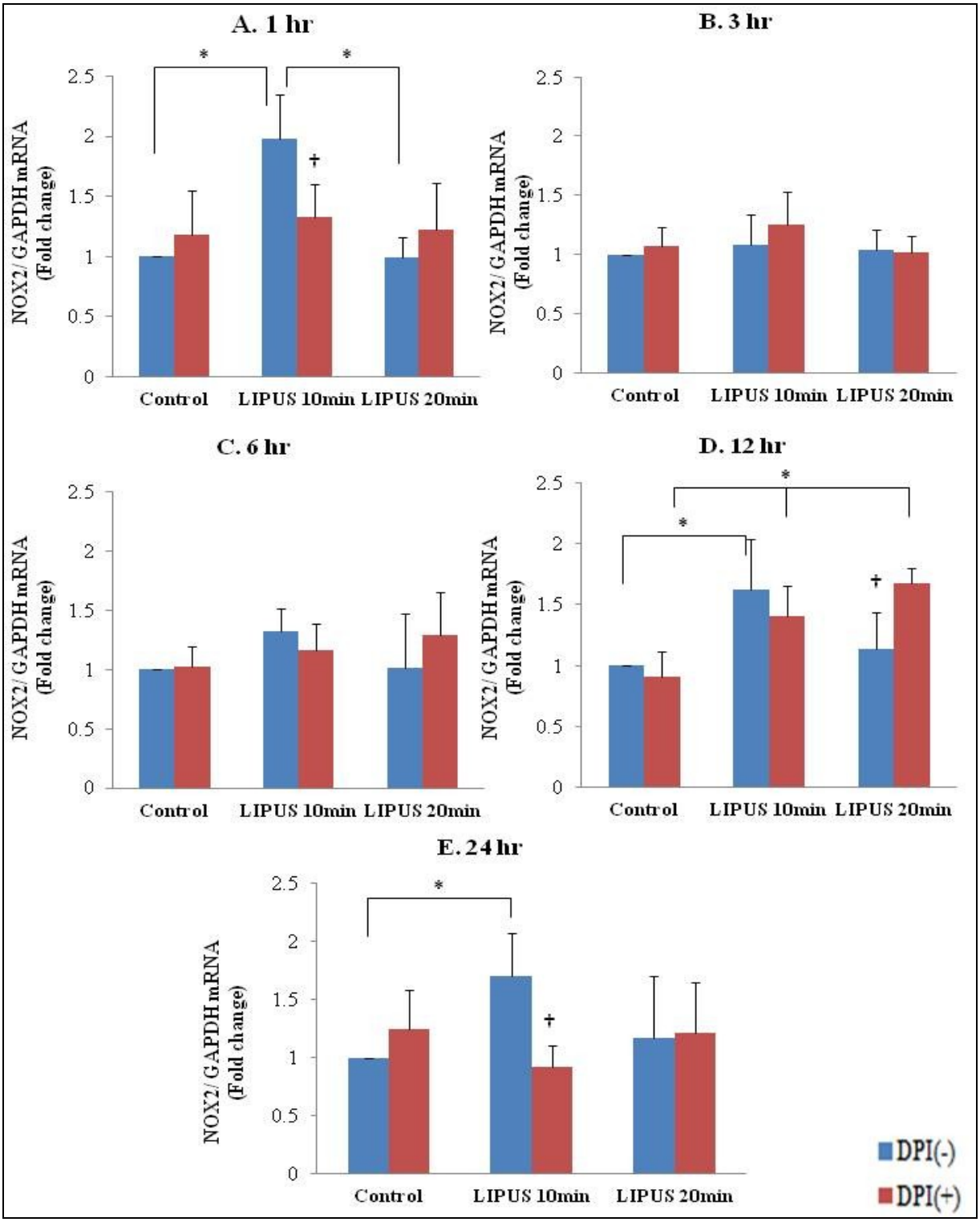

Fig 3.3: NOX2 mRNA expression quantified using RT-qPCR in C28/I2 chondrocytes after LIPUS application in the presence or absence of DPI (10 μM). The samples were collected after A. 1hr, B. 3hr, C. 6hr, D. 12hr and E. 24 hr of LIPUS application. Bar graph showed significant

increase in NOX2 mRNA expression during 1 hour LIPUS application in DPI non-treated group while there was significant increase at 12 hour time point in DPI treated group. (* $p<0.05$; † $p<0.05$ between the corresponding DPI treated and non-treated groups.)

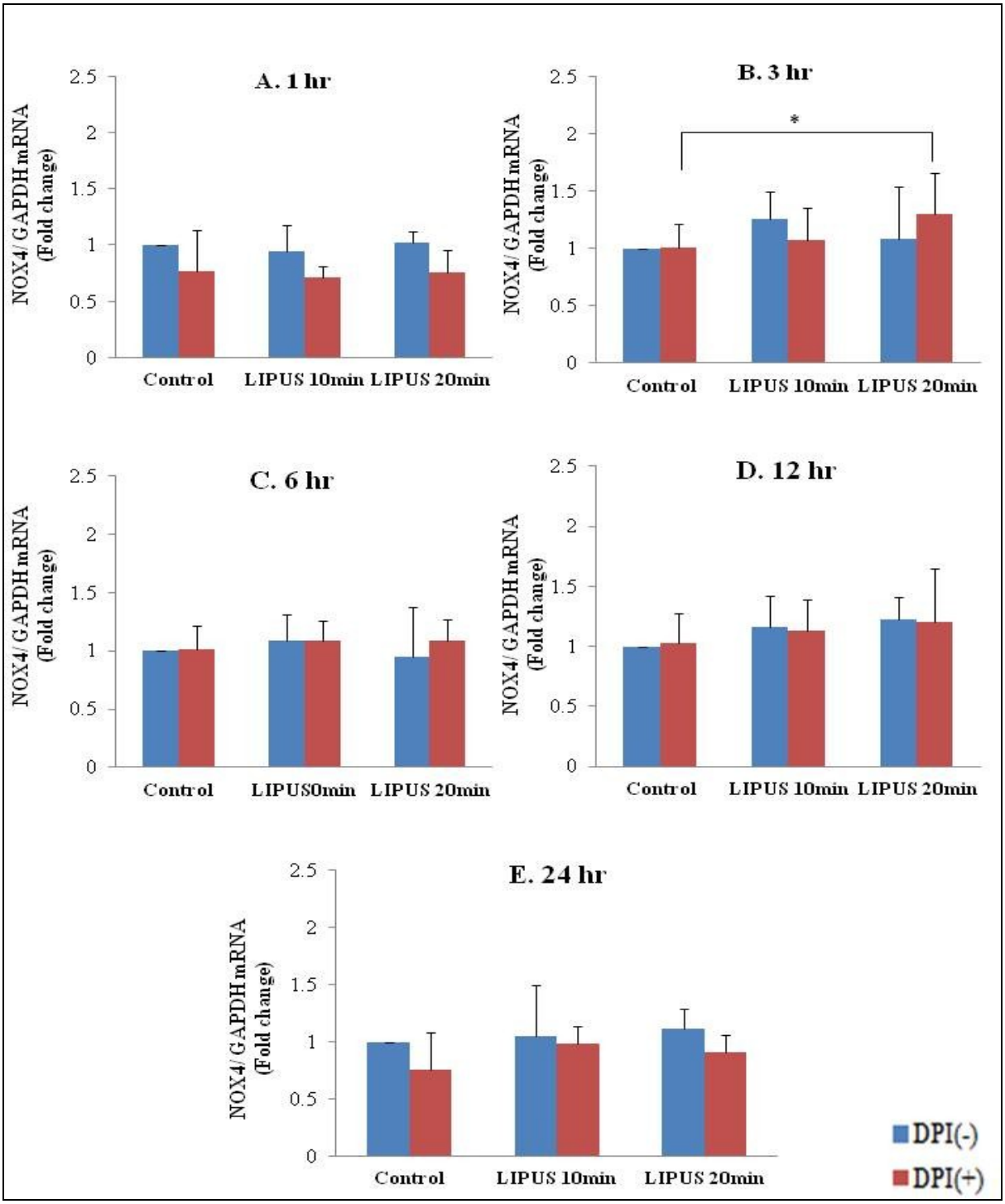

Fig 3.4: NOX4 mRNA expression quantified using RT-qPCR in C28/I2 chondrocytes after LIPUS application in the presence or absence of DPI (10 μM). The samples were collected after A. 1hr, B. 3hr, C. 6hr, D. 12hr and E. 24 hr of LIPUS application. Bar graph showed no significant difference in NOX4 mRNA expression in DPI non-treated group while there was significant increase at 3 hr time point in DPI treated group. (* $p<0.05$; † $p<0.05$ between the corresponding DPI treated and non-treated groups.)

3.3.4. SOX9, ACAN and COL2A1 gene expression with LIPUS stimulation:

In order to study the effect of LIPUS on C28/I2 chondrocytes in the presence or absence of DPI, the gene expression of chondrocytes specific markers i.e. *SOX9*, *ACAN* and *COL2A1* were analyzed. *SOX9* expression was significantly higher at 6 hrs in LIPUS groups as compared to the control in DPI non treated groups. *SOX9* expression was higher at 1 hr in LIPUS 20 min DPI (+) as compared to control and the expression level decreased at later time points (Fig 3.5). *ACAN* and *COL2A1* mRNA expression were higher in LIPUS groups at 12 and 24 hrs in DPI non-treated groups. While there was no significant changes in DPI treated groups at any time points in case of *ACAN* mRNA expression. For *COL2A1* expression, LIPUS groups showed significant increase at 24 hrs in DPI treated groups (Fig 3.6 and 3.7).

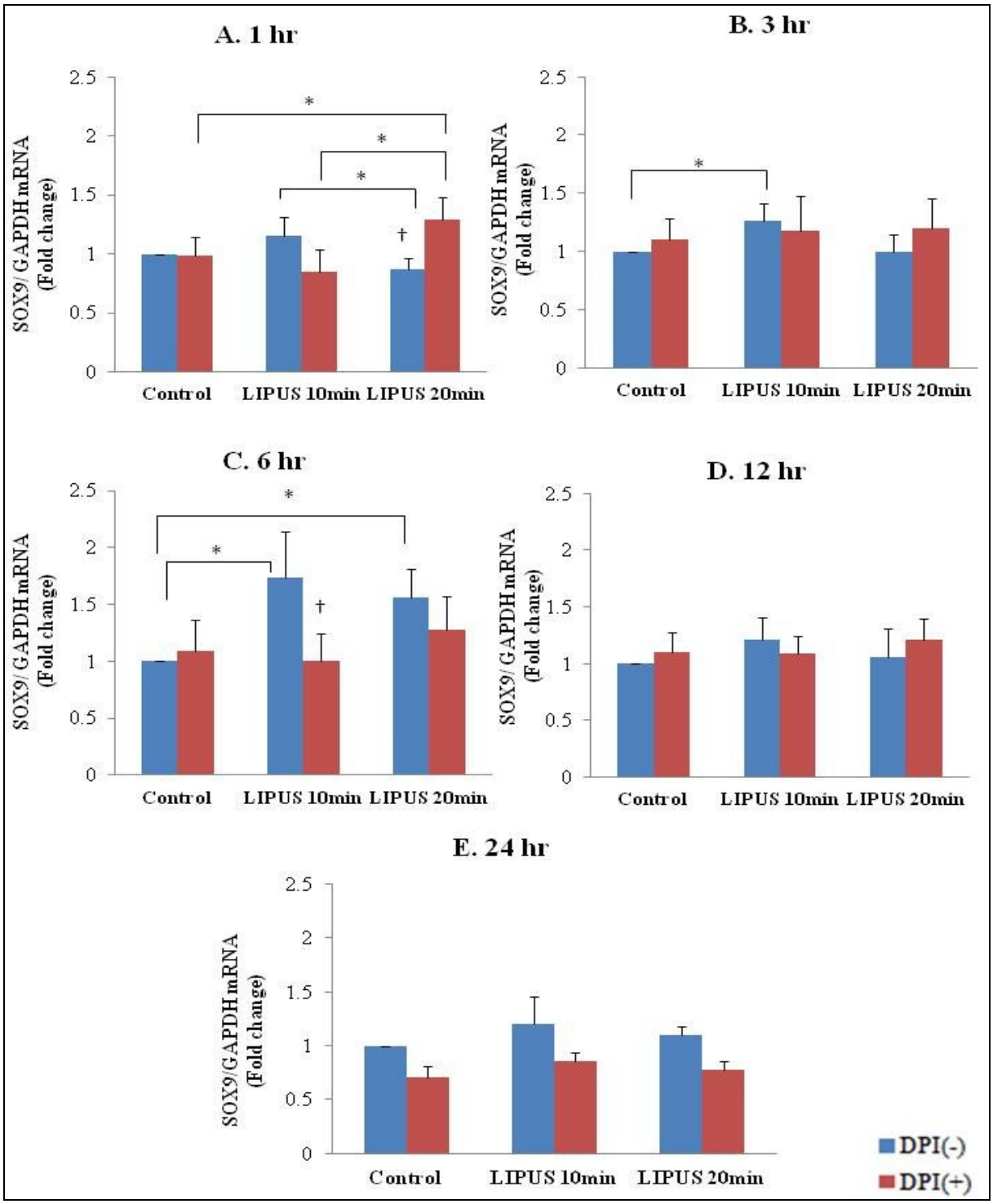

Fig 3.5: *SOX9* mRNA expression quantified using RT-qPCR in C28/I2 chondrocytes after LIPUS application in the presence or absence of DPI (10 µM). The samples were collected after A. 1hr, B. 3hr, C. 6hr, D. 12hr and E. 24 hr of LIPUS application. Bar graph showed significant increase in *SOX9* mRNA expression at 1, 3 and 6 hrs time points in LIPUS treated group as compared to control. (* $p<0.05$; † $p<0.05$ between the corresponding DPI treated and non-treated groups.)

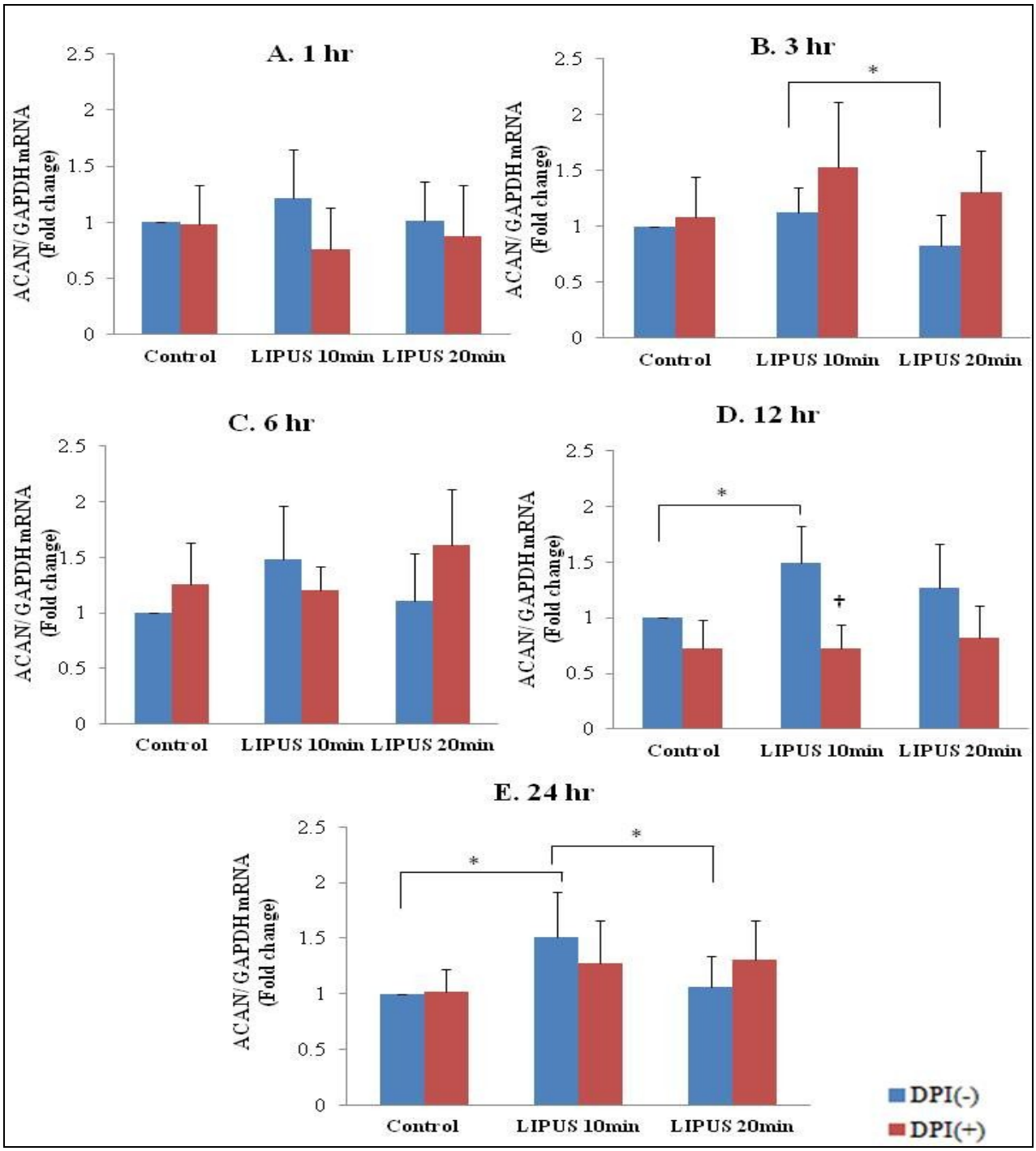

Fig 3.6: *ACAN* mRNA expression quantified using RT-qPCR in C28/I2 chondrocytes after LIPUS application in the presence or absence of DPI (10 µM). The samples were collected after A. 1hr, B. 3hr, C. 6hr, D. 12hr and E. 24 hr of LIPUS application. Bar graph showed significant increase in *ACAN* mRNA expression at 12 and 24 hrs time points in LIPUS treated group as compared to control in DPI non-treated groups. DPI treated groups showed no significant difference at any time pint. (* $p<0.05$; † $p<0.05$ between the corresponding DPI treated and non-treated groups.)

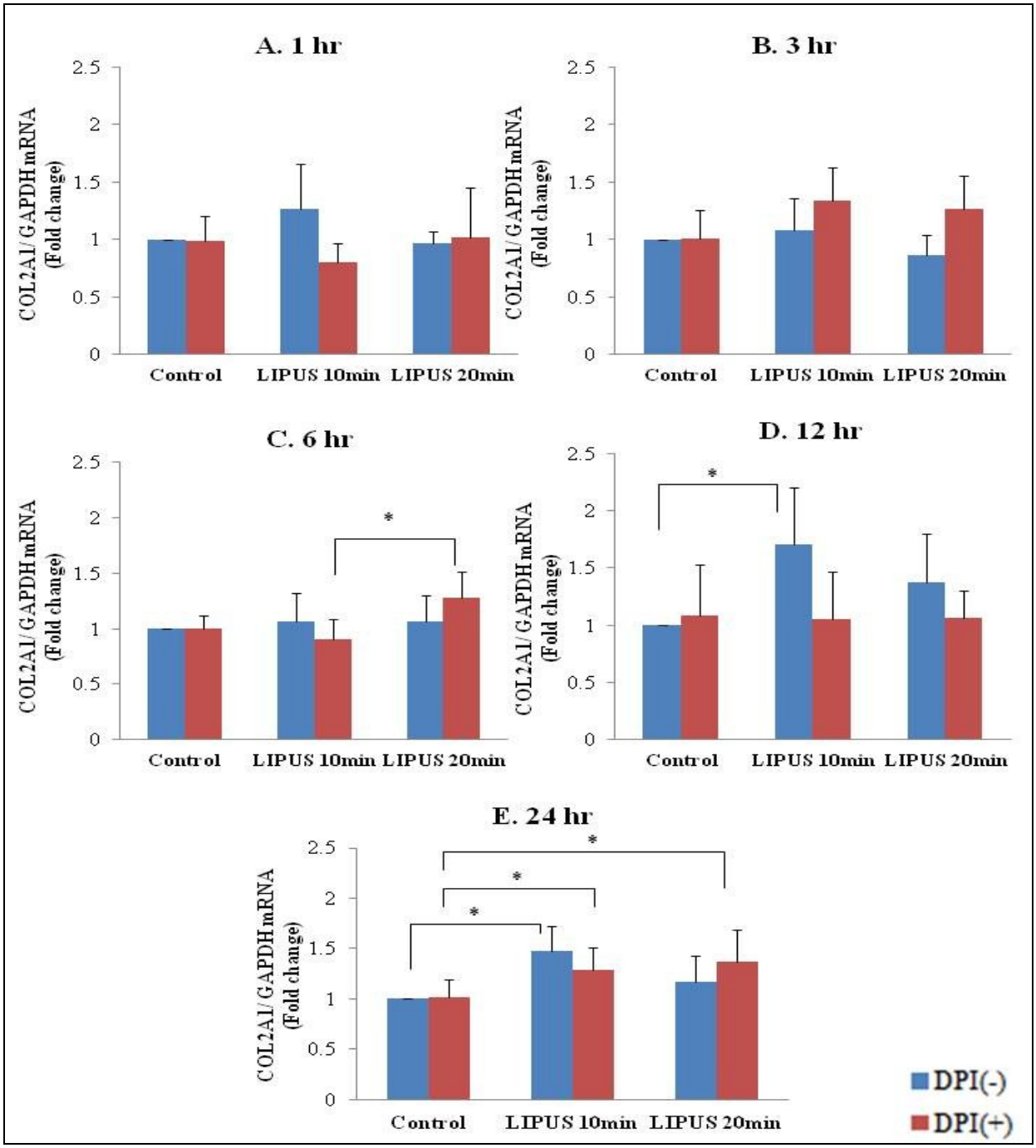

Fig 3.7: RT-qPCR analysis of *COL2A1* mRNA expression in C28/I2 chondrocytes after LIPUS application in the presence or absence of DPI (10 μM). The samples were collected after A. 1hr, B. 3hr, C. 6hr, D. 12hr and E. 24 hr of LIPUS application. Bar graph represents the values in mean ± SD. The graph showed significant increase in *COL2A1* expression at 12 and 24 hrs time points in LIPUS treated group as compared to control in DPI non-treated groups. DPI treated groups showed no significant difference at any time pint. (* $p<0.05$; † $p<0.05$ between the corresponding DPI treated and non-treated groups.)

3.3.5. MAPKs activation with LIPUS stimulation:

In order to examine the effect of LIPUS application and ROS generation on MAPKs phosphorylation, the cells were stimulated with LIPUS in the presence and absence of DPI. ERK1/2 phosphorylation was significantly increased at 6 and 12 hrs after LIPUS application while in DPI treated groups, there was significant reduction in ERK1/2 phosphorylation after 1 hr and the phosphorylation level reduced further on the following time points (Fig 3.8). On the other hand, p38 and JNK phosphorylation showed no significant changes on all the studied time points both in DPI treated and non-treated groups (Fig 3.9 and 3.10).

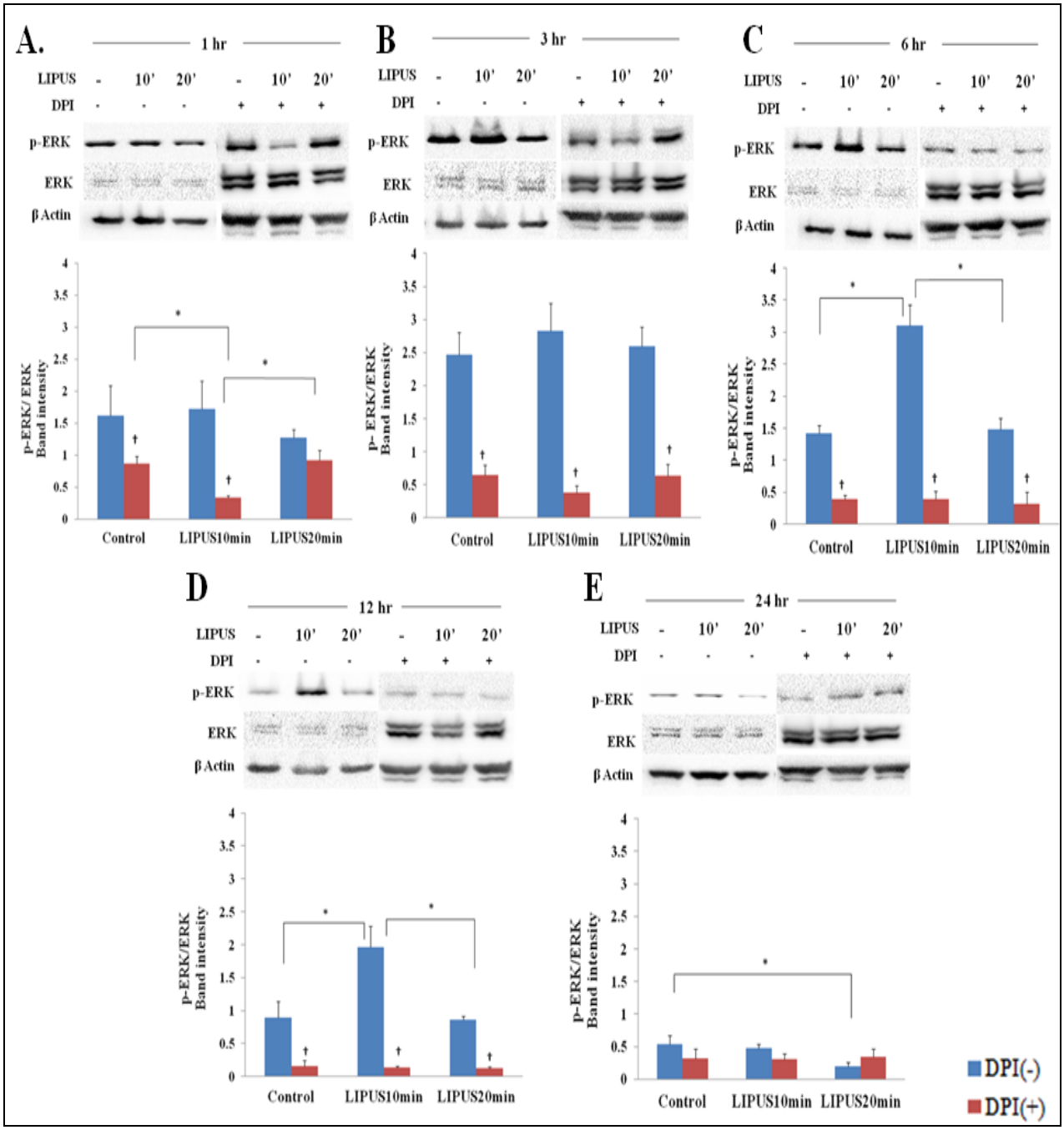

Fig 3.8: Immunoblot analysis of ERK1/2 activation by LIPUS application. C28/I2 chondrocytes were treated with LIPUS in the presence or absence of DPI (10 μM). The samples were harvested for immunoblot analysis after A. 1hr, B. 3hr, C. 6hr, D. 12 hr and E. 24 hrs of LIPUS application. Phosphorylation level of ERK1/2 relative to total ERK1/2 was determined by the quantification of the band intensity using ImageJ software. LIPUS groups showed significant increase in the phosphorylation level at 6 hr and 12 hr time point in DPI non-treated group while phosphorylation level significantly decreased in DPI treated group. (* $p<0.05$; † $p<0.05$ between the corresponding DPI treated and non-treated groups.)

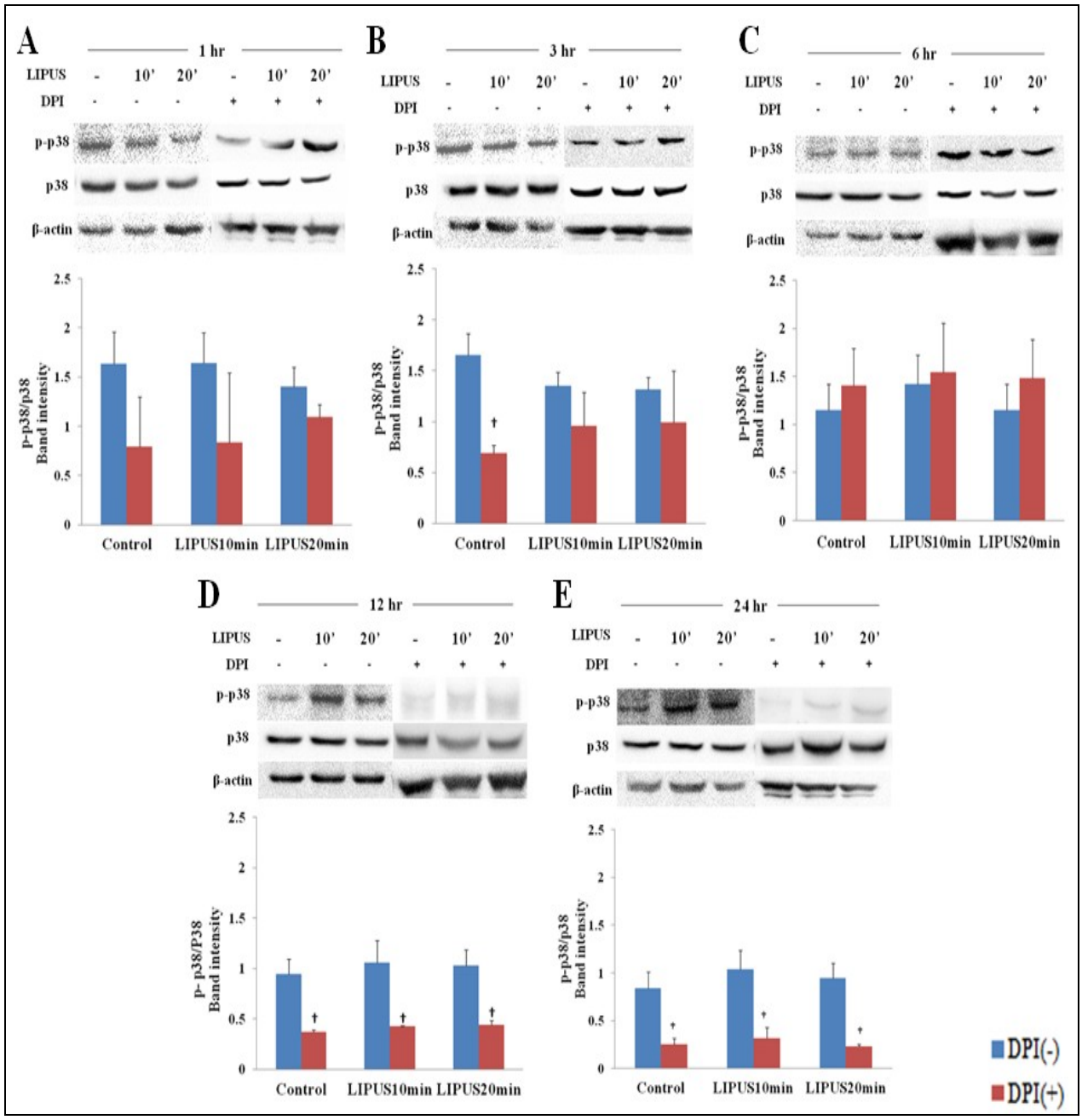

Fig 3.9: Immunoblot analysis of p38 activation by LIPUS application. C28/I2 chondrocytes were treated with LIPUS in the presence or absence of DPI (10 μM). The samples were harvested for immunoblot analysis after A. 1hr, B. 3hr, C. 6hr, D. 12 hr and E. 24 hrs of LIPUS application. LIPUS stimulation showed no significant difference in the phosphorylation level at any time point in DPI treated and non-treated groups. (* $p<0.05$; † $p<0.05$ between the corresponding DPI treated and non-treated groups.)

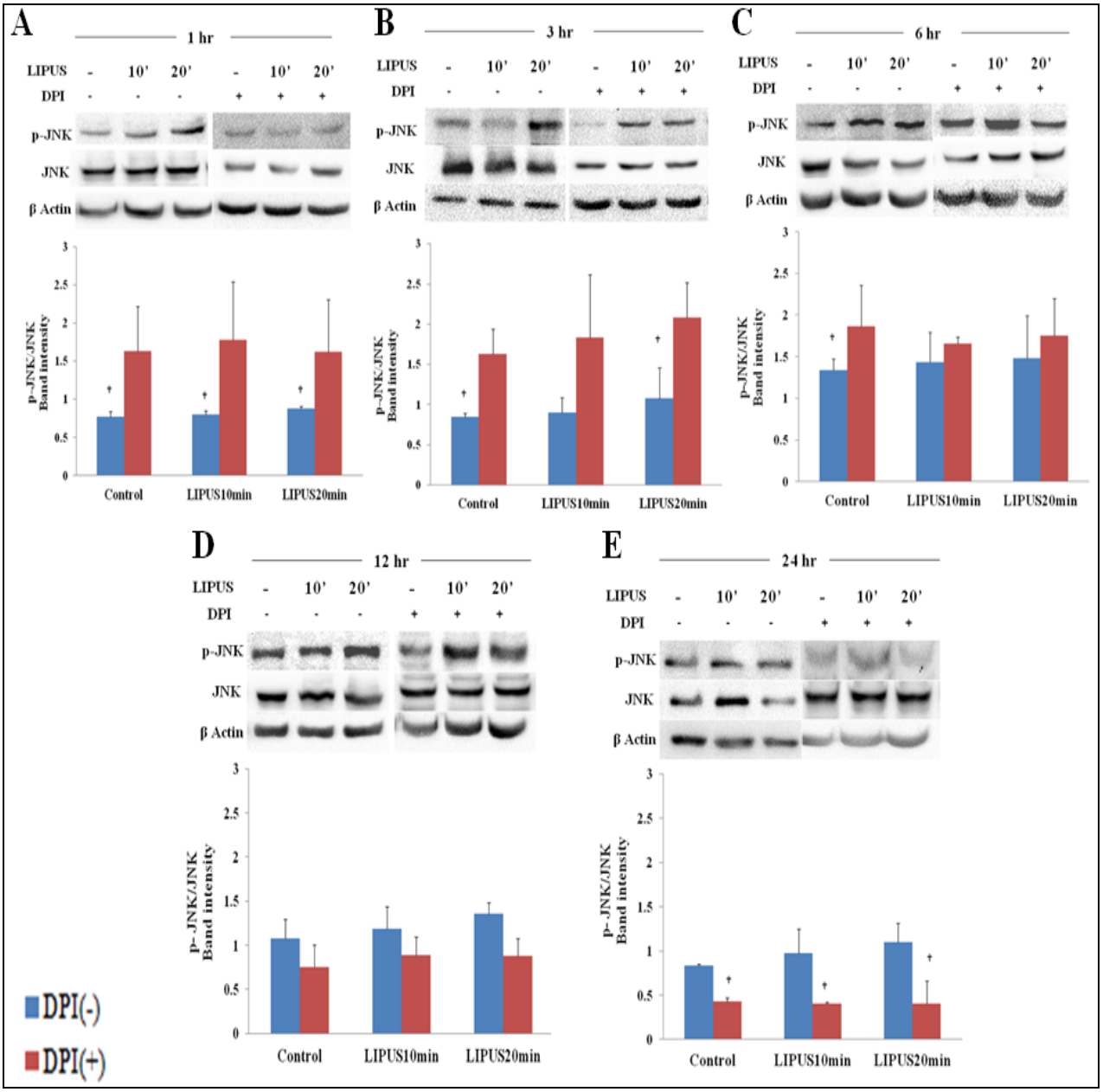

Fig 3.10: Immunoblot analysis of JNK activation by LIPUS application. C28/I2 chondrocytes were treated with LIPUS in the presence or absence of DPI (10 μM). The samples were harvested for immunoblot analysis after A. 1hr, B. 3hr, C. 6hr, D. 12 hr and E. 24 hrs of LIPUS application. LIPUS stimulation showed no significant difference in the phosphorylation level at any time point in DPI treated and non-treated groups. (* $p<0.05$; † $p<0.05$ between the corresponding DPI treated and non-treated groups.)

3.4. Discussion:

LIPUS is a mechanical wave that triggers intracellular signaling in the cell (mechanotransduction) but the mechanism by which LIPUS generate intracellular signals is still unclear. Many intracellular signaling pathways like integrin, stretch-activated ion channels, calcium signaling has been extensively characterized in the context of LIPUS (17) (28) (29). In this study, we investigated the association of ROS generated by LIPUS on immortalized human chondrocyte cell viability and activation of MAPK signaling pathway. We hypothesized that LIPUS stimulates chondrocyte viability and increased mRNA expression of SOX9, AGR and Col 2a1 and activation of MAPK signaling.

In order to study the effect of LIPUS on ROS generation, we used DHE, a blue fluorescent dye in the cytosol. In the presence of superoxide, DHE becomes oxidized to generate red fluorescent hydroxyethidium (30) and intercalates with cellular DNA. Our study showed an increase in fluorescence with LIPUS 10 min application followed by LIPUS 20 min. Since DHE is superoxide-specific indicator, our study demonstrated that ROS generated after LIPUS application is superoxide. However, using a plate-based assay cannot preclude the formation of hydroxyl radical which can also form a fluorescent product; the only way to distinguish superoxide from hydroxyl radical in this assay would be to use HPLC/FD (31) however, we did not employ such methods in this study. For ROS inhibition, we used DPI, which is most commonly used as a NOX inhibitor. DPI is a flavoprotein oxidoreductase inhibitor that from phenol radical which

attack flavin adenine dinucleotide (FAD) of NOX enzyme (32). In DPI-treated groups, there was a significant reduction in superoxide generation in LIPUS 10 min and LIPUS 20 min. A significant stimulatory effect of LIPUS treatment on chondrocytes was observed in the MTT assay, especially in LIPUS 10 min DPI (-) group. While in DPI-treated groups, there was noteworthy difference in LIPUS treated groups than DPI non-treated groups. This could be due to toxic effect of DPI. As mentioned earlier, DPI is a flavoprotein inhibitor and most likely, it caused inhibition of other enzymes in the cell that are important for cell survival.

LIPUS has shown an important role in chondrogenesis. SOX9 is a transcription factor that regulates differentiation of stem cells towards chondrocyte and activates chondrocyte-specific markers like *COL2A1* and *ACAN*. *SOX9* binds to the enhancer element of Col II gene and hence upregulate its expression (33). Col II is the most abundant protein in ECM of the cartilage while ACAN is the cartilage specific proteoglycan core protein. These two components provide resistance against compressive loads and hence contribute to the viscoelastic properties of the cartilage (34). Real-time qPCR data of our study showed a significant increase in mRNA expression of *SOX9* in LIPUS 10 min with the peak at 6 hr. *ACAN* and *COL2A1* mRNA expression were also stimulated by LIPUS 10 min DPI (-) both at 12 hr. There was a significant reduction in gene expression of *SOX9, ACAN and COL2A1* in DPI-treated groups as compared to DPI non-treated one. The previous study by Morita et al (35) showed the role of ROS in chondrocyte differentiation in endochondral ossification both

in vitro and in vivo. In that study, N-acetyl Cysteine (NAC, a ROS scavenger) inhibited chondrocyte hypertrophy in ATDC5 chondrogenic cell line, similar results were seen when NAC was administered to normal mice. We found increased gene expression of *NOX2* gene in LIPUS 10 min DPI (-) group while *NOX4* expression level remained unchanged in DPI-treated and non-treated groups. An immunohistochemistry study of mouse femur showed increased expression of NOX1 protein in proliferative and pre-hypertrophic cartilage layer while increased NOX4 level was observed in osteoblast layer underlying the cartilage (36). Our study results are complimentary to this study as *NOX4* expression was not altered which proves that *NOX4* did not contribute to ROS generation. An important feature about NOX4 is that it leads to the expression of H_2O_2 directly in contrast to superoxide (37). This also suggested that ROS generated in our study was superoxide.

Finally, our study strongly indicated that superoxide played an important role in MAPK signaling during LIPUS application. In independent studies, LIPUS showed increased phosphorylation of MAPKs in osteoblasts, synovial cells, cementoblast and chondrocytes (15), (37-39). Our results also confirm the previous findings of these studies. Phosphorylation of ERK1/2 was significantly increased in LIPUS treated groups in the absence of DPI. Further, the phosphorylation level was significantly reduced in DPI-treated groups due to reduced ROS generation. In the case of p38 MAPK, the level of phosphorylation was increased in LIPUS treated DPI non treated groups but the difference was not significant. Interestingly, the suppression of ROS

generation led to increase in the phosphorylation level of JNK, however, the difference was not significant. MAPKs activation leads to their translocation to the nucleus and increased phosphorylation of various intracellular molecules involved in cellular signaling like transcription factors, nuclear pore protein, cytoskeleton elements etc (24). This study proves that the levels of phosphorylation of MAPKs are regulated by ROS generated during LIPUS application. ROS generated by LIPUS exposure has revealed to be indispensible for the intracellular signaling in chondrocytes.

3.5 Conclusion:

Since their initial discovery, ROS have been considered to cause deleterious effects in cells. In time, however, their role as intracellular secondary messengers has been recognized. These radicals play dual roles in cells as both injurious and positive signals, depending upon the amount produced and the availability of the cellular antioxidants (40). Our study proved that superoxide produced by LIPUS exposure correlated with activation of MAPKs pathway (ERK1/2 and p38) and hence increased gene expression of chondrocyte specific markers – *SOX9, COL2A1* and *ACAN*. Meanwhile, superoxide generation was downregulated by DPI, which was accompanied by inactivation of ERK and p38 and reduced chondrocyte marker genes expression. Our study strongly suggested that superoxide generation by LIPUS application led to MAPKs pathway activation in chondrocytes. Collectively, we conclude that ROS generated by LIPUS exposure played a key role in MAPK activation and matrix production.

3.6 References

1. Whitney NP, Lamb AC, Louw TM, Subramanian A. Integrin-mediated mechanotransduction pathway of low-intensity continuous ultrasound in human chondrocytes. Ultrasound Med Biol. 2012 Oct;38(10):1734–43.

2. Fanghänel J, Gedrange T. On the development, morphology and function of the temporomandibular joint in the light of the orofacial system. Annals of Anatomy - Anatomischer Anzeiger. 2007 Jul 11;189(4):314–9.

3. Jortikka MO, Inkinen RI, Tammi MI, Parkkinen JJ, Haapala J, Kiviranta I, et al. Immobilisation causes longlasting matrix changes both in the immobilised and contralateral joint cartilage. Ann Rheum Dis. 1997 Apr;56(4):255–61.

4. Sato H, Kawamura A, Yamaguchi M, Kasai K. Relationship between masticatory function and internal structure of the mandible based on computed tomography findings. Am J Orthod Dentofacial Orthop. 2005 Dec;128(6):766–73.

5. Tanaka E, Kuroda S, Horiuchi S, Tabata A, El-Bialy T. Low-Intensity Pulsed Ultrasound in Dentofacial Tissue Engineering. Ann Biomed Eng. 2015 Feb 12;

6. Claes L, Willie B. The enhancement of bone regeneration by ultrasound. Prog Biophys Mol Biol. 2007 Apr;93(1–3):384–98.

7. Busse JW, Kaur J, Mollon B, Bhandari M, Tornetta P 3rd, Schünemann HJ, et al. Low intensity pulsed ultrasonography for fractures: systematic review of randomised controlled trials. BMJ. 2009;338:b351.

8. Wu S, Kawahara Y, Manabe T, Ogawa K, Matsumoto M, Sasaki A, et al. Low-intensity pulsed ultrasound accelerates osteoblast differentiation and promotes bone formation in an osteoporosis rat model. Pathobiology. 2009 May;76(3):99–107.

9. Cheung W-H, Chow SK, Sun M-H, Qin L, Leung K-S. Low-Intensity Pulsed Ultrasound Accelerated Callus Formation, Angiogenesis and Callus Remodeling in Osteoporotic Fracture Healing. Ultrasound in Medicine & Biology. 2011 Feb;37(2):231–8.

10. Hasanova GI, Noriega SE, Mamedov TG, Guha Thakurta S, Turner JA, Subramanian A. The effect of ultrasound stimulation on the gene and protein expression of chondrocytes seeded in chitosan scaffolds. J Tissue Eng Regen Med. 2011 Nov;5(10):815–22.

11. Korstjens CM, van der Rijt RHH, Albers GHR, Semeins CM, Klein-Nulend J. Low-intensity pulsed ultrasound affects human articular chondrocytes in vitro. Med Biol Eng Comput. 2008 Dec;46(12):1263–70.

12. El-Bialy T, El-Shamy I, Graber TM. Growth modification of the rabbit mandible using therapeutic ultrasound: is it possible to enhance functional appliance results? Angle Orthod. 2003 Dec;73(6):631–9.

13. El-Bialy T. Nonsurgical treatment of hemifacial microsomia by therapeutic ultrasound and hybrid functional appliance. J Clin Trials. 2010 Mar;29.

14. Kaur H, Uludağ H, El-Bialy T. Effect of nonviral plasmid delivered basic fibroblast growth factor and low intensity pulsed ultrasound on mandibular condylar growth: a preliminary study. Biomed Res Int. 2014;2014:426710.

15. Li X, Li J, Cheng K, Lin Q, Wang D, Zhang H, et al. Effect of low-intensity pulsed ultrasound on MMP-13 and MAPKs signaling pathway in rabbit knee osteoarthritis. Cell Biochem Biophys. 2011 Nov;61(2):427–34.

16. Cheng K, Xia P, Lin Q, Shen S, Gao M, Ren S, et al. Effects of Low-Intensity Pulsed Ultrasound on Integrin-FAK-PI3K/Akt Mechanochemical Transduction in

Rabbit Osteoarthritis Chondrocytes. Ultrasound in Medicine & Biology. 2014 Jul;40(7):1609–18.

17. Sato M, Nagata K, Kuroda S, Horiuchi S, Nakamura T, Karima M, et al. Low-Intensity Pulsed Ultrasound Activates Integrin-Mediated Mechanotransduction Pathway in Synovial Cells. Ann Biomed Eng. 2014 Aug 6;

18. Takeuchi R, Ryo A, Komitsu N, Mikuni-Takagaki Y, Fukui A, Takagi Y, et al. Low-intensity pulsed ultrasound activates the phosphatidylinositol 3 kinase/Akt pathway and stimulates the growth of chondrocytes in three-dimensional cultures: a basic science study. Arthritis Res Ther. 2008;10(4):R77.

19. Uddin SMZ, Hadjiargyrou M, Cheng J, Zhang S, Hu M, Qin Y-X. Reversal of the detrimental effects of simulated microgravity on human osteoblasts by modified low intensity pulsed ultrasound. Ultrasound Med Biol. 2013 May;39(5):804–12.

20. Kusuyama J, Bandow K, Shamoto M, Kakimoto K, Ohnishi T, Matsuguchi T. Low intensity pulsed ultrasound (LIPUS) influences the multilineage differentiation of mesenchymal stem and progenitor cell lines through ROCK-Cot/Tpl2-MEK-ERK signaling pathway. J Biol Chem. 2014 Apr 11;289(15):10330–44.

21. Fujisawa T, Takeda K, Ichijo H. ASK family proteins in stress response and disease. Mol Biotechnol. 2007 Sep;37(1):13–8.

22. Li J, Zhao Z, Liu J, Huang N, Long D, Wang J, et al. MEK/ERK and p38 MAPK regulate chondrogenesis of rat bone marrow mesenchymal stem cells through delicate interaction with TGF-beta1/Smads pathway. Cell Prolif. 2010 Aug;43(4):333–43.

23. Sauer H, Wartenberg M, Hescheler J. Reactive oxygen species as intracellular messengers during cell growth and differentiation. Cell Physiol Biochem. 2001;11(4):173–86.

24. Son Y, Kim S, Chung H-T, Pae H-O. Reactive oxygen species in the activation of MAP kinases. Meth Enzymol. 2013;528:27–48.

25. Reher P, Harris M, Whiteman M, Hai H., Meghji S. Ultrasound stimulates nitric oxide and prostaglandin e2 production by human osteoblasts. Bone. 2002 Jul;31(1):236–41.

26. Li L, Yang Z, Zhang H, Chen W, Chen M, Zhu Z. Low-intensity pulsed ultrasound regulates proliferation and differentiation of osteoblasts through osteocytes. Biochem Biophys Res Commun. 2012 Feb 10;418(2):296–300.

27. Hsu S, Huang T. Bioeffect of ultrasound on endothelial cells in vitro. Biomol Eng. 2004 Nov;21(3–5):99–104.

28. Mortimer AJ, Dyson M. The effect of therapeutic ultrasound on calcium uptake in fibroblasts. Ultrasound Med Biol. 1988;14(6):499–506.

29. Choi BH, Choi MH, Kwak M-G, Min B-H, Woo ZH, Park SR. Mechanotransduction pathways of low-intensity ultrasound in C-28/I2 human chondrocyte cell line. Proc Inst Mech Eng H. 2007 Jul;221(5):527–35.

30. Peshavariya HM, Dusting GJ, Selemidis S. Analysis of dihydroethidium fluorescence for the detection of intracellular and extracellular superoxide produced by NADPH oxidase. Free Radic Res. 2007 Jun;41(6):699–712.

31. Zielonka J, Hardy M, Kalyanaraman B. HPLC study of oxidation products of hydroethidine in chemical and biological systems: Ramifications in superoxide measurements. Free Radic Biol Med. 2009 Feb 1;46(3):329–38.

32. Li N, Ragheb K, Lawler G, Sturgis J, Rajwa B, Melendez JA, et al. DPI induces mitochondrial superoxide-mediated apoptosis. Free Radical Biology and Medicine. 2003 Feb 15;34(4):465–77.

33. Oralová V, Matalová E, Janečková E, Drobná Krejčí E, Knopfová L, Šnajdr P, et al. Role of c-Myb in chondrogenesis. Bone. 2015 Jul;76:97–106.

34. Kuroda S, Tanimoto K, Izawa T, Fujihara S, Koolstra JH, Tanaka E. Biomechanical and biochemical characteristics of the mandibular condylar cartilage. Osteoarthr Cartil. 2009 Nov;17(11):1408–15.

35. Morita K, Miyamoto T, Fujita N, Kubota Y, Ito K, Takubo K, et al. Reactive oxygen species induce chondrocyte hypertrophy in endochondral ossification. J Exp Med. 2007 Jul 9;204(7):1613–23.

36. Ambe K, Watanabe H, Takahashi S, Nakagawa T. Immunohistochemical localization of Nox1, Nox4 and Mn-SOD in mouse femur during endochondral ossification. 2014.

37. Martyn KD, Frederick LM, von Loehneysen K, Dinauer MC, Knaus UG. Functional analysis of Nox4 reveals unique characteristics compared to other NADPH oxidases. Cell Signal. 2006 Jan;18(1):69–82.

38. Ikeda K, Takayama T, Suzuki N, Shimada K, Otsuka K, Ito K. Effects of low-intensity pulsed ultrasound on the differentiation of C2C12 cells. Life Sci. 2006 Oct 12;79(20):1936–43.

39. Rego EB, Inubushi T, Kawazoe A, Tanimoto K, Miyauchi M, Tanaka E, et al. Ultrasound stimulation induces PGE(2) synthesis promoting cementoblastic differentiation through EP2/EP4 receptor pathway. Ultrasound Med Biol. 2010 Jun;36(6):907–15.

40. Bartosz G. Reactive oxygen species: Destroyers or messengers? Biochemical Pharmacology. 2009 Apr 15; 77(8):1303–15.

Chapter 4: Role of reactive oxygen species during low intensity pulsed ultrasound application to MC-3T3 E1 pre-osteoblast cell culture.

4.1. Introduction:

Bone is a vital organ that is under the continuous influence of mechanical loads caused by muscular activity and gravity. In order to preserve the balance of bone strength and mass, mechanical load is indispensible for bone homeostasis (1). On the contrary, loss of gravity and muscle activity due to nerve damage lead to bone degeneration. Hence, mechanical loading is imperative not only for regulating cellular function like gene expression, protein and extracellular matrix (ECM) synthesis, cellular differentiation and apoptosis but also for the maintenance of micro-architecture, integrity and metabolic activity of bone as a whole (2).

Osteoblasts are the pivotal bone forming cells involved in bone matrix production and mineralization. These cells are equipped with special machinery to sense the changes in mechanical properties of ECM and convert them to intracellular signaling by the process of mechanotransduction. Integrins, G-protein receptors, stretch ion channels and mitogen-activated protein kinases (MAPKs) are specific cellular components involved in mechanotransduction (3). MAPKs are primitive multifunctional and widely studied signaling pathway that is involved in the regulation of bone mass and osteoblast differentiation. It consists of three serine-threonine kinases – Extracellular signal-regulated kinase (ERK1/2), p38 and c-Jun N-terminal kinase (JNK); that mediate the response to a variety of stimuli. ERK1/2 is preferentially activated in response to growth factors while p38 and JNK are more responsive to stress impulses. Studies in mice with ERK1/2 germline deletion showed reduced bone mineralization (4) and p38 deletion

leads to osteopenia in long bones (5). ERK1/2 and p38 have shown to exert their osteoblast differentiation effect by regulating runt related transcription factor 2 (RUNX2) phosphorylation which is a transcription factor critical for osteoblast differentiation and gene and protein expression from osteoblast and hypertrophic chondrocytes (6).

Hydrostatic pressure and cyclic compression are shear stress cited in the literature to apply mechanical stress in cell culture system. One additional method is the application of Low intensity pulsed ultrasound (LIPUS). Ultrasound has been used effectively in the medical field for over five decades as a diagnostic, operative and therapeutic tool. In-vitro studies have shown increased cell proliferation, differentiation of osteoblast, gingival fibroblast, periodontal ligament cells and chondrocytes (7). Recent literature is more focused on the use of LIPUS for the treatment of osteoarthritis, bone regeneration as a supplementary method with scaffolds because of the proliferative and angiogenic properties of LIPUS. Studies have shown integrin activation (8), calcium channels signaling (9) and intracellular activation of MAPK and phosphatidylinositide 3 kinase (PI3K) (10) in relation to LIPUS application. However, the potential mechanism of action is not completely understood.

Reactive oxygen species (ROS) are generated during aerobic cell metabolism through reduction-oxidation reaction. Since the time of their discovery, ROS has been considered to have deleterious effects in the living system as they were involved in the aging, cancer metastasis, diabetic neuropathy. It is only during the last decade that their

favorable effects are investigated in the cellular function as the second messenger in the intracellular signaling engaged in proliferation and differentiation (11). Indeed, they are considered harmful when generated in higher level and cause oxidation of macromolecules like DNA, proteins and lipids due to oxidative stress. Living tissue has a variety of enzymes and antioxidants like catalase, superoxide dismutase, glutathione that keeps a check on the amount of ROS generated. The amount generated is a critical factor in cellular homeostasis. When generated in lower level they act as signaling molecule in cell growth and differentiation. NADPH oxidase (NOX) are involved in ROS generation and there are seven subtypes- NOX1-5 and DUOX1 and 2. NOX2 and NOX4 are involved in bone homeostasis (12). ROS modify the proteins comprising of cysteine, methionine, and selenocysteine. One such enzyme that is involved in MAPK functioning is protein tyrosine phosphatase (PTP) which is the target of ROS activity and hence ROS is indirectly involved in MAPK activation (13).

Based on this information, our aim was to investigate the role of ROS generation during LIPUS application and its role in MAPK activation. We hypothesized that LIPUS stimulation increased ROS generation in MC-3T3 E1 pre-osteoblast cell which in turn leads to MAPK activation and increased gene expression of osteoblast specific markers – *RUNX2, OCN,* and *OPN*.

4.2 Materials and Methods:

4.2.1 Reagents:

MC-3T3 E1 cell line was purchased from American Type Culture Collection (ATCC, VA, USA); Dulbecco's modified eagle's medium F12 (DMEM F12) with L-glutamine and HEPES, fetal bovine serum (FBS), and Dulbecco's phosphate buffered saline (DPBS) and Hank's balanced salt solution (HBSS) were purchased from Life technologies, NY, USA; penicillin and streptomycin (Hyclone GE, Utah, USA). dihydroethidine (DHE), diphenylene iodonium (DPI), MTT [(3-(4, 5-dimethylthiazol–2-yl)-2, 5- diphenyltetrazolium bromide], chloroform, isopropanol, bovine serum albumin (BSA), and dimethyl sulfoxide (DMSO) all were purchased from Sigma Aldrich, MO, USA. Sodium dodecyl sulfate (SDS), polyacrylamide and nitrocellulose membrane were purchased from BioRad, Japan. High capacity reverse transcription kit for cDNA preparation was purchased from Applied Biosystems, USA. Antibodies used in immunoblot analysis – anti ERK1/2, anti phospho ERK1/2, anti p38, anti phospho p38, anti JNK and anti phospho JNK were purchased from Cell Signaling Technology, USA. For protein estimation, Pierce BCA protein assay kit was purchased from Thermo Fisher, USA. Enhanced chemiluminiscence (ECL) western blot reagent kit was purchased from Amersham GE Health Care.

4.2.2 Cell culture:

1.5 X 10^5 /ml MC 3T3E1 mouse pre-osteoblast cell line were cultured in 6 well plates in the medium containing DMEM/F12, 10% FBS and 50 units/ml of penicillin and 50 μgm/ ml of streptomycin. Cells were incubated at 37º C in a humid chamber with 5% CO_2 and cultured for 24 hours till the first LIPUS application. The cells were washed twice with DPBS and harvested after 1, 3, 6, 12 and 24 hours after LIPUS application for gene and protein expression. For ROS inhibition, cells were cultured with similar cell density and condition. Before the addition of DPI, cells were starved by removing the medium containing FBS and were replaced with DMEM/F 12 only. DPI was added to DMEM/F12 at least 1 hour before LIPUS application.

4.2.3 LIPUS application:

The cells were treated for either 10 min or 20 min LIPUS while the control group received sham transducer for similar periods of time. LIPUS device was provided by Smile Sonica Inc (Edmonton, AB, and Canada) and was custom made for this experiment. The device generated 200 microseconds bursts of 1.5 MHz sine waves with a pulse repetition frequency of 1 kHz and spatially averaged intensity of 30 mW/cm^2 of the transducer's surface area. The six well plates were placed on the surface of transducer and coupling gel was applied to them for the transmission of ultrasound waves. The groups were: Control DPI (-), LIPUS 10 min DPI (-) and LIPUS 20 min DPI (-). In DPI treatment, the groups were: Control DPI (+), LIPUS 10 min DPI (+) and LIPUS 20 min DPI (+).

4.2.4 Measurement of ROS production:

The cells were washed with pre-warmed (37ºC) DPBS solution and were suspended in either DMEM/F12 (without phenol red) in the concentration of 1X 10^5 cells/ ml. The suspended cells were incubated with DHE (25 µM) for 20 min in the incubator before LIPUS application. Cells were sonicated with LIPUS according to the treatment groups and 100 µl of cell suspension was collected from each sample in triplicates at 0', 15', 30', 45', 60', 90' and 120' and were loaded in 96 black wells plate. ROS have very short half-life and hence it is difficult to measure them on long term basis. Hence, we measured ROS production at short time intervals for upto 2 hrs. The fluorescence intensity was quantified using Tecan M2000 micro-plate reader with excitation and emission wavelengths of 480 and 570 nm respectively. To study the effect of ROS inhibitor, 10 µM DPI was added to the cell suspension and the procedure was repeated.

4.2.5 Measurement of cell viability:

The cells were seeded on a six-well plate in the presence and absence of DPI and the readings were taken after 24 hrs of LIPUS application. MTT [(3-(4,5-dimethylthiazol–2-yl)-2,5-diphenyltetrazolium bromide] assay was used as a measure of cell viability. 800 µl of MTT solution (dissolved in HBSS using concentration of 5 mg/ml) was added to each well containing 2 ml of the medium and incubated for 2 hrs at 37 C. The medium was replaced with 2 ml of dimethyl sulfoxide (DMSO) to dissolve

MTT formazan crystals. The optical density was measured at 570 nm using Tecan M2000 micro-plate reader.

4.2.6 RNA extraction, cDNA synthesis, and Real-time qPCR:

Total RNA was prepared using TRIzol reagent according to the manufacturer's instructions. RNA concentration was measured using NanoDrop 2000C Spectrophotometer. The first strand of cDNA was synthesized from 1µg total RNA by using High Capacity cDNA Reverse Transcriptase kit following the kit instruction in the reaction volume of 20 µl. After reverse transcription reaction, 1 out of 10 dilutions was made from the template to be used in real-time qPCR. 10 µl real-time reaction mixture consisting of 3 µl of cDNA, 1 µl each of forward and reverse primers and 5 µl of the master mix containing SYBR green dye. The mixtures were heated at 95º C for 2 min before going through 40 cycles of a denaturation step (15 sec at 95º C) and an annealing step (1 min at 60º C) using 7500 Real-Time PCR system during which the data were collected. Glyceraldehyde-3-phosphate dehydrogenase (GAPDH) was used as an internal control in each run. Normalized fluorescence was plotted against cycle number (amplification plot), and the threshold suggested by the software was used to calculate Ct (cycle at threshold). ΔΔ Ct analysis was used to determine the differences in gene expression as compared to the control. The samples were collected from the groups at 1, 3, 6, 12 and 24 hrs after LIPUS application. The primers used in the study are presented in Table 4.1.

Table 4.1: Primers for Real-time qPCR

	Primer	Direction	Sequence (5'to 3')
1	*RUNX2*	Forward	GGGAACCAAGAAGGCACAGA
		Reverse	GGATGAGGAATGCGCCCTAA
2	*OCN*	Forward	GGCCCAGACCTAGCAGACA
		Reverse	GGGCTTGGCATCTGTGAGG
3	*OPN*	Forward	GCAGCTCAGAGGAGAAGAAGC
		Reverse	TTCTGTGGCGCAAGGAGATT
4	*NOX 2*	Forward	TCATTCTGGTGTGGTTGGGG
		Reverse	CAGTGCTGACCCAAGGAGTT
5	*NOX 4*	Forward	ACCTCTGCCTGCTCATTTGG
		Reverse	TCGCCCAACATTTGGTGAATG
6	*GAPDH*	Forward	GGAGAGTGTTTCCTCGTCCC
		Reverse	CAAATGGCAGCCCTGGTGA

4.2.7 ELISA for Osteopontin detection:

To determine the amount of OPN released, the supernatants were collected at 1, 3, 6, 12 and 24 hrs after LIPUS exposure in the presence or absence of DPI. OPN ELISA was performed according to manufacturer's instructions. OPN concentration (pg per ml) was calculated from a standard curve.

4.2.8 Immunoblotting:

For immunoblotting analysis, the pre-osteoblast cells were cultured for 1, 3, 6, 12 and 24 h after single ultrasound exposure. The cells were then washed with cold PBS twice and then were lysed in NP-40 lysis buffer (50mM Tris-pH8.0, 150mM NaCl, 1% NP-40 and freshly added 10^{-6} M Protease inhibitor). The lysates were used as samples after centrifugation. Total protein concentration was determined using Pierce BCA kit. Cell lysates were separated on 12% polyacrylamide gels and blotted onto a nitrocellulose membrane. The membrane was blocked for 1 h at room temperature with 5% Bovine serum albumin in 1% TBS-Tween. After blocking, blots were probed with following primary antibodies (1:1000): phospho-ERK1/2, ERK1/2, phospho-p38, p38, phospho-JNK, JNK, β-actin in 5% BSA in 1% TBS-Tween overnight at 4^{o}C. After incubation with HRP-conjugated anti-rabbit IgG (1:3000) for 1 h at room temperature, blots were washed and developed with ECL reagent (Amersham, GE healthcare, Buckinghamshire, UK). Blots were further visualized using Biorad ChemiDoc gel imaging system and intensity of bands was quantitatively determined by Image J Software (National Institute of Health, NIH). All tests were performed in triplicates.

4.2.9 Statistical analysis:

The data was summarized as mean ± standard deviation where the error bars represent standard deviation. All data were tested for normal distribution (Kolmogrov Smirnoff test) and equal variance (Levene's test) using SPSS software version SPSS 21.0 (Chicago, IL, USA). Two statistical tests were applied: a) Two-way repeated

measure analysis of variance (ANOVA) was used followed by Bonferroni test as post hoc to study significance for LIPUS applications and detection time. b) To study the effect of DPI at each time point, One-way ANOVA followed by Bonferroni post hoc test was used. The level of significance was set at $p< 0.05$.

4.3 Results:

4.3.1 ROS generation in MC-3T3 E1 pre-osteoblast after LIPUS application:

To investigate the effect of LIPUS application on ROS generation, we first suspended MC-3T3E1 cell in DMEM/F12 (phenol red free) in the concentration of $1X10^5$ cells/ml and incubated the cell suspension in DHE (25 μM) for 20 min and then treated with LIPUS according to the assigned groups. The samples were collected for fluorescence intensity measurement at 0', 15', 30', 45', 60', 90' and 120' after LIPUS application (Fig 4.1). DHE is superoxide-specific fluorescent dye that emits red fluorescence due to the formation of hydroxyethidine when oxidized by superoxide. LIPUS application showed a significant increase in superoxide generation at all the time points except at 0' i.e. immediately after LIPUS application as compared to the control group. LIPUS 10 min showed higher superoxide generation than LIPUS 20 min. For ROS inhibition, 10 μM DPI was added to the cell suspension and then incubated with DHE (25 μM) for 20 min followed by LIPUS stimulation. DPI-treated groups showed a significant decrease in superoxide generation as compared to DPI non-treated groups. Unlike DPI non-treated group, LIPUS 20 min showed higher superoxide in DPI (+) group than LIPUS 10 min and control.

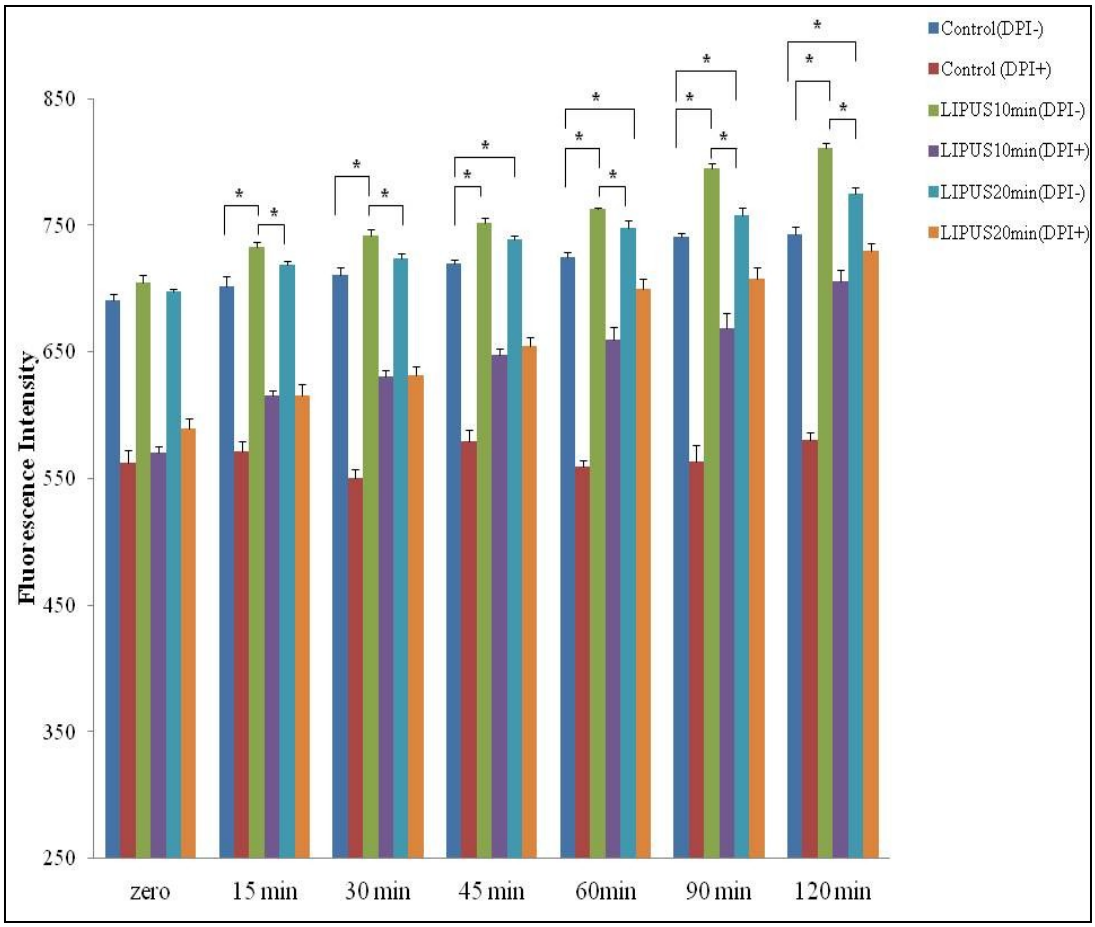

Fig 4.1: LIPUS stimulation induced ROS generation in MC-3T3 E1 pre-osteoblast cells. The osteoblast cells were incubated with DHE (25 µM) and cells were sonicated with LIPUS according to the designated groups. For ROS inhibition, 10 µM DPI was added to DMEM/F12 (phenol red free). The samples were collected at 0' (immediately after LIPUS application), 15', 30', 45', 60', 90' and 120' after LIPUS application. The bar graph depict the time series of DHE fluorescence and the values are presented in Mean ± SD. LIPUS groups showed significant increase in ROS generation from 15 min onwards while DPI treated groups showed significant decrease in ROS generation. (* $p<0.05$; † $p<0.05$ between the corresponding DPI treated and non-treated groups.)

4.3.2 Cell viability after LIPUS application:

In order to study the effect of LIPUS application and ROS generation on the cell viability, MC-3T3 E1 cells were exposed to LIPUS in the presence or absence of DPI. After 24 hrs, the cell viability was determined by the MTT Assay. In DPI non-treated groups, there was significant increase in cell viability in the groups exposed with LIPUS as compared to the control group. There was no difference in cell viability between 10 min and 20 min LIPUS application. In DPI treated groups, there was no statistical difference between the control and LIPUS groups. DPI treatment showed a significant decrease in cell viability of MC 3T3E1 pre-osteoblast cells. (Fig 4.2)

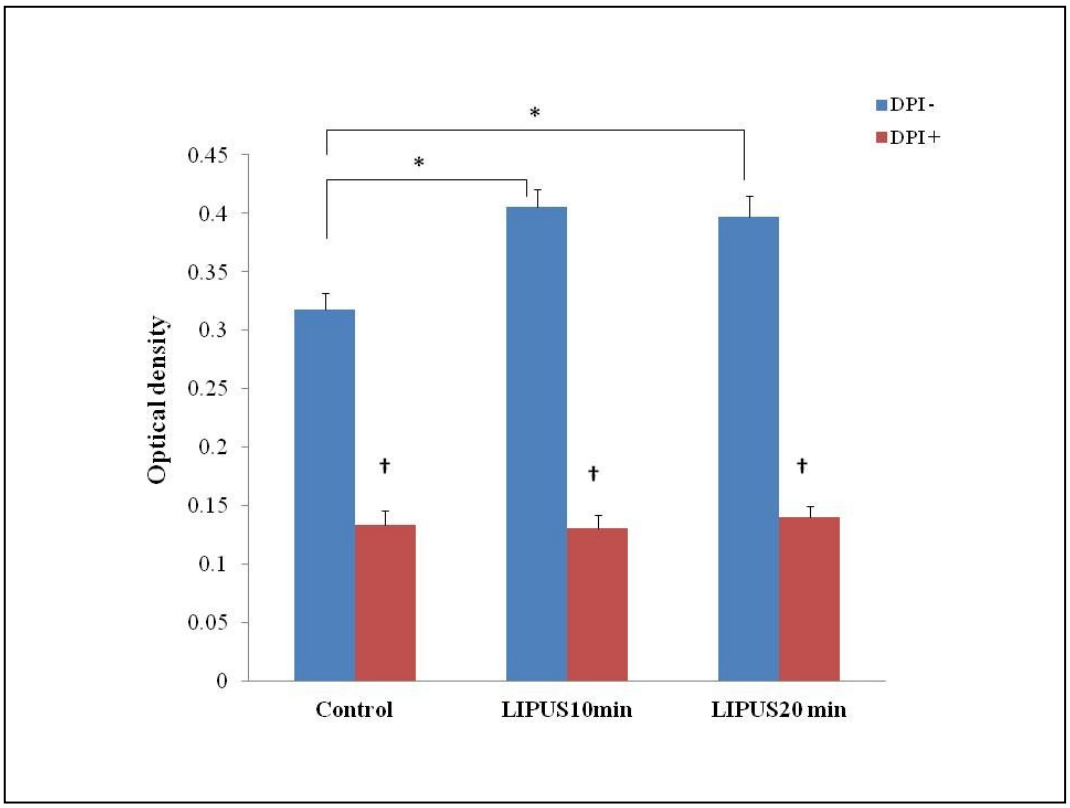

Fig 4.2: Effect of LIPUS stimulation on the cell viability of MC-3T3E1 pre-osteoblast cell as measured by MTT absorbance assay. After 24 hrs of LIPUS application in the presence and absence of DPI (10 µM), the osteoblasts were incubated in MTT solution (5 mg/ml dissolved in HBSS) for 2 hrs. Formazan crystals formed were dissolved in DMSO and absorbance was measured. Values in the bar graph are presented as Mean ± SD. LIPUS stimulation showed significant increase in cell viability as compared to control while DPI-treated groups showed significant decrease in cell viability. (* $p<0.05$; † $p<0.05$ between the corresponding DPI treated and non-treated groups.)

4.3.3 Effect of LIPUS application on NOX2 and NOX4 mRNA expression:

To investigate the effect of LIPUS stimulation on *NOX2* and *NOX 4* expression, MC-3T3E1 pre-osteoblast cells were exposed to LIPUS and the samples were collected after 1 hr, 3 hr, 6 hr, 12 hr, and 24 hr. For ROS inhibition, cells were first treated with DPI (10 μM) and then exposed to LIPUS. Both *NOX2* and *NOX4* mRNA expression were significantly higher in DPI-treated groups at 1 hr time point and then expression level decreased. In DPI non-treated group, *NOX2* and *NOX4* mRNA expression increased at 6 hr time point. By 12 hr, there was no significant difference in their expression levels. (Fig 4.3 and 4.4)

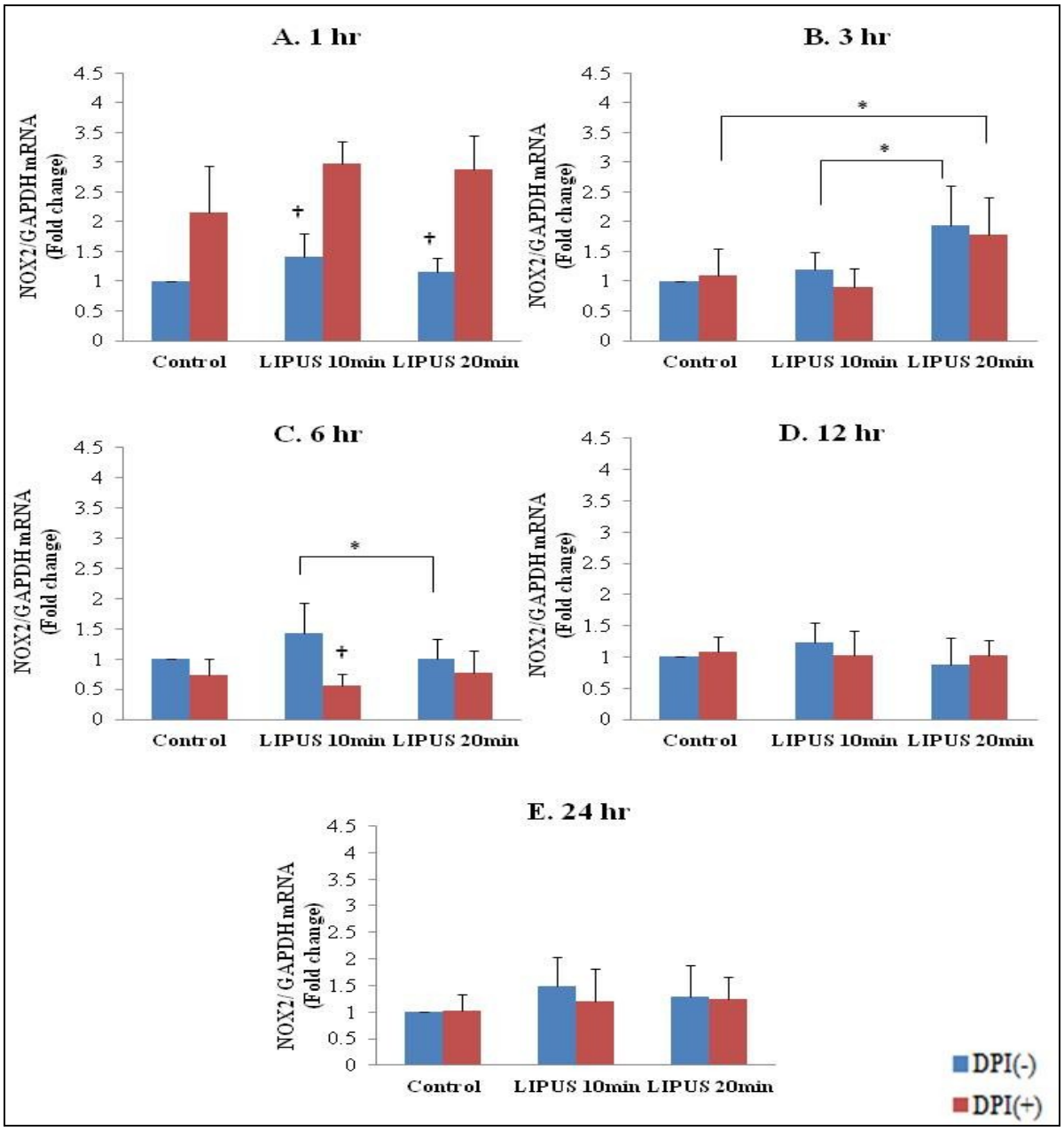

Fig 4.3: Gene expression of NOX2 quantified by RT-qPCR in MC-3T3E1 cells after LIPUS application in the presence or absence of DPI (10 μM). The samples were collected after A. 1hr, B. 3hr, C. 6hr, D. 12hr and E. 24 hr of LIPUS application. Bar graph showed significant increase in NOX2 mRNA expression at 1 hr and 3 hr time points after LIPUS application in DPI-treated group while there was significant increase at 6 hr time point in DPI non-treated group while there was significant increase at 6 hr time point in DPI non-treated group. (* $p<0.05$; † $p<0.05$ between the corresponding DPI treated and non-treated groups.)

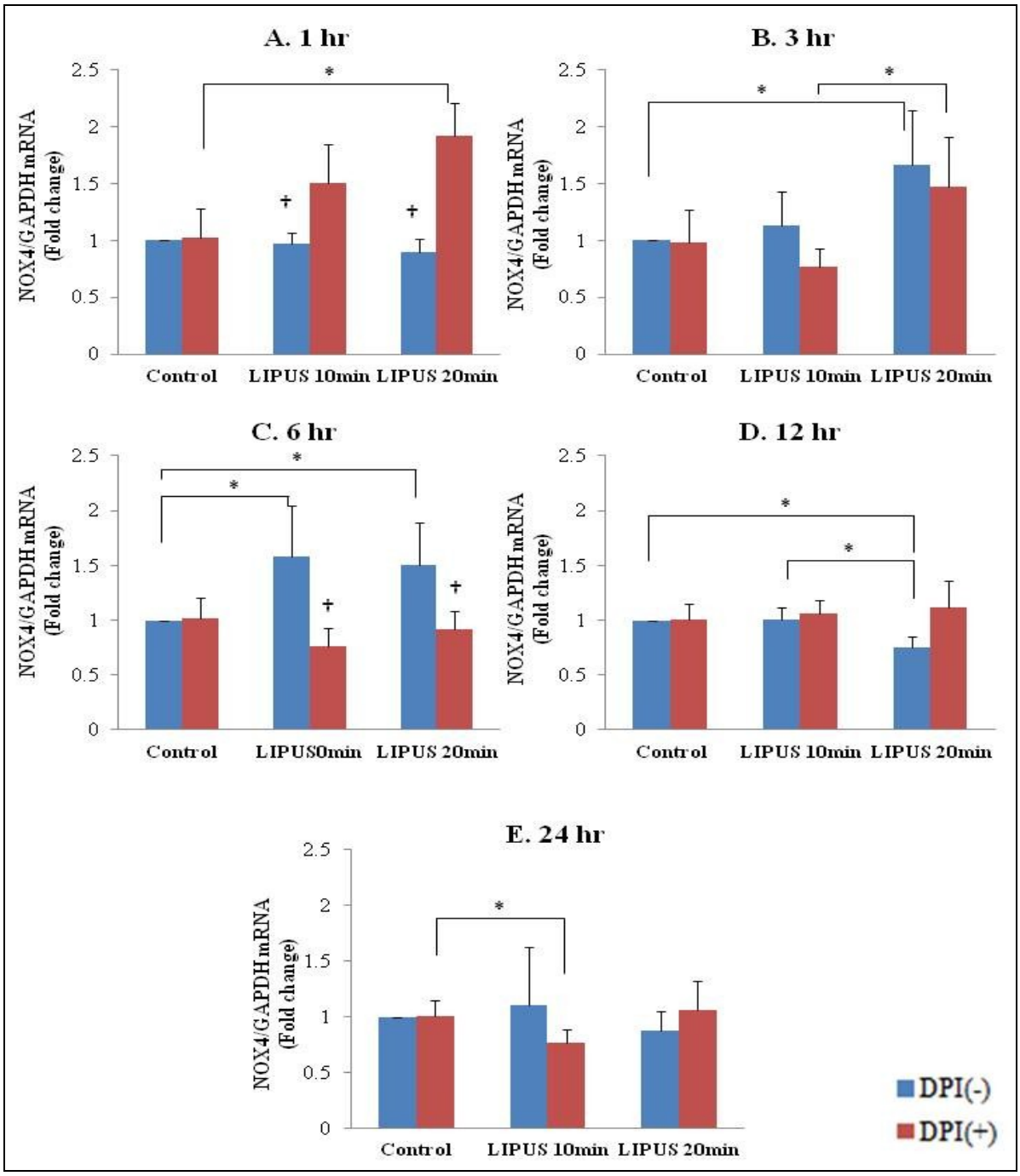

Fig 4.4: Gene expression of *NOX4* quantified by RT-qPCR in MC-3T3E1 pre-osteoblast cells after LIPUS application in the presence or absence of DPI (10 μM). The samples were collected after A. 1hr, B. 3hr, C. 6hr, D. 12hr and E. 24 hr of LIPUS application. Bar graph showed significant increase in *NOX4* mRNA expression at 1 hr and 3 hr time points after LIPUS application in DPI-treated group while there was significant increase at 6 hr time point in DPI non-treated group. (* $p<0.05$; † $p<0.05$ between the corresponding DPI treated and non-treated groups.)

4.3.4 RUNX2, OCN, and OPN mRNA expression after LIPUS application:

To explore the effect of LIPUS stimulation and ROS inhibition, MC-3T3 E1 cells were treated with LIPUS and the samples were investigated for mRNA expression of osteoblast-specific markers. In DPI non-treated group, *RUNX2* expression was significantly increased in LIPUS groups at 3, 6 and 12 hrs time point as compared to the control group while in DPI-treated group, the expression was highest during the first hour and its level decreased on the following time points (Fig 4.5).

In DPI non-treated group, LIPUS showed a significant increase in *OCN* mRNA expression at 24 hr time (Fig 4.6) while *OPN* showed no significant difference (Fig 4.7). In DPI-treated group, *OCN* and *OPN* mRNA showed similar results as *RUNX2*. LIPUS showed a significant increase in expression at 1 hr time point as compared to the control group. However, the expression decreased in the following time points.

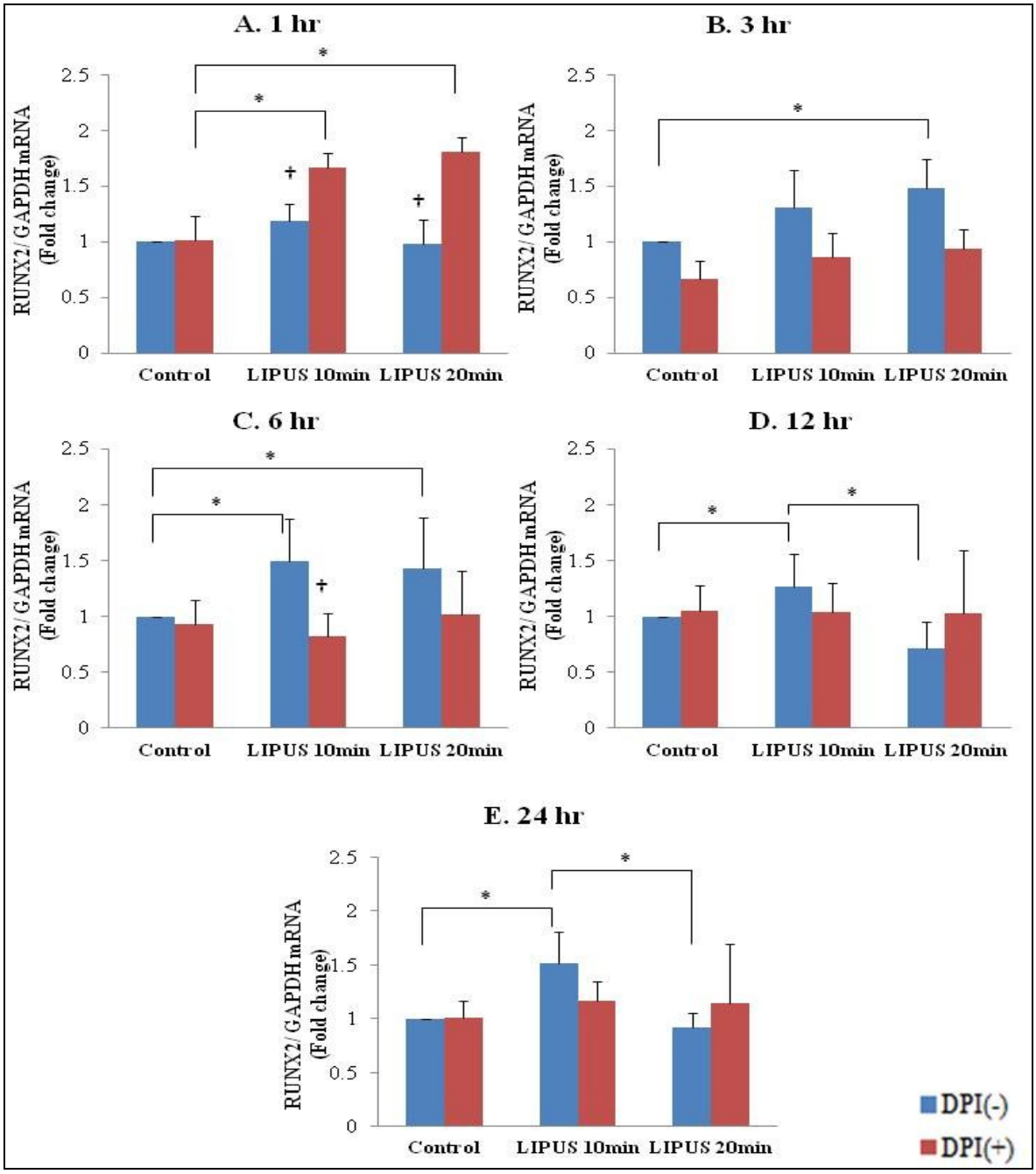

Fig 4.5: *RUNX2* mRNA expression quantified using RT-qPCR in MC-3T3E1 pre-osteoblast cells after LIPUS application in the presence or absence of DPI (10 μM). The samples were collected after A. 1hr, B. 3hr, C. 6hr, D. 12hr and E. 24 hr of LIPUS application. Bar graph showed significant increase in *RUNX2* mRNA expression at 1 hr, and 3 hr time points in LIPUS treated group as compared to control in DPI-treated group while DPI non-treated groups showed significant increase at 6 hr and 12 hrs (* $p<0.05$; † $p<0.05$ between the corresponding DPI treated and non-treated groups.

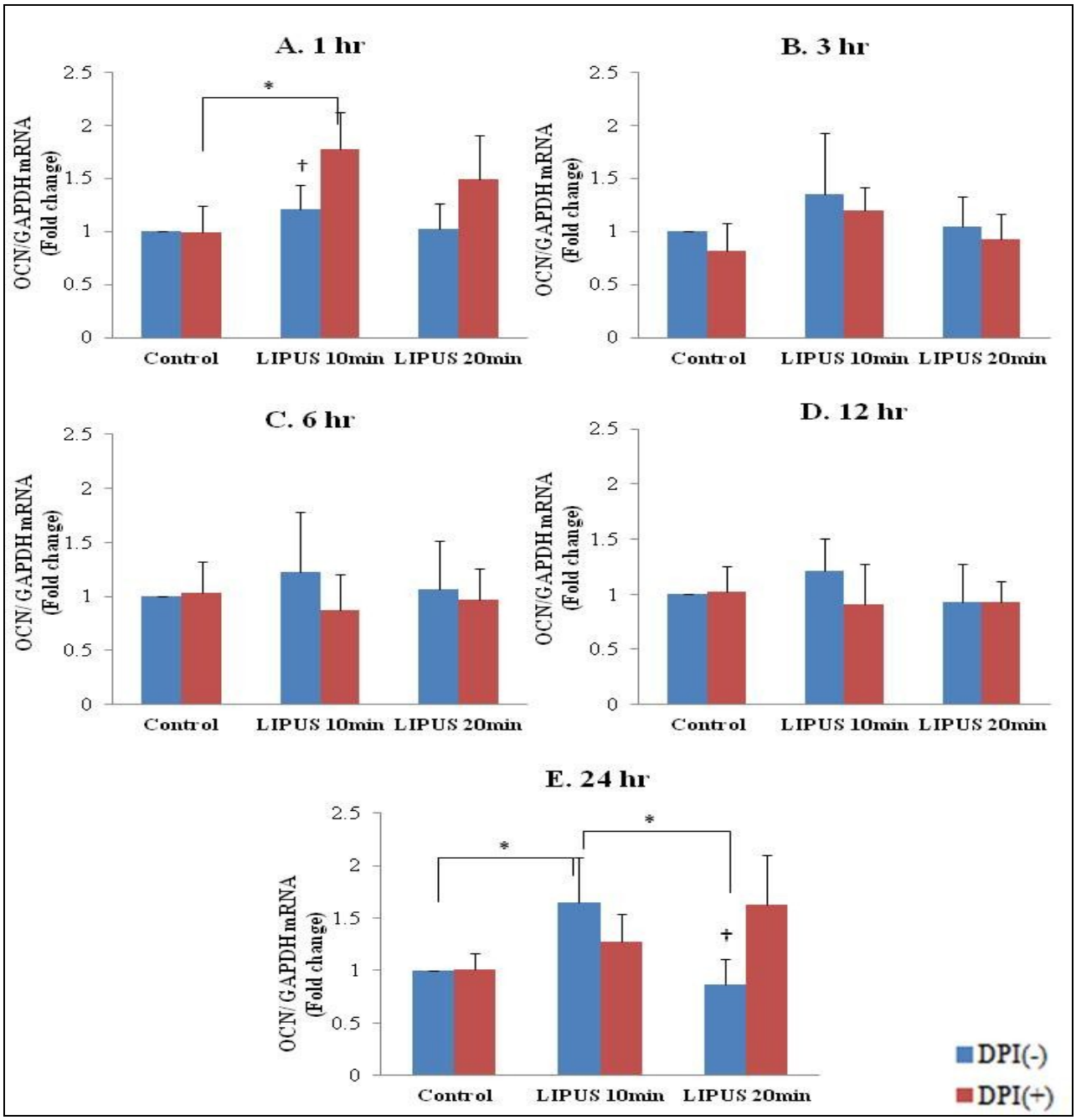

Fig 4.6: *OCN* mRNA expression in MC-3T3E1 pre-osteoblast cells after A. 1hr, B. 3 hr, C. 6 hr, D. 12 hr and E. 24 hrs after LIPUS stimulation. Bar graph showed significant increase in *OCN* mRNA expression at 1 hr in LIPUS group as compared to control in DPI-treated group while DPI non-treated groups showed significant increase at 24 hr between control and LIPUS treated groups. (* $p<0.05$; † $p<0.05$ between the corresponding DPI treated and non-treated groups.)

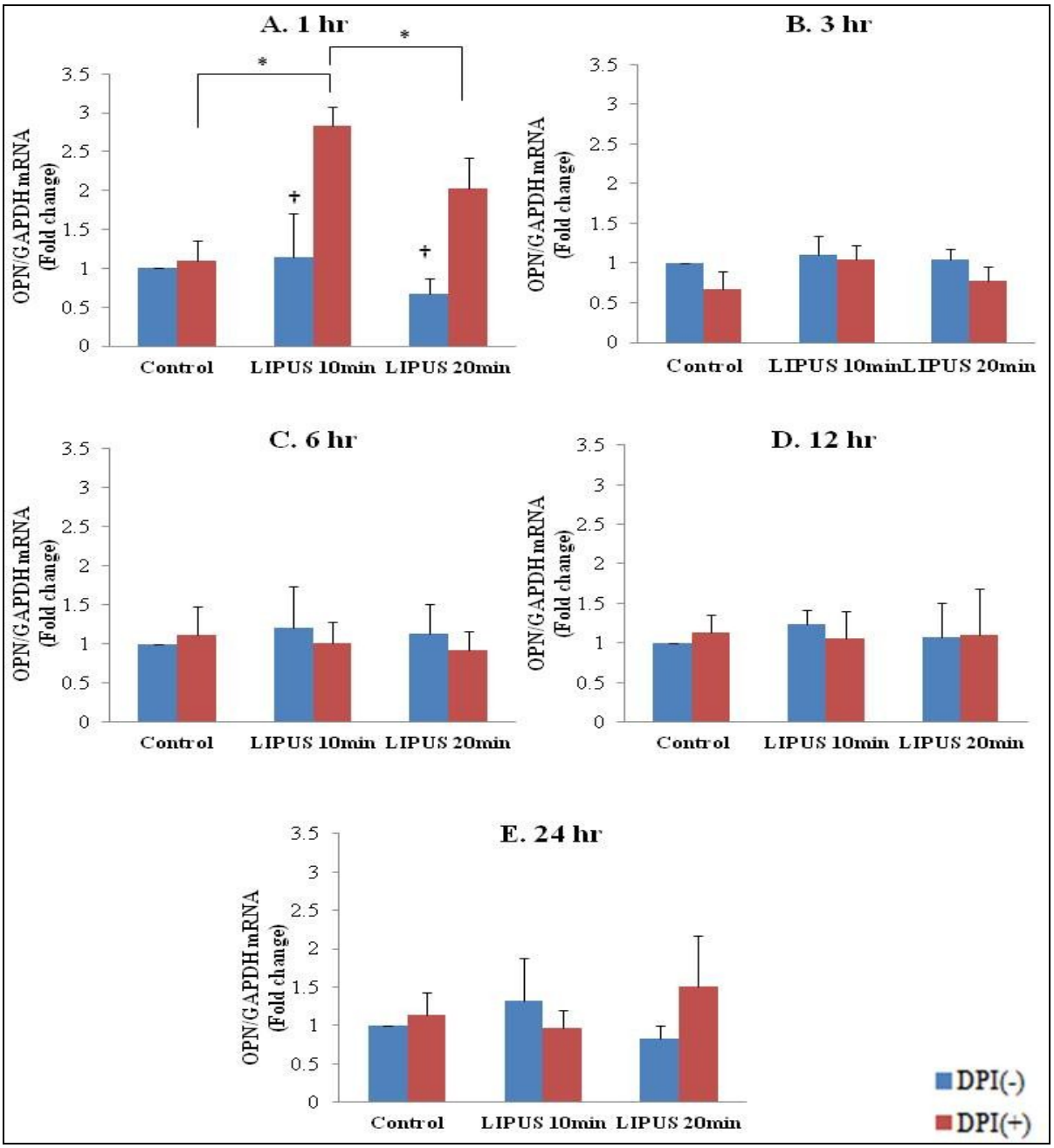

Fig 4.7: *OPN* mRNA expression in MC-3T3E1 pre-osteoblast cells after A. 1hr, B. 3 hr, C. 6 hr, D. 12 hr and E. 24 hrs after LIPUS stimulation. Bar graph showed significant increase in *OPN* mRNA expression at 1 hr in LIPUS treated group as compared to control in DPI-treated group while DPI non-treated groups showed no significant difference in *OPN* between control and LIPUS treated groups. (* $p<0.05$; † $p<0.05$ between the corresponding DPI treated and non-treated groups.)

4.3.5 Effect of LIPUS on OPN protein levels:

Changes in OPN protein level after LIPUS application and ROS inhibition were determined using OPN ELISA by collecting the supernatants from the treatment groups at previously mentioned time points. Contrary to the gene expression, OPN protein level showed a significant increase after 1 hr of LIPUS application in DPI non-treated group while there was a significant decrease in DPI-treated group. Nonetheless, the protein level was higher in DPI non-treated groups after LIPUS application but the differences were not statistically significant. (Fig 4.8)

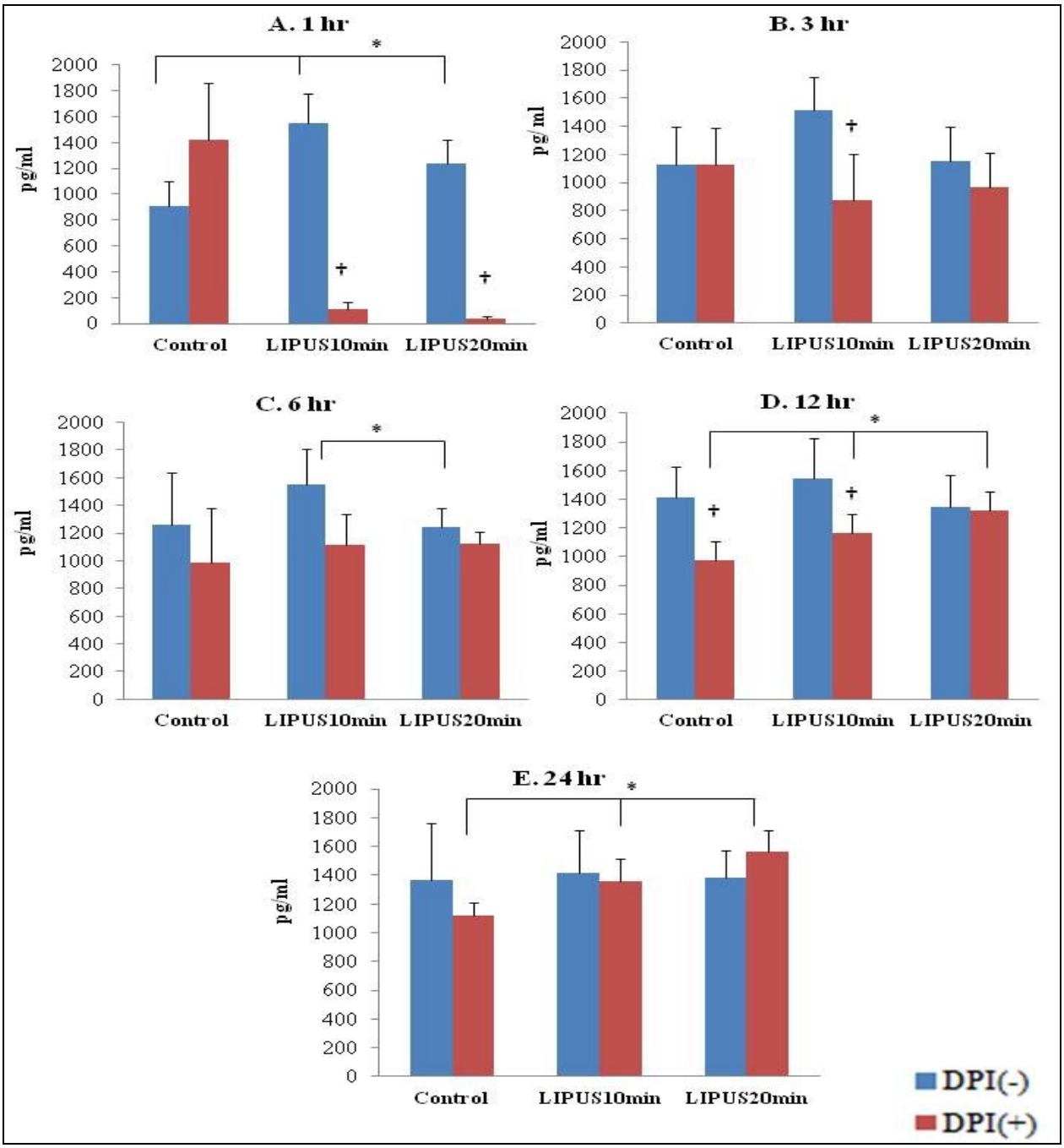

Fig 4.8: Effect of LIPUS exposure on OPN protein expression at A. 1hr, B. 3 hr, C. 6 hr, D. 12 hr and E. 24 hrs was measured by ELISA. The supernatants were collected after LIPUS exposure. In DPI non treated group, LIPUS showed significant increase in OPN protein expression while in ROS inhibition, the level significantly decreased during the first hour. (* $p<0.05$; † $p<0.05$ between the corresponding DPI treated and non-treated groups.)

4.3.6 MAPK activation after LIPUS application:

To examine the effect of LIPUS application and ROS inhibition on MAPK activation, the cells are treated with LIPUS in the presence or absence of DPI. The cells were harvested at the previous mentioned time points. LIPUS stimulation showed a significant increase in ERK1/2 activation at 6, 12 and 24 hrs as compared to control in DPI non-treated group while DPI-treated group showed significant ERK1/2 activation at 1 hr in LIPUS groups (Fig 4.9). p38 and JNK activation level showed no significant difference in LIPUS stimulation as compared to control in both DPI-treated and non-treated groups at any time points. (Fig 4.10 and 4.11)

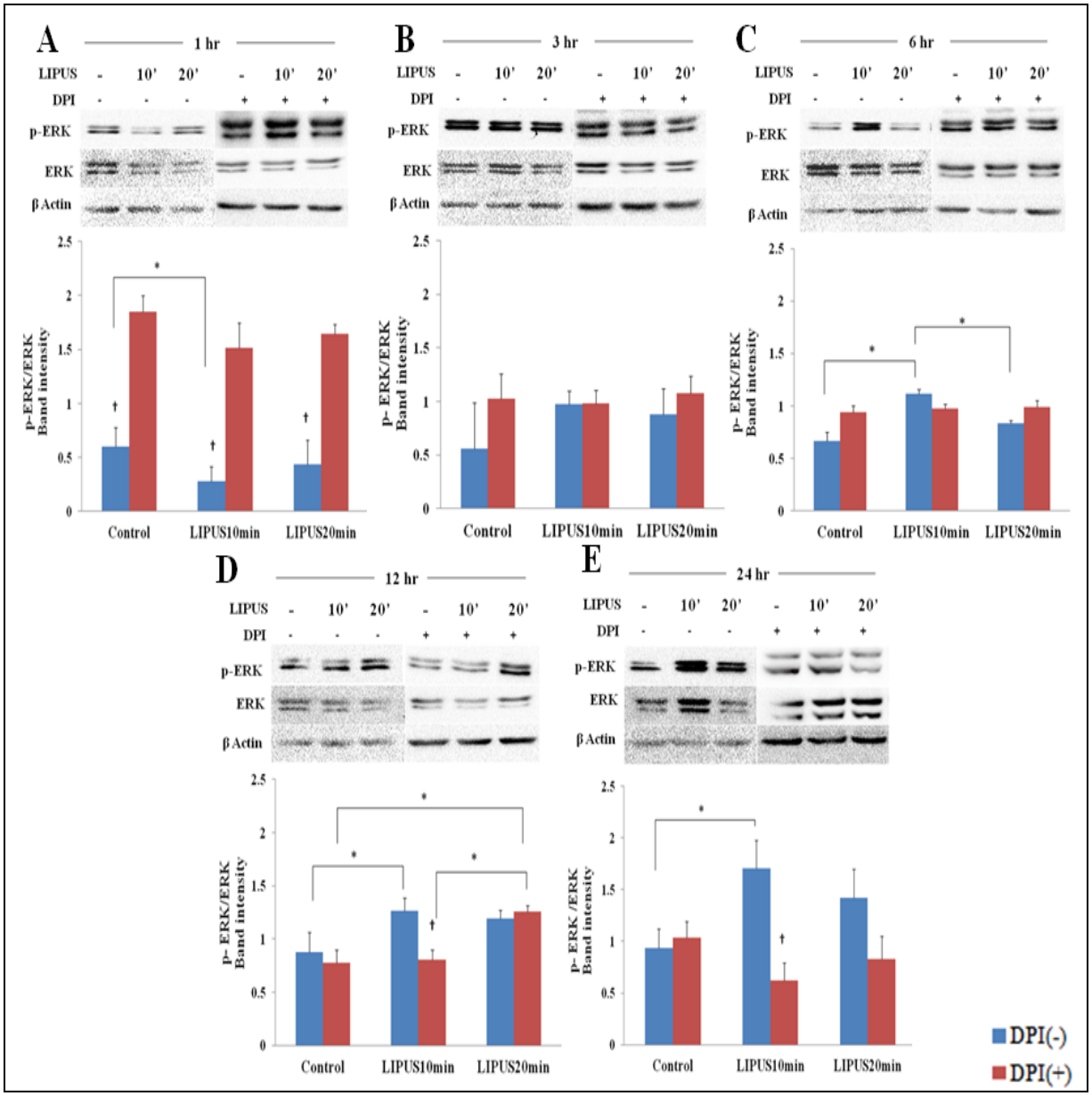

Fig 4.9: ERK1/2 activation after LIPUS application by immunoblot analysis. MC-3T3E1 pre-osteoblast cells were treated with LIPUS in the presence or absence of DPI (10 μM). The samples were harvested for immunoblot analysis after A. 1hr, B. 3hr, C. 6hr, D. 12 hr and E. 24 hrs of LIPUS application. LIPUS groups showed significant increase in the phosphorylation level at 6, 12, and 24 hrs time points in DPI non-treated group while phosphorylation level significantly increased at 1 hr in DPI treated group and the phosphorylation level decreased at latter time points. (* $p<0.05$; † $p<0.05$ between the corresponding DPI treated and non-treated groups.)

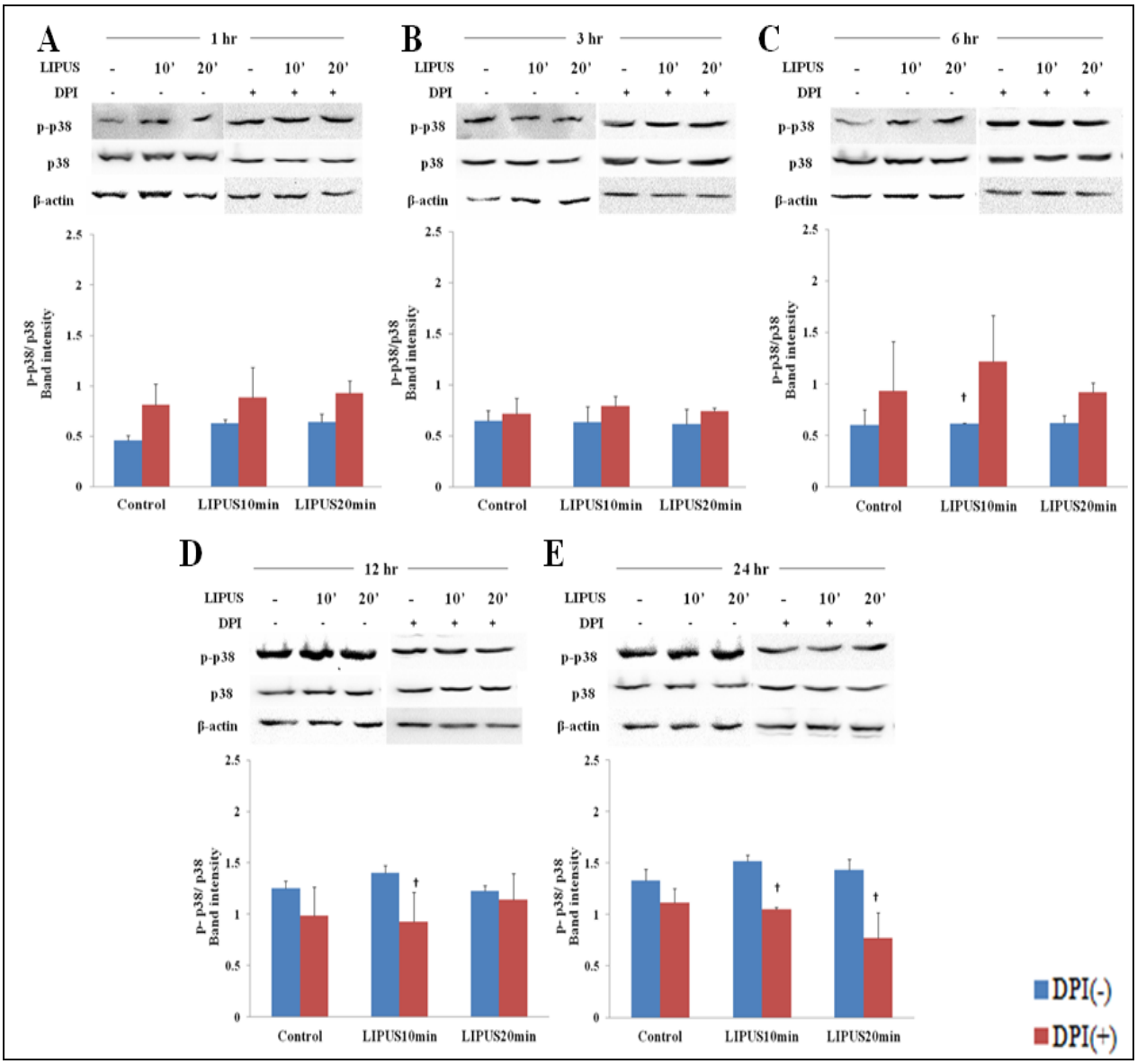

Fig 4.10: Immunoblot analysis of p38 activation by LIPUS application. MC-3T3E1 pre-osteoblasts were treated with LIPUS in the presence or absence of DPI (10 μM). The samples were harvested for immunoblot analysis after A. 1hr, B. 3hr, C. 6hr, D. 12 hr and E. 24 hrs of LIPUS application. Phosphorylation level of p38 relative to total p38 was determined by the quantification of the band intensity using ImageJ software. LIPUS stimulation showed no significant difference in the phosphorylation level at any time point in DPI treated and non-treated groups. (* $p<0.05$; † $p<0.05$ between the corresponding DPI treated and non-treated groups.)

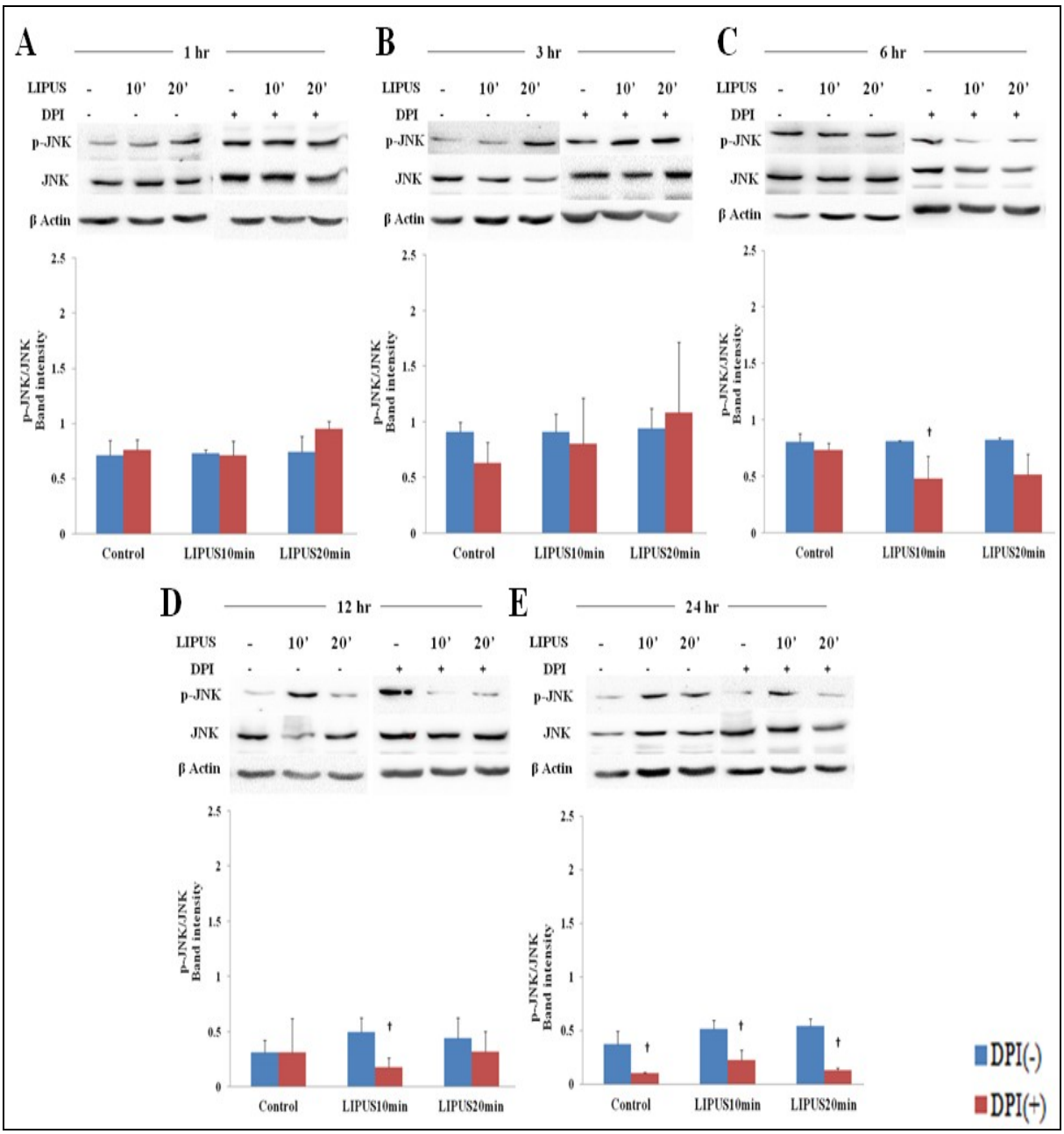

Fig 4.11: Immunoblot analysis of JNK activation by LIPUS application. MC-3T3E1 pre-osteoblasts were treated with LIPUS in the presence or absence of DPI (10 μM). The samples were harvested for immunoblot analysis after A. 1hr, B. 3hr, C. 6hr, D. 12 hr and E. 24 hrs of LIPUS application. LIPUS stimulation showed no significant difference in the phosphorylation level at any time point in DPI treated and non-treated groups. (* $p<0.05$; † $p<0.05$ between the corresponding DPI treated and non-treated groups.)

4.4. Discussion:

LIPUS has shown to increase cell proliferation and promotes osteogenic differentiation of mesenchymal stem cell (14) (15) (16). It has been routinely used in the medical field for the treatment of bone fractures (17) (18) (19). The mechanism of LIPUS has not been completely understood. Several attempts have been made in the past to understand the mechanism of LIPUS interaction with the cell. Based on the previous studies on the potential role of ROS in MAPK activation, we expected LIPUS stimulation to enhance ROS production that facilitates MAPK activation in MC-3T3 E1 pre-osteoblast cells. This would greatly expand our understanding of the usage of LIPUS for fracture healing and more recently its use in tissue engineering and regenerative medicine.

We initially explored ROS generation in pre-osteoblast cells using DHE. The effect was also studied when the cells were treated with a ROS inhibitor, DPI which prevented the organization of NOX enzymes employed in ROS formation. Our study showed a significant increase in ROS generation after LIPUS application which was reduced when DPI was added to the cell culture. Similar results were seen in the study conducted by Loreto et al (14). However, our study is different as we used pulsed wave while their study incorporated continuous waveform. Also, the transducer was placed in the water bath to prevent an increase in temperature in their studies while we used a coupling gel to sonicate the cells directly from the bottom of multiwell plates. DHE is specific for superoxide ion which gets oxidized to form hydroxyl radical (•OH) and

hydrogen peroxide (H_2O_2) in the presence of copper and ferrous ion by Haber-Weiss reaction. H_2O_2 is a stable ROS product that can pass through the cell membrane and cause toxicity. Since ROS are considered harmful due to oxidative stress, MTT cell viability assay was employed to check for the toxicity of ROS generated after LIPUS application. The cell viability significantly increased in LIPUS groups. This shows that the amount of ROS generated by LIPUS in the pre-osteoblast cell culture is not toxic under our experimental conditions.

Since our study showed an increase in ROS production and cell viability, our next step was to determine the expression of NOX enzymes involved in ROS production after LIPUS application. Hence we stimulated MC-3T3E1 pre-osteoblast cells with LIPUS and collected the samples for the gene expression of *NOX2* and *NOX4*. The study showed a significant increase in gene expression for both *NOX2* and *NOX4* at 6 hr in DPI non-treated group, interestingly the expression of both genes was higher at 1 hr time point in DPI-treated group. This could be due to the compensatory mechanism of the cells to generate higher gene in the case of inhibition. NOX enzymes, involved in ROS production, require the organization of additional components for the activation – $p22^{phox}$, $p40^{phox}$, $p47^{phox}$ and $p60^{phox}$. GTP binding protein Rac1 is essential for NOX complex organization and activation (15) LIPUS has previously shown to increase the activation of Rac1 (16). In addition, BMP2, a potent bone-forming morphogenetic protein, has also shown to increase ROS generation by activating NOX enzymes and ROS inhibitors like N-acetyl Cysteine and DPI inhibited BMP2 induced ROS

generation (17). NOX2 and NOX4 play an important role in osteoblast proliferation and differentiation respectively. Additionally, NOX4 protein expression was also higher in osteoblast layer in subchondral bone of mandible condyle (18). Collectively, these studies and our results showed involvement of both *NOX2* and *NOX4* for ROS production in the cells during LIPUS application.

We subsequently investigated the gene expression to explore the effect of ROS generated during LIPUS application on the pre-osteoblast cells at the molecular level. RUNX2 is a transcription factor that is essential for osteoblast differentiation and expression of osteoblast-specific genes, and consequently is important for both intramembranous and endochondral bone formation (19). OCN and OPN are the late differentiation markers of the osteoblast cells. OCN, a non-collagenous protein, is exclusively secreted by osteoblast that undergoes carboxylation as post-translational modification which helps its binding to the mineralized bone matrix (20). OPN, on the other hand, is highly phosphorylated glycoprotein secreted by osteoblast, hypertrophic chondrocytes, and odontoblasts (21). Our results showed a significant increase in *RUNX2* and *OCN* mRNA expression in LIPUS treated group as compared to the control from 6 hr onwards in case of RUNX2 and at 24 hr in *OCN*. These results are supported by other LIPUS treated osteoblast studies from independent labs (22) (23). In ROS inhibition groups, *RUNX2, OCN* and *OPN* mRNA showed increased expression at 1 hr time point. Furthermore, the protein level of OPN increased significantly after LIPUS exposure in DPI non-treated groups while the OPN level was significantly lower in DPI

treated group during the first hour but it changed significantly during the latter time points and reaching to the same level as DPI non-treated group by 24 hr. Since OPN is phosphorylated glycoprotein whose gene expression was higher in ROS inhibition while the protein level was significantly lower. This could be due to ROS that affected the phosphorylation of OPN. To the best of our knowledge, no study has been reported in the literature which stated the interaction of OPN and ROS in osteoblast.

It has been suggested that mechanical stimulus plays a crucial role in MAPK activation in different cell lines. In osteoblasts, ERK1/2 is involved in OCN and bone sialoprotein (BSP) expression through RUNX2 activation. Also, ERK1/2 has involved in post-translational modification of cytoskeleton that helps in cell migration. Similar to ERK, p38 promotes osteoblast differentiation however; JNK activation is not completely understood in the osteoblasts. In-vitro study with JNK inhibition reduced the expression of BSP, OCN and blocks late stage osteoblast differentiation (24). Finally, we tested whether MAPK signaling pathway is activated in MC-3T3E1 pre-osteoblast cells after LIPUS exposure. Our study showed increased ERK1/2 activation in LIPUS treated groups at 6 hr onwards in DPI non-treated group while ROS inhibition led to early activation of ERK1/2. Since ERK1/2 is involved in RUNX2 activation, the results of RUNX2 gene expression followed the similar trend as ERK1/2 activation. These results strongly suggested that ERK1/2 activation after LIPUS stimulation is involved in RUNX2 expression.

Our aim in this study was to understand the potential mechanism of LIPUS in MC 3T3E1 pre-osteoblast cells. Therapeutic ultrasound has been extensively used for imaging fetus, calculi crushing in the urinary tract and in surgical procedures like lumpectomies. Its application is based on the intensity used, ranging from low intensity of 30 mW/cm^2 to high intensity 300 w/cm^2. Therapeutic ultrasound exerts thermal and non-thermal effects on the bone. However, an intensity of 30 mW/cm^2 used in LIPUS is considered low to generate a thermal effect. The non-thermal effect is further divided into cavitation and acoustic streaming. Cavitation involves generation of the gas bubble in the tissue fluid which oscillates with compression and rarefaction of ultrasound waves and collapses to generate a low amount of energy (25) thus causing damage to the cell (26). Like thermal effect, the intensity of LIPUS is low to generate cavitation phenomenon in the bone. Another non-thermal effect by which LIPUS benefit the bone is a generation of a fluid flow along and around the cell membrane. These waves cause radiation forces on the membrane and affect mechanosensitive receptors like integrins (27) along with alteration of micro-environment around the cell by changing concentration gradient of ions, stretching the ion channels, and improving the distribution of growth factors (28). Mechanical stimulation of LIPUS activates integrins (8) that further triggers phosphorylation of focal adhesion molecules like focal adhesion kinase (FAK) and Src (29) (30) which are upstream regulators of MAPK signaling. Recent studies have shown that phosphorylation of MAPK and focal adhesion molecules are controlled by reversible redox modification. ROS oxidize the thiol group

in the focal adhesion molecule and in protein tyrosine phosphatases (PTPs) thus causing conformational changes by forming disulfide bonds (31).

In this study, we tested LIPUS for two time durations- 10 min and 20 min application to pre-osteoblast cells in order to optimize the time for in-vitro study. 20 min LIPUS application is most frequently used in the in-vivo studies and is also approved by US Food and Drug Administration for clinical use, while most of the in-vitro studies have shown increased anabolic effect of LIPUS at 10 min application. This could be due to attenuation of LIPUS while passing through the living tissue. On the other hand, in in-vitro studies the amount of attenuation is lesser. Also, we placed the cell culture plates on the transducer surface using coupling gel as a transfer medium. Using this set-up, temperature increase of up to 3ºC with 20 min application has been reported by Leskinen and Hynynen (32). This temperature increase might have also caused difference in LIPUS effect at the molecular level.

4.5 Conclusion:

Intramembranous ossification and endochondral ossification are two processes of bone formation. Previously it was believed that hypertrophic chondrocytes undergo apoptosis and die but recent studies have shown differentiation of chondrocytes to osteoblasts (33). A study by Gentili et al (34) showed chondrocytes when cultured in the presence of ascorbic acid (another ROS scavenger) led to differentiation into osteoblast like cells. In endochondral bone formation, ROS and ERK1/2 are involved in the differentiation of chondrocytes (35) (36). For now, we can only hypothesize ROS to be

another factor that can regulate chondrocyte differentiation. Our study demonstrates that LIPUS application regulated the expression of osteogenic specific genes and activation of ERK1/2 signaling pathway via ROS generation in MC-3T3E1 pre-osteoblast cells. However, further studies are needed to understand the role of ROS in endochondral ossification.

4.6 References:

1. Haugh MG, Vaughan TJ, McNamara LM. The role of integrin αVβ3 in osteocyte mechanotransduction. J Mech Behav Biomed Mater. 2015 Feb;42:67–75.

2. Tan J, Xu X, Tong Z, Lin J, Yu Q, Lin Y, et al. Decreased osteogenesis of adult mesenchymal stem cells by reactive oxygen species under cyclic stretch: a possible mechanism of age related osteoporosis. Bone Res. 2015;3:15003.

3. Wang JH-C, Thampatty BP. An introductory review of cell mechanobiology. Biomech Model Mechanobiol. 2006 Mar;5(1):1–16.

4. Matsushita T, Chan YY, Kawanami A, Balmes G, Landreth GE, Murakami S. Extracellular Signal-Regulated Kinase 1 (ERK1) and ERK2 Play Essential Roles in Osteoblast Differentiation and in Supporting Osteoclastogenesis. Mol Cell Biol. 2009 Nov;29(21):5843–57.

5. Beardmore VA, Hinton HJ, Eftychi C, Apostolaki M, Armaka M, Darragh J, et al. Generation and Characterization of p38β (MAPK11) Gene-Targeted Mice. Mol Cell Biol. 2005 Dec;25(23):10454–64.

6. Greenblatt MB, Shim J-H, Zou W, Sitara D, Schweitzer M, Hu D, et al. The p38 MAPK pathway is essential for skeletogenesis and bone homeostasis in mice. J Clin Invest. 2010 Jul;120(7):2457–73.

7. Tanaka E, Kuroda S, Horiuchi S, Tabata A, El-Bialy T. Low-Intensity Pulsed Ultrasound in Dentofacial Tissue Engineering. Ann Biomed Eng. 2015 Feb 12;

8. Yang R-S, Lin W-L, Chen Y-Z, Tang C-H, Huang T-H, Lu B-Y, et al. Regulation by ultrasound treatment on the integrin expression and differentiation of osteoblasts. Bone. 2005 Feb 1;36(2):276–83.

9. Parvizi J, Parpura V, Greenleaf JF, Bolander ME. Calcium signaling is required for ultrasound-stimulated aggrecan synthesis by rat chondrocytes. J Orthop Res. 2002 Jan;20(1):51–7.

10. Tang C-H, Lu D-Y, Tan T-W, Fu W-M, Yang R-S. Ultrasound induces hypoxia-inducible factor-1 activation and inducible nitric-oxide synthase expression through the integrin/integrin-linked kinase/Akt/mammalian target of rapamycin pathway in osteoblasts. J Biol Chem. 2007 Aug 31;282(35):25406–15.

11. Sauer H, Wartenberg M, Hescheler J. Reactive oxygen species as intracellular messengers during cell growth and differentiation. Cell Physiol Biochem. 2001;11(4):173–86.

12. Schröder K. NADPH oxidases in bone homeostasis and osteoporosis. Cell Mol Life Sci. 2014 Aug 29;72(1):25–38.

13. Son Y, Kim S, Chung H-T, Pae H-O. Chapter Two - Reactive Oxygen Species in the Activation of MAP Kinases. In: Enrique Cadenas and Lester Packer, editor. Methods in Enzymology [Internet]. Academic Press; 2013 [cited 2013 Dec 11]. p. 27–48. Available from: http://www.sciencedirect.com/science/article/pii/B9780124058811000021

14. Mostafa NZ, Uludağ H, Dederich DN, Doschak MR, El-Bialy TH. Anabolic effects of low-intensity pulsed ultrasound on human gingival fibroblasts. Arch Oral Biol. 2009 Aug;54(8):743–8.

15. Nagasaki R, Mukudai Y, Yoshizawa Y, Nagasaki M, Shiogama S, Suzuki M, et al. A Combination of Low-Intensity Pulsed Ultrasound and Nanohydroxyapatite Concordantly Enhances Osteogenesis of Adipose-Derived Stem Cells From Buccal Fat Pad. Cell Med. 2015 Oct 1;7(3):123–31.

16. Lv Y, Zhao P, Chen G, Sha Y, Yang L. Effects of low-intensity pulsed ultrasound on cell viability, proliferation and neural differentiation of induced pluripotent stem cells-derived neural crest stem cells. Biotechnol Lett. 2013 Dec;35(12):2201–12.

17. Busse JW, Kaur J, Mollon B, Bhandari M, Tornetta P 3rd, Schünemann HJ, et al. Low intensity pulsed ultrasonography for fractures: systematic review of randomised controlled trials. BMJ. 2009;338:b351.

18. Hemery X, Ohl X, Saddiki R, Barresi L, Dehoux E. Low-intensity pulsed ultrasound for non-union treatment: A 14-case series evaluation. Orthopaedics & Traumatology: Surgery & Research. 2011 Feb;97(1):51–7.

19. Waseem Z, Ford M, Syed K, Flannery J. Chronic nonunion in a patient with bilateral supracondylar distal femur fractures treated successfully with twice daily low-intensity pulsed ultrasound. PM R. 2010 Feb;2(2):159–61.

20. Feril LB, Kondo T. Major factors involved in the inhibition of ultrasound-induced free radical production and cell killing by pre-sonication incubation or by high cell density. Ultrason Sonochem. 2005 Apr;12(5):353–7.

21. Bedard K, Krause K-H. The NOX family of ROS-generating NADPH oxidases: physiology and pathophysiology. Physiol Rev. 2007 Jan;87(1):245–313.

22. Claire M. Mahoney, Morgan MR, Harrison A, Humphries MJ, Bass MD. Therapeutic ultrasound bypasses canonical syndecan-4 signaling to activate rac1. J Biol Chem. 2009 Mar 27;284(13):8898–909.

23. Mandal CC, Ganapathy S, Gorin Y, Mahadev K, Block K, Abboud HE, et al. Reactive oxygen species derived from Nox4 mediate BMP2 gene transcription and osteoblast differentiation. Biochem J. 2011 Jan 15;433(2):393–402.

24. Ambe K, Watanabe H, Takahashi S, Nakagawa T. Immunohistochemical localization of Nox1, Nox4 and Mn-SOD in mouse femur during endochondral ossification. 2014.

25. Bruderer M, Richards RG, Alini M, Stoddart MJ. Role and regulation of RUNX2 in osteogenesis. Eur Cell Mater. 2014;28:269–86.

26. Cooper MS, Seibel MJ, Zhou H. Glucocorticoids, bone and energy metabolism. Bone. 2016 Jan;82:64–8.

27. Sodek J, Ganss B, McKee MD. Osteopontin. CROBM. 2000 Jan 1;11(3):279–303.

28. Li JK, Chang WH, Lin JC, Ruaan RC, Liu HC, Sun JS. Cytokine release from osteoblasts in response to ultrasound stimulation. Biomaterials. 2003 Jun;24(13):2379–85.

29. Wu L, Lin L, Qin Y-X. Enhancement of cell ingrowth, proliferation, and early differentiation in a three-dimensional silicon carbide scaffold using low-intensity pulsed ultrasound. Tissue Eng Part A. 2015 Jan;21(1–2):53–61.

30. Greenblatt MB, Shim J-H, Glimcher LH. Mitogen-Activated Protein Kinase Pathways in Osteoblasts. Annual Review of Cell and Developmental Biology. 2013;29(1):63–79.

31. Claes L, Willie B. The enhancement of bone regeneration by ultrasound. Prog Biophys Mol Biol. 2007 Apr;93(1–3):384–98.

32. Johns LD. Nonthermal Effects of Therapeutic Ultrasound: The Frequency Resonance Hypothesis. J Athl Train. 2002;37(3):293–9.

33. Padilla F, Puts R, Vico L, Raum K. Stimulation of bone repair with ultrasound: a review of the possible mechanic effects. Ultrasonics. 2014 Jul;54(5):1125–45.

34. Ebisawa K, Hata K, Okada K, Kimata K, Ueda M, Torii S, et al. Ultrasound Enhances Transforming Growth Factor β-Mediated Chondrocyte Differentiation of Human Mesenchymal Stem Cells. Tissue Engineering. 2004 May;10(5–6):921–9.

35. Gusmão CVB de, Pauli JR, Saad MJA, Alves JM, Belangero WD. Low-intensity Ultrasound Increases FAK, ERK-1/2, and IRS-1 Expression of Intact Rat Bones in a Noncumulative Manner. Clin Orthop Relat Res. 2009 Oct 23;468(4):1149–56.

36. Zhou S, Bachem MG, Seufferlein T, Li Y, Gross HJ, Schmelz A. Low intensity pulsed ultrasound accelerates macrophage phagocytosis by a pathway that requires actin polymerization, Rho, and Src/MAPKs activity. Cellular Signalling. 2008 Apr;20(4):695–704.

37. Fernandes GVO, Cavagis ADM, Ferreira CV, Olej B, de Souza Leão M, Yano CL, et al. Osteoblast Adhesion Dynamics: A Possible Role for ROS and LMW-PTP. J Cell Biochem. 2014 Jun 1;115(6):1063–9.

38. Leskinen JJ, Hynynen K. Study of factors affecting the magnitude and nature of ultrasound exposure with in vitro set-ups. Ultrasound Med Biol. 2012 May;38(5):777–94.

39. Jing Y, Zhou X, Han X, Jing J, Mark K von der, Wang J, et al. Chondrocytes Directly Transform into Bone Cells in Mandibular Condyle Growth. J DENT RES. 2015 Sep 4;22034515598135.

40. Gentili C, Bianco P, Neri M, Malpeli M, Campanile G, Castagnola P, et al. Cell proliferation, extracellular matrix mineralization, and ovotransferrin transient expression during in vitro differentiation of chick hypertrophic chondrocytes into osteoblast-like cells. J Cell Biol. 1993 Aug;122(3):703–12.

41. Chen Z, Yue SX, Zhou G, Greenfield EM, Murakami S. ERK1 and ERK2 regulate chondrocyte terminal differentiation during endochondral bone formation. J Bone Miner Res. 2015 May;30(5):765–74.

42. Morita K, Miyamoto T, Fujita N, Kubota Y, Ito K, Takubo K, et al. Reactive oxygen species induce chondrocyte hypertrophy in endochondral ossification. J Exp Med. 2007 Jul 9;204(7):1613–23.

Chapter 5: Effect of non viral plasmid delivered basic Fibroblast growth factor and low intensity pulsed ultrasound on mandibular condylar growth – a preliminary study.

A version of this chapter was published as: Kaur, H, Uludag H and El-Bialy T. Bio Med Research International, Vol 2014, doi.org/10.1155/2014/426710

5.1 Introduction:

Bone remodeling is a continuous process of bone formation and resorption to maintain its shape and its function. But many conditions like tumors, trauma, skeletal abnormalities and congenital disorders can compromise this dynamic process (1). 700 out of 6000 known congenital syndromes involve craniofacial defects which include but not limited to Treacher Collin Syndrome, Pierre Robin Syndrome etc (2). These problems not only affect the social life but also have the psychological effects on the affected individuals (3)(4)(5). The available treatments of these cases usually include orthopedic surgery, bone grafting and distraction osteogenesis in addition to orthodontic treatment, speech and behavioral management (6). All these treatment modalities have various limitations such as lack of required bone volume, donor site morbidity, long procedure time, graft resorption, disease transmission and known surgical complications. Due to all these limitations, a non conventional form of treatment like gene therapy may be a ray of hope.

The process of bone formation takes place by one of two methods: intramembranous and endochondral bone formation. In endochondral ossification, the chondrocytes present in the cartilage undergo morphogenesis and calcification by the invasion of blood vessels which results in the new bone formation (7). Hence the vascularization is an essential step in the endochondral bone formation. Growth factors like Vascular Endothelial Growth Factor (VEGF) and bFGF play important roles in the process of new blood vessel formation. Many growth factors have been studied for their

regulatory effect in the cell activities like adhesion, proliferation, differentiation in epithelium, bone, connective tissue and the nerves (8). Basic Fibroblast Growth Factor belongs to the family of FGF that comprises of 22 members. It is present in bone matrix and is an important agent in the initial vascularization for the endochondral bone formation (9)(10). bFGF is a potent cytokine that not only help in angiogenesis but it also has a stimulatory role in osteogeneic differentiation of pre-osteoblasts (11), limb development and in fracture healing (10). It exhibit its biological function by binding and activation of FGF receptors1, 2 and 3. bFGF effects the bone formation of the facial region. One study (12) showed that blocking of bFGF leads to the prevention of bone formation at the craniofacial suture sites and study by Hamada et al (13) showed receptors of FGF family present in the condylar cartilage which helps in the differential growth of the condylar cartilage. Rabie et al (6) has successfully studied the effect of adeno virus delivered VEGF on the mandibular condylar growth.

Gene therapy is a fast developing technology that is defined as the treatment of disease by the transfer of the genetic material into the cells in the form of small DNA or RNA fragments. Studies on the treatment of diseases like genetic disorders (14), cancer (15) and neuro-degenerative disease (16). The expected success of gene therapy depends on its delivery system. For the delivery of the gene, either virus or non-virus vectors may be used as the carriers. Viral vectors provide efficient gene delivery to the targeted tissue and longer gene expression. But due to safety concerns associated with viral vectors like immunogenicity and oncogenecity (17) and death of a patient in1999

after adeno viral mediated gene therapy due to disseminated intravascular coagulation and multiple organ failure (18). For these reasons, a non viral vector is a preferred gene delivery approach. Non viral gene delivery involves the transfer of the genetic material either by direct injection of the plasmid or by physical or chemical methods. Plasmid is a linear or circular double stranded DNA. Direct delivery of the plasmid DNA (pDNA) is the most simple and the most convenient method of the gene delivery. Electroporation and sonoporation are two examples of the physical methods used in the gene delivery.

Ultrasound is an acoustic pressure or energy that propagates through the media in the form of waves having the frequency above the human hearing range. The low intensity ultrasound is studied for its role in drug delivery into solid tumor (19), gene delivery to the target tissue (20)(21)(22), treatment of bone fracture, distraction osteogenesis (23)(24) (25)(26), reduction of root resorption after tooth movement (27) and also the growth of the mandibular condyle (28)(29)(30). Out of these, ultrasound application for the treatment of bone fracture has been approved by Food and Drug Association, USA. The exact mechanism is still unclear, however it has been suggested that the effects of LIPUS may be physical or piezoelectric in nature (31). In the recent times, LIPUS has been used as one of the physical method for the gene delivery by using high intensities ranging from 0.4 W/cm^2(32) to 1 W/cm^2 (21) to 2 W/cm^2(22). In a study by Zhou et al (33) for the gene transfection, in the in-vitro procedure intensity applied was 0.75 W/cm^2 and for in-vivo, the intensity used was 2 W/cm^2.

The hypothesis of this pilot study was that bFGF along with LIPUS would enhance the mandibular growth. The objectives were to study the effect of bFGF pDNA delivery on the mandibular condyle and to explore the possible effect of the local injection of bFGF plasmid and daily low intensity pulsed ultrasound (LIPUS) application on the mandibular condylar growth. Changes in height, length, cell proliferation and width of the condylar cartilage were evaluated along with the changes in bone mineral density (BMD), bone volume (BVol) and the ratio of bone volume to tissue volume also known as bone volume fraction (BV/TV).

5.2 Materials and methods:

5.2.1 Animal care and the experimental design:

A total of fifteen late adolescent (~200 gm) adult Sprague Dawley rats were purchased from the Biosciences Laboratory, University of Alberta, Edmonton, Alberta, Canada. All the animal procedures were performed according to the guidelines of the Canadian Council on Animal Care and the study was approved by Animal Welfare Committee at the University of Alberta. Before the procedure, the rats were allowed to acclimatize for a period of 7 days. The rats were housed in pairs in clean cages and were allowed for free access to the standard commercial rat chow (Lab Diet, St. Louis, MO, USA) and tap water. The rats were randomly divided into 5 groups (n=3). Group 1 was the control, Group 2 was injected with blank plasmid (25 µgm gWiz) on the first day of the experiment, Group 3 was injected with 25 µgm bFGF pDNA (description of the plasmid is provided below) on the first day of the experiment, Group 4 received 20 min

of LIPUS for the next 28 days and Group 5 was injected with 25 µgm bFGF pDNA on the first day of the experiment and received LIPUS application for 20 min for 28 days. In all the groups, left mandibular condyle was used as the experimental side. The treatment side of each animal was shaved and coupling gel was applied to ensure the wave propagation. The prepared solutions corresponding to each group were injected to the posterior attachment of the mandibular condyles in the experimental side using ½ cc U-100 Insulin syringe with attached 28½ gauge needle (Becton-Dickinson & Company, Franklin Lakes, NJ, and USA) according to the previously reported technique (6)(34). Before injection, aspiration was performed to make sure that the needle is not into a blood vessel. The content was released slowly over a period of one min to prevent any damage to the surrounding structures. During the ultrasound application, the animals were under inhalation anesthesia of 2.5% Isoflurane with 100% Oxygen. After twenty four hours from the final application of LIPUS, the animals were euthanized by using asphyxiation in CO_2 chamber. The mandibles were extracted from the animals and were placed in formalin solution.

5.2.2 Plasmid material:

The plasmids used in this study were a commercially-available blank plasmid (gWiz) encoding no functional genes and a plasmid (pFGF2-IRES-AcGFP) encoding for both bFGF and Green Fluorescence Protein (GFP) with an internal ribosomal entry site (IRES). The construction and preparation of the latter plasmid was described in

Clements et al (11). The plasmids were mixed with a lipopolymer (linoleic acid substituted 2 kDa polyethyleneimine (35) at plasmid: polymer ratio of 1:5 in 0.15 M NaCl (25 μg plasmid to 125 μg polymer in 100 μL injection volume per rat). The plasmid/polymer mixtures were allowed to incubate for 30 minutes before injection into rats.

5.2.3 Ultrasound application and calibration:

The ultrasound device was custom made and was provided by Smile Sonica Ltd company, Edmonton, Alberta, Canada. The transducer has the emitting surface area of 1.5 cm^2 (12 mm X 13 mm) and generated 200 micro second burst of 1.5 MHz sine wave repeating at 1 kHz that delivered temporal averaged intensity of 30 mW/ cm^2. The ultrasound device was calibrated at the beginning and at the end of the experiment confirmed that the ultrasound device provided stable power output and maintained the desired parameters during the experiment.

5.2.4 Morphometric measurements of the mandible:

The extracted mandibles were divided at the symphyseal junction into two hemi-mandibles. Fig 5.1a shows the points and the linear measurements of the mandible. The mandibles were measured with the help of digital caliper (Fig 5.1b). The description of the points and the parameters are Table 5.1 (36).

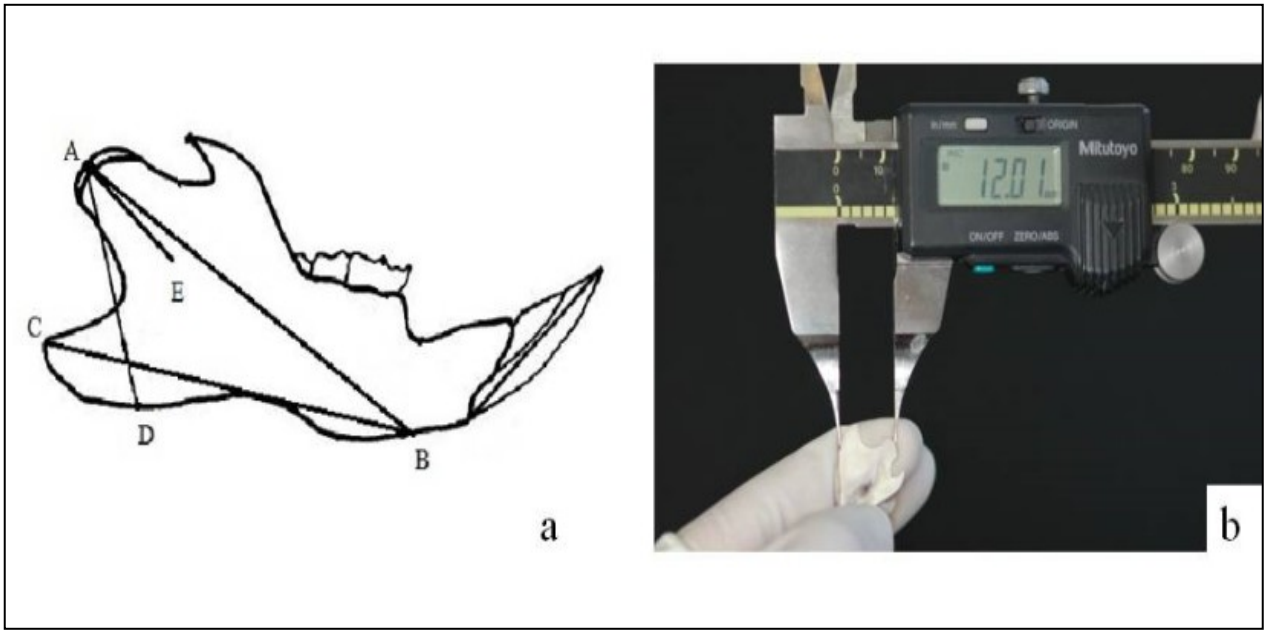

Fig 5.1 A. The diagram illustrating the morphometric points and linear measurements of the mandible (for definition see Table 1)**. B:** The morphometric measurement of the extracted rat mandible with the help of digital caliper.

Table 5.1: Description of the morphometric points and linear measurements.

Points	**Description**
Condylar point (A)	The most posterior and superior point on the mandible condyle.
Menton (B)	The most inferior point on the mandibular symphysis
Gonion point (C)	The most posterior point on the bony contour of the gonial angle of the mandible
Gonion tangent point (D)	Assuming that the mandible is placed on a plane. The point of the mandibular gonion at its junction with that plane.
Mandibular Foramen (E)	The entry of mandibular nerve and blood vessels in the mandibular canal.
Linear measurement	
Menton–Condylar point(A-B)	Total mandibular length. The distance measured between the menton and the condylar point.
Menton – Gonion point (B-C)	Length of mandibular base. The distance measure between the menton and gonion point.
Condylar - GoT(A-D):	Ramus height. The distance measured between the condylar point ar the gonial tangent point.
Condylar process length (A-E)	The distance measured from the mandibular foramen to the condylar point.

5.2.5 Micro CT Imaging:

The mandibles were fixed in 10% neutral buffered formalin (approx 4% formalin, Sigma–Aldrich, Oakville, Ontario, CA) for 24 hours at the room temperature. They were scanned using Micro CT imager, Skyscan 1076, Skyscan NV, Belgium, with resolution of 18 μm at 0.5° step increments with 1180 msec exposure time. The tube voltage and the current were 70 kV and 139 μA respectively. The raw image data reconstructed using modified Feldkamp back projection algorithm with the cross section threshold of 0.00 – 0.04 using NRecon reconstruction software (version 1.4.4, Skyscan NV, Belgium). The analysis of the micro- architecture was done on the vendor supplied CTAN software (Skyscan NV, Belgium). The region of interest (ROI's) was manually selected on the condylar trabecular bone (Fig 5.2). The bone mineral density (BMD) was determined based on the linear correlation between CT attenuation coefficient and bone mineral density. The parameters evaluated from the scans were: bone volume fraction (BV/TV), bone volume (BVol) and bone mineral density (BMD).

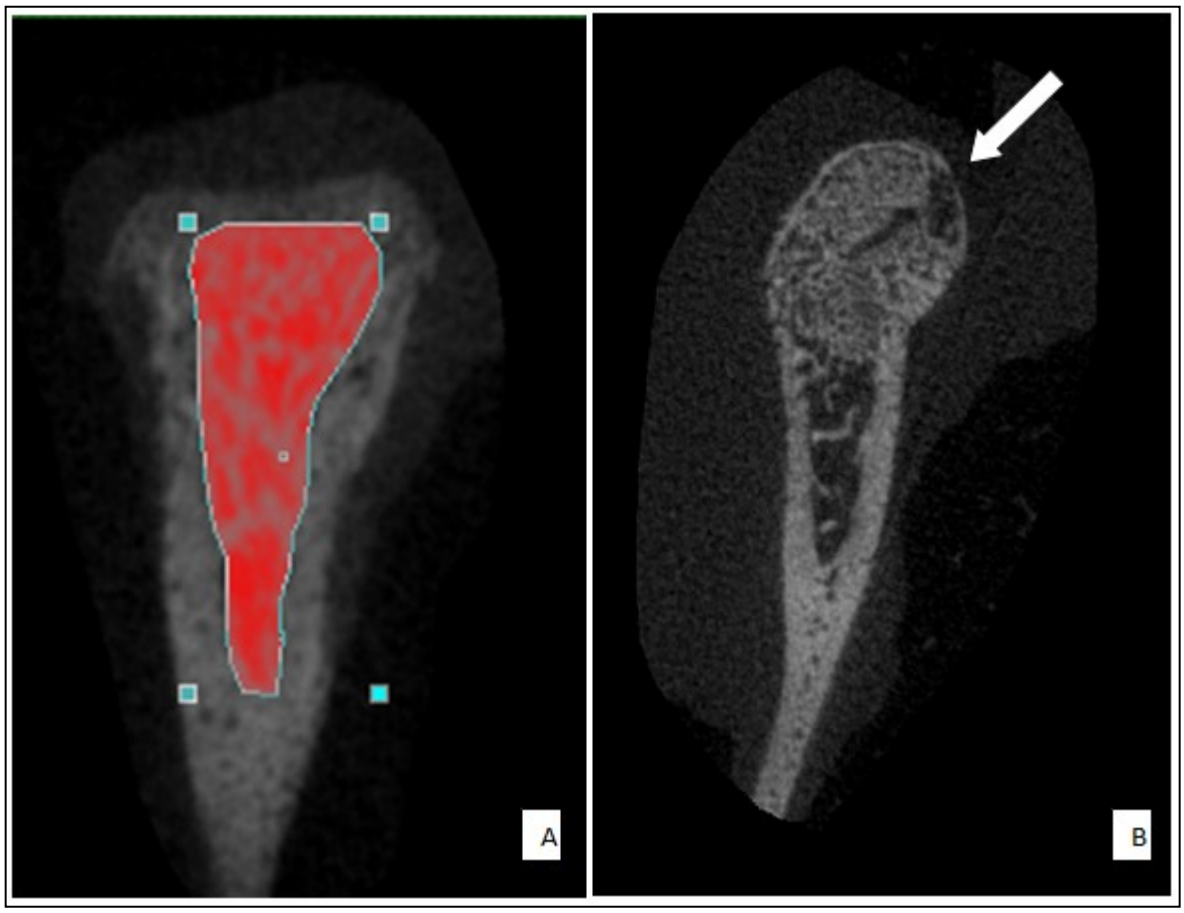

Fig 5.2 : Transaxial view of the MicroCT scan. A. The region of interest was manually drawn to separate trabecular bone from the cortical bone of the condyle and was analysed later using MicroCT Analyser (Skyscan, NV, BE). B. The new bone formation in the bFGF treated group on the mandibular condylar head.

5.2.6 Histology and Histomorphometric analysis:

The mandibles were decalcified using Cal-EX II (Fisher Scientific, Ottawa, CA) (formaldehyde 1.03 M/L, formic acid 2.56 M/L) for about 2 weeks. The samples were processed into paraffin blocks. The sections were in the thickness of 6 μm and were stained with Hematoxylin and Eosin stain. 6 samples were taken from each mandible and the slides were scanned and the photographs were taken using Leica Fluorescent Digital Microscope with charge couple device (CCD) digital camera (Leica, Wetzlar, Germany). The analysis of the images was done using RS Image software 1.73 (Photometric, Roper Scientific Inc, Tucson, AZ, USA). The magnification used was 20X. The cell number and the width of the proliferative and hypertrophic layers were measured. The readings from the six slides of each sample were then averaged to get the final reading for every sample. The condylar cartilage is divided into 4 zones; resting, proliferative, hypertrophic and erosive. Proliferative layer is composed of densely packed mesenchymal cells with high nuclei and cytoplasm ratio. Hypertrophic layer is subdivided into mature chondrocytes and hypertrophic chondrocytes. The cells are larger than the cells in proliferative layer. In this study the mature and hypertrophic chondrocytes were analyzed together as the hypertrophic layer. The proliferative and hypertrophic layers were studied according to their histological characteristics.

5.2.7 Statistical analysis:

The data were collected and processed using SPSS 19.0 (Chicago, IL, USA) by Kruskal-Wallis non parametric test for analysis of all the five groups because of the

relative small sample size. For the comparison between the groups Mann- Whitney U test was used. (The non parametric tests compare the median of the groups.) The mean and standard deviation were presented in the bar graph for each variable and were not compared for statistical analysis. $p = 0.05$ was considered statistically significant.

5.3 Results:

No inflammation or irritation was noted at the injection site. No reduction in weight was noticed during the treatment phase.

***5.3.1 Morphometric analysis**:*

Linear measurements of Condyle-GoT (Ramal height, A-D), Men-GP (mandibular base, B-C) and the Condylar point- Mandibular foramen (Condylar Process, A-E) showed statistically significant increase in the LIPUS. In Fig 5.3, there is significant difference between control and LIPUS treated group and control and bFGF group ($p<0.05$). Ramal height (A-D) showed statistical increase in all the treatment groups compared to the control group ($p=0.02$). There is also significant difference between bFGF and LIPUS groups (Fig 5.4). Men-GP (B-C) showed statistical significant increase in the LIPUS group compared to the control group ($p= 0.02$), bFGF + LIPUS ($p = 0.05$) and statistically significant difference between control and bFGF + LIPUS combination group (Fig 5.5) while the linear measurement of the Condylar point- Men (length of the mandible, A-B) showed no statistically significant difference (data not shown). Overall, by comparing the means of the groups, LIPUS treated group

showed the maximum increase in the anthropometric measurement followed by the combination treatment of bFGF + LIPUS followed by bFGF treated group.

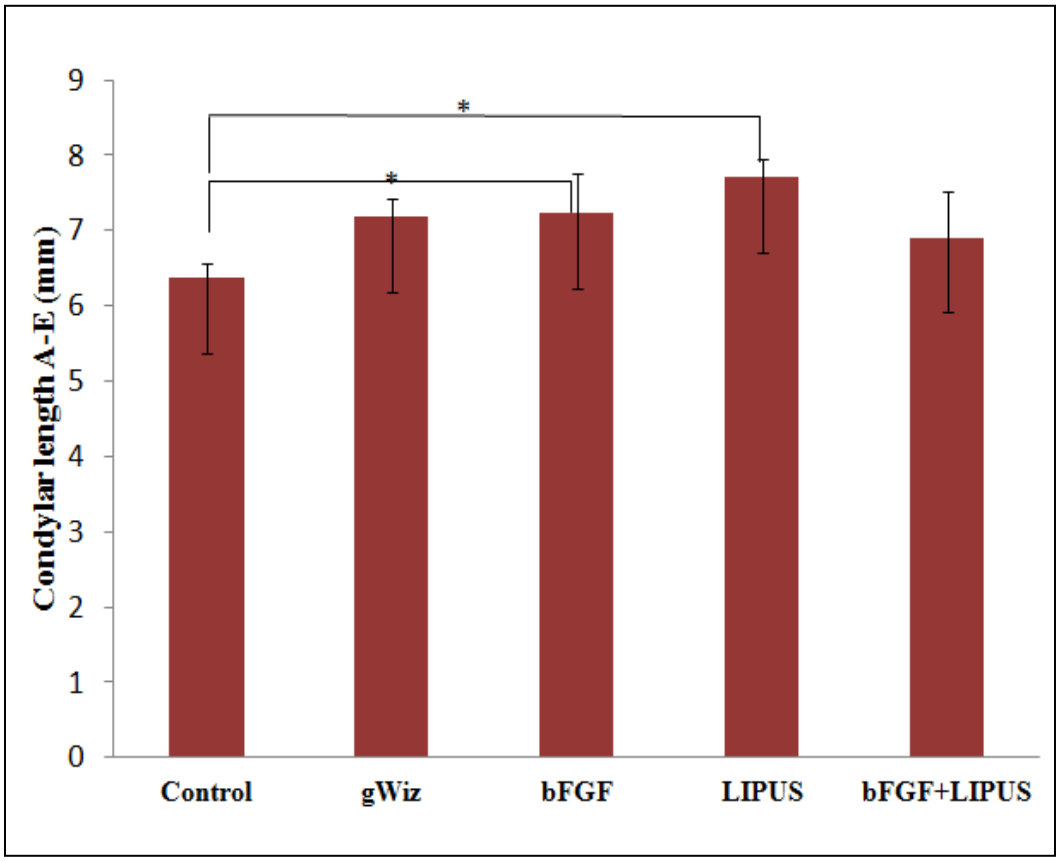

Fig 5.3: The bar chart of the length of the condylar process (A-E) among the five groups showing increase in the length in the LIPUS treated group {* = $p \leq 0.05$}.

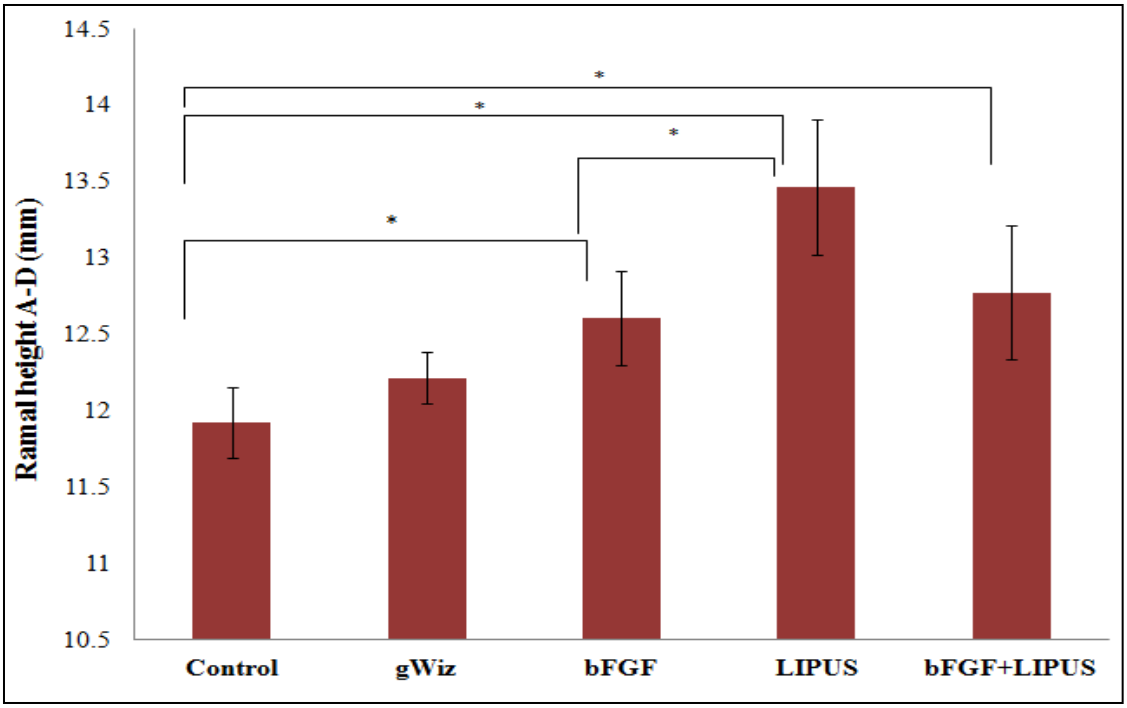

Fig 5.4: The bar chart of the ramal height (A-D) of the mandible among the five groups showing increase in the height of the mandible in LIPUS treated group {* = p≤0.05}.

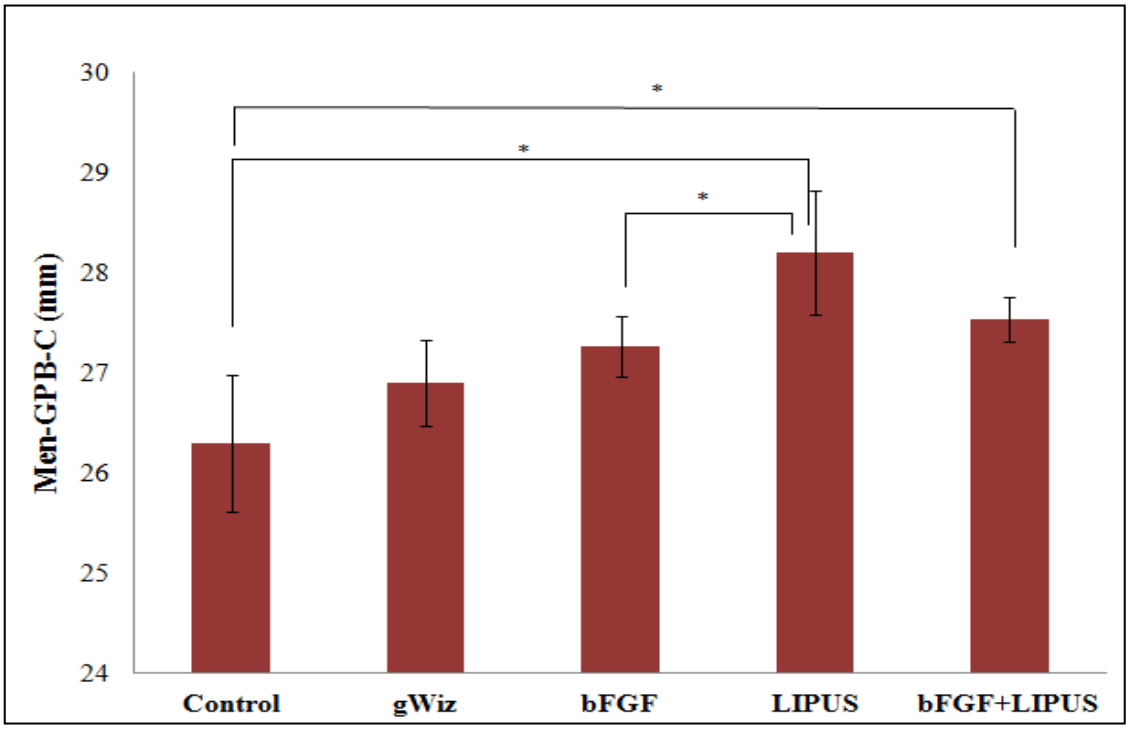

Fig 5.5: The bar chart of the Men-GP (B-C) of the mandible among the five groups showing increase in the height of the mandible in LIPUS treated group {* = p≤0.05}

5.3.2 MicroCT analysis:

Of all the variables measured in the Micro CT analysis, only bone volume fraction showed significant difference among all the five groups (p= 0.05) (Fig 5.6) while the bone volume and BMD showed no significant results (p>0.05) By comparing the means of bone volume and BMD of the groups, the combination treatment of bFGF +LIPUS showed the highest mean followed by bFGF group and LIPUS treated group (Table 5.2).

Table 5.2: Mean and standard deviation of BMD and Bone volume

	Control	gWiz	bFGF	LIPUS	bFGF+LIPUS
BMD Mean	0.0048	0.0053	0.0078	0.0063	0.0086
Std dev	0.001	0	0.003	0	0.001
BVol Mean	0.0926	0.09	0.109	0.1003	0.1069
Std dev	0.017	0.038	0.006	0.021	0.008

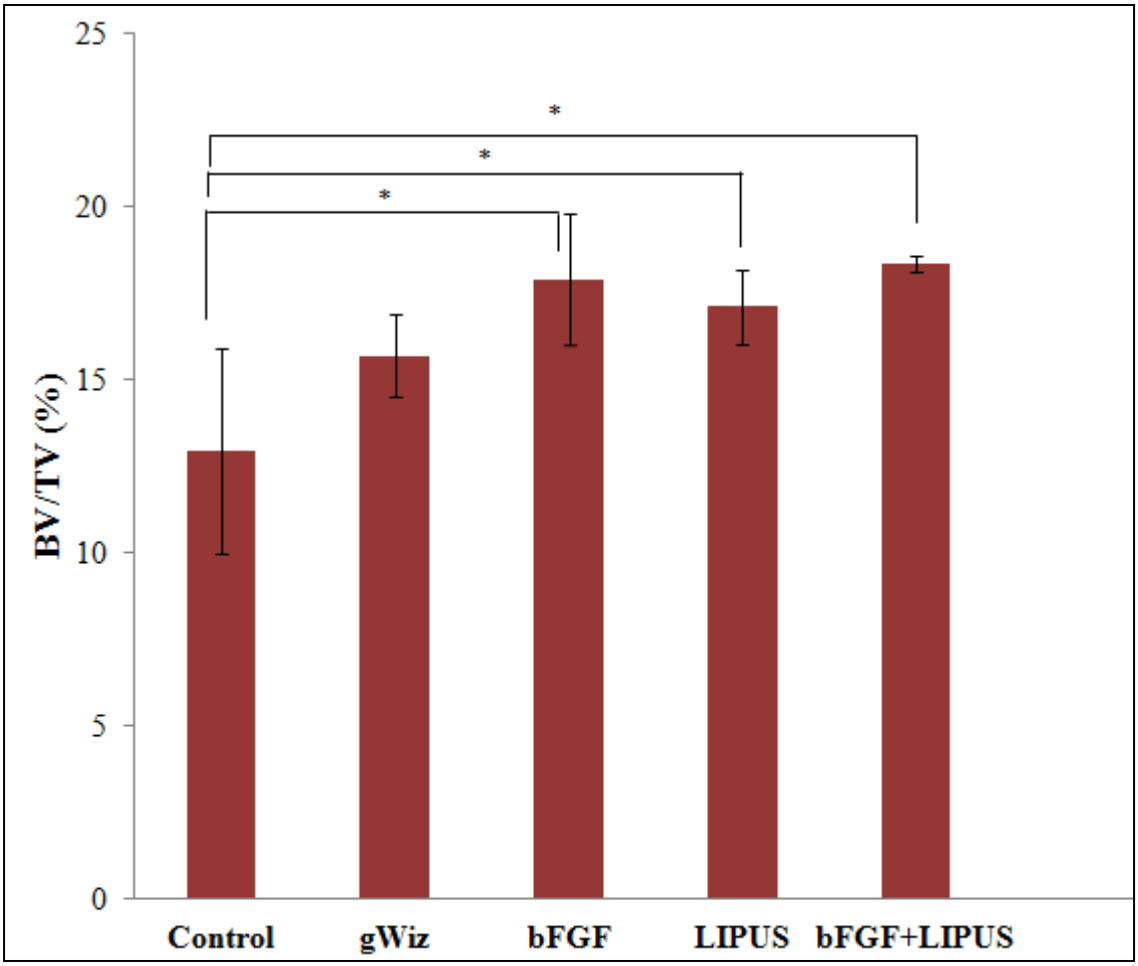

Fig 5.6: The bar chart of the bone volume fraction of the mandible condyle showing increase in bone volume fraction in the combination group (bFGF + LIPUS) {* = $p \leq 0.05$}.

5.3.3 Histomorphometric analysis:

Statistically significant results were seen in all the histomorphometric measured variables, i.e. proliferative cell count ($p = 0.04$), proliferative layer width ($p = 0.02$), hypertrophic cell count ($p = 0.02$) and hypertrophic layer width ($p = 0.05$). Cellular morphological evaluation revealed that the LIPUS treated group showed increase in the cell size of the hypertrophic layer while the bFGF treated group showed increase in the number of the cells in hypertrophic layer but the cell size was small as compared to LIPUS treated group. Moreover, the cells in both the layers were loosely packed in bFGF group as compared to the LIPUS treated and combined treatment groups (Fig 5.7). No significant difference was found between LIPUS and bFGF + LIPUS groups in any of the variables. The mean and the standard deviation of the measured variables are shown in Fig 5.8, 5.9, 5.10 and 5.11. By comparing the means of the groups, LIPUS treated group showed highest cell number in the proliferative layer while bFGF treated group showed the highest increase in the cell number in hypertrophic layer and increase in the width of the proliferative and hypertrophic layers.

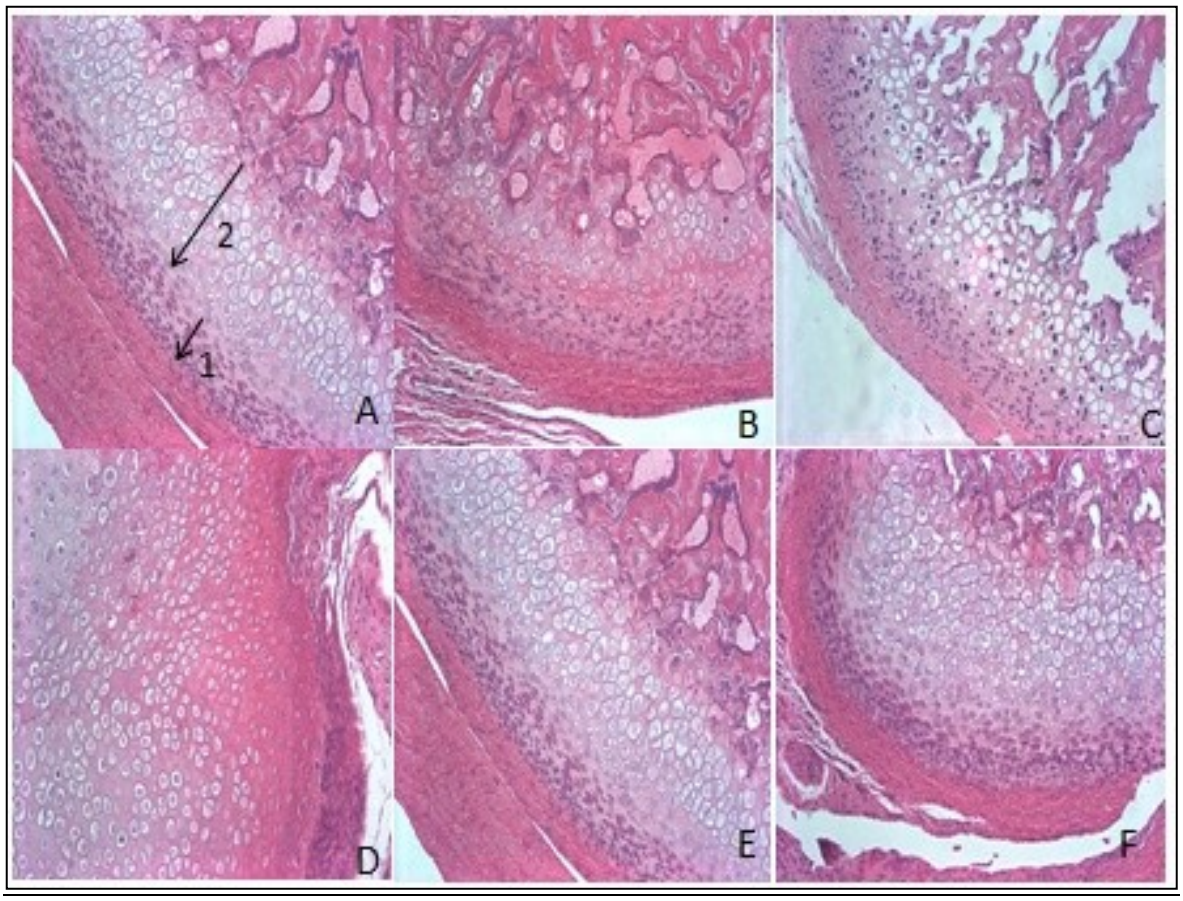

Fig 5.7: H&E stained sections of the articular surface of the condyle in the treatment groups seen in 20 X magnification. A. The proliferative layer marked by arrow 1 and the hypertrophic layer marked by arrow 2 B. Control group C. gWiz group D. bFGF group E. LIPUS group F. bFGF +LIPUS group.

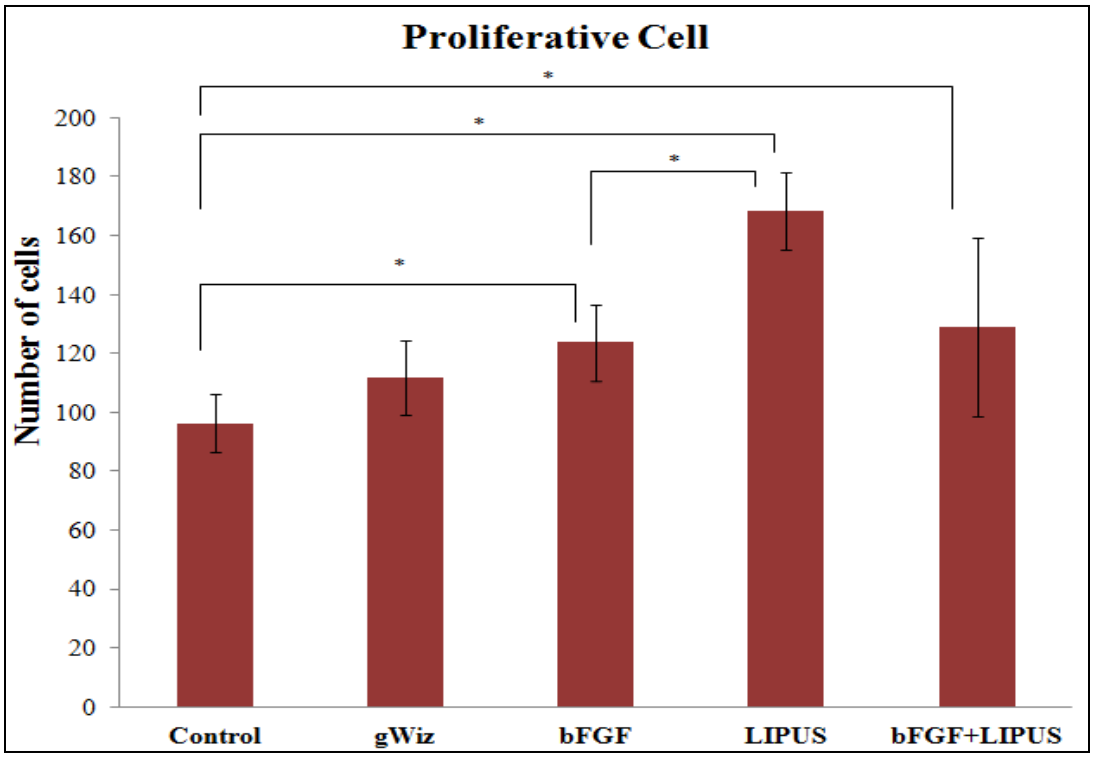

Fig 5.8: The bar chart show increase in proliferative cell count for the LIPUS treated group. {* = p≤0.05}

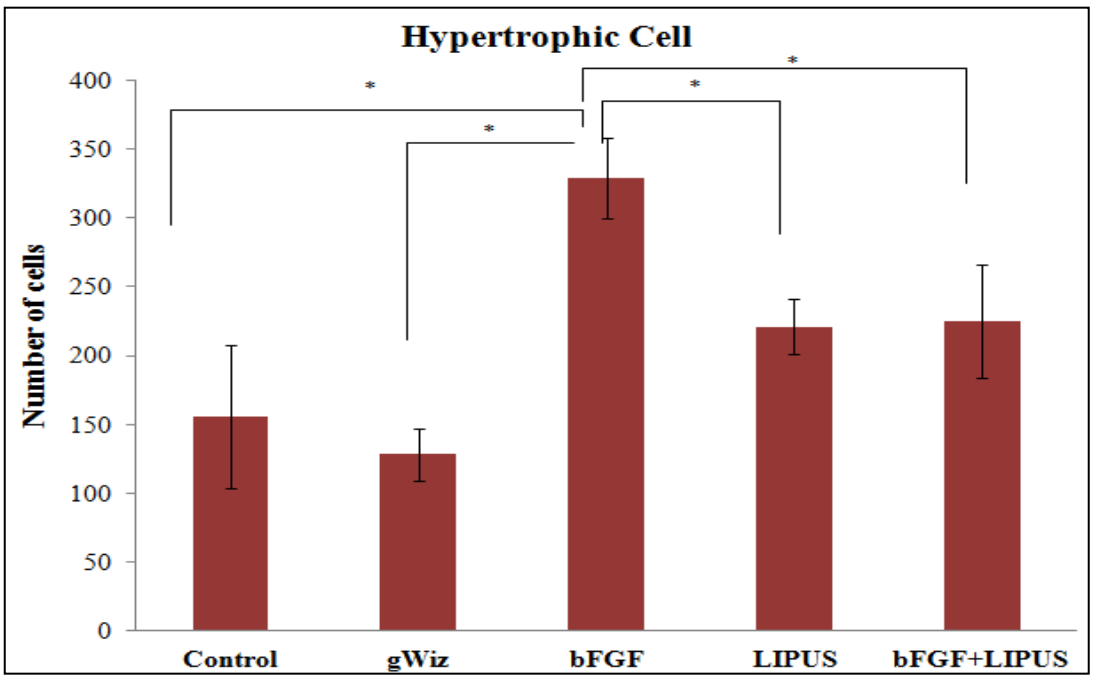

Fig 5.9: The bar chart depicts the result for the hypertrophic cell count of the condyle showing increase in the cell number in the bFGF treated group. {* = p≤0.05}.

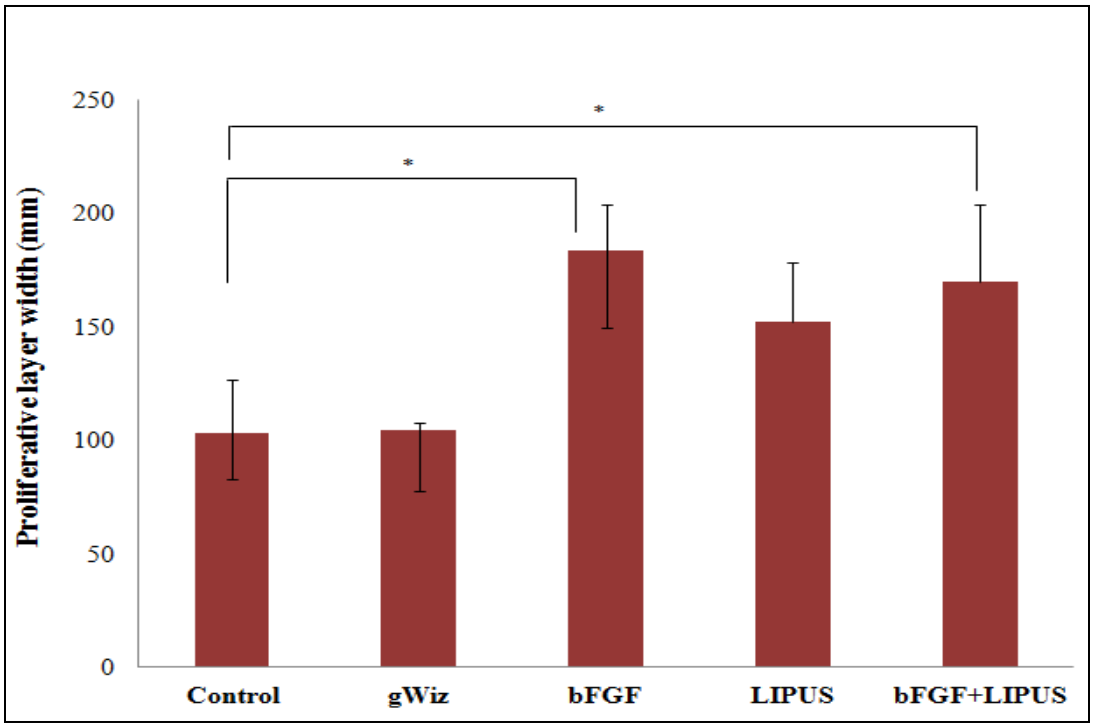

Fig 5.10: The bar chart depicts the result for the width of the proliferative layer of the condyle showing increase in the width in the bFGF treated group {* = p≤0.05}.

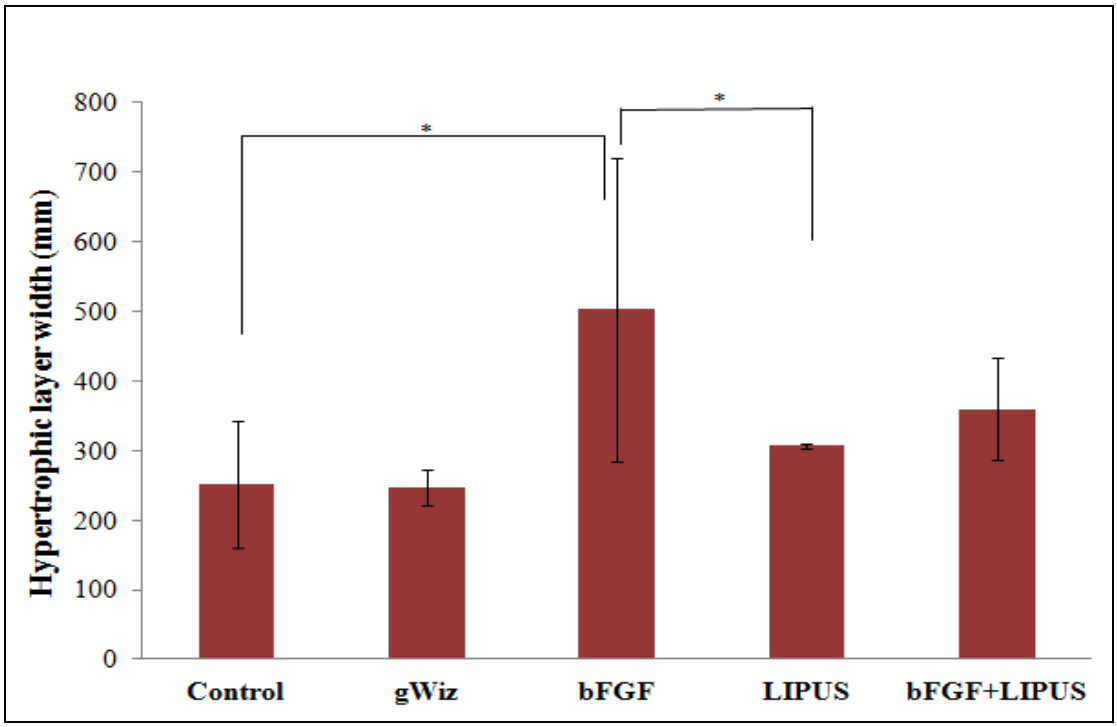

Fig 5.11: The bar chart depicts the result for the width of the hypertrophic layer of the condyle showing increase in the width in the bFGF treated group {* = p≤0.05}.

5.4 Discussion:

This study was performed to evaluate if there is any stimulatory effect of the non-viral plasmid delivered bFGF with or without LIPUS treatment on the condylar cartilage and on the mandibular growth as a whole, in an attempt to optimize mandibular growth stimulation. In our study, we wanted to investigate the effect of plasmid delivered bFGF alone and in combination with LIPUS on the mandibular condyle growth.

In the present study, microbubble was not added to the plasmid solution compared to the previous studies as well the ultrasound parameters used in this study were different from the previous studies as pulsed low intensity ultrasound is used while other studies used continuous wave (37)(38)(39). We also injected the plasmid into the posterior attachment of the condyle to study the effect on the bone growth. The study did not intend to use LIPUS to enhance gene transfection; bFGF plasmid was used to possibly enhance the mandibular growth directly and the main objective of this study was to find if there is any synergetic effect of the combining both techniques or not. The results of this study showed that bFGF and LIPUS alone has a positive effect on the mandibular condylar growth as seen in the histomorphometric and anthropometric measurement respectively while the combination therapy of bFGF and LIPUS showed only increase in the bone volume fraction. Being a pilot study, the objective was only to study the effect of bFGF alone and in the combination with LIPUS and to study the bone growth on the mandibular condylar head and hence no test was conducted to check for the presence of the plasmid at the end of the treatment or assess the duration of gene

expression during the study period. These will require more extensive studies that are planned in the future in the authors' labs.

We investigated the effect of bFGF, LIPUS and the combination therapy on the cell count and the width of proliferative and hypertrophic cell layers of the condyle. Histomorphometric analysis showed significant increase in the proliferative cell count and the width of the proliferative and hypertrophic layers in the bFGF treated group. The proliferative layer consists of undifferentiated mesenchymal cells while the hypertrophic layer consists of mature chondrocytes which is important for the condylar growth (40). The chondrocytes undergo hypertrophic changes in this layer and the first sign of calcification is present in this layer, too. Also the qualitative study of the slides was different in the treated groups. The group treated with LIPUS showed larger cell size compared to the group treated with bFGF which were smaller and loosely packed. The possible reason for the higher values of the histological parameters could be due to the close proximity of the area to the injection site which leads to bone formation on the condylar head (Fig 2b). The difference between LIPUS and bFGF histological sections could be due to the fact that LIPUS was applied to the whole condyle, while bFGF was applied to the posterior part only. Also, this difference might explain the slight increase, while insignificant, in condylar length in LIPUS group compared to plasmid group.

Anthropometric measurement demonstrated there was statistically significant increase in the ramal height (A-D), Men-GP (B-C) measurement and the length of the condylar process (A-E) while no significant difference was seen in case of the length of

the whole mandible (A-B). The LIPUS treated group had the best result among all the groups. These results are in agreement with the previous studies where the linear measurements increased after LIPUS application (24)(28). Although the exact mechanism of action for the LIPUS is still unclear, however it has been suggested that the effects of LIPUS may be physical or piezoelectric in nature (31). LIPUS produces vibration forces in all tissue components, both intracellular as well as extracellular. These vibrations cause movements of the particles in the tissue which causes mechanical stimulation. Therapeutic ultrasound using low intensities (20-50 mW/cm^2) causes small increase of temperature which may affect the cellular mechanism that may cause bone remodeling and growth. According to Wolff's law, the bone in a healthy person and animal will adapt to the load it is placed under. If the loading on the particular bone increases the bone will remodel itself over the time to be stronger to resist the loading (41). Bone is piezoelectric in nature and remodels itself according to the functional demands and environmental forces (42). Ultrasound produces physiological mechanical stress in the bone that causes its deformation. This deformation causes the generation of potential differences in the cells which causes bone remodeling (43). LIPUS produces non thermal effect which causes stable cavitations, micro streaming and mechanical effect on the cell membrane (44). Studies have shown that LIPUS enhance the exchange of ions intracellularly and extracellularly (45), change in the second messenger concentration which lead to alteration in gene expression for the cartilage and bone specific genes (46), increase intracellular concentration of calcium in chondrocytes (47) and increase in the angiogenesis related

cytokines (48). LIPUS used in this study is less likely to produce cavitation without introducing microbubble. Future studies may aim at evaluating this effect both in-vitro and may be in-vivo. It is to be noted that the used LIPUS was not intended to perform sonoporation for the gene delivery. This might explain the non-statistical difference between LIPUS and bFGF + LIPUS groups.

In Micro CT analysis, our study showed that the combination treatment of bFGF and LIPUS has significant effect on the bone volume fraction while all other variables i.e., the bone volume and BMD were non-significant. Although on comparing the means, still the combination therapy showed better results as compared to the other treatment groups except that BV/TV (bone volume fraction) did not increase much in the combination therapy compared to either treatment separately. This might be explained as that there might be minimum synergetic effect between LIPUS and bFGF at the study end point (4 weeks) that is reflected on the bone formation which may warrant future long term study. The bone volume fraction is the ratio of bone volume to the total volume of the region of interest, plays an important role as an interpreter of the mechanical properties of the bone. In this study only the trabecular bone of the condylar process was studied by manually drawing the region of interest to separate the trabecular bone from the cortical bone. The reason for selecting the trabecular bone was that it has high turnover rate as compared to the cortical bone and is the major site to detect the early changes after the therapy (49). The explanation of these results could be that after 4 weeks of treatment, bFGF injection lead to bone formation at the site of the injection and the LIPUS application lead to early maturation and these factors are

combined in the bFGF + LIPUS group while the other treatment groups could still be in the early phases of the growth. This speculation needs to be further evaluated by future studies. The difference between histological and MicroCT data among the groups could be due to the short period of treatment (4 weeks) which could have an effect at the cellular level while the gross anatomy effect might need longer treatment/observation time. This hypothesis also suggests future evaluation.

5.5 Conclusion:

In conclusion, within the limitations of this pilot study, the present study did indicate that the combination treatment of bFGF and LIPUS has selective effect on the mandibular condyle growth. This could be due to the antagonist effect of LIPUS and bFGF but the results of this study must be considered preliminary not only because of the sample size but also due to the method used for the analysis. It is too early to draw the conclusion on the results. More studies are needed not only with larger sample size but also to find the molecular, cellular basis and the long term study with time interval.

5.6 References:

1. Dimitriou R, Jones E, McGonagle D, Giannoudis PV. Bone regeneration: current concepts and future directions. BMC Medicine. 2011 May 31;9(1):66.

2. Thyagarajan T, Totey S, Danton MJS, Kulkarni AB. Genetically altered mouse models: the good, the bad, and the ugly. Crit Rev Oral Biol Med. 2003;14(3):154–74.

3. Krueckeberg SM, Kapp-Simon KA, Ribordy SC. Social skills of preschoolers with and without craniofacial anomalies. Cleft Palate Craniofac J. 1993 Sep;30(5):475–81.

4. Ritto AK. Class II malocclusion: why, when and how to treat this anomaly in mixed dentition with fixed functional appliances. J Gen Orthod. 2001;12(4):9–21.

5. Rankin M, Borah GL. Perceived functional impact of abnormal facial appearance. Plast Reconstr Surg. 2003 Jun;111(7):2140-2146-2148.

6. Rabie ABM, Dai J, Xu R. Recombinant AAV-mediated VEGF gene therapy induces mandibular condylar growth. Gene Ther. 2007 Jun;14(12):972–80.

7. Kronenberg HM. Developmental regulation of the growth plate. Nature. 2003 May 15;423(6937):332–6.

8. Yun Y-R, Won JE, Jeon E, Lee S, Kang W, Jo H, et al. Fibroblast growth factors: biology, function, and application for tissue regeneration. J Tissue Eng. 2010;2010:218142.

9. Eppley BL, Doucet M, Connolly DT, Feder J. Enhancement of angiogenesis by bFGF in mandibular bone graft healing in the rabbit. J Oral Maxillofac Surg. 1988 May;46(5):391–8.

10. Franceschi RT. Biological approaches to bone regeneration by gene therapy. J Dent Res. 2005 Dec;84(12):1093–103.

11. Clements BA, Hsu CYM, Kucharski C, Lin X, Rose L, Uludağ H. Nonviral delivery of basic fibroblast growth factor gene to bone marrow stromal cells. Clin Orthop Relat Res. 2009 Dec;467(12):3129–37.

12. Moore R, Ferretti P, Copp A, Thorogood P. Blocking endogenous FGF-2 activity prevents cranial osteogenesis. Dev Biol. 2002 Mar 1;243(1):99–114.

13. Hamada T, Suda N, Kuroda T. Immunohistochemical localization of fibroblast growth factor receptors in the rat mandibular condylar cartilage and tibial cartilage. J Bone Miner Metab. 1999;17(4):274–82.

14. Stieger K, Lorenz B. [The treatment of inherited dystrophies and neovascular disorders of the retina by rAAV-mediated gene therapy]. Klin Monbl Augenheilkd. 2008 Dec;225(12):1009–23.

15. Gardlik R, Behuliak M, Palffy R, Celec P, Li CJ. Gene therapy for cancer: bacteria-mediated anti-angiogenesis therapy. Gene Ther. 2011 May;18(5):425–31.

16. McMenamin MM, Wood MJA. Progress and prospects: Immunobiology of gene therapy for neurodegenerative disease: prospects and risks. Gene Ther. 2010 Apr;17(4):448–58.

17. Hacein-Bey-Abina S, Von Kalle C, Schmidt M, McCormack MP, Wulffraat N, Leboulch P, et al. LMO2-associated clonal T cell proliferation in two patients after gene therapy for SCID-X1. Science. 2003 Oct 17;302(5644):415–9.

18. Raper SE, Chirmule N, Lee FS, Wivel NA, Bagg A, Gao G, et al. Fatal systemic inflammatory response syndrome in a ornithine transcarbamylase deficient patient following adenoviral gene transfer. Mol Genet Metab. 2003 Oct;80(1–2):148–58.

19. Ziadloo A, Xie J, Frenkel V. Pulsed focused ultrasound exposures enhance locally administered gene therapy in a murine solid tumor model. J Acoust Soc Am. 2013 Mar;133(3):1827–34.

20. Osawa K, Okubo Y, Nakao K, Koyama N, Bessho K. Osteoinduction by microbubble-enhanced transcutaneous sonoporation of human bone morphogenetic protein-2. J Gene Med. 2009 Jul;11(7):633–41.

21. Suzuki R, Maruyama K. Effective In Vitro and In Vivo Gene Delivery by the Combination of Liposomal Bubbles (Bubble Liposomes) and Ultrasound Exposure. In: Weissig V, editor. Liposomes [Internet]. Humana Press; 2010 [cited 2013 Oct 4]. p. 473–86. (Methods in Molecular Biology). Available from: http://link.springer.com.login.ezproxy.library.ualberta.ca/protocol/10.1007/978-1-60327-360-2_33

22. Negishi Y, Tsunoda Y, Endo-Takahashi Y, Oda Y, Suzuki R, Maruyama K, et al. Local gene delivery system by bubble liposomes and ultrasound exposure into joint synovium. J Drug Deliv. 2011;2011:203986.

23. Eberson CP, Hogan KA, Moore DC, Ehrlich MG. Effect of low-intensity ultrasound stimulation on consolidation of the regenerate zone in a rat model of distraction osteogenesis. J Pediatr Orthop. 2003 Feb;23(1):46–51.

24. El-Bialy T, El-Shamy I, Graber TM. Growth modification of the rabbit mandible using therapeutic ultrasound: is it possible to enhance functional appliance results? Angle Orthod. 2003 Dec;73(6):631–9.

25. El-Bialy TH, Elgazzar RF, Megahed EE, Royston TJ. Effects of ultrasound modes on mandibular osteodistraction. J Dent Res. 2008 Oct;87(10):953–7.

26. Schortinghuis J, Bronckers ALJJ, Stegenga B, Raghoebar GM, de Bont LGM. Ultrasound to stimulate early bone formation in a distraction gap: a double blind

randomised clinical pilot trial in the edentulous mandible. Arch Oral Biol. 2005 Apr;50(4):411–20.

27. Inubushi T, Tanaka E, Rego EB, Ohtani J, Kawazoe A, Tanne K, et al. Ultrasound stimulation attenuates resorption of tooth root induced by experimental force application. Bone. 2013 Apr;53(2):497–506.

28. El-Bialy T, Hassan A, Albaghdadi T, Fouad HA, Maimani AR. Growth modification of the mandible with ultrasound in baboons: a preliminary report. Am J Orthod Dentofacial Orthop. 2006 Oct;130(4):435.e7-14.

29. El-Bialy T, Uludag H, Jomha N, Badylak SF. In vivo ultrasound-assisted tissue-engineered mandibular condyle: a pilot study in rabbits. Tissue Eng Part C Methods. 2010 Dec;16(6):1315–23.

30. Oyonarte R, Zárate M, Rodriguez F. Low-intensity pulsed ultrasound stimulation of condylar growth in rats. Angle Orthod. 2009 Sep;79(5):964–70.

31. Erdogan O, Esen E. Biological aspects and clinical importance of ultrasound therapy in bone healing. J Ultrasound Med. 2009 Jun;28(6):765–76.

32. Liao Z-K, Tsai K-C, Wang H-T, Tseng S-H, Deng W-P, Chen W-S, et al. Sonoporation-mediated anti-angiogenic gene transfer into muscle effectively regresses distant orthotopic tumors. Cancer Gene Ther. 2012 Mar;19(3):171–80.

33. Zhou Z, Zhang P, Ren J, Ran H, Zheng Y, Li P, et al. Synergistic effects of ultrasound-targeted microbubble destruction and TAT peptide on gene transfection: An experimental study in vitro and in vivo. Journal of Controlled Release. 2013 Sep 28;170(3):437–44.

34. Khan I, El-Kadi AO, El-Bialy T. Effects of growth hormone and ultrasound on mandibular growth in rats: MicroCT and toxicity analyses. Arch Oral Biol. 2013 Apr 29;

35. Rose LC, Kucharski C, Uludağ H. Protein expression following non-viral delivery of plasmid DNA coding for basic FGF and BMP-2 in a rat ectopic model. Biomaterials. 2012 Apr;33(11):3363–74.

36. Ulgen M, Baran S, Kaya H, Karadede I. The influence of the masticatory hypofunction on the craniofacial growth and development in rats. Am J Orthod Dentofacial Orthop. 1997 Feb;111(2):189–98.

37. Saito M, Mazda O, Takahashi KA, Arai Y, Kishida T, Shin-Ya M, et al. Sonoporation mediated transduction of pDNA/siRNA into joint synovium in vivo. J Orthop Res. 2007 Oct;25(10):1308–16.

38. Sheyn D, Kimelman-Bleich N, Pelled G, Zilberman Y, Gazit D, Gazit Z. Ultrasound-based nonviral gene delivery induces bone formation in vivo. Gene Ther. 2008 Feb;15(4):257–66.

39. Zolochevska O, Xia X, Williams BJ, Ramsay A, Li S, Figueiredo ML. Sonoporation delivery of interleukin-27 gene therapy efficiently reduces prostate tumor cell growth in vivo. Hum Gene Ther. 2011 Dec;22(12):1537–50.

40. Li QF, Rabie ABM. A new approach to control condylar growth by regulating angiogenesis. Arch Oral Biol. 2007 Nov;52(11):1009–17.

41. Frost HM. A 2003 update of bone physiology and Wolff's Law for clinicians. Angle Orthod. 2004 Feb;74(1):3–15.

42. Bassett CA. Electrical effects in bone. Sci Am. 1965 Oct;213(4):18–25.

43. Behari J, Singh S. Ultrasound propagation in “in vivo” bone. Ultrasonics. 1981 Mar;19(2):87–90.

44. Claes L, Willie B. The enhancement of bone regeneration by ultrasound. Prog Biophys Mol Biol. 2007 Apr;93(1–3):384–98.

45. Dinno MA, Dyson M, Young SR, Mortimer AJ, Hart J, Crum LA. The significance of membrane changes in the safe and effective use of therapeutic and diagnostic ultrasound. Phys Med Biol. 1989 Nov;34(11):1543–52.

46. Rawool NM, Goldberg BB, Forsberg F, Winder AA, Hume E. Power Doppler assessment of vascular changes during fracture treatment with low-intensity ultrasound. J Ultrasound Med. 2003 Feb;22(2):145–53.

47. Parvizi J, Parpura V, Greenleaf JF, Bolander ME. Calcium signaling is required for ultrasound-stimulated aggrecan synthesis by rat chondrocytes. J Orthop Res. 2002 Jan;20(1):51–7.

48. Reher P, Doan N, Bradnock B, Meghji S, Harris M. Effect of ultrasound on the production of IL-8, basic FGF and VEGF. Cytokine. 1999 Jun;11(6):416–23.

49. Carballido-Gamio J, Majumdar S. Clinical utility of microarchitecture measurements of trabecular bone. Curr Osteoporos Rep. 2006 Jun;4(2):64–70.

Chapter 6: General Discussion and Conclusion

6.1 Discussion:

The deficient lower jaw (mandible) is a common orofacial anomaly that is present either alone as in the case of class II malocclusion or as one of the features in several syndromic conditions. Depending on the age and severity of deficient mandible, the condition is either treated surgically or with the functional appliance. LIPUS has already shown to reduce the consolidation stage in distraction osteogenesis by stimulating bone healing as well as increase condylar growth when used with FA (1) (2). This thesis addressed the effect of LIPUS either alone or with FA and bFGF gene therapy on the mandibular condylar growth. Also in this study, LIPUS effect on chondrocytes and osteoblasts were investigated to explore its mechanism in more detail. In chapter 1, LIPUS was proposed as a therapeutic tool because of its stimulatory effects on various cell types as well as in different tissue culture set-ups and in various animal models (3) (4) (5) (6) (7).

In the animal study with FA, effects of either of the two LIPUS application timings i.e. either 20 min or 40 min for four weeks were studied. LIPUS application with FA has been investigated previously with 20 min application (2) (8). Based on the studies by Schumann et al, 2006 (9) and Chan et al, 2006 (10) which showed an increase in chondrogenesis and bone healing with 40 min LIPUS application, we hypothesized that 40 min LIPUS will enhance the stimulatory effect on the mandibular condylar growth. By introducing 40 min LIPUS application in this study, we optimized the LIPUS application in the animal studies. The results of this study showed that 20

min LIPUS is optimum for in-vivo study while 40 min application has a deleterious effect on the mandibular condylar growth as shown by all the studied variables. Histomorphometric results showed an increase in cell number and layer width in 20 min LIPUS application while 40 min application in combination with FA showed decreased in cell number and layer width. These results were further strengthened by Micro-CT analysis where 20 min LIPUS application again either alone or in combination with FA showed increased bone volume fraction and BMD with the decrease in trabecular separation. Micro-CT analysis was done upto 100^{th} slice from the first appearance of the trabecular bone on the scan. This was done to study the effect of functional appliance and LIPUS trabecular bone in the posterior part of mandible condyle.

Immunohistology also showed increased expression of SOX9, Aggrecan, Collagen II and X in 20 min groups. Aggrecan is the most abundant proteoglycan in the cartilage while Collagen II and X are most abundant cartilaginous proteins in the mature and hypertrophic layers of MCC. These proteins are protective in nature as they provide strength to the cartilage against tensile, compressive and shear stresses (11). Aggrecan is negatively charged proteoglycan that traps water and hence provides structural and functional integrity. The results showed that LIPUS has a protective effect on the cartilage. Its application for osteoarthritis treatment should be explored for the future.

In this study, the animals treated with LIPUS alone showed better treatment results as compared to when treated in combination with FA. The reason could be the soft diet given to the animals with attached FA. The introduction of soft diet led to a

decrease in the muscular activity which further led to decrease in the mechanical load on the condylar cartilage. Also, the animals could be under psychological stress due to FA which further aggravated the cartilage degradation (12). 40 min LIPUS application caused increase in temperature at the application site. Increased in temperature with 20 min LIPUS application was studied by Xue et al, 2013 (13) during tooth movement, and the study showed approx 2.66ºC increase. So with 40 min, the temperature increase might have been doubled which led to increased expression of matrix metalloproteinase (MMPs) enzymes.

Chapters 3 and 4 demonstrated the effect of LIPUS on C28/I2 chondrocytes and MC-3T3 E1 pre-osteoblasts cell lines. In both the studies, 10 min and 20 min LIPUS were compared to the control for ROS generation, gene and protein expressions. Both the in-vitro studies showed 20 min had detrimental effect while our in-vivo study showed stimulatory effect. The reason could be attenuation of the ultrasound wave in the animal study while passing through the skin, fat tissue and muscles before reaching the mandible condyle while in in-vitro studies, 20 min LIPUS application caused the increase in temperature in the in-vitro set-up (7). The decrease in the cell viability as seen in 20 min LIPUS groups are not due to the toxic effect of ROS generation as the amount generated in 20 min groups is lower than 10 min groups. It might be due to activation of heat shock protein in the cells. The results of our in-vitro studies are in agreement with the other studies where 10 min LIPUS application showed the stimulatory effect of tooth slice organ culture (14) (15). In both the in-vitro studies, the

cell culture plates were placed on the custom made transducers and coupling gel was used for ultrasound transmission. In chondrocyte study, ROS generated by LIPUS application showed increased gene expression of *SOX9*, *ACAN,* and *COL2A1*, and increased phosphorylation of ERK1/2 while p38 and JNK showed no significant difference. This effect was reversed when DPI was used to inhibit ROS generation. Studies by Morita et al, 2007 (16) and Kim et al, 2010 (17) showed that ROS are considered essential for chondrocyte differentiation and in endochondral ossification. Our study results are in agreement with these studies. In MC-3T3 E1 pre-osteoblast study, there was increased phosphorylation of ERK1/2 and increased gene expression of RUNX2, OCN, and OPN when the cells were treated with LIPUS in DPI treated groups. This effect was only during the first hour and was reversed from 3 hr onwards.

We worked on two cell lines - chondrocytes and pre-osteoblasts; as these two cells are involved in the process of EO. Mesenchymal stem cells proliferate and differentiate to chondroblasts which on maturation lay down cartilage matrix and differentiate into hypertrophic chondrocytes (18). EO at the border of cartilage and subchondral bone establishes the mandible structure. Hypertrophic chondrocytes undergo apoptosis and the cartilage matrix is degraded by the invasion of blood vessels from the underlying the subchondral bone (19). Osteoblasts from the subchondral bone deposit new bone in the degrading cartilage. It is believed that hypertrophic chondrocytes undergo apoptosis by blood vessel invasion. However, studies have shown that these cells directly differentiate into the osteoblast. HIF play an important

role in neovascularisation as it is a transcription factor for VEGF. ROS have shown not only to stabilize HIF-1α subunit by preventing its proteasomal degradation (20) but also increase in VEGF expression (21). From this we can hypothesize that ROS can be a factor involved in the transformation of hypertrophic chondrocytes to osteoblasts, however, further studies are needed to understand the role of ROS in EO.

In chapter 5, the effect of bFGF plasmid DNA delivery in combination with LIPUS was investigated to induce bone growth in the mandibular condyle. We found an increase in mandibular length in LIPUS alone group while bFGF plasmid DNA group showed an increase in a number of hypertrophic cell layer and width. The combination group showed an increase in bone volume fraction. These results have shown the potential stimulatory effect of gene delivery and LIPUs on the mandibular growth. However, we recommend further study with larger sample size and also in-vitro study to understand the potential effect of the polymer delivery on cell toxicity, gene and protein expression.

6.2 Limitations and Recommendation for future directions:

In the animal study, we investigated the effect on the mandible growth after four weeks of LIPUS application. Further studies are recommended to study the long-term treatment effect of LIPUS on the mandibular condylar growth. Also, the time-based study is recommended to investigate gene and protein expression at each week interval. Additionally in 40 min LIPUS groups, the animals were under anesthesia for longer time and as mentioned earlier, 40 min LIIPUS could have led to increase in temperature

in the area applied. To avoid this, we recommend 20 minutes LIPUS application twice in a day (like every 12 hrs). This will prevent thermal effect of 40 min application while exposing the mandible condyle to the anabolic effect of 20 min LIPUS.

Another limitation of our FA animal study was different food consistency given to the animals with attached FA. To prevent this, we recommend that all the treatment groups should be given the same type of food and we also recommend anesthetizing the control group as well.

In vitro study results strongly suggested ROS generated by LIPUS application acts as secondary messengers in the cell signaling and amount generated are not toxic to these cells. However, further in-vitro studies are needed to understand ROS generation in the tissue-specific cell line. We recommend isolation of the cells from the MCC or to develop tissue organ culture to understand ROS generation by LIPUS application. Also, we used DHE fluorescence assay for ROS detection which is specific for superoxide ions. We recommend the use of HPLC method to distinguish between the kinds of ROS generated in the cell system.

DPI was used in these studies for NOX inhibition which in reality a flavoprotein inhibitor. Studies have shown DPI to induce oxidative stress and inhibit cell redox metabolism (22) (23). For the future studies, ROS inhibition with the use of siRNA is recommended to better understand ROS generation and its effect with LIPUS application. Also, these in-vitro studies relied on the gene expression results to make the conclusion, while protein expression was done only for OPN in MC-3T3E1 pre-

osteoblast cells. OPN mRNA expression was increased in DPI treated groups while protein expression was significantly reduced. For the future studies, we highly recommend protein expression analysis like western blot or ELISA as the enzymes involved in post translational modification of the functional proteins might be affected by ROS generation.

In the gene therapy study, bFGF was injected in the posterior part of TMJ. However, several other transcription factors and growth factors are involved in EO at TMJ. These factors should be analyzed, either alone or in combination, in an in-vitro set up using either the primary cells extracted from MCC or directly using tissue organ culture. On the other hand, different cells show different transfection ability and also other polymers should be screened first to improve the gene delivery. Other limitations are transfection efficiency and specificity. Although, fluorescent reporter gene – green fluorescent protein (GFP) was attached to bFGF plasmid but at the end of the study, its expression was not studied. For the future, histological examination for the confirmation of transfection should be considered.

6.3 Conclusion:

From both in-vivo and in-vitro studies, we concluded the following findings:

1. 20 min LIPUS application showed in the mandibular condylar growth either alone or in combination with FA.

2. Histomorphometric and immunohistology also showed increased cell number, layer width and increased protein expression of SOX9, Aggrecan, Collagen II and X in 20 min LIPUS groups.
3. There was an increase in BMD and bone volume fraction values in 20 min LIPUS groups.
4. One time LIPUS application in C28/I2 chondrocytes cell culture showed increased ROS generation which further leads to increase in phosphorylation of ERK1/2 and increase in gene expression of SOX9, ACAN, and COL2A1. This effect was reversed when the cells were treated with NOX inhibitor, DPI.
5. A single application of LIPUS in MC-3T3 E1 pre-osteoblasts cell culture showed increase ROS generation. However, the level of phosphorylation of ERK1/2 and gene expression of RUNX2, OCN, and OPN were higher during the first hour in the presence of DPI. This effect later subsided and DPI non-treated groups showed increased ERK1/2 phosphorylation and gene expression of RUNX2, OCN and OPN from 3 hr onwards.
6. In bFGF pilot study, the results showed potential additive effect with LIPUS on the mandibular condylar growth.

6.4 References:

1. Eberson CP, Hogan KA, Moore DC, Ehrlich MG. Effect of low-intensity ultrasound stimulation on consolidation of the regenerate zone in a rat model of distraction osteogenesis. J Pediatr Orthop. 2003 Feb;23(1):46–51.

2. El-Bialy T, El-Shamy I, Graber TM. Growth modification of the rabbit mandible using therapeutic ultrasound: is it possible to enhance functional appliance results? Angle Orthod. 2003 Dec;73(6):631–9.

3. Ikeda K, Takayama T, Suzuki N, Shimada K, Otsuka K, Ito K. Effects of low-intensity pulsed ultrasound on the differentiation of C2C12 cells. Life Sci. 2006 Oct 12;79(20):1936–43.

4. Cheng K, Xia P, Lin Q, Shen S, Gao M, Ren S, et al. Effects of Low-Intensity Pulsed Ultrasound on Integrin-FAK-PI3K/Akt Mechanochemical Transduction in Rabbit Osteoarthritis Chondrocytes. Ultrasound in Medicine & Biology. 2014 Jul;40(7):1609–18.

5. Dalla-Bona DA, Tanaka E, Inubushi T, Oka H, Ohta A, Okada H, et al. Cementoblast response to low- and high-intensity ultrasound. Arch Oral Biol. 2008 Apr;53(4):318–23.

6. Tanaka E, Yamano E, Dalla-Bona DA, Watanabe M, Inubushi T, Shirakura M, et al. Dynamic compressive properties of the mandibular condylar cartilage. J Dent Res. 2006 Jun;85(6):571–5.

7. Padilla F, Puts R, Vico L, Raum K. Stimulation of bone repair with ultrasound: a review of the possible mechanic effects. Ultrasonics. 2014 Jul;54(5):1125–45.

8. El-Bialy T, Hassan A, Albaghdadi T, Fouad HA, Maimani AR. Growth modification of the mandible with ultrasound in baboons: a preliminary report. Am J Orthod Dentofacial Orthop. 2006 Oct;130(4):435.e7-14.

9. Schumann D, Kujat R, Zellner J, Angele MK, Nerlich M, Mayr E, et al. Treatment of human mesenchymal stem cells with pulsed low intensity ultrasound enhances the chondrogenic phenotype in vitro. Biorheology. 2006;43(3–4):431–43.

10. Chan CW, Qin L, Lee KM, Cheung WH, Cheng JCY, Leung KS. Dose-dependent effect of low-intensity pulsed ultrasound on callus formation during rapid distraction osteogenesis. J Orthop Res. 2006 Nov;24(11):2072–9.

11. Kuroda S, Tanimoto K, Izawa T, Fujihara S, Koolstra JH, Tanaka E. Biomechanical and biochemical characteristics of the mandibular condylar cartilage. Osteoarthr Cartil. 2009 Nov;17(11):1408–15.

12. Li Q, Zhang M, Chen Y-J, Zhou Q, Wang Y-J, Liu J. Psychological stress alters microstructure of the mandibular condyle in rats. Physiology and Behavior. 2013;110–111:129–39.

13. Xue H, Zheng J, Cui Z, Bai X, Li G, Zhang C, et al. Low-intensity pulsed ultrasound accelerates tooth movement via activation of the BMP-2 signaling pathway. PLoS ONE. 2013;8(7):e68926.

14. Al-Daghreer S, Doschak M, Sloan AJ, Major PW, Heo G, Scurtescu C, et al. Short-Term Effect of Low-Intensity Pulsed Ultrasound on an Ex-Vivo 3-D Tooth Culture. Ultrasound in Medicine and Biology. 2013 Jun 1;39(6):1066–74.

15. Al-Daghreer S, Doschak M, Sloan AJ, Major PW, Heo G, Scurtescu C, et al. Long term effect of low intensity pulsed ultrasound on a human tooth slice organ culture. Arch Oral Biol. 2012 Jun;57(6):760–8.

16. Morita K, Miyamoto T, Fujita N, Kubota Y, Ito K, Takubo K, et al. Reactive oxygen species induce chondrocyte hypertrophy in endochondral ossification. J Exp Med. 2007 Jul 9;204(7):1613–23.

17. Ki SK, Hae WC, Hee EY, Ick YK. Reactive oxygen species generated by NADPH oxidase 2 and 4 are required for chondrogenic differentiation. Journal of Biological Chemistry. 2010;285(51):40294–302.

18. Rabie ABM, Hägg U. Factors regulating mandibular condylar growth. Am J Orthod Dentofacial Orthop. 2002 Oct;122(4):401–9.

19. Gibson G. Active role of chondrocyte apoptosis in endochondral ossification. Microsc Res Tech. 1998 Oct 15;43(2):191–204.

20. Rankin EB, Giaccia AJ, Schipani E. A central role for hypoxic signaling in cartilage, bone, and hematopoiesis. Curr Osteoporos Rep. 2011 Jun;9(2):46–52.

21. Kosmidou I, Xagorari A, Roussos C, Papapetropoulos A. Reactive oxygen species stimulate VEGF production from C(2)C(12) skeletal myotubes through a PI3K/Akt pathway. Am J Physiol Lung Cell Mol Physiol. 2001 Apr;280(4):L585-592.

22. Lambert AJ, Buckingham JA, Boysen HM, Brand MD. Diphenyleneiodonium acutely inhibits reactive oxygen species production by mitochondrial complex I during reverse, but not forward electron transport. Biochimica et Biophysica Acta (BBA) - Bioenergetics. 2008 May;1777(5):397–403.

23. Riganti C, Gazzano E, Polimeni M, Costamagna C, Bosia A, Ghigo D. Diphenyleneiodonium Inhibits the Cell Redox Metabolism and Induces Oxidative Stress. J Biol Chem. 2004 Nov 12;279(46):47726–31.

Bibliography

Chapter 1: Introduction

1. Shaffer SM, Brismée J-M, Sizer PS, Courtney CA. Temporomandibular disorders. Part 1: anatomy and examination/diagnosis. J Man Manip Ther. 2014 Feb;22(1):2–12.

2. Shibata S, Suda N, Suzuki S, Fukuoka H, Yamashita Y. An in situ hybridization study of Runx2, Osterix, and Sox9 at the onset of condylar cartilage formation in fetal mouse mandible. J Anat. 2006 Feb;208(2):169–77.

3. Symons NBB. Studies on the growth and form of the mandible. Dent Rec (London). 1951 Mar;71(3):41–53.

4. Copray JC, Jansen HW, Duterloo HS. Growth and growth pressure of mandibular condylar and some primary cartilages of the rat in vitro. Am J Orthod Dentofacial Orthop. 1986 Jul;90(1):19–28.

5. Ogston A. The Growth and Maintenance of the Articular Ends of Adult Bones. J Anat Physiol. 1878 Jul;12(Pt 4):503–17.

6. Sperber GH, Sperber SM, Guttmann GD. Craniofacial Embryogenetics and Development. PMPH-USA; 2010. 264 p.

7. Mizoguchi I, Nakamura M, Takahashi I, Kagayama M, Mitani H. An immunohistochemical study of localization of type I and type II collagens in mandibular condylar cartilage compared with tibial growth plate. Histochemistry. 1990 Apr 1;93(6):593–9.

8. Livne E, Oliver C, Silbermann M. Further characterization of the chondroprogenitor zone in mandibular condyles of suckling mice. An ultrastructural and cytochemical study. Acta Anat (Basel). 1987;129(3):231–7.

9. Hinton RJ. Genes that regulate morphogenesis and growth of the temporomandibular joint: a review. Dev Dyn. 2014 Jul;243(7):864–74.

10. Symons NBB. A histochemical study of the secondary cartilage of the mandibular condyle in the rat. Archives of Oral Biology. 1965 Jul;10(4):579–IN3.

11. Glineburg RW, Laskin DM, Blaustein DI. The effects of immobilization on the primate temporomandibular joint: a histologic and histochemical study. J Oral Maxillofac Surg. 1982 Jan;40(1):3–8.

12. Nakao Y, Konno-Nagasaka M, Toriya N, Arakawa T, Kashio H, Takuma T, et al. Proteoglycan Expression Is Influenced by Mechanical Load in TMJ Discs. J DENT RES. 2014 Oct 27;22034514553816.

13. Yamashiro T, Takano-Yamamoto T. Differential responses of mandibular condyle and femur to oestrogen deficiency in young rats. Arch Oral Biol. 1998 Mar;43(3):191–5.

14. Ghafari J, Degroote C. Condylar cartilage response to continuous mandibular displacement in the rat. Angle Orthod. 1986 Jan;56(1):49–57.

15. Meikle MC. In vivo transplantation of the mandibular joint of the rat; an autoradiographic investigation into cellular changes at the condyle. Arch Oral Biol. 1973 Aug;18(8):1011–20.

16. Voudouris JC, Kuftinec MM. Improved clinical use of Twin-block and Herbst as a result of radiating viscoelastic tissue forces on the condyle and fossa in treatment and long-term retention: growth relativity. Am J Orthod Dentofacial Orthop. 2000 Mar;117(3):247–66.

17. Rabie ABM, Hägg U. Factors regulating mandibular condylar growth. Am J Orthod Dentofacial Orthop. 2002 Oct;122(4):401–9.

18. Moffett B. The morphogenesis of the temporomandibular joint. American Journal of Orthodontics. 1966 Jun 1;52(6):401–15.

19. Li QF, Rabie ABM. A new approach to control condylar growth by regulating angiogenesis. Arch Oral Biol. 2007 Nov;52(11):1009–17.

20. Luder HU, Leblond CP, von der Mark K. Cellular stages in cartilage formation as revealed by morphometry, radioautography and type II collagen immunostaining of the mandibular condyle from weanling rats. Am J Anat. 1988 Jul;182(3):197–214.

21. Ohno S, Schmid T, Tanne Y, Kamiya T, Honda K, Ohno-Nakahara M, et al. Expression of superficial zone protein in mandibular condyle cartilage. Osteoarthr Cartil. 2006 Aug;14(8):807–13.

22. Mizoguchi I, Toriya N, Nakao Y. Growth of the mandible and biological characteristics of the mandibular condylar cartilage. Japanese Dental Science Review. 2013 Nov;49(4):139–50.

23. Shibukawa Y, Young B, Wu C, Yamada S, Long F, Pacifici M, et al. Temporomandibular joint formation and condyle growth require Indian hedgehog signaling. Dev Dyn. 2007 Feb;236(2):426–34.

24. Provot S, Schipani E. Molecular mechanisms of endochondral bone development. Biochemical and Biophysical Research Communications. 2005 Mar 18;328(3):658–65.

25. Lefebvre V, Smits P. Transcriptional control of chondrocyte fate and differentiation. Birth Defects Res C Embryo Today. 2005 Sep;75(3):200–12.

26. Shibata S, Suda N, Yoda S, Fukuoka H, Ohyama K, Yamashita Y, et al. Runx2-deficient mice lack mandibular condylar cartilage and have deformed Meckel's cartilage. Anat Embryol. 2004 Jul;208(4):273–80.

27. Fukada K, Shibata S, Suzuki S, Ohya K, Kuroda T. In situ hybridisation study of type I, II, X collagens and aggrecan mRNas in the developing condylar cartilage of fetal mouse mandible. J Anat. 1999 Oct;195 (Pt 3):321–9.

28. Shen G, Rabie AB, Zhao Z-H, Kaluarachchi K. Forward deviation of the mandibular condyle enhances endochondral ossification of condylar cartilage indicated by increased expression of type X collagen. Arch Oral Biol. 2006 Apr;51(4):315–24.

29. Park JH, Park BH, Kim HK, Park TS, Baek HS. Hypoxia decreases Runx2/Cbfa1 expression in human osteoblast-like cells. Molecular and Cellular Endocrinology. 2002 Jun 28;192(1–2):197–203.

30. Hartmann C, Tabin CJ. Dual roles of Wnt signaling during chondrogenesis in the chicken limb. Development. 2000 Jul;127(14):3141–59.

31. Sahni M, Ambrosetti DC, Mansukhani A, Gertner R, Levy D, Basilico C. FGF signaling inhibits chondrocyte proliferation and regulates bone development through the STAT-1 pathway. Genes Dev. 1999 Jun 1;13(11):1361–6.

32. Ornitz DM. FGF signaling in the developing endochondral skeleton. Cytokine Growth Factor Rev. 2005 Apr;16(2):205–13.

33. Yang Z, Jiao H, Chao W, Yan Z, Changhong H, Li G, et al. Application of HIF-1α by gene therapy enhances angiogenesis and osteogenesis in alveolar bone defect regeneration. J Gene Med. 2016 Feb 29;

34. Wink JD, Goldstein JA, Paliga JT, Taylor JA, Bartlett SP. The mandibular deformity in hemifacial microsomia: a reassessment of the Pruzansky and Kaban classification. Plast Reconstr Surg. 2014 Feb;133(2):174e–81e.

35. Vargervik K. Mandibular malformations: growth characteristics and management in hemifacial microsomia and Nager syndrome. Acta Odontol Scand. 1998 Dec;56(6):331–8.

36. Kaneyama K, Segami N, Hatta T. Congenital deformities and developmental abnormalities of the mandibular condyle in the temporomandibular joint. Congenit Anom (Kyoto). 2008 Sep;48(3):118–25.

37. Gonzales B, Henning D, So RB, Dixon J, Dixon MJ, Valdez BC. The Treacher Collins syndrome (TCOF1) gene product is involved in pre-rRNA methylation. Hum Mol Genet. 2005 Jul 15;14(14):2035–43.

38. Dixon J, Jones NC, Sandell LL, Jayasinghe SM, Crane J, Rey J-P, et al. Tcof1/Treacle is required for neural crest cell formation and proliferation deficiencies that cause craniofacial abnormalities. Proc Natl Acad Sci USA. 2006 Sep 5;103(36):13403–8.

39. Jakobsen LP, Ullmann R, Christensen SB, Jensen KE, Mølsted K, Henriksen KF, et al. Pierre Robin sequence may be caused by dysregulation of SOX9 and KCNJ2. J Med Genet. 2007 Jun;44(6):381–6.

40. Battaglia A, Magit A. Nager acrofacial dysostosis with autosomal dominant inheritance: implications for the otolaryngologist. Otolaryngol Head Neck Surg. 2000 Sep;123(3):276–7.

41. Verrotti C, Benassi G, Piantelli G, Magnani C, Giordano G, Gramellini D. Acrofacial dysostosis syndromes: a relevant prenatal dilemma. A case report and brief literature review. J Matern Fetal Neonatal Med. 2007 Jun;20(6):487–90.

42. Friedman RA, Wood E, Pransky SM, Seid AB, Kearns DB. Nager acrofacial dysostosis: management of a difficult airway. Int J Pediatr Otorhinolaryngol. 1996 Mar;35(1):69–72.

43. Pirttiniemi P, Peltomäki T, Müller L, Luder HU. Abnormal mandibular growth and the condylar cartilage. Eur J Orthod. 2009 Feb;31(1):1–11.

44. Tank W, Wright D, Iizuka T. Unilateral dysplasia of the mandibular condyle: report of a case. J Oral Maxillofac Surg. 1998 Jun;56(6):765–9.

45. Saurenmann RK, Rose JB, Tyrrell P, Feldman BM, Laxer RM, Schneider R, et al. Epidemiology of juvenile idiopathic arthritis in a multiethnic cohort: ethnicity as a risk factor. Arthritis Rheum. 2007 Jun;56(6):1974–84.

46. Yang L, Thornton S, Grom AA. Interleukin-15 inhibits sodium nitroprusside-induced apoptosis of synovial fibroblasts and vascular endothelial cells. Arthritis Rheum. 2002 Nov;46(11):3010–4.

47. Hanna VE, Rider SF, Moore TL, Wilson VK, Osborn TG, Rotskoff KS, et al. Effects of systemic onset juvenile rheumatoid arthritis on facial morphology and temporomandibular joint form and function. J Rheumatol. 1996 Jan;23(1):155–8.

48. Kjellberg H. Craniofacial growth in juvenile chronic arthritis. Acta Odontol Scand. 1998 Dec;56(6):360–5.

49. McNamara JA Jr. Components of class II malocclusion in children 8-10 years of age. Angle Orthod. 1981 Jul;51(3):177–202.

50. Proffit WR, Fields HW Jr, Moray LJ. Prevalence of malocclusion and orthodontic treatment need in the United States: estimates from the NHANES III survey. Int J Adult Orthodon Orthognath Surg. 1998;13(2):97–106.

51. Karaiskos N, Wiltshire WA, Odlum O, Brothwell D, Hassard TH. Preventive and interceptive orthodontic treatment needs of an inner-city group of 6- and 9-year-old Canadian children. J Can Dent Assoc. 2005 Oct;71(9):649.

52. Warren JJ, Slayton RL, Yonezu T, Bishara SE, Levy SM, Kanellis MJ. Effects of Nonnutritive Sucking Habits on Occlusal Characteristics in the Mixed Dentition. Pediatric Dentistry. 2005 Nov 1;27(6):445–50.

53. Randerath WJ, Verbraecken J, Andreas S, Bettega G, Boudewyns A, Hamans E, et al. Non-CPAP therapies in obstructive sleep apnoea. Eur Respir J. 2011 May;37(5):1000–28.

54. Kinzinger G, Czapka K, Ludwig B, Glasl B, Gross U, Lisson J. Effects of fixed appliances in correcting Angle Class II on the depth of the posterior airway space: FMA vs. Herbst appliance--a retrospective cephalometric study. J Orofac Orthop. 2011 Aug;72(4):301–20.

55. Sedaghat AR, Anderson ICW, McGinley BM, Rossberg MI, Redett RJ, Ishman SL. Characterization of obstructive sleep apnea before and after tongue-lip adhesion in children with micrognathia. Cleft Palate Craniofac J. 2012 Jan;49(1):21–6.

56. Joshi N, Hamdan AM, Fakhouri WD. Skeletal malocclusion: a developmental disorder with a life-long morbidity. J Clin Med Res. 2014 Dec;6(6):399–408.

57. Ghafournia M, Hajenourozali Tehrani M. Relationship between Bruxism and Malocclusion among Preschool Children in Isfahan. J Dent Res Dent Clin Dent Prospects. 2012;6(4):138–42.

58. Rondeau BH. Class II malocclusion in mixed dentition. J Clin Pediatr Dent. 1994;19(1):1–11.

59. Ritto AK. Class II malocclusion: why, when and how to treat this anomaly in mixed dentition with fixed functional appliances. J Gen Orthod. 2001;12(4):9–21.

60. Bock NC, Ruf S. Dentoskeletal changes in adult Class II division 1 Herbst treatment--how much is left after the retention period? Eur J Orthod. 2012 Dec;34(6):747–53.

61. Camilla Tulloch JF, Lenz BE, Phillips C. Surgical Versus Orthodontic Correction for Class II Patients: Age and Severity in Treatment Planning and Treatment Outcome. Semin Orthod. 1999 Dec;5(4):231–40.

62. Kersey ML, Nebbe B, Major PW. Temporomandibular joint morphology changes with mandibular advancement surgery and rigid internal fixation: a systematic literature review. Angle Orthod. 2003 Feb;73(1):79–85.

63. Ow A, Cheung LK. Skeletal stability and complications of bilateral sagittal split osteotomies and mandibular distraction osteogenesis: an evidence-based review. J Oral Maxillofac Surg. 2009 Nov;67(11):2344–53.

64. Epker BN, Wolford LM, Fish LC. Mandibular deficiency syndrome. II. Surgical considerations for mandibular advancement. Oral Surg Oral Med Oral Pathol. 1978 Mar;45(3):349–63.

65. Graber TM, Rakosi T, Petrovic AG. Dentofacial orthopedics with functional appliances. St. Louis: Mosby; 1997.

66. Graber TM, Vanarsdall RL, Vig KWL. Orthodontics: current principles & techniques. St. Louis: Elsevier Mosby; 2005.

67. Tingey TF, Shapiro PA. Selective inhibition of condylar growth in the rabbit mandible using intra-articular papain. Am J Orthod. 1982 Jun;81(6):455–64.

68. Peltomäki T, Kylämarkula S, Vinkka-Puhakka H, Rintala M, Kantomaa T, Rönning O. Tissue-separating capacity of growth cartilages. Eur J Orthod. 1997 Oct;19(5):473–81.

69. Dannan A. An update on periodontic-orthodontic interrelationships. J Indian Soc Periodontol. 2010 Jan;14(1):66–71.

70. Pancherz H, Ruf S, Thomalske-Faubert C. Mandibular articular disk position changes during Herbst treatment: a prospective longitudinal MRI study. Am J Orthod Dentofacial Orthop. 1999 Aug;116(2):207–14.

71. Kochel J, Meyer-Marcotty P, Witt E, Stellzig-Eisenhauer A. Effectiveness of bionator therapy for Class II malocclusions. J Orofac Orthop. 2012 Apr;73(2):91–103.

72. Angelieri F, Franchi L, Cevidanes LHS, Scanavini MA, McNamara JA. Long-term treatment effects of the FR-2 appliance: a prospective evalution 7 years post-treatment. Eur J Orthod [Internet]. 2013 Jun 4 [cited 2013 Jul 20]; Available from: http://ejo.oxfordjournals.org/content/early/2013/06/03/ejo.cjt026

73. Franchi L, Pavoni C, Faltin K, McNamara JA, Cozza P. Long-term skeletal and dental effects and treatment timing for functional appliances in Class II malocclusion. Angle Orthod. 2013 Mar;83(2):334–40.

74. O'Brien K, Wright J, Conboy F, Chadwick S, Connolly I, Cook P, et al. Effectiveness of early orthodontic treatment with the Twin-block appliance: a multicenter, randomized, controlled trial. Part 2: Psychosocial effects. Am J Orthod Dentofacial Orthop. 2003 Nov;124(5):488-494-495.

75. Siara-Olds NJ, Pangrazio-Kulbersh V, Berger J, Bayirli B. Long-term dentoskeletal changes with the Bionator, Herbst, Twin Block, and MARA functional appliances. Angle Orthod. 2010 Jan;80(1):18–29.

76. Du X, Hägg U, Rabie ABM. Effects of headgear Herbst and mandibular step-by-step advancement versus conventional Herbst appliance and maximal jumping of the mandible. Eur J Orthod. 2002 Apr;24(2):167–74.

77. Bendeus M, Hägg U, Rabie B. Growth and treatment changes in patients treated with a headgear-activator appliance. Am J Orthod Dentofacial Orthop. 2002 Apr;121(4):376–84.

78. Evans CH, Huard J. Gene therapy approaches to regenerating the musculoskeletal system. Nat Rev Rheumatol. 2015 Apr;11(4):234–42.

79. Scheller EL, Krebsbach PH, Kohn DH. Tissue engineering: state of the art in oral rehabilitation. J Oral Rehabil. 2009 May;36(5):368–89.

80. Huang Y-C, Simmons C, Kaigler D, Rice KG, Mooney DJ. Bone regeneration in a rat cranial defect with delivery of PEI-condensed plasmid DNA encoding for bone morphogenetic protein-4 (BMP-4). Gene Ther. 2005 Mar;12(5):418–26.

81. Scheller EL, Villa-Diaz LG, Krebsbach PH. Gene therapy: implications for craniofacial regeneration. J Craniofac Surg. 2012 Jan;23(1):333–7.

82. Hacein-Bey-Abina S, Von Kalle C, Schmidt M, McCormack MP, Wulffraat N, Leboulch P, et al. LMO2-associated clonal T cell proliferation in two patients after gene therapy for SCID-X1. Science. 2003 Oct 17;302(5644):415–9.

83. Jin H, Zhang K, Qiao C, Yuan A, Li D, Zhao L, et al. Efficiently engineered cell sheet using a complex of polyethylenimine-alginate nanocomposites plus bone morphogenetic protein 2 gene to promote new bone formation. Int J Nanomedicine. 2014;9:2179–90.

84. Gugala Z, Davis AR, Fouletier-Dilling CM, Gannon FH, Lindsey RW, Olmsted-Davis EA. Adenovirus BMP2-induced osteogenesis in combination with collagen carriers. Biomaterials. 2007 Oct;28(30):4469–79.

85. Evans CH. Advances in regenerative orthopedics. Mayo Clin Proc. 2013 Nov;88(11):1323–39.

86. Sieker JT, Kunz M, Weißenberger M, Gilbert F, Frey S, Rudert M, et al. Direct bone morphogenetic protein 2 and Indian hedgehog gene transfer for articular cartilage repair using bone marrow coagulates. Osteoarthr Cartil. 2015 Mar;23(3):433–42.

87. Ivkovic A, Pascher A, Hudetz D, Maticic D, Jelic M, Dickinson S, et al. Articular cartilage repair by genetically modified bone marrow aspirate in sheep. Gene Ther. 2010 Jun;17(6):779–89.

88. Goodrich LR, Hidaka C, Robbins PD, Evans CH, Nixon AJ. Genetic modification of chondrocytes with insulin-like growth factor-1 enhances cartilage healing in an equine model. J Bone Joint Surg Br. 2007 May;89(5):672–85.

89. Rabie ABM, Dai J, Xu R. Recombinant AAV-mediated VEGF gene therapy induces mandibular condylar growth. Gene Ther. 2007 Jun;14(12):972–80.

90. Suzuki S, Itoh K, Ohyama K. Local administration of IGF-I stimulates the growth of mandibular condyle in mature rats. J Orthod. 2004 Jun;31(2):138–43.

91. Seifi M, Maghzi A, Gutknecht N, Mir M, Asna-Ashari M. The effect of 904 nm low level laser on condylar growth in rats. Lasers Med Sci. 2010 Jan;25(1):61–5.

92. Wan Q, Li Z-B. Intra-articular injection of parathyroid hormone in the temporomandibular joint as a novel therapy for mandibular asymmetry. Med Hypotheses. 2010 Apr;74(4):685–7.

93. Liu Q, Wan Q, Yang R, Zhou H, Li Z. Effects of intermittent versus continuous parathyroid hormone administration on condylar chondrocyte proliferation and differentiation. Biochem Biophys Res Commun. 2012 Jul 20;424(1):182–8.

94. Kasturi G, Adler RA. Mechanical means to improve bone strength: ultrasound and vibration. Curr Rheumatol Rep. 2011 Jun;13(3):251–6.

95. Bashardoust Tajali S, Houghton P, MacDermid JC, Grewal R. Effects of low-intensity pulsed ultrasound therapy on fracture healing: a systematic review and meta-analysis. Am J Phys Med Rehabil. 2012 Apr;91(4):349–67.

96. El-Bialy TH, Elgazzar RF, Megahed EE, Royston TJ. Effects of ultrasound modes on mandibular osteodistraction. J Dent Res. 2008 Oct;87(10):953–7.

97. Shimazaki A, Inui K, Azuma Y, Nishimura N, Yamano Y. Low-intensity pulsed ultrasound accelerates bone maturation in distraction osteogenesis in rabbits. J Bone Joint Surg Br. 2000 Sep;82(7):1077–82.

98. Katano M, Naruse K, Uchida K, Mikuni-Takagaki Y, Takaso M, Itoman M, et al. Low intensity pulsed ultrasound accelerates delayed healing process by reducing the time required for the completion of endochondral ossification in the aged mouse femur fracture model. Exp Anim. 2011;60(4):385–95.

99. Doan N, Reher P, Meghji S, Harris M. In vitro effects of therapeutic ultrasound on cell proliferation, protein synthesis, and cytokine production by human fibroblasts, osteoblasts, and monocytes. J Oral Maxillofac Surg. 1999 Apr;57(4):409–419; discussion 420.

100. Sun JS, Hong RC, Chang WH, Chen LT, Lin FH, Liu HC. In vitro effects of low-intensity ultrasound stimulation on the bone cells. J Biomed Mater Res. 2001 Dec 5;57(3):449–56.

101. Li JK, Chang WH, Lin JC, Ruaan RC, Liu HC, Sun JS. Cytokine release from osteoblasts in response to ultrasound stimulation. Biomaterials. 2003 Jun;24(13):2379–85.

102. Naruse K, Sekiya H, Harada Y, Iwabuchi S, Kozai Y, Kawamata R, et al. Prolonged endochondral bone healing in senescence is shortened by low-intensity pulsed ultrasound in a manner dependent on COX-2. Ultrasound Med Biol. 2010 Jul;36(7):1098–108.

103. Naruse K, Miyauchi A, Itoman M, Mikuni-Takagaki Y. Distinct Anabolic Response of Osteoblast to Low-Intensity Pulsed Ultrasound. Journal of Bone and Mineral Research. 2003;18(2):360–369.

104. Ikeda K, Takayama T, Suzuki N, Shimada K, Otsuka K, Ito K. Effects of low-intensity pulsed ultrasound on the differentiation of C2C12 cells. Life Sci. 2006 Oct 12;79(20):1936–43.

105. Takayama T, Suzuki N, Ikeda K, Shimada T, Suzuki A, Maeno M, et al. Low-intensity pulsed ultrasound stimulates osteogenic differentiation in ROS 17/2.8 cells. Life Sci. 2007 Feb 13;80(10):965–71.

106. Parvizi J, Wu CC, Lewallen DG, Greenleaf JF, Bolander ME. Low-intensity ultrasound stimulates proteoglycan synthesis in rat chondrocytes by increasing aggrecan gene expression. J Orthop Res. 1999 Jul;17(4):488–94.

107. Parvizi J, Parpura V, Greenleaf JF, Bolander ME. Calcium signaling is required for ultrasound-stimulated aggrecan synthesis by rat chondrocytes. J Orthop Res. 2002 Jan;20(1):51–7.

108. Mukai S, Ito H, Nakagawa Y, Akiyama H, Miyamoto M, Nakamura T. Transforming growth factor-beta1 mediates the effects of low-intensity pulsed ultrasound in chondrocytes. Ultrasound Med Biol. 2005 Dec;31(12):1713–21.

109. Zhang Z-J, Huckle J, Francomano CA, Spencer RGS. The effects of pulsed low-intensity ultrasound on chondrocyte viability, proliferation, gene expression and matrix production. Ultrasound Med Biol. 2003 Nov;29(11):1645–51.

110. Zhang Z i-Jun, Huckle J, Francomano CA, Spencer RGS. The influence of pulsed low-intensity ultrasound on matrix production of chondrocytes at different stages of differentiation: an explant study. Ultrasound Med Biol. 2002 Dec;28(11–12):1547–53.

111. Mitragotri S. Healing sound: the use of ultrasound in drug delivery and other therapeutic applications. Nat Rev Drug Discov. 2005 Mar;4(3):255–60.

112. Dyson M. Non-thermal cellular effects of ultrasound. Br J Cancer Suppl. 1982 Mar;5:165–71.

113. Frenkel V. Ultrasound mediated delivery of drugs and genes to solid tumors. Adv Drug Deliv Rev. 2008 Jun 30;60(10):1193–208.

114. Padilla F, Puts R, Vico L, Raum K. Stimulation of bone repair with ultrasound: a review of the possible mechanic effects. Ultrasonics. 2014 Jul;54(5):1125–45.

115. Sarvazyan A. Diversity of biomedical applications of acoustic radiation force. Ultrasonics. 2010 Feb;50(2):230–4.

116. Krasovitski B, Frenkel V, Shoham S, Kimmel E. Intramembrane cavitation as a unifying mechanism for ultrasound-induced bioeffects. Proc Natl Acad Sci USA. 2011 Feb 22;108(8):3258–63.

117. Wang N, Tytell JD, Ingber DE. Mechanotransduction at a distance: mechanically coupling the extracellular matrix with the nucleus. Nat Rev Mol Cell Biol. 2009 Jan;10(1):75–82.

118. Wang JH-C, Thampatty BP. An introductory review of cell mechanobiology. Biomech Model Mechanobiol. 2006 Mar;5(1):1–16.

119. Schmidt CE, Horwitz AF, Lauffenburger DA, Sheetz MP. Integrin-cytoskeletal interactions in migrating fibroblasts are dynamic, asymmetric, and regulated. J Cell Biol. 1993 Nov;123(4):977–91.

120. Wang N, Butler JP, Ingber DE. Mechanotransduction across the cell surface and through the cytoskeleton. Science. 1993 May 21;260(5111):1124–7.

121. Urbich C, Dernbach E, Reissner A, Vasa M, Zeiher AM, Dimmeler S. Shear stress-induced endothelial cell migration involves integrin signaling via the fibronectin receptor subunits alpha(5) and beta(1). Arterioscler Thromb Vasc Biol. 2002 Jan;22(1):69–75.

122. Juffermans LJM, van Dijk A, Jongenelen CAM, Drukarch B, Reijerkerk A, de Vries HE, et al. Ultrasound and microbubble-induced intra- and intercellular bioeffects in primary endothelial cells. Ultrasound Med Biol. 2009 Nov;35(11):1917–27.

123. Uddin SMZ, Hadjiargyrou M, Cheng J, Zhang S, Hu M, Qin Y-X. Reversal of the detrimental effects of simulated microgravity on human osteoblasts by modified low intensity pulsed ultrasound. Ultrasound Med Biol. 2013 May;39(5):804–12.

124. Yang R-S, Lin W-L, Chen Y-Z, Tang C-H, Huang T-H, Lu B-Y, et al. Regulation by ultrasound treatment on the integrin expression and differentiation of osteoblasts. Bone. 2005 Feb 1;36(2):276–83.

125. Guilak F. The deformation behavior and viscoelastic properties of chondrocytes in articular cartilage. Biorheology. 2000;37(1–2):27–44.

126. Lee HS, Millward-Sadler SJ, Wright MO, Nuki G, Salter DM. Integrin and mechanosensitive ion channel-dependent tyrosine phosphorylation of focal adhesion proteins and beta-catenin in human articular chondrocytes after mechanical stimulation. J Bone Miner Res. 2000 Aug;15(8):1501–9.

127. Salter DM, Millward-Sadler SJ, Nuki G, Wright MO. Differential responses of chondrocytes from normal and osteoarthritic human articular cartilage to mechanical stimulation. Biorheology. 2002;39(1–2):97–108.

128. Wu QQ, Chen Q. Mechanoregulation of chondrocyte proliferation, maturation, and hypertrophy: ion-channel dependent transduction of matrix deformation signals. Exp Cell Res. 2000 May 1;256(2):383–91.

129. Giancotti FG, Ruoslahti E. Integrin signaling. Science. 1999 Aug 13;285(5430):1028–32.

130. Campbell ID, Humphries MJ. Integrin structure, activation, and interactions. Cold Spring Harb Perspect Biol. 2011 Mar;3(3).

131. Kuo J-C, Han X, Hsiao C-T, Yates JR, Waterman CM. Analysis of the myosin-II-responsive focal adhesion proteome reveals a role for β-Pix in negative regulation of focal adhesion maturation. Nat Cell Biol. 2011 Apr;13(4):383–93.

132. Schiller HB, Friedel CC, Boulegue C, Fässler R. Quantitative proteomics of the integrin adhesome show a myosin II-dependent recruitment of LIM domain proteins. EMBO Rep. 2011 Mar;12(3):259–66.

133. Whitney NP, Lamb AC, Louw TM, Subramanian A. Integrin-mediated mechanotransduction pathway of low-intensity continuous ultrasound in human chondrocytes. Ultrasound Med Biol. 2012 Oct;38(10):1734–43.

134. Watabe H, Furuhama T, Tani-Ishii N, Mikuni-Takagaki Y. Mechanotransduction activates $\alpha_5\beta_1$ integrin and PI3K/Akt signaling pathways in mandibular osteoblasts. Exp Cell Res. 2011 Nov 1;317(18):2642–9.

135. Iwabuchi Y, Tanimoto K, Tanne Y, Inubushi T, Kamiya T, Kunimatsu R, et al. Effects of low-intensity pulsed ultrasound on the expression of cyclooxygenase-2 in mandibular condylar chondrocytes. J Oral Facial Pain Headache. 2014;28(3):261–8.

136. Lee D-Y, Yeh C-R, Chang S-F, Lee P-L, Chien S, Cheng C-K, et al. Integrin-mediated expression of bone formation-related genes in osteoblast-like cells in response to fluid shear stress: roles of extracellular matrix, Shc, and mitogen-activated protein kinase. J Bone Miner Res. 2008 Jul;23(7):1140–9.

137. Yang R-S, Lin W-L, Chen Y-Z, Tang C-H, Huang T-H, Lu B-Y, et al. Regulation by ultrasound treatment on the integrin expression and differentiation of osteoblasts. Bone. 2005 Feb;36(2):276–83.

138. Schumann D, Kujat R, Zellner J, Angele MK, Nerlich M, Mayr E, et al. Treatment of human mesenchymal stem cells with pulsed low intensity ultrasound enhances the chondrogenic phenotype in vitro. Biorheology. 2006;43(3–4):431–43.

139. Cheng K, Xia P, Lin Q, Shen S, Gao M, Ren S, et al. Effects of Low-Intensity Pulsed Ultrasound on Integrin-FAK-PI3K/Akt Mechanochemical Transduction in Rabbit Osteoarthritis Chondrocytes. Ultrasound in Medicine & Biology. 2014 Jul;40(7):1609–18.

140. Barberis L, Wary KK, Fiucci G, Liu F, Hirsch E, Brancaccio M, et al. Distinct roles of the adaptor protein Shc and focal adhesion kinase in integrin signaling to ERK. J Biol Chem. 2000 Nov 24;275(47):36532–40.

141. Choi BH, Choi MH, Kwak M-G, Min B-H, Woo ZH, Park SR. Mechanotransduction pathways of low-intensity ultrasound in C-28/I2 human chondrocyte cell line. Proc Inst Mech Eng H. 2007 Jul;221(5):527–35.

142. Greenblatt MB, Shim J-H, Glimcher LH. Mitogen-Activated Protein Kinase Pathways in Osteoblasts. Annual Review of Cell and Developmental Biology. 2013;29(1):63–79.

143. Stanton L-A, Underhill TM, Beier F. MAP kinases in chondrocyte differentiation. Dev Biol. 2003 Nov 15;263(2):165–75.

144. Kyriakis JM, Avruch J. Mammalian MAPK signal transduction pathways activated by stress and inflammation: a 10-year update. Physiol Rev. 2012 Apr;92(2):689–737.

145. Li X, Li J, Cheng K, Lin Q, Wang D, Zhang H, et al. Effect of low-intensity pulsed ultrasound on MMP-13 and MAPKs signaling pathway in rabbit knee osteoarthritis. Cell Biochem Biophys. 2011 Nov;61(2):427–34.

146. Ren L, Yang Z, Song J, Wang Z, Deng F, Li W. Involvement of p38 MAPK pathway in low intensity pulsed ultrasound induced osteogenic differentiation of human periodontal ligament cells. Ultrasonics. 2012 Nov 5;

147. Sato M, Nagata K, Kuroda S, Horiuchi S, Nakamura T, Karima M, et al. Low-Intensity Pulsed Ultrasound Activates Integrin-Mediated Mechanotransduction Pathway in Synovial Cells. Ann Biomed Eng. 2014 Aug 6;

148. Xia P, Ren S, Lin Q, Cheng K, Shen S, Gao M, et al. Low-Intensity Pulsed Ultrasound Affects Chondrocyte Extracellular Matrix Production via an Integrin-Mediated p38 MAPK Signaling Pathway. Ultrasound Med Biol. 2015 Jun;41(6):1690–700.

149. Chen M-H, Sun J-S, Liao S-Y, Tai P-A, Li T-C, Chen M-H. Low-intensity pulsed ultrasound stimulates matrix metabolism of human annulus fibrosus cells mediated by transforming growth factor β1 and extracellular signal-regulated kinase pathway. Connect Tissue Res. 2015 Jun;56(3):219–27.

150. Son Y, Kim S, Chung H-T, Pae H-O. Reactive oxygen species in the activation of MAP kinases. Meth Enzymol. 2013;528:27–48.

151. Klebanoff SJ. Oxygen metabolism and the toxic properties of phagocytes. Ann Intern Med. 1980 Sep;93(3):480–9.

152. Sauer H, Wartenberg M, Hescheler J. Reactive oxygen species as intracellular messengers during cell growth and differentiation. Cell Physiol Biochem. 2001;11(4):173–86.

153. Bedard K, Krause K-H. The NOX family of ROS-generating NADPH oxidases: physiology and pathophysiology. Physiol Rev. 2007 Jan;87(1):245–313.

154. Suzuki YJ, Forman HJ, Sevanian A. Oxidants as stimulators of signal transduction. Free Radic Biol Med. 1997;22(1–2):269–85.

155. Slutsky V, Kozyrev D. Handbook of Free Radicals : Formation, Types and Effects. New York: Nova Science Publishers; 2010. (Cell Biology Research Progress Series).

156. Morita K, Miyamoto T, Fujita N, Kubota Y, Ito K, Takubo K, et al. Reactive oxygen species induce chondrocyte hypertrophy in endochondral ossification. J Exp Med. 2007 Jul 9;204(7):1613–23.

157. Bartosz G. Reactive oxygen species: Destroyers or messengers? Biochemical Pharmacology. 2009 Apr 15;77(8):1303–15.

158. Hobbs GA, Mitchell LE, Arrington ME, Gunawardena HP, DeCristo MJ, Loeser RF, et al. Redox regulation of Rac1 by thiol oxidation. Free Radical Biology and Medicine. 2015 Feb;79:237–50.

159. Poli G, Leonarduzzi G, Biasi F, Chiarpotto E. Oxidative stress and cell signalling. Current Medicinal Chemistry. 2004;11(9):1163–82.

160. Goldstein BJ, Mahadev K, Kalyankar M, Wu X. Redox paradox: insulin action is facilitated by insulin-stimulated reactive oxygen species with multiple potential signaling targets. Diabetes. 2005 Feb;54(2):311–21.

161. El-Bialy T, El-Shamy I, Graber TM. Growth modification of the rabbit mandible using therapeutic ultrasound: is it possible to enhance functional appliance results? Angle Orthod. 2003 Dec;73(6):631–9.

162. El-Bialy T, Hassan A, Albaghdadi T, Fouad HA, Maimani AR. Growth modification of the mandible with ultrasound in baboons: a preliminary report. Am J Orthod Dentofacial Orthop. 2006 Oct;130(4):435.e7-14.

163. El-Bialy T. Nonsurgical treatment of hemifacial microsomia by therapeutic ultrasound and hybrid functional appliance. J Clin Trials. 2010 Mar;29.

164. Chan CW, Qin L, Lee KM, Cheung WH, Cheng JCY, Leung KS. Dose-dependent effect of low-intensity pulsed ultrasound on callus formation during rapid distraction osteogenesis. J Orthop Res. 2006 Nov;24(11):2072–9.

Chapter 2: Effect of increasing daily Low Intensity Pulsed Ultrasound application and Functional Appliance on mandibular condyle in growing rats.

1. Delatte M, Von den Hoff JW, van Rheden REM, Kuijpers-Jagtman AM. Primary and secondary cartilages of the neonatal rat: the femoral head and the mandibular condyle. Eur J Oral Sci. 2004 Apr;112(2):156–62.

2. McNamara JA Jr. Components of class II malocclusion in children 8-10 years of age. Angle Orthod. 1981 Jul;51(3):177–202.

3. Ritto AK. Class II malocclusion: why, when and how to treat this anomaly in mixed dentition with fixed functional appliances. J Gen Orthod. 2001;12(4):9–21.

4. Proffit WR, Fields HW Jr, Moray LJ. Prevalence of malocclusion and orthodontic treatment need in the United States: estimates from the NHANES III survey. Int J Adult Orthodon Orthognath Surg. 1998;13(2):97–106.

5. Bock NC, Ruf S. Dentoskeletal changes in adult Class II division 1 Herbst treatment--how much is left after the retention period? Eur J Orthod. 2012 Dec;34(6):747–53.

6. Graber TM, Rakosi T, Petrovic AG. Dentofacial orthopedics with functional appliances. St. Louis: Mosby; 1997.

7. El-Bialy T, El-Shamy I, Graber TM. Growth modification of the rabbit mandible using therapeutic ultrasound: is it possible to enhance functional appliance results? Angle Orthod. 2003 Dec;73(6):631–9.

8. Cozza P, Baccetti T, Franchi L, De Toffol L, McNamara JA Jr. Mandibular changes produced by functional appliances in Class II malocclusion: a systematic review. Am J Orthod Dentofac Orthop Off Publ Am Assoc Orthod Its Const Soc Am Board Orthod. 2006 May;129(5):599.e1-12; discussion e1-6.

9. Pangrazio MNK, Pangrazio-Kulbersh V, Berger JL, Bayirli B, Movahhedian A. Treatment effects of the mandibular anterior repositioning appliance in patients with Class II skeletal malocclusions. Angle Orthod. 2012 Nov;82(6):971–7.

10. Owtad P, Park JH, Shen G, Potres Z, Darendeliler MA. The biology of TMJ growth modification: a review. J Dent Res. 2013 Apr;92(4):315–21.

11. Ustun Y, Erdogan O, Kurkcu M, Akova T, Damlar I. Effects of low-intensity pulsed ultrasound on dental implant osseointegration: a preliminary report. Eur J Dent. 2008 Oct;2(4):254–62.

12. Baker KG, Robertson VJ, Duck FA. A Review of Therapeutic Ultrasound: Biophysical Effects. Phys Ther. 2001 Jul 1;81(7):1351–8.

13. Doan N, Reher P, Meghji S, Harris M. In vitro effects of therapeutic ultrasound on cell proliferation, protein synthesis, and cytokine production by human fibroblasts, osteoblasts, and monocytes. J Oral Maxillofac Surg Off J Am Assoc Oral Maxillofac Surg. 1999 Apr;57(4):409–419; discussion 420.

14. Snyder BM, Conley J, Koval KJ. Does low-intensity pulsed ultrasound reduce time to fracture healing? A meta-analysis. Am J Orthop Belle Mead NJ. 2012 Feb;41(2):E12-19.

15. Dudda M, Hauser J, Muhr G, Esenwein SA. Low-intensity pulsed ultrasound as a useful adjuvant during distraction osteogenesis: a prospective, randomized controlled trial. J Trauma. 2011 Nov;71(5):1376–80.

16. El-Bialy T, Hassan A, Albaghdadi T, Fouad HA, Maimani AR. Growth modification of the mandible with ultrasound in baboons: a preliminary report. Am J Orthod Dentofac Orthop Off Publ Am Assoc Orthod Its Const Soc Am Board Orthod. 2006 Oct;130(4):435.e7-14.

17. El-Bialy T. Nonsurgical treatment of hemifacial microsomia by therapeutic ultrasound and hybrid functional appliance. Open Access J Clin Trials. 2010 Mar;29.

18. Schumann D, Kujat R, Zellner J, Angele MK, Nerlich M, Mayr E, et al. Treatment of human mesenchymal stem cells with pulsed low intensity ultrasound enhances the chondrogenic phenotype in vitro. Biorheology. 2006;43(3–4):431–43.

19. Chan CW, Qin L, Lee KM, Cheung WH, Cheng JCY, Leung KS. Dose-dependent effect of low-intensity pulsed ultrasound on callus formation during rapid distraction osteogenesis. J Orthop Res Off Publ Orthop Res Soc. 2006 Nov;24(11):2072–9.

20. Rabie ABM, She TT, Hägg U. Functional appliance therapy accelerates and enhances condylar growth. Am J Orthod Dentofacial Orthop. 2003 Jan;123(1):40–8.

21. Rabie AB, Zhao Z, Shen G, Hägg EU, Dr O, Robinson W. Osteogenesis in the glenoid fossa in response to mandibular advancement. Am J Orthod Dentofac Orthop Off Publ Am Assoc Orthod Its Const Soc Am Board Orthod. 2001 Apr;119(4):390–400.

22. Rabie ABM, Xiong H, Hägg U. Forward mandibular positioning enhances condylar adaptation in adult rats. Eur J Orthod. 2004 Aug;26(4):353–8.

23. Oyonarte R, Zárate M, Rodriguez F. Low-intensity pulsed ultrasound stimulation of condylar growth in rats. Angle Orthod. 2009 Sep;79(5):964–70.

24. Rawool NM, Goldberg BB, Forsberg F, Winder AA, Hume E. Power Doppler assessment of vascular changes during fracture treatment with low-intensity ultrasound. J Ultrasound Med Off J Am Inst Ultrasound Med. 2003 Feb;22(2):145–53.

25. Fajardo RJ, Müller R. Three-dimensional analysis of nonhuman primate trabecular architecture using micro-computed tomography. Am J Phys Anthropol. 2001 Aug;115(4):327–36.

26. Kazama JJ, Koda R, Yamamoto S, Narita I, Gejyo F, Tokumoto A. Cancellous bone volume is an indicator for trabecular bone connectivity in dialysis patients. Clin J Am Soc Nephrol CJASN. 2010 Feb;5(2):292–8.

27. Kim H, Oh E, Im H, Mun J, Yang M, Khim J-Y, et al. Oxidative damages in the DNA, lipids, and proteins of rats exposed to isofluranes and alcohols. Toxicology. 2006 Mar 15;220(2–3):169–78.

28. Sachs F. Mechanical transduction by membrane ion channels: a mini review. Mol Cell Biochem. 1991 Jun 29;104(1–2):57–60.

29. Bassett CA. Electrical effects in bone. Sci Am. 1965 Oct;213(4):18–25.

30. Behari J, Singh S. Ultrasound propagation in “in vivo” bone. Ultrasonics. 1981 Mar;19(2):87–90.

31. Schortinghuis J, Stegenga B, Raghoebar GM, de Bont LGM. Ultrasound stimulation of maxillofacial bone healing. Crit Rev Oral Biol Med Off Publ Am Assoc Oral Biol. 2003;14(1):63–74.

32. Schuster A, Schwab T, Bischof M, Klotz M, Lemor R, Degel C, et al. Cell specific ultrasound effects are dose and frequency dependent. Ann Anat Anat Anz Off Organ Anat Ges. 2013 Jan;195(1):57–67.

33. Whitney NP, Lamb AC, Louw TM, Subramanian A. Integrin-mediated mechanotransduction pathway of low-intensity continuous ultrasound in human chondrocytes. Ultrasound Med Biol. 2012 Oct;38(10):1734–43.

34. Cheng K, Xia P, Lin Q, Shen S, Gao M, Ren S, et al. Effects of Low-Intensity Pulsed Ultrasound on Integrin-FAK-PI3K/Akt Mechanochemical Transduction in Rabbit Osteoarthritis Chondrocytes. Ultrasound Med Biol. 2014 Jul;40(7):1609–18.

35. Marques MR, Hajjar D, Oliveira Crema V, Kimura ET, Santos MF. A mandibular propulsive appliance modulates collagen-binding integrins distribution in the young rat condylar cartilage. Biorheology. 2006;43(3–4):293–302.

36. Marques MR, Hajjar D, Franchini KG, Moriscot AS, Santos MF. Mandibular appliance modulates condylar growth through integrins. J Dent Res. 2008 Feb;87(2):153–8.

37. Xue H, Zheng J, Cui Z, Bai X, Li G, Zhang C, et al. Low-intensity pulsed ultrasound accelerates tooth movement via activation of the BMP-2 signaling pathway. PloS One. 2013;8(7):e68926.

38. Leskinen JJ, Hynynen K. Study of factors affecting the magnitude and nature of ultrasound exposure with in vitro set-ups. Ultrasound Med Biol. 2012 May;38(5):777–94.

39. Kuroda S, Tanimoto K, Izawa T, Fujihara S, Koolstra JH, Tanaka E. Biomechanical and biochemical characteristics of the mandibular condylar cartilage. Osteoarthr Cartil OARS Osteoarthr Res Soc. 2009 Nov;17(11):1408–15.

40. Bozzini C, Picasso E, Champin G, Bozzini CE, Alippi RM. Effect of physical consistency of food on the biomechanical behaviour of the mandible in the growing rat. Eur J Oral Sci. 2015 Sep 4;

41. Li Q, Zhang M, Chen Y-J, Zhou Q, Wang Y-J, Liu J. Psychological stress alters microstructure of the mandibular condyle in rats. Physiol Behav. 2013;110–111:129–39.

Chapter 3: Superoxide mediates Low Intensity Pulsed Ultrasound induced Mitogen Activated Protein Kinases activation in C28/I2 human chondrocytes.

1. Whitney NP, Lamb AC, Louw TM, Subramanian A. Integrin-mediated mechanotransduction pathway of low-intensity continuous ultrasound in human chondrocytes. Ultrasound Med Biol. 2012 Oct;38(10):1734–43.

2. Fanghänel J, Gedrange T. On the development, morphology and function of the temporomandibular joint in the light of the orofacial system. Annals of Anatomy - Anatomischer Anzeiger. 2007 Jul 11;189(4):314–9.

3. Jortikka MO, Inkinen RI, Tammi MI, Parkkinen JJ, Haapala J, Kiviranta I, et al. Immobilisation causes longlasting matrix changes both in the immobilised and contralateral joint cartilage. Ann Rheum Dis. 1997 Apr;56(4):255–61.

4. Sato H, Kawamura A, Yamaguchi M, Kasai K. Relationship between masticatory function and internal structure of the mandible based on computed tomography findings. Am J Orthod Dentofacial Orthop. 2005 Dec;128(6):766–73.

5. Tanaka E, Kuroda S, Horiuchi S, Tabata A, El-Bialy T. Low-Intensity Pulsed Ultrasound in Dentofacial Tissue Engineering. Ann Biomed Eng. 2015 Feb 12;

6. Claes L, Willie B. The enhancement of bone regeneration by ultrasound. Prog Biophys Mol Biol. 2007 Apr;93(1–3):384–98.

7. Busse JW, Kaur J, Mollon B, Bhandari M, Tornetta P 3rd, Schünemann HJ, et al. Low intensity pulsed ultrasonography for fractures: systematic review of randomised controlled trials. BMJ. 2009;338:b351.

8. Wu S, Kawahara Y, Manabe T, Ogawa K, Matsumoto M, Sasaki A, et al. Low-intensity pulsed ultrasound accelerates osteoblast differentiation and promotes

bone formation in an osteoporosis rat model. Pathobiology. 2009 May;76(3):99–107.

9. Cheung W-H, Chow SK, Sun M-H, Qin L, Leung K-S. Low-Intensity Pulsed Ultrasound Accelerated Callus Formation, Angiogenesis and Callus Remodeling in Osteoporotic Fracture Healing. Ultrasound in Medicine & Biology. 2011 Feb;37(2):231–8.

10. Hasanova GI, Noriega SE, Mamedov TG, Guha Thakurta S, Turner JA, Subramanian A. The effect of ultrasound stimulation on the gene and protein expression of chondrocytes seeded in chitosan scaffolds. J Tissue Eng Regen Med. 2011 Nov;5(10):815–22.

11. Korstjens CM, van der Rijt RHH, Albers GHR, Semeins CM, Klein-Nulend J. Low-intensity pulsed ultrasound affects human articular chondrocytes in vitro. Med Biol Eng Comput. 2008 Dec;46(12):1263–70.

12. El-Bialy T, El-Shamy I, Graber TM. Growth modification of the rabbit mandible using therapeutic ultrasound: is it possible to enhance functional appliance results? Angle Orthod. 2003 Dec;73(6):631–9.

13. El-Bialy T. Nonsurgical treatment of hemifacial microsomia by therapeutic ultrasound and hybrid functional appliance. J Clin Trials. 2010 Mar;29.

14. Kaur H, Uludağ H, El-Bialy T. Effect of nonviral plasmid delivered basic fibroblast growth factor and low intensity pulsed ultrasound on mandibular condylar growth: a preliminary study. Biomed Res Int. 2014;2014:426710.

15. Li X, Li J, Cheng K, Lin Q, Wang D, Zhang H, et al. Effect of low-intensity pulsed ultrasound on MMP-13 and MAPKs signaling pathway in rabbit knee osteoarthritis. Cell Biochem Biophys. 2011 Nov;61(2):427–34.

16. Cheng K, Xia P, Lin Q, Shen S, Gao M, Ren S, et al. Effects of Low-Intensity Pulsed Ultrasound on Integrin-FAK-PI3K/Akt Mechanochemical Transduction in Rabbit Osteoarthritis Chondrocytes. Ultrasound in Medicine & Biology. 2014 Jul;40(7):1609–18.

17. Sato M, Nagata K, Kuroda S, Horiuchi S, Nakamura T, Karima M, et al. Low-Intensity Pulsed Ultrasound Activates Integrin-Mediated Mechanotransduction Pathway in Synovial Cells. Ann Biomed Eng. 2014 Aug 6;

18. Takeuchi R, Ryo A, Komitsu N, Mikuni-Takagaki Y, Fukui A, Takagi Y, et al. Low-intensity pulsed ultrasound activates the phosphatidylinositol 3 kinase/Akt pathway and stimulates the growth of chondrocytes in three-dimensional cultures: a basic science study. Arthritis Res Ther. 2008;10(4):R77.

19. Uddin SMZ, Hadjiargyrou M, Cheng J, Zhang S, Hu M, Qin Y-X. Reversal of the detrimental effects of simulated microgravity on human osteoblasts by modified low intensity pulsed ultrasound. Ultrasound Med Biol. 2013 May;39(5):804–12.

20. Kusuyama J, Bandow K, Shamoto M, Kakimoto K, Ohnishi T, Matsuguchi T. Low intensity pulsed ultrasound (LIPUS) influences the multilineage differentiation of mesenchymal stem and progenitor cell lines through ROCK-Cot/Tpl2-MEK-ERK signaling pathway. J Biol Chem. 2014 Apr 11;289(15):10330–44.

21. Fujisawa T, Takeda K, Ichijo H. ASK family proteins in stress response and disease. Mol Biotechnol. 2007 Sep;37(1):13–8.

22. Li J, Zhao Z, Liu J, Huang N, Long D, Wang J, et al. MEK/ERK and p38 MAPK regulate chondrogenesis of rat bone marrow mesenchymal stem cells through delicate interaction with TGF-beta1/Smads pathway. Cell Prolif. 2010 Aug;43(4):333–43.

23. Sauer H, Wartenberg M, Hescheler J. Reactive oxygen species as intracellular messengers during cell growth and differentiation. Cell Physiol Biochem. 2001;11(4):173–86.

24. Son Y, Kim S, Chung H-T, Pae H-O. Reactive oxygen species in the activation of MAP kinases. Meth Enzymol. 2013;528:27–48.

25. Reher P, Harris M, Whiteman M, Hai H., Meghji S. Ultrasound stimulates nitric oxide and prostaglandin e2 production by human osteoblasts. Bone. 2002 Jul;31(1):236–41.

26. Li L, Yang Z, Zhang H, Chen W, Chen M, Zhu Z. Low-intensity pulsed ultrasound regulates proliferation and differentiation of osteoblasts through osteocytes. Biochem Biophys Res Commun. 2012 Feb 10;418(2):296–300.

27. Hsu S, Huang T. Bioeffect of ultrasound on endothelial cells in vitro. Biomol Eng. 2004 Nov;21(3–5):99–104.

28. Mortimer AJ, Dyson M. The effect of therapeutic ultrasound on calcium uptake in fibroblasts. Ultrasound Med Biol. 1988;14(6):499–506.

29. Choi BH, Choi MH, Kwak M-G, Min B-H, Woo ZH, Park SR. Mechanotransduction pathways of low-intensity ultrasound in C-28/I2 human chondrocyte cell line. Proc Inst Mech Eng H. 2007 Jul;221(5):527–35.

30. Peshavariya HM, Dusting GJ, Selemidis S. Analysis of dihydroethidium fluorescence for the detection of intracellular and extracellular superoxide produced by NADPH oxidase. Free Radic Res. 2007 Jun;41(6):699–712.

31. Zielonka J, Hardy M, Kalyanaraman B. HPLC study of oxidation products of hydroethidine in chemical and biological systems: Ramifications in superoxide measurements. Free Radic Biol Med. 2009 Feb 1;46(3):329–38.

32. Li N, Ragheb K, Lawler G, Sturgis J, Rajwa B, Melendez JA, et al. DPI induces mitochondrial superoxide-mediated apoptosis. Free Radical Biology and Medicine. 2003 Feb 15;34(4):465–77.

33. Oralová V, Matalová E, Janečková E, Drobná Krejčí E, Knopfová L, Šnajdr P, et al. Role of c-Myb in chondrogenesis. Bone. 2015 Jul;76:97–106.

34. Kuroda S, Tanimoto K, Izawa T, Fujihara S, Koolstra JH, Tanaka E. Biomechanical and biochemical characteristics of the mandibular condylar cartilage. Osteoarthr Cartil. 2009 Nov;17(11):1408–15.

35. Morita K, Miyamoto T, Fujita N, Kubota Y, Ito K, Takubo K, et al. Reactive oxygen species induce chondrocyte hypertrophy in endochondral ossification. J Exp Med. 2007 Jul 9;204(7):1613–23.

36. Ambe K, Watanabe H, Takahashi S, Nakagawa T. Immunohistochemical localization of Nox1, Nox4 and Mn-SOD in mouse femur during endochondral ossification. 2014.

37. Martyn KD, Frederick LM, von Loehneysen K, Dinauer MC, Knaus UG. Functional analysis of Nox4 reveals unique characteristics compared to other NADPH oxidases. Cell Signal. 2006 Jan;18(1):69–82.

38. Ikeda K, Takayama T, Suzuki N, Shimada K, Otsuka K, Ito K. Effects of low-intensity pulsed ultrasound on the differentiation of C2C12 cells. Life Sci. 2006 Oct 12;79(20):1936–43.

39. Rego EB, Inubushi T, Kawazoe A, Tanimoto K, Miyauchi M, Tanaka E, et al. Ultrasound stimulation induces PGE(2) synthesis promoting cementoblastic differentiation through EP2/EP4 receptor pathway. Ultrasound Med Biol. 2010 Jun;36(6):907–15.

40. Bartosz G. Reactive oxygen species: Destroyers or messengers? Biochemical Pharmacology. 2009 Apr 15; 77(8):1303–15.

Chapter 4: Role of reactive oxygen species during low intensity pulsed ultrasound application in MC-3T3 E1 pre-osteoblast cell culture.

1. Haugh MG, Vaughan TJ, McNamara LM. The role of integrin αVβ3 in osteocyte mechanotransduction. J Mech Behav Biomed Mater. 2015 Feb;42:67–75.

2. Tan J, Xu X, Tong Z, Lin J, Yu Q, Lin Y, et al. Decreased osteogenesis of adult mesenchymal stem cells by reactive oxygen species under cyclic stretch: a possible mechanism of age related osteoporosis. Bone Res. 2015;3:15003.

3. Wang JH-C, Thampatty BP. An introductory review of cell mechanobiology. Biomech Model Mechanobiol. 2006 Mar;5(1):1–16.

4. Matsushita T, Chan YY, Kawanami A, Balmes G, Landreth GE, Murakami S. Extracellular Signal-Regulated Kinase 1 (ERK1) and ERK2 Play Essential Roles in Osteoblast Differentiation and in Supporting Osteoclastogenesis. Mol Cell Biol. 2009 Nov;29(21):5843–57.

5. Beardmore VA, Hinton HJ, Eftychi C, Apostolaki M, Armaka M, Darragh J, et al. Generation and Characterization of p38β (MAPK11) Gene-Targeted Mice. Mol Cell Biol. 2005 Dec;25(23):10454–64.

6. Greenblatt MB, Shim J-H, Zou W, Sitara D, Schweitzer M, Hu D, et al. The p38 MAPK pathway is essential for skeletogenesis and bone homeostasis in mice. J Clin Invest. 2010 Jul;120(7):2457–73.

7. Tanaka E, Kuroda S, Horiuchi S, Tabata A, El-Bialy T. Low-Intensity Pulsed Ultrasound in Dentofacial Tissue Engineering. Ann Biomed Eng. 2015 Feb 12;

8. Yang R-S, Lin W-L, Chen Y-Z, Tang C-H, Huang T-H, Lu B-Y, et al. Regulation by ultrasound treatment on the integrin expression and differentiation of osteoblasts. Bone. 2005 Feb 1;36(2):276–83.

9. Parvizi J, Parpura V, Greenleaf JF, Bolander ME. Calcium signaling is required for ultrasound-stimulated aggrecan synthesis by rat chondrocytes. J Orthop Res. 2002 Jan;20(1):51–7.

10. Tang C-H, Lu D-Y, Tan T-W, Fu W-M, Yang R-S. Ultrasound induces hypoxia-inducible factor-1 activation and inducible nitric-oxide synthase expression through the integrin/integrin-linked kinase/Akt/mammalian target of rapamycin pathway in osteoblasts. J Biol Chem. 2007 Aug 31;282(35):25406–15.

11. Sauer H, Wartenberg M, Hescheler J. Reactive oxygen species as intracellular messengers during cell growth and differentiation. Cell Physiol Biochem. 2001;11(4):173–86.

12. Schröder K. NADPH oxidases in bone homeostasis and osteoporosis. Cell Mol Life Sci. 2014 Aug 29;72(1):25–38.

13. Son Y, Kim S, Chung H-T, Pae H-O. Chapter Two - Reactive Oxygen Species in the Activation of MAP Kinases. In: Enrique Cadenas and Lester Packer, editor. Methods in Enzymology [Internet]. Academic Press; 2013 [cited 2013 Dec 11]. p. 27–48. Available from: http://www.sciencedirect.com/science/article/pii/B9780124058811000021

14. Mostafa NZ, Uludağ H, Dederich DN, Doschak MR, El-Bialy TH. Anabolic effects of low-intensity pulsed ultrasound on human gingival fibroblasts. Arch Oral Biol. 2009 Aug;54(8):743–8.

15. Nagasaki R, Mukudai Y, Yoshizawa Y, Nagasaki M, Shiogama S, Suzuki M, et al. A Combination of Low-Intensity Pulsed Ultrasound and Nanohydroxyapatite

Concordantly Enhances Osteogenesis of Adipose-Derived Stem Cells From Buccal Fat Pad. Cell Med. 2015 Oct 1;7(3):123–31.

16. Lv Y, Zhao P, Chen G, Sha Y, Yang L. Effects of low-intensity pulsed ultrasound on cell viability, proliferation and neural differentiation of induced pluripotent stem cells-derived neural crest stem cells. Biotechnol Lett. 2013 Dec;35(12):2201–12.

17. Busse JW, Kaur J, Mollon B, Bhandari M, Tornetta P 3rd, Schünemann HJ, et al. Low intensity pulsed ultrasonography for fractures: systematic review of randomised controlled trials. BMJ. 2009;338:b351.

18. Hemery X, Ohl X, Saddiki R, Barresi L, Dehoux E. Low-intensity pulsed ultrasound for non-union treatment: A 14-case series evaluation. Orthopaedics & Traumatology: Surgery & Research. 2011 Feb;97(1):51–7.

19. Waseem Z, Ford M, Syed K, Flannery J. Chronic nonunion in a patient with bilateral supracondylar distal femur fractures treated successfully with twice daily low-intensity pulsed ultrasound. PM R. 2010 Feb;2(2):159–61.

20. Feril LB, Kondo T. Major factors involved in the inhibition of ultrasound-induced free radical production and cell killing by pre-sonication incubation or by high cell density. Ultrason Sonochem. 2005 Apr;12(5):353–7.

21. Bedard K, Krause K-H. The NOX family of ROS-generating NADPH oxidases: physiology and pathophysiology. Physiol Rev. 2007 Jan;87(1):245–313.

22. Claire M. Mahoney, Morgan MR, Harrison A, Humphries MJ, Bass MD. Therapeutic ultrasound bypasses canonical syndecan-4 signaling to activate rac1. J Biol Chem. 2009 Mar 27;284(13):8898–909.

23. Mandal CC, Ganapathy S, Gorin Y, Mahadev K, Block K, Abboud HE, et al. Reactive oxygen species derived from Nox4 mediate BMP2 gene transcription and osteoblast differentiation. Biochem J. 2011 Jan 15;433(2):393–402.

24. Ambe K, Watanabe H, Takahashi S, Nakagawa T. Immunohistochemical localization of Nox1, Nox4 and Mn-SOD in mouse femur during endochondral ossification. 2014.

25. Bruderer M, Richards RG, Alini M, Stoddart MJ. Role and regulation of RUNX2 in osteogenesis. Eur Cell Mater. 2014;28:269–86.

26. Cooper MS, Seibel MJ, Zhou H. Glucocorticoids, bone and energy metabolism. Bone. 2016 Jan;82:64–8.

27. Sodek J, Ganss B, McKee MD. Osteopontin. CROBM. 2000 Jan 1;11(3):279–303.

28. Li JK, Chang WH, Lin JC, Ruaan RC, Liu HC, Sun JS. Cytokine release from osteoblasts in response to ultrasound stimulation. Biomaterials. 2003 Jun;24(13):2379–85.

29. Wu L, Lin L, Qin Y-X. Enhancement of cell ingrowth, proliferation, and early differentiation in a three-dimensional silicon carbide scaffold using low-intensity pulsed ultrasound. Tissue Eng Part A. 2015 Jan;21(1–2):53–61.

30. Greenblatt MB, Shim J-H, Glimcher LH. Mitogen-Activated Protein Kinase Pathways in Osteoblasts. Annual Review of Cell and Developmental Biology. 2013;29(1):63–79.

31. Claes L, Willie B. The enhancement of bone regeneration by ultrasound. Prog Biophys Mol Biol. 2007 Apr;93(1–3):384–98.

32. Johns LD. Nonthermal Effects of Therapeutic Ultrasound: The Frequency Resonance Hypothesis. J Athl Train. 2002;37(3):293–9.

33. Padilla F, Puts R, Vico L, Raum K. Stimulation of bone repair with ultrasound: a review of the possible mechanic effects. Ultrasonics. 2014 Jul;54(5):1125–45.

34. Ebisawa K, Hata K, Okada K, Kimata K, Ueda M, Torii S, et al. Ultrasound Enhances Transforming Growth Factor β-Mediated Chondrocyte Differentiation of Human Mesenchymal Stem Cells. Tissue Engineering. 2004 May;10(5–6):921–9.

35. Gusmão CVB de, Pauli JR, Saad MJA, Alves JM, Belangero WD. Low-intensity Ultrasound Increases FAK, ERK-1/2, and IRS-1 Expression of Intact Rat Bones in a Noncumulative Manner. Clin Orthop Relat Res. 2009 Oct 23;468(4):1149–56.

36. Zhou S, Bachem MG, Seufferlein T, Li Y, Gross HJ, Schmelz A. Low intensity pulsed ultrasound accelerates macrophage phagocytosis by a pathway that requires actin polymerization, Rho, and Src/MAPKs activity. Cellular Signalling. 2008 Apr;20(4):695–704.

37. Fernandes GVO, Cavagis ADM, Ferreira CV, Olej B, de Souza Leão M, Yano CL, et al. Osteoblast Adhesion Dynamics: A Possible Role for ROS and LMW-PTP. J Cell Biochem. 2014 Jun 1;115(6):1063–9.

38. Leskinen JJ, Hynynen K. Study of factors affecting the magnitude and nature of ultrasound exposure with in vitro set-ups. Ultrasound Med Biol. 2012 May;38(5):777–94.

39. Jing Y, Zhou X, Han X, Jing J, Mark K von der, Wang J, et al. Chondrocytes Directly Transform into Bone Cells in Mandibular Condyle Growth. J DENT RES. 2015 Sep 4;22034515598135.

40. Gentili C, Bianco P, Neri M, Malpeli M, Campanile G, Castagnola P, et al. Cell proliferation, extracellular matrix mineralization, and ovotransferrin transient expression during in vitro differentiation of chick hypertrophic chondrocytes into osteoblast-like cells. J Cell Biol. 1993 Aug;122(3):703–12.

41. Chen Z, Yue SX, Zhou G, Greenfield EM, Murakami S. ERK1 and ERK2 regulate chondrocyte terminal differentiation during endochondral bone formation. J Bone Miner Res. 2015 May;30(5):765–74.

42. Morita K, Miyamoto T, Fujita N, Kubota Y, Ito K, Takubo K, et al. Reactive oxygen species induce chondrocyte hypertrophy in endochondral ossification. J Exp Med. 2007 Jul 9;204(7):1613–23.

Chapter 5: Effect of non viral plasmid delivered basic Fibroblast growth factor and low intensity pulsed ultrasound on mandibular condylar growth – a preliminary study.

1. Dimitriou R, Jones E, McGonagle D, Giannoudis PV. Bone regeneration: current concepts and future directions. BMC Medicine. 2011 May 31;9(1):66.

2. Thyagarajan T, Totey S, Danton MJS, Kulkarni AB. Genetically altered mouse models: the good, the bad, and the ugly. Crit Rev Oral Biol Med. 2003;14(3):154–74.

3. Krueckeberg SM, Kapp-Simon KA, Ribordy SC. Social skills of preschoolers with and without craniofacial anomalies. Cleft Palate Craniofac J. 1993 Sep;30(5):475–81.

4. Ritto AK. Class II malocclusion: why, when and how to treat this anomaly in mixed dentition with fixed functional appliances. J Gen Orthod. 2001;12(4):9–21.

5. Rankin M, Borah GL. Perceived functional impact of abnormal facial appearance. Plast Reconstr Surg. 2003 Jun;111(7):2140-2146-2148.

6. Rabie ABM, Dai J, Xu R. Recombinant AAV-mediated VEGF gene therapy induces mandibular condylar growth. Gene Ther. 2007 Jun;14(12):972–80.

7. Kronenberg HM. Developmental regulation of the growth plate. Nature. 2003 May 15;423(6937):332–6.

8. Yun Y-R, Won JE, Jeon E, Lee S, Kang W, Jo H, et al. Fibroblast growth factors: biology, function, and application for tissue regeneration. J Tissue Eng. 2010;2010:218142.

9. Eppley BL, Doucet M, Connolly DT, Feder J. Enhancement of angiogenesis by bFGF in mandibular bone graft healing in the rabbit. J Oral Maxillofac Surg. 1988 May;46(5):391–8.

10. Franceschi RT. Biological approaches to bone regeneration by gene therapy. J Dent Res. 2005 Dec;84(12):1093–103.

11. Clements BA, Hsu CYM, Kucharski C, Lin X, Rose L, Uludağ H. Nonviral delivery of basic fibroblast growth factor gene to bone marrow stromal cells. Clin Orthop Relat Res. 2009 Dec;467(12):3129–37.

12. Moore R, Ferretti P, Copp A, Thorogood P. Blocking endogenous FGF-2 activity prevents cranial osteogenesis. Dev Biol. 2002 Mar 1;243(1):99–114.

13. Hamada T, Suda N, Kuroda T. Immunohistochemical localization of fibroblast growth factor receptors in the rat mandibular condylar cartilage and tibial cartilage. J Bone Miner Metab. 1999;17(4):274–82.

14. Stieger K, Lorenz B. [The treatment of inherited dystrophies and neovascular disorders of the retina by rAAV-mediated gene therapy]. Klin Monbl Augenheilkd. 2008 Dec;225(12):1009–23.

15. Gardlik R, Behuliak M, Palffy R, Celec P, Li CJ. Gene therapy for cancer: bacteria-mediated anti-angiogenesis therapy. Gene Ther. 2011 May;18(5):425–31.

16. McMenamin MM, Wood MJA. Progress and prospects: Immunobiology of gene therapy for neurodegenerative disease: prospects and risks. Gene Ther. 2010 Apr;17(4):448–58.

17. Hacein-Bey-Abina S, Von Kalle C, Schmidt M, McCormack MP, Wulffraat N, Leboulch P, et al. LMO2-associated clonal T cell proliferation in two patients after gene therapy for SCID-X1. Science. 2003 Oct 17;302(5644):415–9.

18. Raper SE, Chirmule N, Lee FS, Wivel NA, Bagg A, Gao G, et al. Fatal systemic inflammatory response syndrome in a ornithine transcarbamylase deficient patient following adenoviral gene transfer. Mol Genet Metab. 2003 Oct;80(1–2):148–58.

19. Ziadloo A, Xie J, Frenkel V. Pulsed focused ultrasound exposures enhance locally administered gene therapy in a murine solid tumor model. J Acoust Soc Am. 2013 Mar;133(3):1827–34.

20. Osawa K, Okubo Y, Nakao K, Koyama N, Bessho K. Osteoinduction by microbubble-enhanced transcutaneous sonoporation of human bone morphogenetic protein-2. J Gene Med. 2009 Jul;11(7):633–41.

21. Suzuki R, Maruyama K. Effective In Vitro and In Vivo Gene Delivery by the Combination of Liposomal Bubbles (Bubble Liposomes) and Ultrasound Exposure. In: Weissig V, editor. Liposomes [Internet]. Humana Press; 2010 [cited 2013 Oct 4]. p. 473–86. (Methods in Molecular Biology). Available from: http://link.springer.com.login.ezproxy.library.ualberta.ca/protocol/10.1007/978-1-60327-360-2_33

22. Negishi Y, Tsunoda Y, Endo-Takahashi Y, Oda Y, Suzuki R, Maruyama K, et al. Local gene delivery system by bubble liposomes and ultrasound exposure into joint synovium. J Drug Deliv. 2011;2011:203986.

23. Eberson CP, Hogan KA, Moore DC, Ehrlich MG. Effect of low-intensity ultrasound stimulation on consolidation of the regenerate zone in a rat model of distraction osteogenesis. J Pediatr Orthop. 2003 Feb;23(1):46–51.

24. El-Bialy T, El-Shamy I, Graber TM. Growth modification of the rabbit mandible using therapeutic ultrasound: is it possible to enhance functional appliance results? Angle Orthod. 2003 Dec;73(6):631–9.

25. El-Bialy TH, Elgazzar RF, Megahed EE, Royston TJ. Effects of ultrasound modes on mandibular osteodistraction. J Dent Res. 2008 Oct;87(10):953–7.

26. Schortinghuis J, Bronckers ALJJ, Stegenga B, Raghoebar GM, de Bont LGM. Ultrasound to stimulate early bone formation in a distraction gap: a double blind randomised clinical pilot trial in the edentulous mandible. Arch Oral Biol. 2005 Apr;50(4):411–20.

27. Inubushi T, Tanaka E, Rego EB, Ohtani J, Kawazoe A, Tanne K, et al. Ultrasound stimulation attenuates resorption of tooth root induced by experimental force application. Bone. 2013 Apr;53(2):497–506.

28. El-Bialy T, Hassan A, Albaghdadi T, Fouad HA, Maimani AR. Growth modification of the mandible with ultrasound in baboons: a preliminary report. Am J Orthod Dentofacial Orthop. 2006 Oct;130(4):435.e7-14.

29. El-Bialy T, Uludag H, Jomha N, Badylak SF. In vivo ultrasound-assisted tissue-engineered mandibular condyle: a pilot study in rabbits. Tissue Eng Part C Methods. 2010 Dec;16(6):1315–23.

30. Oyonarte R, Zárate M, Rodriguez F. Low-intensity pulsed ultrasound stimulation of condylar growth in rats. Angle Orthod. 2009 Sep;79(5):964–70.

31. Erdogan O, Esen E. Biological aspects and clinical importance of ultrasound therapy in bone healing. J Ultrasound Med. 2009 Jun;28(6):765–76.

32. Liao Z-K, Tsai K-C, Wang H-T, Tseng S-H, Deng W-P, Chen W-S, et al. Sonoporation-mediated anti-angiogenic gene transfer into muscle effectively regresses distant orthotopic tumors. Cancer Gene Ther. 2012 Mar;19(3):171–80.

33. Zhou Z, Zhang P, Ren J, Ran H, Zheng Y, Li P, et al. Synergistic effects of ultrasound-targeted microbubble destruction and TAT peptide on gene transfection: An experimental study in vitro and in vivo. Journal of Controlled Release. 2013 Sep 28;170(3):437–44.

34. Khan I, El-Kadi AO, El-Bialy T. Effects of growth hormone and ultrasound on mandibular growth in rats: MicroCT and toxicity analyses. Arch Oral Biol. 2013 Apr 29;

35. Rose LC, Kucharski C, Uludağ H. Protein expression following non-viral delivery of plasmid DNA coding for basic FGF and BMP-2 in a rat ectopic model. Biomaterials. 2012 Apr;33(11):3363–74.

36. Ulgen M, Baran S, Kaya H, Karadede I. The influence of the masticatory hypofunction on the craniofacial growth and development in rats. Am J Orthod Dentofacial Orthop. 1997 Feb;111(2):189–98.

37. Saito M, Mazda O, Takahashi KA, Arai Y, Kishida T, Shin-Ya M, et al. Sonoporation mediated transduction of pDNA/siRNA into joint synovium in vivo. J Orthop Res. 2007 Oct;25(10):1308–16.

38. Sheyn D, Kimelman-Bleich N, Pelled G, Zilberman Y, Gazit D, Gazit Z. Ultrasound-based nonviral gene delivery induces bone formation in vivo. Gene Ther. 2008 Feb;15(4):257–66.

39. Zolochevska O, Xia X, Williams BJ, Ramsay A, Li S, Figueiredo ML. Sonoporation delivery of interleukin-27 gene therapy efficiently reduces prostate tumor cell growth in vivo. Hum Gene Ther. 2011 Dec;22(12):1537–50.

40. Li QF, Rabie ABM. A new approach to control condylar growth by regulating angiogenesis. Arch Oral Biol. 2007 Nov;52(11):1009–17.

41. Frost HM. A 2003 update of bone physiology and Wolff's Law for clinicians. Angle Orthod. 2004 Feb;74(1):3–15.

42. Bassett CA. Electrical effects in bone. Sci Am. 1965 Oct;213(4):18–25.

43. Behari J, Singh S. Ultrasound propagation in "in vivo" bone. Ultrasonics. 1981 Mar;19(2):87–90.

44. Claes L, Willie B. The enhancement of bone regeneration by ultrasound. Prog Biophys Mol Biol. 2007 Apr;93(1–3):384–98.

45. Dinno MA, Dyson M, Young SR, Mortimer AJ, Hart J, Crum LA. The significance of membrane changes in the safe and effective use of therapeutic and diagnostic ultrasound. Phys Med Biol. 1989 Nov;34(11):1543–52.

46. Rawool NM, Goldberg BB, Forsberg F, Winder AA, Hume E. Power Doppler assessment of vascular changes during fracture treatment with low-intensity ultrasound. J Ultrasound Med. 2003 Feb;22(2):145–53.

47. Parvizi J, Parpura V, Greenleaf JF, Bolander ME. Calcium signaling is required for ultrasound-stimulated aggrecan synthesis by rat chondrocytes. J Orthop Res. 2002 Jan;20(1):51–7.

48. Reher P, Doan N, Bradnock B, Meghji S, Harris M. Effect of ultrasound on the production of IL-8, basic FGF and VEGF. Cytokine. 1999 Jun;11(6):416–23.

49. Carballido-Gamio J, Majumdar S. Clinical utility of microarchitecture measurements of trabecular bone. Curr Osteoporos Rep. 2006 Jun;4(2):64–70.

Chapter 6: General Discussion and Conclusion

1. Eberson CP, Hogan KA, Moore DC, Ehrlich MG. Effect of low-intensity ultrasound stimulation on consolidation of the regenerate zone in a rat model of distraction osteogenesis. J Pediatr Orthop. 2003 Feb;23(1):46–51.

2. El-Bialy T, El-Shamy I, Graber TM. Growth modification of the rabbit mandible using therapeutic ultrasound: is it possible to enhance functional appliance results? Angle Orthod. 2003 Dec;73(6):631–9.

3. Ikeda K, Takayama T, Suzuki N, Shimada K, Otsuka K, Ito K. Effects of low-intensity pulsed ultrasound on the differentiation of C2C12 cells. Life Sci. 2006 Oct 12;79(20):1936–43.

4. Cheng K, Xia P, Lin Q, Shen S, Gao M, Ren S, et al. Effects of Low-Intensity Pulsed Ultrasound on Integrin-FAK-PI3K/Akt Mechanochemical Transduction in Rabbit Osteoarthritis Chondrocytes. Ultrasound in Medicine & Biology. 2014 Jul;40(7):1609–18.

5. Dalla-Bona DA, Tanaka E, Inubushi T, Oka H, Ohta A, Okada H, et al. Cementoblast response to low- and high-intensity ultrasound. Arch Oral Biol. 2008 Apr;53(4):318–23.

6. Tanaka E, Yamano E, Dalla-Bona DA, Watanabe M, Inubushi T, Shirakura M, et al. Dynamic compressive properties of the mandibular condylar cartilage. J Dent Res. 2006 Jun;85(6):571–5.

7. Padilla F, Puts R, Vico L, Raum K. Stimulation of bone repair with ultrasound: a review of the possible mechanic effects. Ultrasonics. 2014 Jul;54(5):1125–45.

8. El-Bialy T, Hassan A, Albaghdadi T, Fouad HA, Maimani AR. Growth modification of the mandible with ultrasound in baboons: a preliminary report. Am J Orthod Dentofacial Orthop. 2006 Oct;130(4):435.e7-14.

9. Schumann D, Kujat R, Zellner J, Angele MK, Nerlich M, Mayr E, et al. Treatment of human mesenchymal stem cells with pulsed low intensity ultrasound enhances the chondrogenic phenotype in vitro. Biorheology. 2006;43(3–4):431–43.

10. Chan CW, Qin L, Lee KM, Cheung WH, Cheng JCY, Leung KS. Dose-dependent effect of low-intensity pulsed ultrasound on callus formation during rapid distraction osteogenesis. J Orthop Res. 2006 Nov;24(11):2072–9.

11. Kuroda S, Tanimoto K, Izawa T, Fujihara S, Koolstra JH, Tanaka E. Biomechanical and biochemical characteristics of the mandibular condylar cartilage. Osteoarthr Cartil. 2009 Nov;17(11):1408–15.

12. Li Q, Zhang M, Chen Y-J, Zhou Q, Wang Y-J, Liu J. Psychological stress alters microstructure of the mandibular condyle in rats. Physiology and Behavior. 2013;110–111:129–39.

13. Xue H, Zheng J, Cui Z, Bai X, Li G, Zhang C, et al. Low-intensity pulsed ultrasound accelerates tooth movement via activation of the BMP-2 signaling pathway. PLoS ONE. 2013;8(7):e68926.

14. Al-Daghreer S, Doschak M, Sloan AJ, Major PW, Heo G, Scurtescu C, et al. Short-Term Effect of Low-Intensity Pulsed Ultrasound on an Ex-Vivo 3-D Tooth Culture. Ultrasound in Medicine and Biology. 2013 Jun 1;39(6):1066–74.

15. Al-Daghreer S, Doschak M, Sloan AJ, Major PW, Heo G, Scurtescu C, et al. Long term effect of low intensity pulsed ultrasound on a human tooth slice organ culture. Arch Oral Biol. 2012 Jun;57(6):760–8.

16. Morita K, Miyamoto T, Fujita N, Kubota Y, Ito K, Takubo K, et al. Reactive oxygen species induce chondrocyte hypertrophy in endochondral ossification. J Exp Med. 2007 Jul 9;204(7):1613–23.

17. Ki SK, Hae WC, Hee EY, Ick YK. Reactive oxygen species generated by NADPH oxidase 2 and 4 are required for chondrogenic differentiation. Journal of Biological Chemistry. 2010;285(51):40294–302.

18. Rabie ABM, Hägg U. Factors regulating mandibular condylar growth. Am J Orthod Dentofacial Orthop. 2002 Oct;122(4):401–9.

19. Gibson G. Active role of chondrocyte apoptosis in endochondral ossification. Microsc Res Tech. 1998 Oct 15;43(2):191–204.

20. Rankin EB, Giaccia AJ, Schipani E. A central role for hypoxic signaling in cartilage, bone, and hematopoiesis. Curr Osteoporos Rep. 2011 Jun;9(2):46–52.

21. Kosmidou I, Xagorari A, Roussos C, Papapetropoulos A. Reactive oxygen species stimulate VEGF production from C(2)C(12) skeletal myotubes through a PI3K/Akt pathway. Am J Physiol Lung Cell Mol Physiol. 2001 Apr;280(4):L585-592.

22. Lambert AJ, Buckingham JA, Boysen HM, Brand MD. Diphenyleneiodonium acutely inhibits reactive oxygen species production by mitochondrial complex I during reverse, but not forward electron transport. Biochimica et Biophysica Acta (BBA) - Bioenergetics. 2008 May;1777(5):397–403.

23. Riganti C, Gazzano E, Polimeni M, Costamagna C, Bosia A, Ghigo D. Diphenyleneiodonium Inhibits the Cell Redox Metabolism and Induces Oxidative Stress. J Biol Chem. 2004 Nov 12;279(46):47726–31.